

CRANFIELD UNIVERSITY

EMMANUEL OZIOMA OSIGWE

TECHNO-ECONOMIC AND RISK ANALYSIS OF CLOSED-CYCLE
GAS TURBINE SYSTEMS FOR SUSTAINABLE ENERGY
CONVERSION

SCHOOL OF AEROSPACE TRANSPORT AND MANUFACTURING
Power Propulsion Engineering Center

Doctor of Philosophy (PhD Full Time)
Academic Year: 2015 - 2018

Supervisor: Professor Pericles Pilidis
Associate Supervisor: Dr Suresh Sampath, Dr Theoklis Nikolaidis
April 2018

CRANFIELD UNIVERSITY

SCHOOL OF AEROSPACE TRANSPORT AND MANUFACTURING
Power Propulsion Engineering Center

Doctor of Philosophy (PhD Full Time)

Academic Year 2015 - 2018

EMMANUEL OZIOMA OSIGWE

TECHNO-ECONOMIC AND RISK ANALYSIS OF CLOSED-CYCLE
GAS TURBINE SYSTEMS FOR SUSTAINABLE ENERGY
CONVERSION

Supervisor: Professor Pericles Pilidis
Associate Supervisor: Dr. Suresh Sampath, Dr. Theoklis Nikolaidis
April 2018

© Cranfield University 2018. All rights reserved. No part of this
publication may be reproduced without the written permission of the
copyright owner.

ABSTRACT

With renewed interest in research and development on the closed-cycle gas turbine technology, it is almost certain this energy conversion system may well emerge in the foreseeable future as a viable option in power generation and utility industry due to: (a) its easy adaptability to a wide spectrum of working fluids and heat sources (b) very high fuel utilization efficiency (c) reduction in pollution and energy consumption, (d) potential for high degree of availability, reliability and low maintenance cost and (e) high part-load performance characteristics. In Europe, power plants up to 50MWe have operated successfully on arrays of gaseous, liquid and solid fuels, and have demonstrated a high degree of availability and reliability, with both helium and air used as working fluids. Waste heat thermal energy from these plants, in form of hot water, has been utilized for industrial and urban district heating with results of over 80% fuel utilization efficiency met. However, despite the many advantages of the closed-cycle gas turbine system, it has not enjoyed widespread commercialization. This is because its features do not come free and the diffidence exploring the technology for future investment may be related to limited experience in design and operation for several variables such as working fluid options. Therefore, for the full potentials of the closed-cycle gas turbine to be realized, its suitability in the choice component design, cycle performance, economic potentials with minimum risk have to be proven in several off-setting conditions before any appropriate investment decision can be made.

This research seeks to address the knowledge gap on the effect of selected working fluids such as helium, air, nitrogen, and carbon dioxide on the overall component design, cycle performance, and economics of the closed-cycle gas turbine power plant. To implement the research aim, a robust decision support framework for closed-cycle gas turbine using the Techno-economic, Environmental and Risk Analysis (TERA) method has been adopted in this research, as a multidisciplinary tool for strategic decision making in closed-cycle gas turbine technology investments. The governing principles of TERA arise

from different module integration, which allows for design considerations and/or operating areas such as performance, environment, economics and risk analysis. In this research, each of the operating areas was modelled to achieve the central goal of the research.

The results from the performance perspective show that the overall cycle efficiency of the closed-cycle gas turbine is maximum for working fluid with a high ratio of specific heats at lower pressure ratio. Also, the research shows that working fluid have great influence on design choice configuration, gas turbine component sizing and the initial cost of investment in closed-cycle gas turbine technology. In the economic assessment, competitive cost information was generated with helium showing a higher risk of investment due to its limited supply. Most significantly, the research provides a representative of trade-offs on the plant thermodynamic performance characteristics, economics and impact of working fluids on closed-cycle gas turbine system technology.

Keywords:

Sustainable Energy, Component design, TERA, Cycle Performance, Working Fluid

ACKNOWLEDGMENT

Foremost, I am eternally grateful to the Almighty God for divine help throughout this research and for giving me the patience to complete this doctorate.

My deepest thanks go to Prof. Pilidis for his unwavering guidance, support and opportunities he gave me, without whom this thesis could not have been completed. I would also express my unreserved gratitude to Dr. Sampath for his advice and support in supervising my work. To Dr. Nikolaidis, I cannot thank you enough for your supervision and critical reviews of my papers. Thank you for being so helpful.

Most especially, my heartfelt appreciation goes to my lovely wife, Nimi, and daughter Rhema. Thanks to you both for your patience, understanding and moral support.

PUBLICATIONS

Osigwe, E.O., Pilidis, P., Sampath, S., Nikolaidis, T., Gad-Briggs, A., (2018). "Performance Analysis of Generation IV Nuclear Reactor using CO₂ and N₂: Case Study of a Recuperated Brayton Gas Turbine Cycle". ASME 26th ICONE Conference, ICONE26-82373, July 22-26, 2018, London

Osigwe, E.O., Pilidis, P., Sampath, S., Nikolaidis, T., Gad-Briggs, A., (2018). "Multi-Fluid Gas Turbine Components Scaling for a Generation IV Nuclear Reactor Power Plant Performance Simulation". ASME 26th ICONE Conference, ICONE26-82373, July 22-26, 2018, London

Osigwe, E.O., Pilidis, P., Sampath, S., Nikolaidis, T., (2018). "GT- ACYSS: Gas Turbine Arekret-Cycle Simulation Tool for Training and Educational Purposes". AIAA Modelling and Simulation Technologies Conference and Journal Publication

TABLE OF CONTENTS

ABSTRACT	i
ACKNOWLEDGMENT	iii
LIST OF FIGURES	x
LIST OF TABLES	xv
LIST OF EQUATIONS.....	xvi
LIST OF ABBREVIATIONS	xxii
1 RESEARCH OVERVIEW	1
1.1 Background and Motivation	1
1.2 Contribution to Knowledge.....	3
1.3 Scope of Work and Objectives.....	3
1.3.1 Technical and Performance Objectives.....	4
1.3.2 Economic Objectives.....	4
1.3.3 Risk Objectives	4
1.4 Approach	5
1.4.1 Concept of TERA	6
1.5 Thesis Structure.....	6
2 CLOSED-CYCLE GAS TURBINE DESIGN AND OPERATIONS: A STATE – OF – THE – ART REVIEW	9
2.1 Background.....	9
2.2 The Closed-Cycle Gas Turbine Technology	11
2.2.1 Comparison with Open Cycle.....	13
2.2.2 Cycle and Shaft Configurations.....	14
2.2.3 Direct and Indirect Coupling	16
2.3 Historical Development and Potential Application.....	18
2.3.1 Applications of the closed-cycle gas turbine technology	21
2.4 Niche Market Potentials	25
2.4.1 Working Fluid Potentials.....	25
2.4.2 Heat Source Alternative	26
2.4.3 Energy Utilization Potentials.....	29
2.5 Summary of R&D Programmes	32
2.5.1 Advances in working fluid studies and component design	32
2.5.2 Modelling and Simulation studies for Closed-cycle with different fluid	33
2.6 Setbacks and Future Prospects.....	34
2.6.1 Explore working fluid options for different heat source application and economic assessment.....	34
2.6.2 The need for a robust simulation and demonstration plant.....	35
2.6.3 Turbomachinery and heat exchanger design and performance analysis	35
2.6.4 Future prospect	36

2.7 Knowledge Gap and Research Novelty	36
2.8 The TERA Approach and Application	37
2.9 Chapter Conclusion	39
3 RESEARCH METHODOLOGY	41
3.1 Background.....	41
3.2 The justification for TERA Approach	42
3.3 TERA for Closed-Cycle Gas Turbine Technology.....	43
3.3.1 Performance Module	44
3.3.2 Component Design and Sizing Model	45
3.3.3 Economic Module.....	46
3.3.4 Risk Analysis Module	47
3.3.5 Model Limitations and Potential Improvements	47
3.4 Chapter Conclusion	48
4 DEVELOPMENT OF GT- ACYSS PERFORMANCE CODE	49
4.1 Background.....	49
4.1.1 Justification of the need for the Code Development	49
4.2 Code Structure.....	50
4.3 Engine Configuration Options	53
4.4 Components Simulation Modelling	53
4.4.1 Turbomachinery Component.....	53
4.4.2 Heat Exchangers.....	55
4.4.3 Heat Source	57
4.4.4 Cycle Performance Calculation	57
4.5 Component Matching.....	58
4.6 Multi-Fluid Component Scaling for Single Shaft Configuration	60
4.6.1 Turbomachinery Component Map Scaling	61
4.6.2 Heat Exchangers Scaling at Off-design Operation	63
4.7 Working Fluid Options.....	65
4.7.1 Modelling of Fluid Properties in GT-ACYSS.....	65
4.8 Control Options and Strategy.....	69
4.8.1 Inventory Control (ICS).....	71
4.8.2 Bypass Control (BCS)	76
4.8.3 Heat Source Temperature Control (HST).....	78
4.8.4 Combined Control Mode	80
4.9 Solution Convergence Method.....	80
4.10 Application of GT-ACYSS Performance Code and Control Options	83
4.11 Results and Discussions.....	83
4.11.1 Application 1: Simulation of three closed-cycle gas turbine plant... ..	83
4.11.2 Application 2: Control Option performance analysis and Load Rejection	92
4.12 Technical studies on Inventory Control	108
4.12.1 Method of Analysis	110

4.12.2 Results and Discussion	111
4.13 Chapter Conclusion	114
5 EFFECT OF WORKING FLUID ON PERFORMANCE AND DESIGN OF CLOSED-CYCLE GAS TURBINE	116
5.1 Background.....	116
5.2 Working Fluid and Material Compatibility	117
5.2.1 Working Fluid Safety Issues.....	118
5.3 Performance Parametric Analysis.....	118
5.3.1 Influence of Cycle Configuration	119
5.3.2 Influence of working fluid properties on cycle efficiency and specific power	124
5.3.3 Influence of compressor entry conditions	127
5.4 Sensitivity Analysis	132
5.4.1 Effect of Pressure Drop	133
5.4.2 Effect of Component Efficiency	137
5.4.3 Effect of Heat Exchanger Effectiveness	140
5.5 Effect on Inventory Control Systems.....	142
5.5.1 Case Study.....	143
5.6 Effect on Component Design, Sizing, and Operational Performance ...	148
5.6.1 Turbomachinery Preliminary Design and Sizing Model.....	149
5.6.2 Heat Exchanger Preliminary Design and Sizing Model	152
5.6.3 Inventory Tank Design Sizing and Weight Model.....	154
5.6.4 Case Studies.....	157
5.7 Chapter Conclusion	170
6 TECHNO-ECONOMIC ANALYSIS ON DESIGN AND OPERATIONAL PERFORMANCE WITH DIFFERENT WORKING FLUID	175
6.1 Background.....	175
6.2 Working Fluid Economics and Availability.....	176
6.3 Method of Analysis.....	177
6.4 Equipment Component Cost.....	178
6.4.1 Turbomachinery	179
6.4.2 Heat Exchangers.....	179
6.4.3 Generator	180
6.5 Economic Model of Inventory Control System	180
6.5.1 Cost of Transfer compressor.....	181
6.6 Cash Flows	182
6.6.1 Revenue and Expenses	182
6.6.2 Operating Income and Annual Net Cash Flow	184
6.7 Measure of Economic Assessment.....	184
6.7.1 Levelized Annual Revenue.....	184
6.7.2 Net Present Value	185
6.7.3 Internal Rate of Return (IRR)	186

6.7.4 Discounted Pay-back Period.....	186
6.8 Case Studies	187
6.9 Results and Discussions.....	189
6.10 Chapter Conclusion	191
7 RISK ANALYSIS	193
7.1 Background.....	193
7.2 Technology Risk	194
7.2.1 Material technology for high temperature and pressure	195
7.2.2 Working fluid gas management.....	196
7.2.3 Technology maturity level.....	197
7.3 Financial Risk	201
7.3.1 Cost of working fluid	201
7.3.2 Sensitivity to pressure ratio and mass flow	202
7.3.3 Legislation	203
7.4 Chapter Conclusion	203
8 CONCLUSION AND RECOMMENDATIONS.....	205
8.1 Summary of a research study	205
8.2 Conclusion of results.....	207
8.3 Concluding Discussions.....	208
8.4 Limitation of Studies.....	209
8.5 Recommendations for Future Work	210
REFERENCES.....	211
APPENDICES	227
Appendix A GT – ACYSS: Additional Information.....	227
Appendix B Effect of Working Fluid – Additional Results.....	238
Appendix C Effect of Working Fluid – Additional Results.....	242

LIST OF FIGURES

Figure 1-1 Flow Chart for Overview of Research Methodology	5
Figure 2-1 Gas Turbine Working Fluid Configurations [4]	10
Figure 2-2 Gas turbine classification and flexibility of closed-cycle gas turbine	10
Figure 2-3 : Evolution of turbine entry temperature of closed-cycle gas turbines [14,15].....	11
Figure 2-4 Direct and indirect coupling of closed-cycle gas turbine [33].....	17
Figure 2-5: Examples of closed-cycle gas turbine built and licensed by Escher Wyss [2].....	18
Figure 2-6 Land based Application of closed-cycle gas turbine.....	22
Figure 2-7 General Electric HTRE3 and HTRE1 (Nuclear Powered airplane engines) at the Idaho National Laboratory in Arco, Idaho [52].....	23
Figure 2-8 Tupolev Tu-95LAL nuclear test-bed airplane [54]	23
Figure 2-9 Conceptual solar powered closed-cycle gas turbine cogeneration [14]	29
Figure 2-10 Simplified Aim of TERA.....	38
Figure 3-1 Basic architecture of TERA	41
Figure 3-2 TERA framework for closed-cycle gas turbine technology	43
Figure 3-3 Structure of Performance Model	44
Figure 3-4 Flow process for component design and sizing module.....	45
Figure 3-5 Structure of economic Model	46
Figure 4-1 Structure of GT- ACYSS: Closed - Cycle Gas Turbine Simulation Code.....	51
Figure 4-2 Schematic Diagram of Intercooled - Recuperated Closed - Cycle Gas Turbine Plant	59
Figure 4-3 Flow chart of Multi - Fluid Scaling Method used for Turbomachinery Component Maps	61
Figure 4-4 Comparison of GT-ACYSS Model for Air Specific Heat Capacity with Tables - Variation with Temperature at Pressure of 1atm.....	68
Figure 4-5 Comparison of GT-ACYSS Model for N2 Specific Heat Capacity with Tables - Variation with Temperature at Pressure of 1atm.....	68
Figure 4-6 Comparison of GT-ACYSS Model for CO2 Specific Heat Capacity with Tables - Variation with Temperature at Pressure of 1atm	69

Figure 4-7 Scheme of Reference Plant Circuit with Different Control Options .	71
Figure 4-8 Iteration Procedure using Inventory Control Strategy at steady-state	73
Figure 4-9 Iteration Procedure using Bypass Control Strategy at steady-state	78
Figure 4-10 Iteration Procedure using HST Control Strategy at steady-state...	79
Figure 4-11: Structure of Simulation Convergence in GT-ACYSS.....	82
Figure 4-12 Schematic of reference plant modelled for case 1 [27,138–140] ..	84
Figure 4-13 Compressor performance comparisons with GT-ACYSS at full speed.....	86
Figure 4-14 Heat power requirement comparisons from full to part-load.....	86
Figure 4-15 Variation in performance due to changes in compressor inlet temperature for fixed power operation	88
Figure 4-16 Schematic of reference plant modelled for case 3	89
Figure 4-17 Part Load Performance Comparison.....	90
Figure 4-18 Engine rotational Speed as a function of pressure ratio and corrected mass flow.....	91
Figure 4-19: Effect of compressor inlet temperature	92
Figure 4-20 Effect of Part Load Performance on PR and Compressor Pressures using ICS.....	94
Figure 4-21 Effect of Part Load Performance on Mass Flow and Cycle Efficiency using ICS.....	95
Figure 4-22 : Effect of Part Load Performance on Mass Flow and Cycle Efficiency using BCS	96
Figure 4-23 : Effect of Part Load Performance on PR and Compressor Pressures using BCS.....	97
Figure 4-24 Effect of Part Load Performance on Mass Flow and Cycle Efficiency using HST	98
Figure 4-25 Effect of Part Load Performance on PR and Compressor Pressures using HST	98
Figure 4-26 Comparison of Efficiency for Different Control Strategy at Part Load	99
Figure 4-27 Comparison of shaft speed for Different Control Strategy at Part Load.....	100
Figure 4-28 Effect of CIT on Mass Flow and Cycle Efficiency using ICS	101

Figure 4-29 Effect of CIT on PR and Compressor Pressures using ICS	102
Figure 4-30 Effect of CIT on PR and Compressor Pressures using HST	102
Figure 4-31 Effect of CIT on Mass Flow and Cycle Efficiency using HST	103
Figure 4-32 Comparison of Efficiency for Different Control Strategy at Changes in CIT	103
Figure 4-33 Estimation of Pseudo-Transient Behaviour with bypass control (speed & load released).....	106
Figure 4-34 Estimation of Pseudo-Transient Behaviour with bypass control (system temperatures).....	107
Figure 4-35 Estimation of Pseudo-Transient Behaviour with bypass control (system pressure ratios)	107
Figure 4-36 Inventory Control with Multi – Storage Tank using Natural pressure differential	109
Figure 4-37 Inventory Control with Transfer Compressor (TC).....	109
Figure 4-38 Procedure for Analysis	110
Figure 4-39 Effect of Tank Pressure on Inventory Control Level	111
Figure 4-40 Effect of Number of Tanks	111
Figure 4-41 Weight and Cost Analysis of ICS	112
Figure 4-42 Cost Economics of Inventory Control Options.....	113
Figure 5-1 Effect of cycle configuration on cycle efficiency at different pressure ratios and working fluids	120
Figure 5-2 Effect of cycle configuration on specific power at different pressure ratios and working fluids	121
Figure 5-3 Effect of working fluid properties on cycle efficiency at different PR and TET.....	126
Figure 5-4 Effect of working fluid properties on specific power at different PR and TET.....	127
Figure 5-5: Influence of compressor entry temperature on cycle efficiency at fixed PR and TET	129
Figure 5-6 Influence of compressor entry temperature on specific power at fixed PR and TET	130
Figure 5-7 Influence of compressor entry pressure on cycle efficiency at fixed PR and TET	131

Figure 5-8 Influence of compressor entry pressure on specific power at fixed PR and TET.....	132
Figure 5-9 Effect of pre-cooler (PC) pressure drop on the cycle efficiency	135
Figure 5-10 Effect of recuperator low-pressure-side (LPS) pressure drop on the cycle efficiency	135
Figure 5-11 Effect of Gas Heater (GH) pressure drop on the cycle efficiency	136
Figure 5-12 Effect of recuperator high-pressure-side (HPS) pressure drop on the cycle efficiency	136
Figure 5-13 Effect of recuperator LPS & HPS pressure drop on the cycle efficiency.....	137
Figure 5-14 Sensitivity of compressor efficiency on cycle efficiency	139
Figure 5-15 Sensitivity of turbine efficiency on cycle efficiency	139
Figure 5-16 Sensitivity of pre-cooler effectiveness on cycle efficiency	140
Figure 5-17 Sensitivity of gas heater effectiveness on cycle efficiency	141
Figure 5-18 Sensitivity of recuperator effectiveness on cycle efficiency.....	141
Figure 5-19 Effect of Reynolds number on cycle efficiency at part-load operation	144
Figure 5-20 Mass of Inventory tank and GT cycle before part-load operations	146
Figure 5-21 Mass of working fluid leaving the GT cycle during part-load operation.....	146
Figure 5-22 Total mass of ICT during part-load operation.....	147
Figure 5-23 Total volume of inventory tank during part-load operation	147
Figure 5-24 Working fluid response to part-load operation.....	148
Figure 5-25 Chart for Determining Optimum Diameter of Pressure Vessel Storage Tank [153,154]	155
Figure 5-26 Schematic representation of the Gen-IV reactor indirectly coupled with a recuperated closed-cycle gas turbine.....	160
Figure 5-27 Case1 – Turbomachinery number of stages (same output power for all working fluids	161
Figure 5-28 Case1 – Length of the compressor, turbine and recuperator (same output power for all working fluids	161
Figure 5-29 Case2 – Turbomachinery Number of stages (same rotational speed for all working fluids).....	165

Figure 5-30 Case2 - Length of the compressor, turbine and recuperator (same rotational speed for all working fluids.....	165
Figure 5-31 Case2 – compressor characteristics (same rotational speed for all working fluids.....	166
Figure 5-32 Case3 – Turbomachinery Number of stages (same geometry)...	168
Figure 5-33 Case3 - Length of the compressor, turbine and recuperator (same geometry for all working fluids	168
Figure 6-1 Scheme of economic analysis.....	178
Figure 6-2 present annual net cash flow comparison for nitrogen	188
Figure 6-3 Internal rate of return for nitrogen.....	189
Figure 7-1: Scheme for Risk Analysis	194
Figure 7-2 NASA Technology Readiness Level (TRL)	198

LIST OF TABLES

Table 2-1 Major characteristics of cycle selection for closed-cycle gas turbine	16
Table 4-1 Summary of GT-ACYSS Modelling Framework	52
Table 4-2 Comparison of Simulated results and Published Design Point Data for case 1	85
Table 4-3 Comparison of Simulated results and Published Design Point Data for case 2	88
Table 4-4 Comparison of Simulated results and Published Design Point Data for case 3	90
Table 4-5 Summary of Power Plant Design Point Description.....	93
Table 4-6 Summary of Power Plant Design Point Description.....	108
Table 5-1 Remarks on Working Fluid	118
Table 5-2 Baseline Parameter for Parametric study	119
Table 5-3 Summary of Power Plant Design Point Description.....	143
Table 5-4 Simulated cycle performance at constant mass flow.....	143
Table 5-5 Summary of reference plant design point description.....	159
Table 5-6 Case1 – Compressor Characteristics (same output power for all working fluids).....	163
Table 5-7 Case1 – Recuperator Characteristics (same output power for all working fluids).....	163
Table 5-8 Case1 – Turbine Characteristics (same output power for all working fluids).....	164
Table 5-9 Case2 – Compressor Characteristics (same rotational speed for all working fluids).....	167
Table 5-10 Case3 - Compressor Characteristics (same geometry for all working fluids).....	169
Table 6-1 Cost of Working Fluid [156,157]	177
Table 6-2 General assumptions for economic analysis	187
Table 6-3 Estimated closed cycle gas turbine capital cost for different working fluids	188
Table 6-4: Economic performance results.....	189

LIST OF EQUATIONS

(4-1).....	54
(4-2).....	54
(4-3).....	54
(4-4).....	54
(4-5).....	54
(4-6).....	55
(4-7).....	55
(4-8).....	55
(4-9).....	55
(4-10).....	56
(4-11).....	56
(4-12).....	56
(4-13).....	56
(4-14).....	56
(4-15).....	56
(4-16).....	56
(4-17).....	57
(4-18).....	57
(4-19).....	57
(4-20).....	57
(4-21).....	58
(4-22).....	59
(4-23).....	59
(4-24).....	60
(4-25).....	60
(4-26).....	60
(4-27).....	62
(4-28).....	62

(4-29).....	62
(4-30).....	62
(4-31).....	63
(4-32).....	63
(4-33).....	63
(4-34).....	63
(4-35).....	63
(4-36).....	63
(4-37).....	64
(4-38).....	64
(4-39).....	64
(4-40).....	64
(4-41).....	64
(4-42).....	64
(4-43).....	64
(4-44).....	65
(4-45).....	65
(4-46).....	65
(4-47).....	66
(4-48).....	66
(4-49).....	67
(4-50).....	67
(4-51).....	67
(4-52).....	67
(4-53).....	74
(4-54).....	74
(4-55).....	74
(4-56).....	74
(4-57).....	75

(4-58).....	75
(4-59).....	75
(4-60).....	75
(4-61).....	75
(4-62).....	75
(4-63).....	76
(4-64).....	76
(4-65).....	77
(4-66).....	77
(4-67).....	77
(5-1).....	145
(5-2).....	145
(5-3).....	150
(5-4).....	150
(5-5).....	150
(5-6).....	150
(5-7).....	150
(5-8).....	150
(5-9).....	151
(5-10).....	151
(5-11).....	151
(5-12).....	151
(5-13).....	151
(5-14).....	151
(5-15).....	151
(5-16).....	151
(5-17).....	152
(5-18).....	152
(5-19).....	152

(5-20).....	153
(5-21).....	153
(5-22).....	153
(5-23).....	154
(5-24).....	154
(5-25).....	154
(5-26).....	154
(5-27).....	155
(5-28).....	155
(5-29).....	156
(5-30).....	156
(5-31).....	156
(5-32).....	156
(5-33).....	157
(5-34).....	157
(5-35).....	157
(5-36).....	157
(5-37).....	157
(5-38).....	157
(5-39).....	157
(5-40).....	158
(5-41).....	159
(6-1).....	179
(6-2).....	179
(6-3).....	179
(6-4).....	179
(6-5).....	180
(6-6).....	180
(6-7).....	180

(6-8).....	180
(6-9).....	180
(6-10).....	181
(6-11).....	181
(6-12).....	181
(6-13).....	182
(6-14).....	183
(6-15).....	183
(6-16).....	183
(6-17).....	183
(6-18).....	183
(6-19).....	184
(6-20).....	184
(6-21).....	184
(6-22).....	185
(6-23).....	185
(6-24).....	185
(6-25).....	185
(6-26).....	185
(6-27).....	186
(6-28).....	186
(A2-1)	229
(A2-2)	229
(A2-3)	229
(A2-4)	229
(A2-5)	229
(A2-6)	229
(A2-7)	229
(A2-8)	230

(A2-9)	230
(A2-10)	230
(A2-11)	230

LIST OF ABBREVIATIONS

A	Area
ASME	American Society of Mechanical Engineers
BCS	Bypass Control
BVC	Bypass Valve Close
BVO	Bypass Valve Open
CBC	Closed Brayton Cycle
CET	Compressor Entry Temperature
CH	Corrected enthalpy drop
CMF	Corrected Mass Flow
CS	Corrected Speed
CW	Compressor Work
DP	Design Point
DPBP	Discounted Payback Period
EGT	Exhaust Gas Temperature
FOM	Figure of Merit
GH	Gas Heater
GT	Gas Turbine
HPC	High-Pressure Compressor
HPCDP	High-Pressure Compressor Discharge Pressure
HPCPR	High-Pressure Compressor Pressure ratio
HPS	High-Pressure-Side
HST	Heat Source Temperature Control
IC	Intercooler
ICC	Initial Capital Cost
ICR	Intercooled Recuperated Cycle
ICS	Inventory Control System
ICT	Inventory Control Tank
ICV	Inventory Control Valves
IRR	Internal Rate of Return
LCOE	Levelized Cost of Electricity
LPC	Low-pressure Compressor
LPCIP	Low-Pressure Compressor Inlet Pressure
LPCPR	Low-Pressure Compressor Pressure ratio
LPS	Low-Pressure-Side
NCF	Net Cash Flow
NDCW	Nondimensional Compressor work
NPV	Net Present Value

NTU	Number of transfer units
OD	Off-design
OPR	Overall pressure ratio
PC	Pre-cooler
PR	Pressure ratio
RX	Recuperator Heat Exchanger
SOP	Shaft Output Power
SP	Specific Power
TERA	Techno-economic, Environment and Risk Analysis
TET	Turbine Entry Temperature
TMF	Turbine Mass Flow
TPR	Turbine Pressure ratio
TW	Turbine Work
UW	Useful Work

NOTATION

C_{old}	Heat Capacity of the cold fluid stream (J/kgK)
C_{hot}	Heat Capacity of the hot fluid stream (J/kgK)
C_{max}	Maximum Heat Capacity (J/kgK)
C_{min}	Minimum Heat Capacity (J/kgK)
C_P	Specific heat capacity at constant pressure (J/kgK)
D	Diameter (m)
D_m	Mean Diameter
D_h	Hub Diameter (m)
D_t	Tip Diameter (m)
G	Torque (Nm)
L	Length (m)
M	Mach Number
M_T	Mass of Inventory Control tank (kg)
M_{GT}	Mass of Gas Turbine Cycle loop (kg)
N	Rotational Speed (rpm)
P	Pressure (Pa)
P_{ref}	Reference pressure (Pa)
P_{Cin}	Inlet compressor Pressure (Pa)
P_{Cout}	Exit Compressor Pressure (Pa)
PR_C	Compressor Pressure ratio
PR_t	Turbine Pressure ratio
Q	Heat Transfer rate
Q_g	Heat gained

R	Fluid Specific Gas constant (J/kgK)
Re	Reynold number
R_{stage}	Pressure ratio per stage
T	Temperature (K)
T_{cap}	Insulation temperature for Inventory tank (K)
T_{Cin}	Inlet Compressor temperature (K)
T_{Cout}	Exit Compressor temperature (K)
T_{ref}	Reference temperature (K)
V	Velocity (m/s)
V_a	Axial Velocity (m/s)
V_T	Volume of Inventory tank (m ³)
W	Mass flow (kg/s)
ε	Effectiveness
γ	Ratio of heat capacity
η	Efficiency
η_c	Compressor efficiency
η_t	Turbine Efficiency
η_m	Mechanical Efficiency
η_{aux}	Auxiliary Losses
η_{HEX}	Heat exchanger efficiency
θ	Referred temperature parameter
δ	Referred pressure parameter
ρ	Density (kg/m ³)
Δ	Changes/Difference
ω	Angular velocity
f	Friction factor
μ	Viscosity (Ns/m ²)

1 RESEARCH OVERVIEW

1.1 Background and Motivation

The International Energy Agency's (IEA) report of 2015 projected a significant (37%) growth in the World's energy demand over the next 30 years [1]. This increase will be as a result of population growth and urbanization, as well as industrial and economic expansion, especially in developing countries like India, China, Nigeria, and Brazil. The greater part of this energy demand will be met using non-renewable fuels with limited supply. The question we need to confront as a global community is:

- **How does one provide a sustainable energy conversion system with total energy utilization from its heat source that would service the growing population, economic and industrial demand, yet reduce the primary energy from non-renewable energy sources?**

It is also important to consider the environmental impact related to energy conversion. Not until recently, the focus on energy impact to the environment was seen as a local phenomenon, but increased awareness on the likeliness of a global climate change associated with this process has shifted our concerns to proffering efficient technological solutions . Hence, the future of any energy conversion system is linked to its impact on the environment.

- **How can one decrease emission of CO₂ and other green-house gases (GHG) to the atmosphere associated with energy conversion systems?**

The closed-cycle gas turbine plant has the potential to meet the two questions raised above and to complement the existing conventional power plants and open cycle gas turbine. In the last few years, there has been considerable interest in closed-cycle gas turbine power plant due to [2–4]: (a) its easy adaptability to wide range of heat source (b) flexibility to changes in working fluid (c) high efficiency at part load (d) high level of availability and low maintenance cost, as well as (d) reduction in pollution (f) the enormous

achievement in the areas of high-temperature reactors and the development of the Generation IV nuclear reactors.

In Europe, closed-cycle power plants up to 50MWe [2] have operated successfully on arrays of gaseous, liquid and solid fuels, and have demonstrated high availability/reliability index with helium and air as working fluids. Waste heat energy from these plants, in form of hot water, has been utilized for industrial and urban heating with results of over 80% fuel utilization efficiency met. Recently, the UK government gave final approval to £18bn Hinkley Point C closed-cycle nuclear plant in Somerset [5], which is an indication of future prospects for closed cycle gas turbine technology.

However, the advantageous features of this power conversion system do not come free. Thus, for the potentials of the closed-cycle gas turbine to be fully realized, its suitability, when coupled with any heat source has to be explored and performance compared for various possible working fluids over a large variation of a possible number of combinations in the operating conditions and power demand. The choice of the power plant set-up which includes: (a) type of working fluid, (b) cycle configuration, (c) heat source, and other factors must be proven to be cost and performance effective in several off-setting conditions before any appropriate investment decision is made. Hence, a robust decision support framework encompassing every aspect of research in closed-cycle technology is required to satisfy or act as a reference for any future investment.

To this end, the research topic presented originates from answering these questions and curiosities raised above with a special focus on the effect of selected working fluid on the performance, design and economic assessment of the closed-cycle gas turbine. The working fluids considered in this study include air, carbon dioxide, helium, and nitrogen. The overall goal of this study is to undertake a **Techno-economic and Risk Analysis (TERA)** from design and operational perspective for the listed working fluids on closed-cycle gas turbine technology. Thus, the study comprises of four parts: part one focuses on performance modelling and assessment, while part two deals with component designs. Part three shows a techno-economic assessment while part four is the

risk analysis. In all the parts of this research, selected case studies are presented and discussed in details.

1.2 Contribution to Knowledge

Having performed a state-of-the-art review of relevant literatures, it is clear that although design and performance assessment has been performed for specific fluid such as references [5–13], there has not been a detailed comparison for the fluids used in this study in terms of its economic assessment, and influence on component design, cycle performance and inventory control system.

To this end, the contribution to knowledge of this research is to develop and integrate multidisciplinary models using TERA (Techno-economic, Environment and Risk Analysis) approach, to analyse the effect of working fluids in closed-cycle gas turbine engine systems performance and design. The research novelties are highlighted as follow:

- **Development of simulation tool called GT-ACYSS with extended features of different working fluid, cycle configuration, control system options, and component design options**
- **The economic viability of the closed-cycle gas turbine technology for different working fluids**
- **Cycle performance assessment with air, nitrogen, helium and carbon dioxide**
- **The risk analysis on implementing this technology.**

The models and methodology developed hopes to provide useful decision-making support for any investment in closed-cycle gas turbine technology.

1.3 Scope of Work and Objectives

The aim of this research is to implement a TERA on a proposed development of a closed-cycle gas turbine system for sustainable energy conversion. In this study, an environmental assessment was not included as part of the research scope. Thus, in order to accomplish the desired expectation, a breakdown of objectives which defines the scope of this research is specified as follows:

1.3.1 Technical and Performance Objectives

- Develop a performance simulation tool with capability for different working fluid options, cycle configuration, control options and preliminary component design.
- To investigate design point and off-design point performance of an industrial application using different working fluids.
- To understand the technical requirements and design considerations of the closed-cycle gas turbine components under the influence of thermodynamic properties, pressure losses, and component losses. The above property effects will be compared to assess the working fluid selection for optimum cycle performance.

1.3.2 Economic Objectives

An economic analysis of the gas turbine systems will be investigated considering components size and performance, cost of operation and maintenance considerations. This objective seeks to translate into economic terms the relationship of performance, component sizing, working fluid and different configurations. The following scope will be investigated under this objective:

- To establish a techno-economic assessment on the power plant considering the current price of electricity, capital investment, energy sources, working fluids, operations and maintenance costs using Net Present Value.
- To understand the economic implications in the components thermodynamic performance characteristics.

1.3.3 Risk Objectives

- To develop a financial risk model considering the sensitivity of component(s) to the investment.

- Establish the technology risk of working fluid management, technology maturity, and components design selections.
- Investigation of the dependency of working fluid selections on the equipment size.

All these objectives will be incorporated into the TERA framework as a tool for decision making for both, the manufacturer and operator (investor).

1.4 Approach

To implement the central aim of this research, a methodology based on TERA approach was developed. The governing principles of TERA arise from different module integration, which allows for design consideration and/or operating areas such as performance, economic and risk analysis. Each of module components of the TERA was targeted at achieving the specific objective of the research.

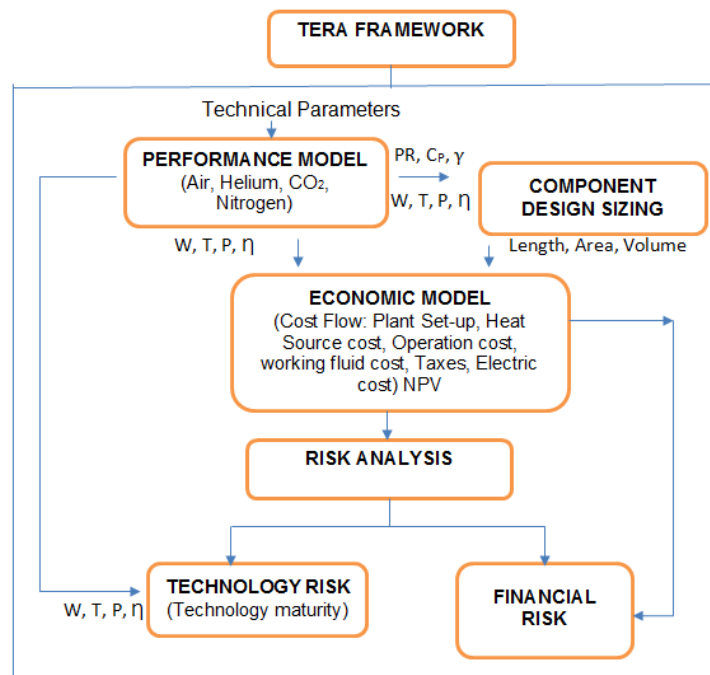


Figure 1-1 Flow Chart for Overview of Research Methodology

An overview of the research methodology is shown in Fig. 1-1. For purpose of brevity, a detail description of the research method is discussed in chapter three of this thesis.

1.4.1 Concept of TERA

TERA is an acronym for Techno-economic, Environmental and Risk Analysis. It provides a method which incorporates multi-disciplinary aspects of modelling plant performance, estimation of environmental impact, assessment of economic feasibility and identification of potential risk and critical elements associated with a proposed technology. It is used to exploit potential technology design solutions of an engineering problem, thereby reducing computational time and costs. In this way, an optimum solution can be selected with a reduced error in the decision-making process. The TERA tool can be greatly utilized to influence the decision of any future investment in the closed-cycle gas turbine technology considering a wide range of possible conditions.

1.5 Thesis Structure

This research thesis is structured into eight (8) chapters as follows:

Chapter one (1) gives a general overview of the research which includes: knowledge gap as a motivation for this research, the scope, and objectives, a diagrammatic representation of methodology to be implemented to achieve the research aim. The novelty/ contribution to knowledge is mentioned in section 1.2 of this chapter. It also discusses the previous works by other investigators in areas such as the development of Generation IV nuclear power plant and modelling. It further gives an overview of the proposed methodology adopted in this research, the research aim, objectives and the contribution to knowledge. It closes with a thesis structure breakdown.

In Chapter two (2) the review of relevant literature on advancement made in closed Brayton Cycle technology and TERA tool and discussed to establish a background knowledge and understanding of the research. It summarizes theoretical work on the closed cycle gas turbine and operating experiences from actual plants. It also presents the setbacks and future prospect of the closed-cycle gas turbine technology.

Chapter three (3) discusses a breakdown of the methodology to be implemented for the research study using TERA approach. The governing

principles of TERA arise from different module integration, which allows for design consideration and/or operating areas such as performance, economic and risk analysis. Each of module components of the TERA was targeted at achieving the specific objective of the research. This chapter discusses a breakdown of the general approach implemented in the research.

Chapter four (4) introduces GT-ACYSS, a program developed by the author for closed-cycle gas turbine steady-state performance simulation and component design using different working fluids. It describes the structure of the code, computational models used, and verifications based on open literature of reference power plant.

The content of chapter five (5) is principally to present analyses for the effect of selected working fluids on the design and performance of the closed-cycle gas turbine. The purpose of the working fluid study is to identify the influence of candidate fluids on components and overall design and performance of the closed-cycle gas turbine, as well as its suitability for the plant operations without major modification on the engine configuration.

Chapter six (6) provides an economic assessment of the influence of selected working fluids on the overall plant cost, maintenance, and operations. The economic assessment was based on the plant component design and working fluid cost.

Chapter seven (7) gives an assessment of the uncertainties and operational challenges based on set assumptions. Most significantly, it provides a representative of trade-offs on the plant thermodynamic performance characteristics, working fluid selection, the effect of legislation and impact of technology maturity.

Finally, chapter (8) provides an overview of the conducted research and contributions made from the various studies carried out. It then goes further to lists areas for further improvements and research which the research could not cover.

2 CLOSED-CYCLE GAS TURBINE DESIGN AND OPERATIONS: A STATE – OF – THE – ART REVIEW

2.1 Background

Over the past four decades gas turbines have become one of the widely used energy conversion systems for large-scale power generation, and as a prime mover for different types of applications (airborne, land and sea). Contributing to its continuous usage in the applications mentioned is as a result of its high thermal efficiency, availability, high power to weight ratio and low emissions compared with other conventional energy conversion systems. Gas turbine engines operate on Brayton cycle which is usually described as a thermodynamic cycle that converts heat energy gained by the working fluid to useful work while operating at constant pressure during heat addition to the gas cycle. Based on the working fluid path in the Brayton cycle, gas turbines are classified as either open cycle, closed cycle or semi-closed cycle as shown in Fig 2-1; with the open cycle being the most common configuration in use for airborne and land-based applications. In the open cycle, the expanded working fluid is released into the environment while in the closed-cycle the expanded working fluid is cooled and reused continuously in the cycle loop.

As previously mentioned, the open cycle has been the most commonly used gas turbine due to its simplicity and availability of clean fuel. However, in the last few years, there has been a renewed growing interest in the closed-cycle gas turbine as an alternative or additional sustainable energy conversion system due to its suitability for the different non-oxygenated application (submarines, space), high part load performance, working fluid flexibility and other potential benefits it can offer. In retrospect, the closed-cycle gas turbine technology is ahead of its time in terms of technology readiness and great prospects of practically coupling it with different heat sources, and heat sink utilization, towards the realization of a high efficiency and pollution free environment. With this growing interest, it now seems that a new race is emerging; the competition between the open and closed-cycle gas turbines.

Hence, it is the purpose of this chapter to present a state-of-the-art review on the closed-cycle gas turbine technology and to discuss emerging issues from current researches and development studies which can add value to any potential future investment, as well as establish a basis (knowledge gap) for the thesis. The aim of the chapter is to give an introduction of the relevant concept necessary to achieve a basic understanding of past experiences, recent progress and to give future research outlook of the closed-cycle gas turbine technology.

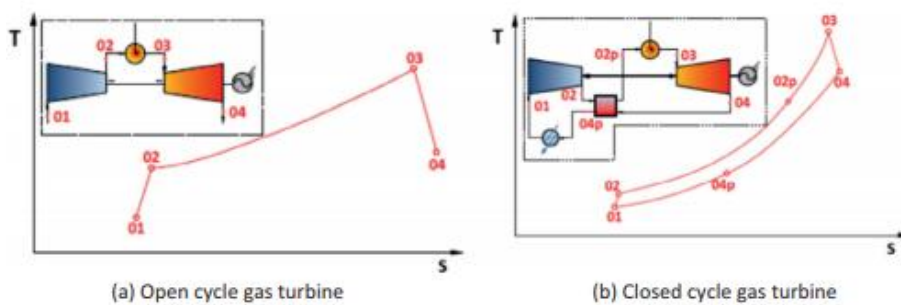


Figure 2-1 Gas Turbine Working Fluid Configurations [4]

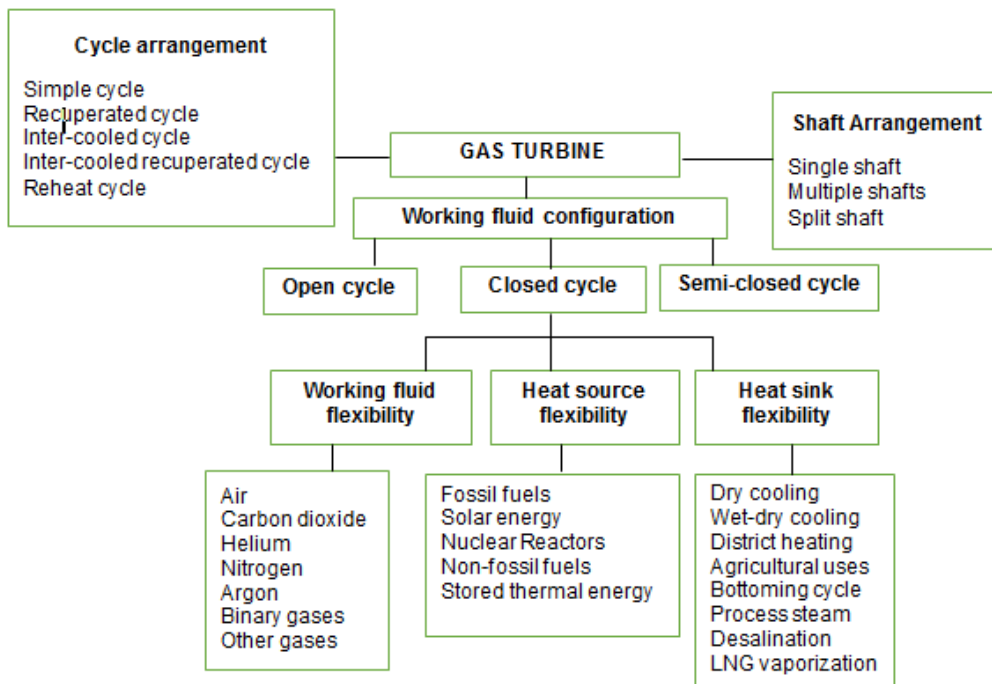


Figure 2-2 Gas turbine classification and flexibility of closed-cycle gas turbine

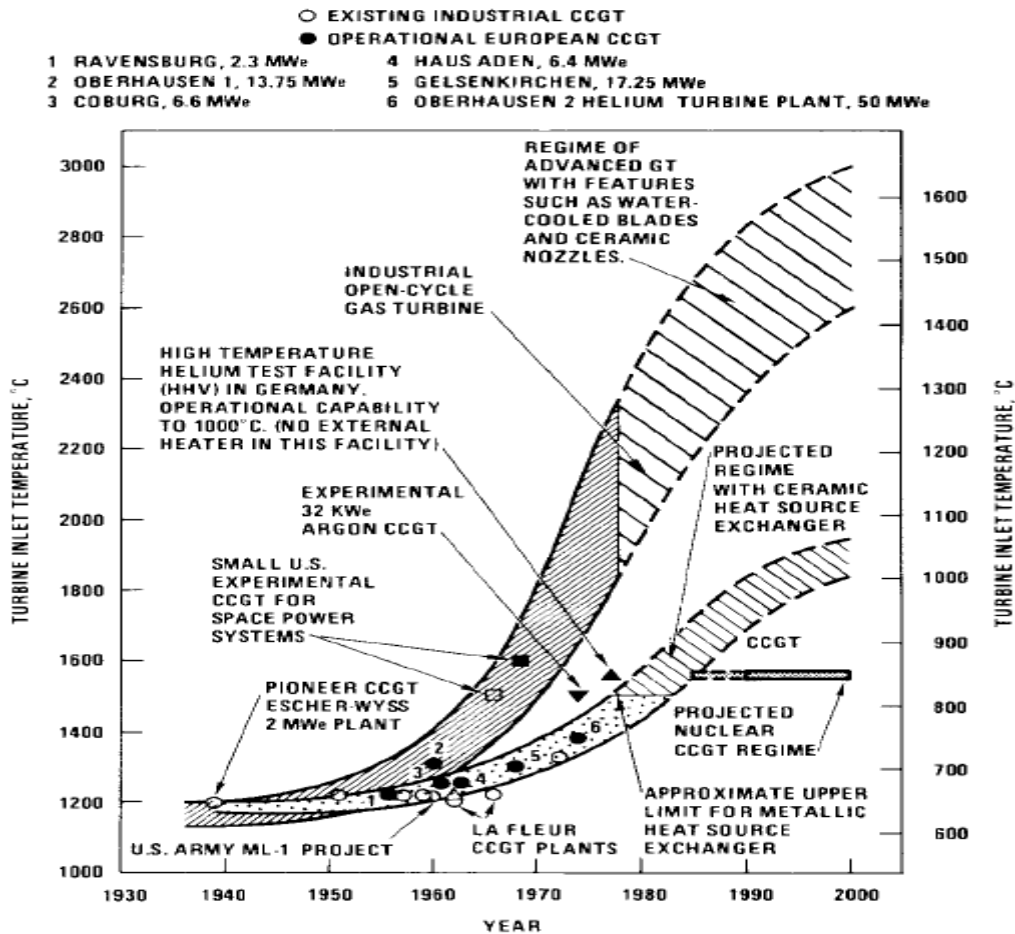


Figure 2-3 : Evolution of turbine entry temperature of closed-cycle gas turbines [14,15]

2.2 The Closed-Cycle Gas Turbine Technology

The closed-cycle gas turbine is a prime mover, in which thermal energy is transferred from an external heat source to the gaseous working fluid. After work is done by the working fluid to the turbine, heat is rejected to a sink before recycling the working fluid into the compressor. The distinctive feature of the closed-cycle operation compared to the open cycle is the isolation of the working fluid from the outside environment within a control volume. This makes it possible for any working gas to be adopted in the circuit, and with a self-contained working fluid, the closed-cycle gas turbine can be used in environments with no oxygenated atmosphere. The isolation of the working fluid

permits the possibility of having it free from moisture and contamination, which is important for high-temperature surfaces that could be corroded and/or fouled, by particulate contaminants.

The closed Brayton cycle and the Carnot cycle can be assumed to be similar in efficiency within the given temperature range. Both cycles need isothermal compression and expansion over a moderate cycle pressure ratio, the major difference being that the CBC requires heat transfer apparatus to accomplish its temperature range while Carnot cycle requires the use of additional machinery. However, the performance and application of closed Brayton cycles has been demonstrated in the closed-cycle gas turbine power plant with an increase in the turbine entry temperature as shown in Fig 2-3

The closed-cycle gas turbine characteristics are in consonance with goals of resource conservation and high overall efficiency potential. The external heat source and multiple heat exchangers deployed in this type of plant make it more complex compared to other Brayton cycles. However, bearing in mind the impact of energy conversion due to increased public concern about the environment, the perceived advantages of the cycle makes it a viable future option for sustainable energy conversion. The motivation, however, to select the closed cycle gas turbine over any energy conversion is hinged on the following:

- The capability of pressurizing the system and using the pressure level to achieve high part-load efficiency. The capability to operate at high pressure can reduce the size of components, hence, the cost of the closed-cycle gas turbine unit
- A self-contained working fluid system with the option of flexibility in the choice of fluid and cleanliness of fluid as shown in Fig 2-2. Having a self-contained working fluid allows it to be used in wide environmental application such as space power systems, submarine propulsion, terrestrial transportation, aircraft and electric power generation. The flexibility to use any working fluid allows for the potential use of high-temperature materials such as molybdenum alloys due to the non-

oxidizing atmosphere and reduces the danger of fouling, corrosion or efficiency loss due to contamination.

- Operational flexibility and adaptability to a wide range of heat sources and fuel as listed in Fig.2-2. The closed-cycle can quick adapt to changes in heat source since the energy conversion system can be indirectly coupled with much complexity.
- High energy utilization efficiency with a wide range of heat sink system. Due to the arrangement of the closed-cycle, the cooling medium provides high overall energy utilization with minimum environmental impact.
- The closed-cycle also offers high reliability, compactness of machines and components since there is no moving part on the machines in high-temperature region, and reduction of thermal stresses with the steady temperature at all load.

2.2.1 Comparison with Open Cycle

Both the open and closed-cycle gas turbine have made a reasonable contribution towards meeting the world's energy demands in terms of power generation. In the open cycle, heat addition takes place in a combustor by burning the fuel in the working fluid stream, with resultant products of combustion mixing with and becoming part of the working fluid and the cycle heat rejection is accomplished by discharging the low-pressure exhaust gas into the system surroundings and recharging the open circuit with fresh ambient air. The closed-cycle working fluid flow is not allowed to mix with the system surroundings; hence, heat addition and rejection are accomplished through heat exchangers; a high-temperature heater and a low-temperature cooler, respectively.

In terms of performance, the closed-cycle gas turbine was originally conceived as a means of effecting good control of the system over a wide range of loads with essentially no loss no significant loss in cycle thermal efficiency with a reduction in load down to around 30%. This is in contrast to the performance characteristics of conventional open cycle gas turbine in which control is

accomplished by varying the TET. That not only reduces the cycle efficiency but also leads to a mismatch of the turbo-set because of the reduction in flow rate through the turbine, changes in relative velocities entering and leaving the turbine. Reference [16] compared the performance of closed and open cycle using a simple and recuperated configuration at constant pressure ratios, turbine entry temperatures, and effectiveness. The results showed that the closed-cycle have lower pressure losses compared to the open cycle, however, the heating efficiency of the open cycle and the fuel flow addition to the working fluid gives it an advantage in cycle efficiency. Similarly, in the work of reference [17], the closed-cycle have its peak performance characteristics at lower pressure ratios as against the open cycle configuration.

With this mind, one may be tempted to conclude that despite the many benefits of the closed-cycle gas turbine, the open cycle have been more popular due to its potentials to achieving very high turbine entry temperature making it more efficient, and less costly while the closed-cycle firing temperature is limited by the maximum allowable temperature of the heat exchangers. Hence, the closed-cycle may not be able to totally replace the open cycle but could gain more usefulness in an application where the open cycle cannot be deployed such as in a non-oxygenated environment [4,18].

2.2.2 Cycle and Shaft Configurations

The design choice for performance operating cycles based on the physical layout or configuration of the closed-cycle gas turbine power plant is driven by the thermo-economic analysis of the system so as to get the right balance between thermal efficiency and capital cost [19,20]. Simple closed-cycle gas turbine component arrangements usually consist of the cooling heat exchanger and a turbomachinery set as shown in Fig.2-1. In order to improve the cycle efficiency, the simple cycle arrangement can be modified with recuperation, intercooling, reheating, and recompressing as well as other unique configurations. Gad-Briggs et al., [19] compared the performance and technical advantages of simple and intercooled recuperated for Generation IV reactor power plants. The results showed that intercooled-recuperated cycle had a

better cycle performance than the simple cycle arrangement. Similarly, reference [21] compared the performance of a recuperated cycle, recompression and simple cycle arrangement for supercritical carbon dioxide cycle application.

A decision to improve cycle performance using recuperation means that additional heat exchanger will be incorporated to the simple arrangement, in which a portion of the sensible heat in the turbine exhaust is used to preheat the working fluid prior to entering the heat source. This increases the cycle efficiency at every pressure ratio for which recuperation is possible [22–24]. Similarly, for intercooled cycle, the compressor work and exit temperature are reduced by incorporating a heat exchanger to cool the working fluid before further compression is achieved. This increases the input thermal power with a slight improvement in the cycle efficiency and significant increase in the output power. References [21,25,26] presented an analysis of the optimal number of intercooling stages and the trade-off between the cycle performance and the initial cost of the overall system. On the other hand, reheating the system increases the cycle efficiency and output power by increasing the average temperature of heat addition. Other factors that can affect the design choice of the cycle arrangement are the choice of working fluid, the environmental application and technology readiness level for the closed-cycle application. The added complexity to the simple plant design, to only marginally improve the cycle performance may not be warranted in terms of capital cost, but the long-term operations will recoup the initial investment. Table 2-1 gives an overview of the cycle selection on major characteristics of the closed-cycle gas turbine. An overview of the diagrammatic representation of these cycle arrangements discussed is presented in Appendix A.1

Just like in open cycle application, different shaft arrangements (single or multi-shaft) can be deployed in the closed-cycle gas turbine. The decision to use either the single or multi-shaft arrangement depends on the control system, working fluid to use, and cost. In the single-shaft configuration, the turbo-set and generator are connected by a single rotor shaft as applied in GTHTR300

[27] and GT-MHR [28], while the multi-shaft arrangement has sets of the turbomachinery components coupled in pairs of several rotor shafts as applied in PMBR [29,30].

Comparing the different shaft arrangement, reference [31] analysed the merits and demerits of both configurations based on steady-state and transient control simulation. The results showed that single shaft required more power at a transient operation than three-shaft configuration. Similarly, reference [32] showed that the turbomachinery overall volume for a two-shaft configuration is less than a single shaft configuration. Hence, adopting a multi-shaft arrangement has improved performance benefits than single shaft such as improve the dynamic performance of the rotating shaft and flexibility in part load operation whereas the single shaft is difficult managing the part load performance. The main advantage of the single shaft arrangement in closed-cycle gas turbine application is the simplicity and reduced cost it offers.

Table 2-1 Major characteristics of cycle selection for closed-cycle gas turbine

Comparison	SC	RC	ICR	IC	RH
High-efficiency potential	NE	G	G	NE	NE
Plant layout	S	A	A	A	A
Technology Maturity	P	P	P	NP	NP
Component size	P	A	A	A	A
Future prospect	A	G	G	-	-
Potential heat sink usage	VG	G	A	G	VG

Key:
 SC – simple cycle, RC – recuperated cycle, RH – reheat cycle
 IC – intercooled cycle, ICR – intercooled-recuperated cycle
 VG – very good
 G – good
 A – acceptable
 P – proven
 NE – not economical
 NP – not proven
 S - simple

2.2.3 Direct and Indirect Coupling

Closed-cycle gas turbines can be coupled directly with its heat source as seen in most closed-cycle operations coupled to nuclear reactors. Similarly, for other design reasons and ease of maintainability, some plant are coupled indirectly to

it heat source as shown in Fig. 2-4. In a plant with indirect coupling, an extra heat exchanger is required working fluid in the reactor and the gas turbine system can be different, while for the direct coupling the working fluid in the reactor and the gas turbine system are the same. There are several researches comparing the benefits of indirect and direct coupling of the closed-cycle gas turbine. El-Genk [33] compared the performance of VHTR plants with direct and indirect closed-cycle gas turbine. The result showed that with indirect coupling, the size and number of stages of the turbomachine are reduced, which translates into better dynamic stability for the rotor and substantial cost saving for the turbomachine. However, this is achieved at the expense of decreasing the plant cycle efficiency. The work identified some other advantages of indirect coupling such as the reduced impact of changing the operation conditions of the cycle loop and the electrical load demand on the VHTR operation. Secondly, is the flexibility in the plant maintenance and operation which the indirect coupling arrangement offers.

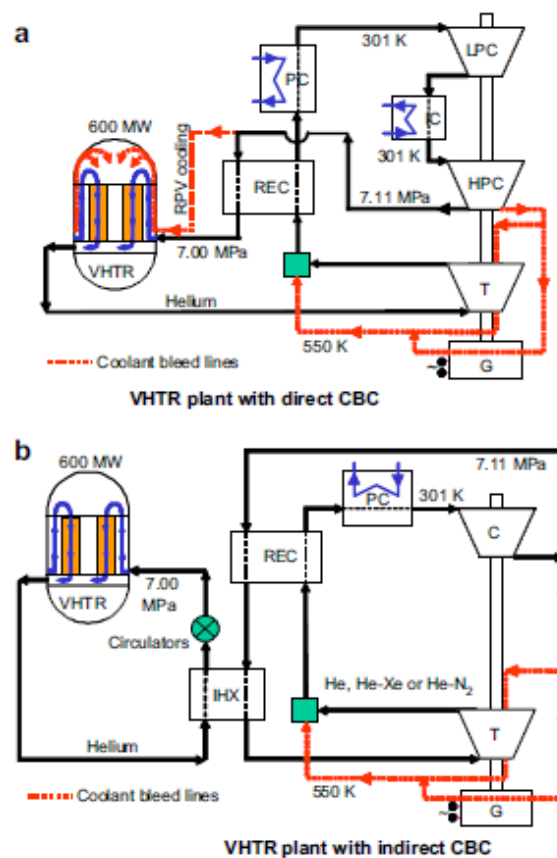
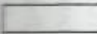



Figure 2-4 Direct and indirect coupling of closed-cycle gas turbine [33]

2.3 Historical Development and Potential Application

The conceptual idea of the closed-cycle gas turbine also known as Ackeret-Keller or AK cycle [14,34] was earliest published by J. Ackeret and C. Keller in 1939 [14]; which was later first designed and commercialized by Escher Wyss, Ltd. of Zurich, Switzerland. Fifteen years down the line of this conceptual idea and thereafter has witnessed over 25 closed-cycle plants (Pilot and Commercial) built across the global. The variations of closed-cycle gas turbine plants that were built by Escher Wyss Ltd. and Licensees have been well documented [2,14]. Some of these plants have operated for over 150,000 hours; have demonstrated an optimum level of reliability and availability [2]. Thus, its ability to operate on different fuels and the possibility for the cogeneration of heat and power contributed to the popularity of the closed-cycle gas turbine at that time. Some of the pioneer experiences, research, and development in the closed-cycle gas turbine field are extensively outlined in [2,24,35–42]. Figure 2-5 shows plant built by Escher Wyss and its licensees for testing and industrial applications.

EXPERIMENTAL				INDUSTRIAL															
				0.7 - 2.3 MW				6.0 - 6.6 MW				12 - 50 MW							
Plant	Fuel	MW	Mf	Plant	Fuel	MW	Mf	Plant	Fuel	MW	Mf	Plant	Fuel	MW	Mf				
AK-36	39	0	2.0	E	Coventry ⁵⁾	49	H	0.7	J	Coburg	61	B	6.6	G	Paris ⁶⁾	52	O	12	E
Clydebank	50	B	1.0	J	Ravensburg	56	BO	2.3	EG	Haus Aden	63	MB	6.4	G	Dundee ⁶⁾	54	O	12	J
Clydebank	51	P	0.4	J	Toyotomi	57	N	2.0	EF	Phoenix ³⁾	66	N	6.0	EL	Oberhausen I	60	BC	14	EG
Tuco-52	55	0	1.5	E	Altnabreak	59	P	2.2	J	4) Thermodynamic heated test bed (HHT-Project) 5) Heat utilization from retorters of a gas work 6) Reheated twin shaft 7) He-turbine plant				Kashira	61	L	12	EK	
IN-10 ¹⁾	61	0	7.0	M	Roths	60	S	2.0	J					Nippon Kokan	61	F	12	F	
ML-1 ²⁾	62	R	0.4							Gelsenkirchen	67	F	17	G					
La Fleur ³⁾	62	N	2.0	L						Vienna	72	Q	30	EW					
Wau ⁴⁾	81	-	-40	B						Oberhausen II ⁷⁾	74	C	50	GS					

	100,000 - 150,000 operating hours	Manufacturers: B Brown Boveri
	Nearly 100,000 operating hours	E Escher Wyss
		F Fuji Electric
		G Gute Hoffnungs Hütte
		J John Brown
		K EVT (KSG)
		L La Fleur
		M Mitsui
		S Sulzer Brothers
		W Waagner Biro

Fuels:		
○ Light oil	C Cok furnace gas	L Lignite
○ Heavy fuel oil	F Blast furnace gas	P Peat
○ Natural gas	B Bituminous coal	R Nuclear
○ Mine gas	S Coal slurry	H Waste heat

Figure 2-5: Examples of closed-cycle gas turbine built and licensed by Escher Wyss [2]

The pioneer closed-cycle gas turbine plant built by Escher Wyss in 1939 was an oil-fired plant which generated 2.0 MW and operated successfully with an efficiency of 32.6 percent, a turbine inlet temperature of 973K and Air was used as working fluid [2,43]. This plant was in service for more than 6000 hours of operation and proved the viability of the closed-cycle concept as a technological base for future fossil-fired closed-cycle gas turbine plant. With the post-war economic situation of 1948, installation of the first commercial closed-cycle gas turbine plant was commissioned in 1956 at the Escher Wyss AG works in Ravensburg, Germany. The pulverized coal and heavy or light oil closed-cycle gas turbine plant in Ravensburg supplied 2.3 MW output power of electricity to furnaces, fabrication buildings and forging works in the factory. This plant was operational for about 125,000 hours and had an availability of 87 percent. Other closed-cycle gas turbine plants developed between 1939 and 1965 has been documented in [2,14,44,45] and summarized in Fig 2-5 above.

Similarly, in the same year, the first closed-cycle gas turbine plant was built, a 4.0 MW open gas turbine was developed by Brown, Boveri and Cie (BBC, now ABB), which achieved an efficiency of 17.0 percent and a turbine inlet temperature of 823K. The initial reason for the Ackeret-Keller or AK cycle success was hinged on the utilization of coal, hence with an external gas heater system; the problem of turbine erosion from combustion products was prevented. However, with the fuel supply situation in Europe as at that time, there were changes from coal to gaseous and liquid fossil fuels. As fossil fuels (gas and oil) became abundant between the 1950s and 1960s, the open-cycle gas turbine was rapidly utilized for both industrial and aerospace application. By this time, the open-cycle in combined-cycle mode could match the performance of the presumed fossil-fired closed-cycle gas turbine plant and this slowed the development of the closed-cycle gas turbine. Withal, in the mid-1970s due to the economics of increasing demand and decreasing availability of cleaner fuels, the closed-cycle gas turbine with its external combustion system offered a possible modern prime mover, capable of burning dirty fuels in an environmentally acceptable manner. This resuscitated further development activities in Europe and the U.S for the closed-cycle gas turbine plant.

In 1972, the city of Vienna commissioned Escher Wyss in Zurich to build another plant with an output of 30.0 MW. It supplied electricity and heat for the Spittelauer general hospital, with an efficiency of 31.0 percent, turbine inlet temperature of 993K and Air as working fluid [2]. Similarly, Oberhausen II, Helium closed-cycle gas turbine plant was initiated in 1974, designed with for an output power of 50.0 MW, cycle efficiency of 34.5 percent and high-temperature reactor with turbine inlet temperature of 1023K. The second demonstration facility for the helium high-temperature reactor was built in 1981. After 1981, large concept closed cycle gas turbine was not pursued due to lack of technology readiness, hence, current investigation has become limited to conceptual design.

However, by 1987, research focus on helium gas turbines shifted to high-temperature small modular reactor gas turbine systems, which resulted in a conceptual design of the modular high-temperature gas-cooled reactor gas turbine MGR-GT developed in Massachusetts Institute of Technology (MIT) [46]. Also, within this period, the first design of the modular helium reactor gas turbine (MHR-GT) was developed by General Atomics (GA) in USA [20,47]. The breakthrough in high-temperature reactors brought about a renewed growing interest in the closed cycle gas turbine. This new interest was also seen in supercritical carbon dioxide cycles between the 1990s and 2000s; a collaboration of MIT with Sandia National Laboratories (SNL), Idaho National Laboratories (INL) and Argonne National Laboratories (ANL) developed a supercritical carbon dioxide turbomachinery, compact heat exchangers and heat source technologies [13,48,49]. By 1994, ESKOM Company in South Africa started the development of a 400MWth Pebble Bed Modular Reactor couple with a direct closed cycle gas turbine [4,28]. The Gas Turbine High-Temperature Reactor (GTHTR300) programme was initiated by the Japan Atomic Research Institute in 2001 [27]. Similarly, by 2003 the Chinese Institute of Nuclear and New Energy Technology (INET) began an experimental 10MW helium cooled high-temperature reactor gas turbine (HTR-10GT) at Tsinghua University [4,50]. In 2004, the AREVA new technology advanced reactor energy supply (ANTARES) began the French high/very high-temperature reactors

comprising a topping of the helium-nitrogen mixture. In 2012, the final design and installation of S-CO₂ recompression Brayton cycle test assembly were realized by SNL. Similar, by 2014, an 8MW closed-cycle gas turbine using supercritical carbon dioxide was presented for commercial demonstration by Echogen Power Systems [4].

The capability to generate and control a large amount of heating power without impeding the electric power generation made the closed-cycle gas turbine plant a viable advantage for various municipalities with the large heating grid. In total, the closed-cycle gas turbines have accumulated over 750,000 operating hours. However, due to the wide range of applicability of the closed-cycle gas turbine, there have been numerous research and development with varied successes documented in reference [4].

2.3.1 Applications of the closed-cycle gas turbine technology

As previously mentioned, one of the advantages of the closed-cycle gas turbine is its application in the different environment, especially in the non-oxygenated environment. This section presents the successful and potential application of the closed cycle gas turbine.

2.3.1.1 Land-Based application

Most of the closed-cycle gas turbine plants designed and built were used for the terrestrial land-based operation. In Europe, especially Switzerland and Germany, the benefits of the closed-cycle gas turbine was long recognized for terrestrial combined electrical power generation, and its acceptance laid on the utilization of the high-grade heat sink for industrial, cogeneration and urban district heating. The closed-cycle gas turbine which allows for a wide range of heat sources was utilized in both fossil-fired and nuclear sources for the land-based application. Typical examples of this application are the closed-cycle gas turbine plants built in Germany; the 2MWe Ravensburg plant, the cogeneration plant in Gelsenkirchen which supplied the steel mill with 17.25MW power and a heating power of 29MW, to the Oberhausen I and II 50 MWe plant which has been described extensively in [2,4,14,18,43–45] and in Fig 2-5. Other Land-

based application built include the Coburg and Haus Aden plants in Germany, Toyotomi plant in Japan, the Kashira 12MW plant in Russia with district heating and the Nippon Kokan plant in Japan.

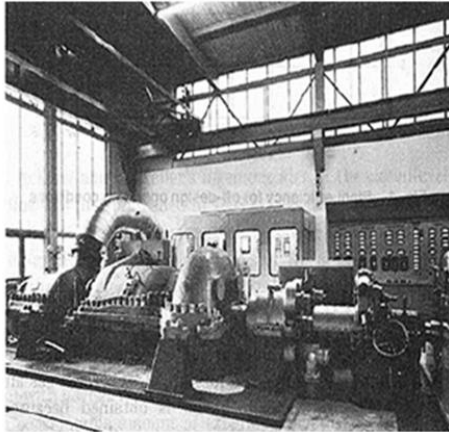


Figure I: 6.6MWe Power Station at Coburg, Germany

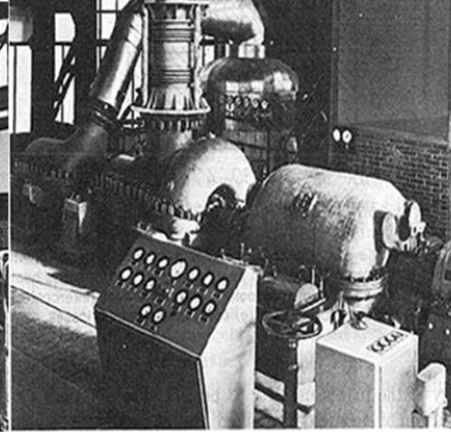


Figure II : 6.4MWe Power Station at Haus Aden, Germany

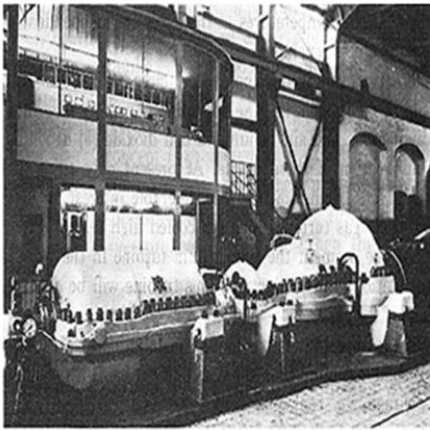


Figure III: 13.75MWe Power Station at Oberhausen, Germany

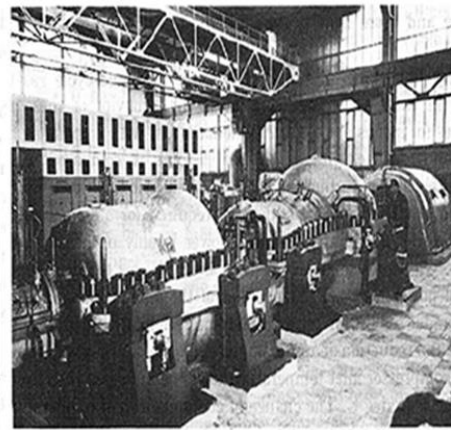


Figure IV: 17.7MWe Power Station at Geisenk, Germany

Figure 2-6 Land-based Application of closed-cycle gas turbine

As reported in reference [51], the closed-cycle gas turbine now has a growing interest in the field of Liquefied Natural Gas (LNG) vaporization with the potential yielding efficiency of 58 percent and overall plant efficiency of 80 percent. As a result of a constant increase in the demand for LNG, there has been renewed interest for improved technique in liquefaction and regasification of the LNG by utilizing the closed-cycle gas turbine thermodynamic potential for simultaneous power generation without affecting the environment. This concept

is to utilize the heat sink from the closed-cycle gas turbine for regasification and, at the same time, to take advantage of the low LNG temperature for cooling the closed-cycle working fluid before compression. This leads to an appreciable increase in the available gas turbine output and of the plant efficiency, thereby reducing the overall operating cost.

2.3.1.2 Aerospace application

In the 1950s, a program for Aircraft Nuclear Propulsion (ANP) was initiated by the Atomic Energy Commission in the US to redesign B-36 which was later renamed NB-36 [18,52,53]. By 1960s progressed was made with both direct and indirect closed-cycle engines tested, using air as working fluid [52].



Figure 2-7 General Electric HTRE3 and HTRE1 (Nuclear Powered airplane engines) at the Idaho National Laboratory in Arco, Idaho [52]



Figure 2-8 Tupolev Tu-95LAL nuclear test-bed airplane [54]

Similarly, after extensive experimentation with different engines and transfer systems, the Soviet Engineers developed the Tu-95LAL and 34 more research flights completed between the 1950s and 1960s using the closed-cycle gas turbine technology [54]. Feasibility studies using closed-cycle gas turbine engine for unmanned aircraft has been documented [55]; the study evaluated the benefit of the closed-cycle gas turbine at high altitude performance, operation in polluted air environment using generic thermal heat sources.

The high power conversion efficiencies and power to weight ratio provided by the closed-cycle gas turbine has demonstrated renewed interest in adapting the system for space power application. It allows for suitability of the system to a wide variety of missions like lunar, deep space and earth orbit missions. These missions applicability can be adapted from a wide range of heat sources (radioisotope, nuclear, solar). The NASA-Lewis Research Centre developed a radioisotope closed-cycle gas turbine power generation unit in the 1960s which achieved an output power between 2 KW and 10 KW [56,57]. Similarly, the NASA Space Station Freedom selected a solar-powered CBC for space power system application.

Several researches and development programs have been deployed to show the technology readiness of the closed-cycle gas turbine in aerospace application [53,55,58].

2.3.1.3 Marine application

Over the last few years, there has been appreciable interest in the closed-cycle gas turbine for marine propulsion because of its excellent part-load efficiency [24,42]. In 1961, Mitsui Shipbuilding in Tamano, Japan built an experimental fast attack boat for the Navy, using air as working fluid, turbine inlet temperature of 998K and cycle efficiency of 27.0 percent was achieved [2]. Although the IN-10 ship propulsion turbine did not progress beyond the test operation, however, the concept was used for a small laboratory engine of 30 KW using argon as working fluid, built and tested with a resistance type electric heater energy source and turbine inlet temperature of 1144K [41,59]. Analytical studies on performance improvement potentials of this engine have been performed [60].

Between 1958 and 1962, the concept was developed for Maritime Gas-Cooled Reactor (MGCR) with a closed-cycle nuclear propulsion system, which delivered 15MWe. The power cycle comprised of a beryllium-oxide, helium-cooled reactor which was coupled to a closed-cycle gas turbine [61]. Current researches in marine propulsion are focused on implementation of lighter closed-cycle gas turbine propulsion systems that will improve strategic and tactical operational capabilities as a result of increased speed, endurance time, increased payload or reduction in ship size and cost [24]. Relevant experiences in closed-cycle gas turbine design have also been applied to a range of the unmanned underwater vehicle by Allied-Signal CBC Company in the US [42,62,63].

2.4 Niche Market Potentials

It is almost certain that the closed-cycle gas turbine technology will reappear as a viable option in power generation. The closed cycle gas turbine has great market potentials for utilizing coal, biomass and waste oils for remote on-site power generation and space heating/cooling; which may provide for potential economic gains not available with current technologies. Some of these potentials will create the market niche for the closed-cycle gas turbine in the future, which are discussed as follows:

2.4.1 Working Fluid Potentials

The freedom to choose which working fluid essentially suits one's design makes the closed-cycle gas turbine a desirable energy conversion system. This is because it gives the designer the freedom to select fluid that enables compact design, affordable and efficient in terms of cycle performance. From the viewpoint of thermodynamic performance, all permanent gases can be utilized for closed-cycle gas turbine working fluids; however, considerations on thermal stability, inflammability, chemical inertness, and toxicity are important in selecting a suitable fluid for the system. The fluid will be operated in the gaseous region beyond its critical temperature all through the cycle. Among these gases, air has been the most common working fluid utilized in land-based closed-cycle gas turbine power plants, whereas for closed-cycle gas turbine space power

applications, where weight and size are important, monatomic gases like helium, argon, and mixtures of helium and xenon can be utilized [36,64,65]. For a nuclear heat source, helium and carbon dioxide have been successfully implemented in past for reactor cooling and steam generation [2].

Considerations on the compatibility of the working fluid with the material used in closed-cycle gas turbine construction, particularly the heat exchangers, are important in the selection of the working fluid. Other working fluids that have been used in the past include air, carbon-dioxide, nitrogen, argon, and mixtures of gases.

2.4.2 Heat Source Alternative

As previously highlighted and listed in Fig 2-2, the closed-cycle gas turbine offers appreciable heat source flexibility and adaptability, which include: Fossil-fired, Nuclear, Solar and Stored Thermal Energy. Salient characteristics of these heat sources are discussed as follow:

2.4.2.1 Fossil-fired heat source

Fossil-Fired closed-cycle gas turbine has been extensively demonstrated in Europe, especially the use of dirty (coal, peat, lignite, etc.) fuels. Experiences from these plants have been based on burning pulverized solid fuels and there are appreciable statistics of gas heaters designed for this purpose [39]. Evaluations on the pulverized fossil-fired system with the aim of comparing predicted and actual operating life of the plant has continued with growing interest. In the US, development strides to increase the turbine inlet temperature above 1000K, by utilizing ceramic heat exchangers, plant operation in cogeneration mode and meeting the environmental standard is at its advance phase.

In recent years, research has been directed towards fluidized bed, coal-fired closed-cycle gas turbine system embodying both metallic and ceramic in-bed heat exchangers [14,38,39], like the large Atmospheric Fluidized Bed (AFB) combustor and gas heater developed by Rocketdyne Division of Rockwell International, and other activities are underway in support of future fossil-fired

closed-cycle gas turbine plant. In the fluidized bed combustion process, coal is burned in a bed of limestone, which reacts with the sulphur dioxide released from the coal to form calcium sulphate. At temperatures between 1000K and 1300K, the limestone sorbent in the bed will capture a major portion of the objectionable atmospheric pollutants, which are removed as dry granular solid and easily handled for disposal.

Apart from coal and other dirty fossil fuels, high-cost clean fuels like gas and oil have been also used to fire closed-cycle gas turbine plants. Examples of plants in operation with fossil-fired include Oberhausen I and II in Germany which is fired with coke-oven gas, the Altnabreac plant in the UK fired with peat, the Toyotomi plant in Japan fired with natural gas as listed in Fig. 2-5

2.4.2.2 The nuclear-powered heat source

In retrospect of the development of nuclear reactors for energy conversion, especially using gaseous coolant, from a gas cooled reactor had appeared interesting to any engineers. Together with growing development in the closed-cycle gas turbine, the elimination or substitution of the fossil-fired heat exchanger which was structurally and metallurgical limited in its maximum cycle temperature became necessary with the advent of a high-temperature gas cooled reactor core. This new interaction has enabled the full potential of the closed-cycle gas turbine to be realized. Although gas cooled reactors were developed for use with steam turbine conversion systems, but the potential benefits for the closed-cycle gas turbine driven by reactor coolant became attractive; direct power conversion from single-cycle system afforded better improvements in the plant size, capital cost, efficiency and waste rejection compared to a steam power system. This was made possible due to direct expansion of the high-temperature reactor core coolant and the high-temperature graphite reactor core which did not impose metallurgical limitations on maximum cycle temperature above 1000K.

As the design and research on High-Temperature Gas Reactor (HTGR) progressed in the 1970s, especially by GA Technology (formerly General Atomic Company), the plant configurations and thermodynamic cycle translated

from investigating the best means to satisfying the various economic, performance, safety and operational goals. Plant sizes ranging from 800MW to 1200MW was conceived and extensively studied by GA Technology in the US, and a similar program established by European High-Temperature Helium Turbine (HHT) project documented in [3,28,66,67]. In the late 1970s, a reference plant design was established, without intercoolers, 1130K turbine inlet temperature and with dry cooling [67].

The development of power-producing fusion reactors is at a point where the emphasis is being placed on technology and engineering designs. A prime mover which seems well suited to coupling with a fusion reactor is the closed-cycle gas turbine, and various studies have been performed. Thermonuclear fusion reactors offer the promise of virtually unlimited energy source. Deuterium, the basic fuel for fusion reactors, is plentiful to supply world's energy needs for one billion years at present rate of consumption. It is projected that the coupling of a closed-cycle gas turbine to a fusion reactor represents perhaps the most exciting and challenging task for gas turbine engineers in the 21st century, and indeed may well be regarded as the ultimate application of the gas turbine.

2.4.2.3 Solar powered and Thermal Storage

Solar energy has always been known as an inexhaustible heat source but was ignored in the last century in favour of fossil fuels which were readily available at low cost and convenient use. As evidenced in several publications [68–70], the analysis and design of the solar energy systems are hinged on established engineering knowledge. Hence, there is appreciable interest in its utilization for solar-powered closed-cycle gas turbine conversion systems. This concept presumes to utilize the intensity of solar radiation during the adequate period of sunshine. However, areas with optimal insolation characteristics are usually arid and lack adequate water supply, which makes it essential to provide closed-cycle gas turbine power plant designs with dry cooling.

The philosophy of this technology is to position the closed-cycle gas turbine at the focal point of a parabolic dish concentrator, with the heat receiver, turbo-

generator set, and heat exchangers housed, to avoid a shadowing effect [38]. The receiver captures the solar radiation energy and transfers it to the gaseous working fluid and the energy contained in the working fluid is transported via pipelines to the closed-cycle gas turbine conversion assembly unit. However, to provide a continuous supply of electrical power and heat, it is important to create an alternative heat source for the closed-cycle gas turbine for times when the sun is not shining as described in [14] and presented in Fig 2-8

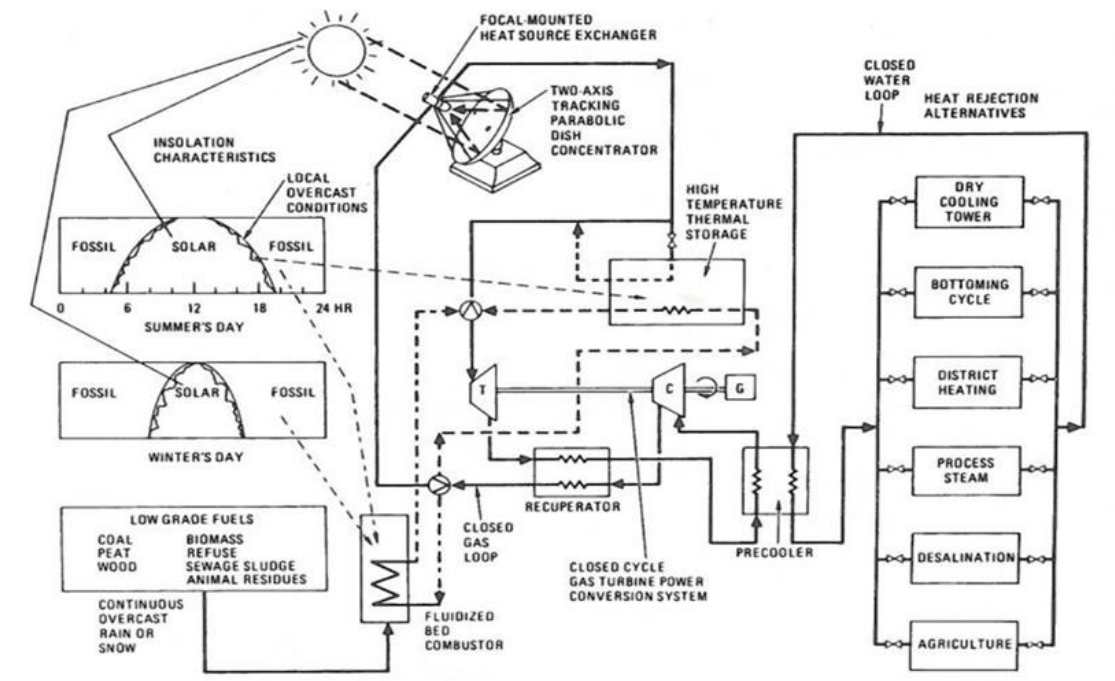


Figure 2-9 Conceptual solar powered closed-cycle gas turbine cogeneration [14]

During conditions of local overcast, the closed-cycle gas turbine would operate with a high-temperature thermal storage system together with an inventory control. However, when there is inadequate solar radiation, fossil-fired with external combustion can be utilized as shown in the conceptual design above. Several research in solar-powered closed-cycle gas turbine has been documented in [53,69–71].

2.4.3 Energy Utilization Potentials

Energy utilization focuses on technologies that can lead to new and potentially more efficient ways of maximizing the total energy content from a given unit of “energy carrier”. Hence, the closed-cycle gas turbine has good potentials of

utilizing its waste heat energy for other applications as highlighted in Fig 2-2. Of interest today is the process of cogeneration in which the supply process heat and the generation of electricity are combined in an integrated mode. According to reference [14], the intrinsic economic worth of any power plant will be assessed based on the usage of its multiple heat rejection which is too valuable to be discharged to the environment. This puts the closed-cycle gas turbine as a viable option for total energy utilization potentials. Heat is removed from the closed-cycle gas turbine process using the pre-cooler and compressor intercoolers. There are several possibilities for direct utilization of heat from the closed-cycle gas turbine plant. The following heat rejection alternatives have been employed in most closed-cycle gas turbines in operation today.

2.4.3.1 District Heating and Process steam supply

The flexibility with regard to combined electrical and heat production is an important feature of the closed-cycle gas turbine technology that may not have been fully appreciated by many. The closed-cycle gas turbine advantage is that its high water rejects temperature could allow air to be heated at the end-user point [14,36,38]. The upper-temperature range of the working medium in the coolers can be easily used for providing heating energy. The 50MW Oberhausen II helium turbine plant in Germany has thermal heat rejected of 54MW used for combined power and district heating plant [14].

In reference [72], the author identified that raising the compressor inlet temperature by throttling the cooling water evidently increases the amount of waste heat which can be used for district heating. This method has been used most often in cogeneration plants. This is in contrast to a steam turbine plant that requires steam extraction for water heating or back pressuring, with a significant penalty paid in the electrical output.

The closed-cycle gas turbine exhibits attractive high power-to-heat ratios, hence, has great potentials for process steam supply. Process steam which is typically used at 450K can be generated from heat leaving the closed-cycle gas turbine with the electrical output, cycle efficiency and power cost from the plant not essentially affected by the process steam generation [2,72,73]. From the

study of reference [73], the cogeneration capacity for an advanced 1000MW nuclear powered closed-cycle gas turbine shows that the steam generation envelop is dependent on the reactor outlet temperature and by the turbine extraction requirements which occurs at the upstream of the high-pressure turbine.

2.4.3.2 Desalination

Access to clean water is essential for a living but approximately 20% of the world's population, lack safe drinking water and unfortunately, 94% of the world's water is salt water [1]. In this regard, the development and use of water desalination technology are essential. Desalination of water requires a heat source, but the energy required can be achieved at relatively low temperatures. Waste heat from power plants is sufficient for this purpose and the closed-cycle gas turbine has the potential to plug that need, particularly in a dual capacity by providing water in addition to greenhouse-gas-free energy. Preliminary studies for a nuclear closed-cycle gas turbine coupled to a desalination plant have been performed by reference [74]. The studies showed that the temperature required for desalination is at 400K, which can be easily met by the pre-cooler of the closed-cycle gas turbine plant without interfering with the cycle performance. However, reference [14] identified that the desalination process may require minor modifications in the basic multistage-flash-evaporation.

2.4.3.3 Bottoming Rankine Cycles

In bottoming cycle, the heat removed in the pre-cooler can be dissipated to the environment in a dry cooling tower, which can be used for further generation in a secondary or binary cycle. The closed-cycle gas turbine also has the potential of operating with a bottoming Rankine cycle with a high thermodynamic efficiency of over 50%. In the work of reference [75], a coal-fired cogeneration was studied for potential ethyl production. Other researches documented on closed-cycle gas turbine coupled with a bottoming cycle is documented in references [2,14].

2.5 Summary of R&D Programmes

In the last two decades, there has been growing efforts in research and development of closed-cycle gas turbine technology design and operations which has led to various pilot component designs, performance testing, and feasibility demonstration of different working fluid for the closed-cycle gas turbine. This section provides an updated review of research and development within the last two decades, on the use of different working fluids for the closed-cycle gas turbine. It also provides an overview of literature modelling and simulation studies as well as tools employed for closed-cycle gas turbine steady-state thermodynamic analysis. This review sets the foundation for the knowledge gap which this thesis seeks to address.

2.5.1 Advances in working fluid studies and component design

As previously mentioned, the closed-cycle gas turbine working fluids commonly employed include the monoatomic inert gases and mixtures thereof, as well as air and nitrogen. Thus, many studies have been carried out exploring the potentials of helium and helium mixtures. El-Genk and Tournier [33] analyzed the cycle thermodynamic performance and turbomachinery design of helium and its binary mixtures such as helium-xenon, and helium-nitrogen for a very high-temperature gas reactor plant coupled with the closed-cycle gas turbine. The study showed that cycle with pure helium have better cycle performance, however, the use of binary mixtures have a significant impact on the turbomachinery design in terms number of stages and length of the shaft. In another analysis, El-Genk and Tournier [12] investigated the effect of helium and its mixtures on the turbomachinery shaft speed and size. In the work of Gronchiwa [76], cycle performance was compared for helium and supercritical carbon dioxide using different cycle configuration for a generation IV nuclear power plant. Similarly, Wang and Gu [9] presented a comparative study of helium, nitrogen, and air for a high-temperature gas reactor and the results showed variation in cycle performance for the different fluid with helium have more favourable outcome. Najjar and Zammout [77] also carried out a comparative study of combustion gases, helium, and air for a recuperated

closed-cycle gas turbine. Lee et al., [64] analysed the effect of thermodynamic and transport properties of different gases at fixed pressure ratio factor, for optimum selection of a coal-fired closed-cycle gas turbine design.

For fluid like carbon dioxide, Kato et al [78] presented a performance and design analysis for medium temperature carbon dioxide gas turbine reactor, comparing the influence of intercoolers on the cycle performance for a nuclear reactor. Olumayegun et al. [32] presented a preliminary study of nitrogen cycle performance and component design for a sodium fast reactor comparing the single and dual shaft arrangements. Ulizar and Pilidis [79], described the possibility of handling a closed-cycle gas turbine with carbon dioxide and argon. Alpy et al [80] compared gas testing for nitrogen and carbon dioxide in a closed-cycle gas turbine component design prototype. Other researches that have explored several options of working fluid for closed cycle gas turbine technology are documented in references [8,28,81].

2.5.2 Modelling and Simulation studies for Closed-cycle with different fluid

A great deal of research work has been expended to develop analytical tools capable of evaluating the steady-state performance, dynamic performance, and control system of closed-cycle gas turbine engines. Broadly speaking, a review of the available simulations model; both analog and non-linear digital have been discussed by [4,82–85]. Vavra [86] described a method that graphically illustrated the fundamentals of matching components in the closed-cycle gas turbine. The investigations of Dostal [13] and Dyreby [49] also covers various aspects of simulations programs with S-CO₂ cycles. Their approach essentially consisted of synthesizing the thermodynamic-relationships that described each engine component. Dynamic equations describing the transient behaviour of GT-HTGR have been documented in Badia [87] and Yan [46]. Dupont et al., [88] described a computer code called Tugsim-10 developed for transient simulation of nuclear plants.

Sanchez et al. [89] presented a performance model comparing supercritical carbon dioxide closed cycle gas turbine with a hybrid system using air in open

cycle arrangement. The modelling technique and results presented using a molten carbonated fuel cell and coal-fired Brayton cycle show that the supercritical carbon dioxide bottoming cycle has a very high potential as an efficient power generator for hybrid systems. Reference [90] developed the gas plant analyser and system simulator for hydrogen for dynamic modelling of gas cooled reactors. Also, reference [90], compared RELP5 and Aspen Custom Modeller (ACM) modelling of load rejection and part-load transient of the ACACIA plant.

The review by [4] covers various aspects of simulations for closed-cycle gas turbines. However, most of the documented models in open literature [91–95] were developed mainly for open-cycle gas turbine operations and specific closed-cycle projects which are not accessible for commercial use.

2.6 Setbacks and Future Prospects

Despite the advantages and initial successes by the early pioneers, the closed-cycle gas turbine plant has not penetrated the market as expected. Some of the diffidence exploring this technology is related to the higher capital cost, material limitations for high temperature and high-pressure applications, lack of sufficient turbomachinery design experience for different working fluids, bearings, seals, heat exchanger designs and perhaps unfamiliarity with the utilities with a seemingly non-steam system.

A review of the current research and development programme shows that for full-scale commercial deployment of the closed-cycle gas turbine to be realised, there is need to address some of the featured gaps or challenges highlighted through continuous research in this field. Summarising these gaps is as follows:

2.6.1 Explore working fluid options for different heat source application and economic assessment

A lot has been done on fluids like helium and there are growing numbers of researches for carbon dioxide as working fluid as observed in literature reviewed. However, more fluid options such as nitrogen, xenon, and mixture gases need to be explored in terms of cycle performance, component design

and compatibility with heat source options especially solar, fusion reactors and thermal storages. Apart from the performance or design viewpoint, an economic and risk assessment comparing various fluid options in terms of cost is another area that could give value to investment in closed-cycle gas turbine technology.

2.6.2 The need for a robust simulation and demonstration plant

Before design, manufacture and commercial deployment, of the closed-cycle gas turbine, a lot of variables have to be proven and these can be largely addressed using computer simulation and demonstration tools. Computer simulations tool has become increasingly important in all aspects of the closed-cycle gas turbine design process. As modelling techniques have improved, and as computers have progressed, simulations have assumed an essential role in planning, executing and evaluation operations, to reduce acquisition costs, increase system performance and improve maintenance. The demonstration of plant performance or component capability will enable the verification of the system performance and component integrity for any production process to be done.

From the brief review of the published work cited here. It would appear that the modelling tools mentioned above were mostly developed for specific closed-cycle projects, design-point analysis with specific fluid type and applications, which are not made available for commercial use in research and development. Hence, there is still need for a general model that may be used to represent different closed-cycle engine configurations, different working fluid capability and to study particularly at the conceptual design stage, the effect of component performance on the overall performance of the engine, independent control system of closed-cycle gas turbine and scaling approach for turbomachinery maps from one fluid to another

2.6.3 Turbomachinery and heat exchanger design and performance analysis

There is still a gap in research and development of the aerodynamic design for compressor and turbine using fluid options other than air. This has been

identified as one of the main setbacks in closed-cycle gas turbine technology. Nowadays, where sophisticated computer software is available, it should become a lot easier to explore different turbomachinery design models for different working fluids. Also, further analysis of high-temperature materials for heat exchanger design needs to be explored as identified in the literature reviews. The maximum theoretical temperature for closed-cycle gas turbine heat exchanger is currently at 1123K.

2.6.4 Future prospect

With increasing attention being given to Green-House Gases (GHG) emission as a result of fossil fuels for international air and marine transport, and the excellent safety record of closed-cycle gas turbine powered generation, the use of the closed-cycle system will increase due to the requirement of meeting the tightened regulations on environmental emission reduction. This will lead to:

- A rethinking of the public heating system using more total energy plants, thereby utilizing the energy source by over 75 percent.
- There will be a speed-up in the introduction of helium turbine coupled in a closed-cycle with gas cooled, high-temperature reactors.
- Improvement in material technology for a potential increase in the turbine entry temperature, thereby increasing the closed-cycle performance.
- With the availability of advance numerical computational tools, improved design of the heat exchangers and turbomachinery aerodynamics will put the closed-cycle gas turbine technology as a viable option for energy conversion now and in the future.

2.7 Knowledge Gap and Research Novelty

The knowledge gathered from the various literature reviewed has shown that the application of the closed-cycle gas turbine technology and its features cannot be achieved without proven trade-offs of design variables and economic merit, which has to be optimized by careful analysis before investment decisions can be made. **The** viability of the closed-cycle gas turbine for the application proposed in this research is hinged on selecting the appropriate

working fluid, operating and design conditions which satisfy external regulatory constraints, high cycle performance, investment cost and return on investment. For this to be achieved, a robust simulation tool with various capabilities for different research study needs to be developed.

Therefore, the contribution to knowledge of this research is to develop a techno-economic, and risk analysis model for closed-cycle gas turbine technology, comparing the influence of the thermodynamic and transport properties of air, helium, carbon dioxide and nitrogen as working fluid on the cycle performance and components design. This is aimed at supporting investment decision on any proposed closed-cycle gas turbine system for sustainable energy conversion.

TERA approach which is described as Techno-economic, Environmental and Risk Analysis framework were used in this research to exploit the potential technology design solutions for closed-cycle gas turbine technology for different working fluid options. In this way, an optimum solution can be selected with a reduced error in the decision-making process.

2.8 The TERA Approach and Application

Engineering design requires a great deal of compromise to arrive at an optimum characteristic selection. Hence, it is important to develop a tool that can enable one to make adequate comparisons which are critical to decision making. The concept of TERA is a Techno-economic, Environmental and Risk Analysis framework used to exploit potential technology design solutions of an engineering problem, thereby reducing computational time and costs. In this way, an optimum solution can be selected with a reduced error in the decision-making process. It can be used as an appraisal and optimization technique applied to any mechanical system with a set of objective functions and can provide the specific insight necessary for preliminary design decisions [96].

Kyprianidis et al. [97] precisely described TERA as “an adaptable decision making a support system for preliminary analysis of complex mechanical systems”. He further argued, “A TERA approach during the preliminary design

process of complex mechanical systems will soon become the only affordable, and hence, feasible way of producing optimized and sound designs if the whole spectrum of possible impacts is to be taken into account". TERA has also been defined by others as a multi-disciplinary technique for engine asset management and modeling of gas turbines [96,98–102].

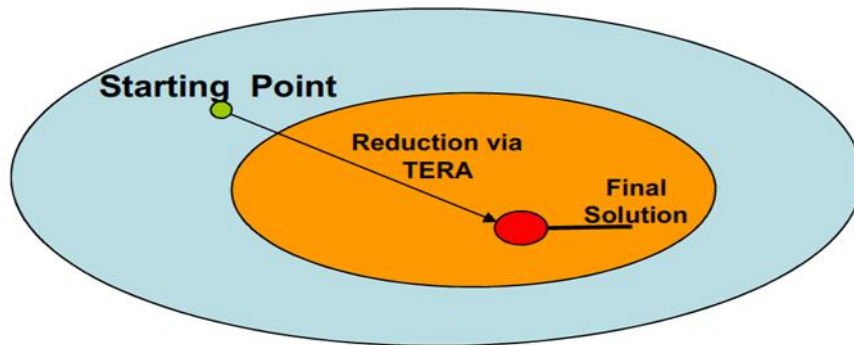


Figure 2-10 Simplified Aim of TERA

Whellens and Singh described how TERA method can be used for modelling design process to make traditional decision procedure easier [96,99]. The different modules that makeup TERA have extensively documented by [102]. The author presented architecture of performance, emissions, risk and economic module from which this research an upshot application. Vicente and Gayraud were among the pioneer conception of TERA tool at Cranfield University for aircraft and industrial applications respectively [101,103].

TERA has been successfully applied to several engineering design concept applicable in aviation, Industrial and marine operation. The philosophy of TERA was developed in Cranfield University for selection of gas turbines in the aviation industry, which was later supported by EU to significantly reduce aircraft noise, emissions and fuel consumption in a project called VITAL. While Vicente pioneered the aviation application, Gayraud used this tool for selection of industrial gas turbines.

Subsequently, this tool has been used in the marine application through the Advanced Marine Electric Propulsion Systems (AMEPS) project [98,104]. Other

areas where TERA have been applied are documented in [47,96–100,102–104].

2.9 Chapter Conclusion

A state-of-the-art review of closed-cycle gas turbine technology and research work carried out so far is provided in this chapter. These include its historical development, major concepts and features of the closed-cycle gas turbine plant, and important research and development. Based on the reviews and previous operating experiences, the challenges that have hindered its large-scale deployment and the future prospect of the closed-cycle gas turbine was also presented. This review set the background for the present gap which this research contribution was defined.

In general, it can be concluded that the closed-cycle gas turbine has the potential for improved efficiency of electricity generation, compact and simple design, and reduced emissions and therefore could complement conventional power generation plants.

3 RESEARCH METHODOLOGY

3.1 Background

This chapter describes the overall methodology used in this study to analyse the effect of selected working fluids on closed-cycle gas turbine technology and economic assessment.

The TERA approach is used in this research as a multidisciplinary framework for strategic decision making in closed-cycle gas turbine technology investments. TERA is a conceptual model used to assess gas turbine engines with minimum impact on the environment and lowest cost of ownership. This model has been applied to different areas of gas turbine technology. The governing principles of TERA arise from different module integration, which allows for design considerations and/or operating areas such as performance assessment, environmental assessment, economics and risk analysis.

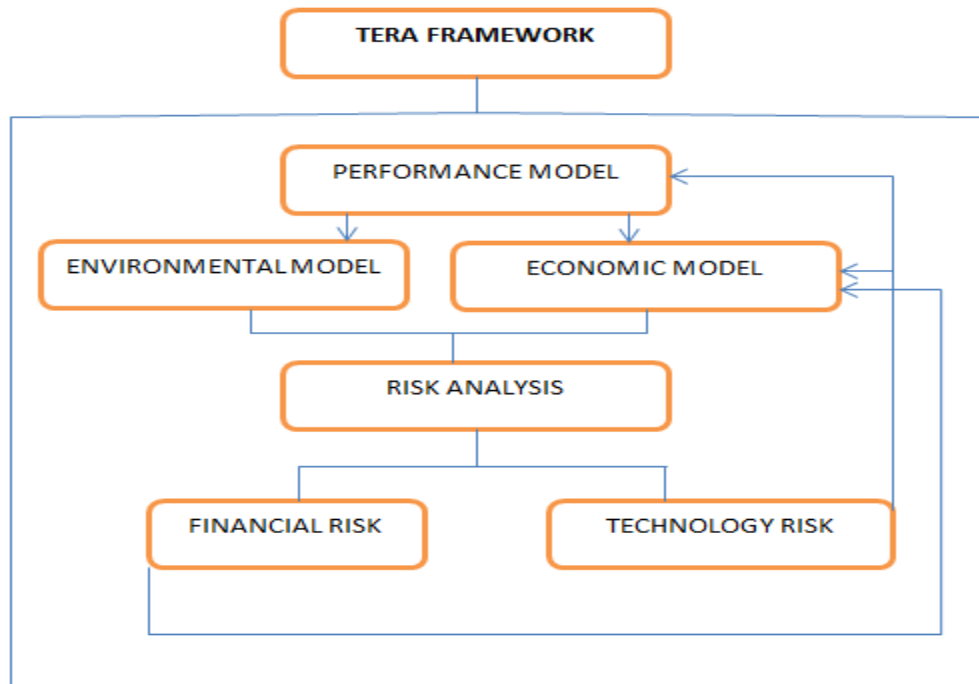


Figure 3-1 Basic architecture of TERA

Fig 3-1 represents the basic concept of TERA upon which the decision making procedure for the closed-cycle gas turbine power plant can be evaluated. The framework starts with the thermodynamic performance model of the power plant in a wide range of operating conditions

The performance model at a wide range of operating conditions facilitates a transparent and consistent performance comparison of the proposed closed-cycle gas turbine technology. Performance analysis only is not enough to justify the viability of any technology including the closed-cycle gas turbine, hence, further analysis modules are required, such as environmental, and economics as shown in figure 3-1. This is done to give quantifying indices and an indication of the attractiveness of the proposed technology investment. The quantifying indicators for these models include Pay-Back Period (PBP), Net Present Value (NPV) and level of impact to the environment.

Subsequently, risk analysis is needed to identify the challenges and risk emanating from each technology scenario. The risk can be analyzed as either a technological risk or financial risk. The aim is to assess the impact of changes in the system component details and cost of decision making. Finally, a techno-economic optimization may also be included in the TERA approach find to give an optimum solution to the research goal.

3.2 The justification for TERA Approach

Life cycle analysis has been notably used for assessment of new or existing technology. This also involves using different tools to analyse the impact of a technology on the environment and the cost implication of manufacture. Also, a similar concept to TERA called Environmental Design Space (EDS) has been independently developed in the USA by the FAA, Georgia Institute of Technology and Michigan Institute of Technology [105,106]. The model was designed to assess performance, noise, and emission of different engine configurations, taking into account the different economic and policy scenarios.

However, TERA has been widely used in Cranfield University because of the existing tools which can be easily used by the researcher to achieve the

different modules in TERA. For example the performance simulation tool, economic model tool, emission prediction tool, component sizing tool and other useful tools one can easily use as a reference to their models.

3.3 TERA for Closed-Cycle Gas Turbine Technology

The development of a quick and robust decision support framework for closed-cycle gas turbine technology is a difficult and time-consuming task, of which this research work can be considered as a first step, especially within the time frame of this report. However, reflecting on the basic multidisciplinary architecture of TERA presented in Fig 3-1 and exploded in Fig 3-2, the process of implementing the methodology proposed for the effect of different working fluid thermodynamic properties on the closed-cycle gas turbine technology is organized in the following serial connection modules:

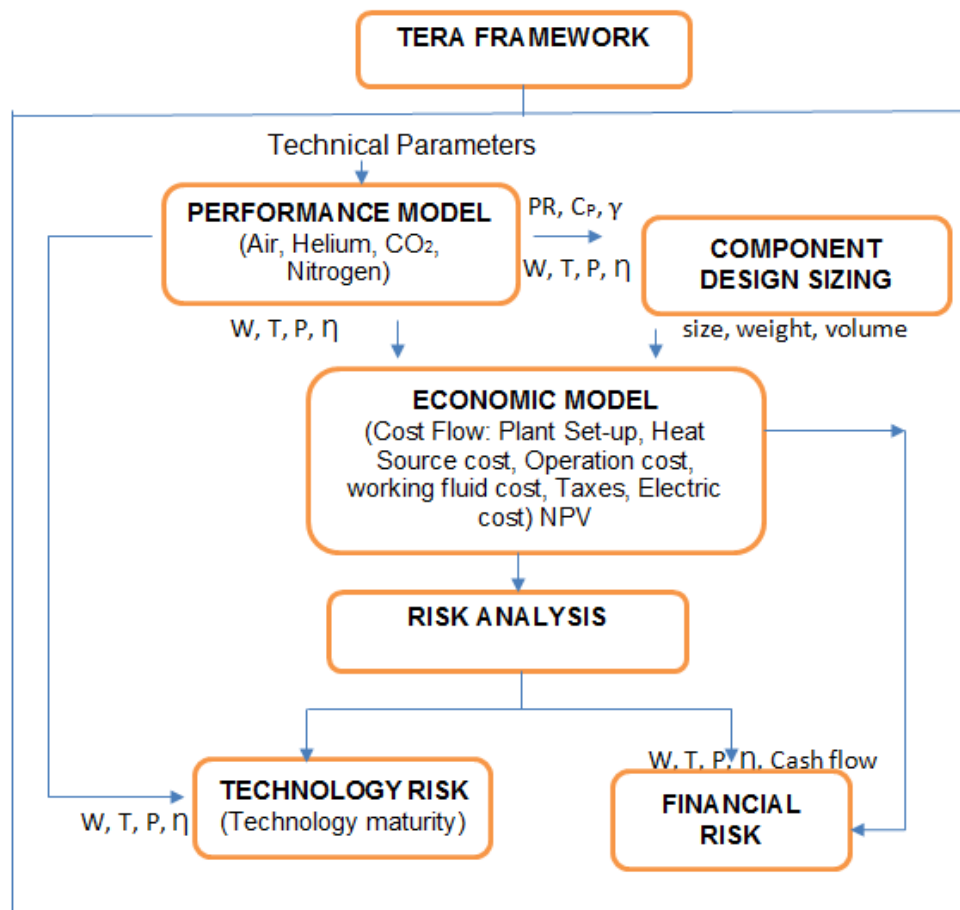


Figure 3-2 TERA framework for closed-cycle gas turbine technology

3.3.1 Performance Module

The performance model forms a fundamental part of the TERA and this research. The basic structure of the performance module to be implemented is presented in Fig 3-3. The performance module is used to assess the closed-cycle power plant performance. This module is used to develop the general mathematical thermodynamic characteristics of the closed-cycle gas turbine components at different cycle configuration, working fluid, heat source and operating conditions. The essence of this module is to help create an understanding of the phenomena observed in a real system and to allow for assessment of the plant behaviour at different conditions. The result from this module is used as input characteristics for the other modules. An important of the performance is the modelling the selected working fluid (air, helium, nitrogen, carbon dioxide) as real gas especially carbon dioxide which is greatly influenced by changes in temperature and pressure. Also, the module is developed for different cycle configuration studies, control option studies and component effects and large variation of operating conditions.

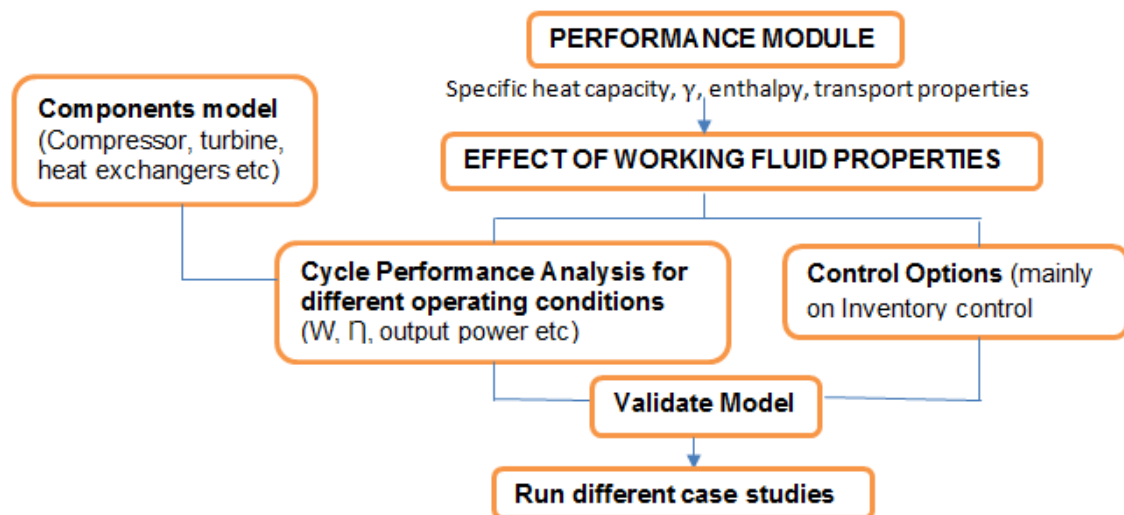


Figure 3-3 Structure of Performance Model

To achieve the aim of the module, the author developed a simulation tool called GT-ACYSS which is designed to meet various simulations needs for this study. The development of this tool is one of the novelties of this research. A detailed description of the tool is described in the next chapter. From Fig 3-3, the model

is validated using existing closed-cycle power plant data available in the literature. The fluid properties were also validated similar to the cycle performance and control option studies.

3.3.2 Component Design and Sizing Model

An important step in the TERA framework is a way to analyze the effect of the selected working fluids on the overall size and weight of the power plant. The results from the performance module are fed onto the component design and sizing module. This module is developed to perform preliminary component design and sizing for the main components of the closed-cycle gas turbine such as the compressor, turbine, heat exchangers, and inventory control system. The model developed for this operation uses the different fluid properties to compute the component design and sizing.

Several methods are available that aim to predict the layout and overall sizing of the engine, however, for the turbomachinery components, Sargerser et al's [107] method was used to determine the overall length of the turbo-set. This method was adapted from an aircraft application to give a preliminary assessment of the turbo-sets. A detailed description of each component design and sizing is described in chapter five. Figure 3-4 gives an overview of the basic concept of the model.

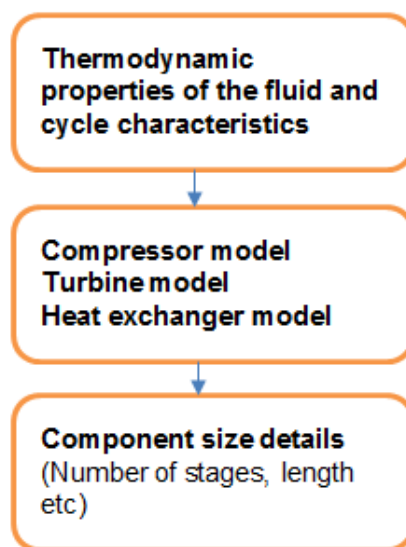


Figure 3-4 Flow process for component design and sizing module

3.3.3 Economic Module

Making the decision for an investment comprises different criteria, one of which is hinged on the profits generated at the end of the project. Therefore, economic evaluations provide useful information for making quality investment decisions, with the ultimate purpose of ensuring that the expected future returns would justify the initial investment cost. However, the main objective of this module is to access the initial capital cost of the closed-cycle gas turbine plant based on the effect of the selected working fluids properties on the component size. This module is used to access the economic attractiveness of the proposed closed-cycle gas turbine power plant in terms of cost. A structure of the economic model is shown in Fig 3-5.

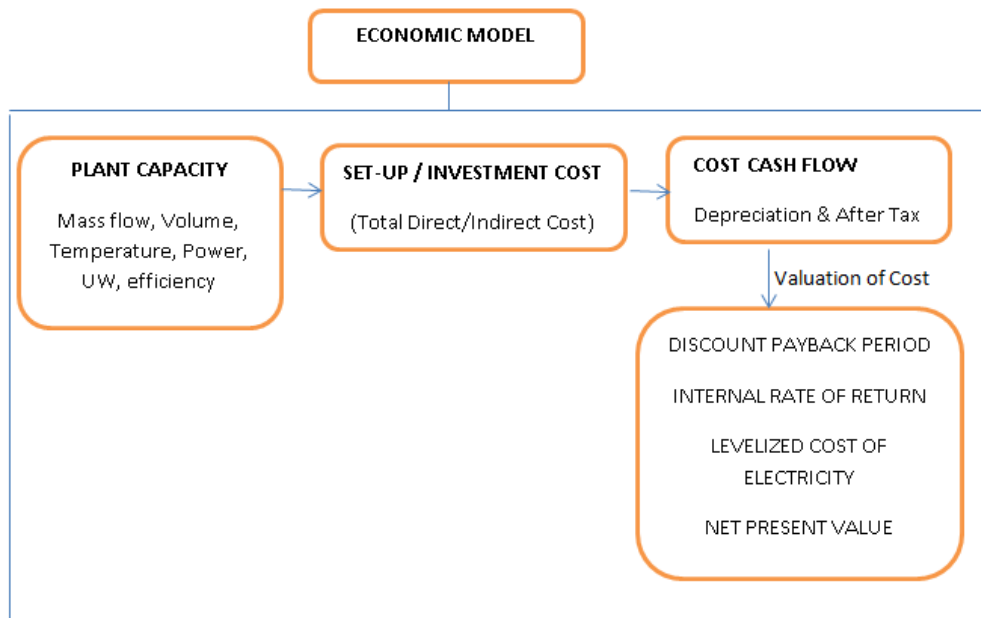


Figure 3-5 Structure of economic Model

The bottom-to-top approach is used in this research to analyze the cost of the plant. This approach estimates the overall cost of a system based on the aggregate cost of its components. Details from the result of the performance module like, efficiency, output power, heat source, plant components and working fluid management are plug into this module for analysis. This is achieved by modifying some existing FORTRAN programs to calculate the cost cash flow of plant setup, fuel, working fluid management and operations. The

study uses the economic performance indicators such as the net present value, internal rate of return, discounted pay-back period and levelised cost of electricity to measure the economic performance of the various working fluid effect used. The sets of equations used in the economic analysis for this research is discussed in chapter six.

3.3.4 Risk Analysis Module

This module provides an assessment of the uncertainties and operational challenges that may be associated with the implementation of the closed-cycle gas turbine technology. Most significantly, risk module is a representative of the plant performance, in that there is a trade-off on the thermodynamic performance characteristics of the plant. This module will focus on technology risk which aims at characterizing the impact that technology maturity of the system component, will have on the plant performance and the cost sensitivity of the system component, which will be used as a measure of analyzing the financial risk involved. An overview of the structure of risk analysis model is presented in chapter seven. Each block is defined as an integrated unit based on input values from the performance, component design, and economic model results.

3.3.5 Model Limitations and Potential Improvements

The models presented so far has the capability to predict to the cycle performance and component design assessment to reasonable level of accuracy based on assumptions made. For the component sizing, comprehensive losses model was not considered and the results were based on the preliminary component design to give a quick solution of the model objective. For the performance model, the properties of the cooling medium were assumed (for example the type of cooling medium – air or water, the temperature of the cooling medium). Also, several other assumptions have been used to carry out calculations or analysis of each module in the TERA framework, which are described in chapter four, five, six, and seven. Some of the assumptions were made because there were no available published data.

Several improvements can be made to the codes to improve its functionality and prediction accuracy, for which there was not sufficient time to implement.

3.4 Chapter Conclusion

This chapter presented the research methodology based on TERA approach. It discussed each component of the TERA framework and the procedure for development of each module that makes up the TERA. The chapter also provides an overview of the limitation of the research methodology.

4 DEVELOPMENT OF GT- ACYSS PERFORMANCE CODE

4.1 Background

This chapter introduces GT-ACYSS, a performance simulation code developed by the author for closed-cycle gas turbine steady-state and pseudo transient performance simulation. It describes the structure of the code, computational models used, and verifications based on open literature of reference power plant. The code allows the choice of key design point parameters and computes the cycle performance at different off-design conditions, i.e. at varying temperatures, pressures, rotational speeds and part-load. This code can be a useful educational tool since it allows the student to monitor gas path properties throughout the closed-cycle without laborious calculations and to carry out preliminary component design assessment. The purpose of this code is to create an understanding of the phenomena observed in real systems and to allow for assessment of different working fluid on the power plant behaviour at different operating conditions.

4.1.1 Justification of the need for the Code Development

Performance calculation which gives the user the flexibility to simulate different working fluids is the main objective of this research in both the design and operation of the closed-cycle gas turbines. Hence, the need for a simulation tool which has several specific features and applicability that meets the research objectives. This will assist in the task of explaining, by making it possible to observe what is happening within each individual component and the overall engine behaviour.

To this end, review of available simulation models; both analog and non-linear digital have been discussed by references [4,82,108] and in this thesis literature review section. Broadly speaking, most of the documented simulation codes in open literature were developed mainly for either open-cycle gas turbine operations or closed-cycle design point analysis or for specific closed-cycle power plant projects which are not accessible for commercial use. Based on

this reviews, there was still need to develop a code that has the applicability for simulating different closed-cycle engine configurations, different working fluid capability, off-design condition assessment and to enable studies particularly at the conceptual design stage, the effects of component parameters and working fluid thermodynamic properties on the overall design performance of the engine.

Consequently, a great deal of research time was expended to develop this simulation code called GT-ACYSS. Other benefits of the code development include:

- Modular code structure, where parts and models can be changed, replaced or added for further application
- The capability of utilizing different control options for independent performance analysis
- More component map characteristics can be introduced for off-design calculations.
- Selected working fluids were modelled as real gas which changes properties at varying pressure and temperature.
- Maybe possible to integrate the code into TURBOMATCH if required, since the code is written in FORTRAN
- Single-shaft configuration which includes simple cycle, recuperated cycle, intercooled cycle and intercooled recuperated cycle
- Multi-fluid component scaling approach which allows the effect of changes in working fluid to be accommodated in the simulation process
- The heat exchangers model can be used for performance analysis of the low-pressure side and high-pressure side

Therefore, for these reasons described, it became essentially helpful to develop this code in order to meet the research objective criteria. The GT-ACYSS model presented is envisioned as building blocks for further modifications.

4.2 Code Structure

The code was developed in FORTRAN 90 and enables the performance and component sizing analysis of single-shaft closed-cycle gas turbine. The main

objective of its development was to produce a user-friendly programme for closed-cycle gas turbine performance simulation to support teaching and training purpose like the TURBOMATCH code [109], already developed in Cranfield University for open cycle gas turbine configurations performance simulations.

The possibility of estimating performance parameters and cycle details, for any operating conditions encountered is of fundamental importance to any technique of performance monitoring. Engine performance computer models are used for this purpose. Such models are based on a conceptual division of the engine into its components as shown in figure 4-1.

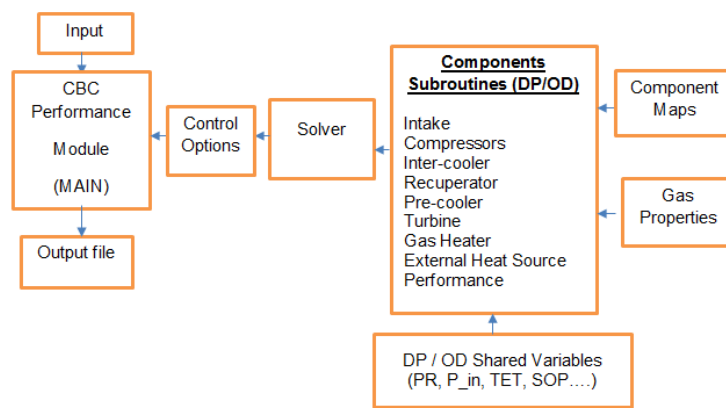


Figure 4-1 Structure of GT- ACYSS: Closed - Cycle Gas Turbine Simulation Code

The overall program structure shown in figure 4-1 consists of modules and subroutines that inter-connect to simulate the steady state performance of the listed engine configurations. The major advantage of this kind of structure is that it creates flexibility in case of any further modification or improvement. The functions of the files listed in figure 4-1 have been described Table 4-1.

The basic concept of the program input description follows an almost similar pattern to those used in TURBOMATCH. Codewords were used to develop the input file and to identify or specify each component input parameters/requirements for design point, off-design point, and preliminary component sizing simulation. A typical example of the input file description can be found in Appendix A-3.

Table 4-1 Summary of GT-ACYSS Modelling Framework

List Name	Class Name	Filename	Description
DP/OD shared Variables	Module	shared_variables.f90 offdesign_variables.f90	Contains list of defined shared variables for Design, Off-design Point and Components sizing (P,W, T etc)
Control Options	Subroutine	Control_files.f90	Defines the engine configuration, control handle, working fluid, & calculations
CBC Main	Program	CBC_main.f90	Part of the code which calls all modules and subroutines
Component	Module	Component_name.f90	Contains components performance and sizing calculations
Input and Output	Import/export files	name.dat, name.txt	Contains input files and writes output files
Solver	Subroutine	Design_Point_Solver Offdesign_Solver.f90	Contains the off-design point solver based on analytical or component map calculation. Calls all component modules based on cycle configuration
Gas properties	Subroutine	Gas_properties.f90	Contains all the fluid properties model
Component Maps	Subroutine	Compressor_map.f90 Turbine_map.f90	Contains component maps and does scaling calculations

4.3 Engine Configuration Options

The gas turbine is an assembly of different components or modules. The characteristic of each component is classified according to the kind of thermodynamic process it accomplishes in the engine operation theory. Similar to the open cycle gas turbine, a closed-cycle gas turbine may either have a single or multi-shaft arrangement of simple, recuperated, or intercooled cycle configuration. Hence, the need for any simulation programs to have the capability of simulating various types of cycle configurations will give it a usage advantage over other available programs.

A closed-cycle simulation tool should allow the user to assemble engine component in the desired configuration. Considering this requirement, GT-ACYSS was developed to be modular. At the moment, the code is capable of simulating single-shaft recuperated, intercooled, intercooled-recuperated and simple cycle configurations. Since the code is modular in structure, other cycle configuration can be incorporated to it in the future. Typical representations of selected engine configurations enabled in GT-ACYSS are shown in Appendix A-1

4.4 Components Simulation Modelling

The overall performance of the closed-cycle gas turbine is mainly determined by its components. The mathematical model which describes the physical behaviour of the system components were created using analytical and empirical equations described in references [23,110–113].

4.4.1 Turbomachinery Component

The behaviour of both the compressor and turbine are described by dimensionless parameters. The performance characteristics are usually plotted as pressure ratio against non-dimensional or corrected mass flow and speed. The dimensionless parameters can be represented by the following equations

$$CMF = \left(\frac{W\sqrt{\theta}}{\delta} \times \sqrt{\frac{R}{\gamma}} \right), \quad CS = \left(\frac{N}{\sqrt{\theta R \gamma}} \right), \quad CH = \left(\frac{\Delta H}{\sqrt{\theta R \gamma}} \right) \quad (4-1)$$

Where,

$$\theta = \frac{T}{T_{ref}}, \text{ and } \delta = \frac{P}{P_{ref}}$$

The temperature at the exit of the compressor is obtained from the inlet temperature, isentropic efficiency, pressure ratio and ratio of specific heats, given by the expression

$$T_{c_{out}} = T_{c_{in}} + \frac{T_{c_{in}}}{\eta_c} \left[\left(\frac{P_{c_{out}}}{P_{c_{in}}} \right)^{\frac{\gamma-1}{\gamma}} - 1 \right] \quad (4-2)$$

Where, the compressor discharge pressure $P_{c_{out}}$ is derived from the given pressure ratio

$$PR_c = \frac{P_{c_{out}}}{P_{c_{in}}} = f(CMF, CS) \quad (4-3)$$

The corrected compressor work (NDCW) is derived as

$$NDCW = \left(\frac{CW}{\delta\sqrt{\theta}} \right) = f(CMF, CS) \quad (4-4)$$

Where CW is the compressor work, which is a product of the mass flow rate, specific heat capacity at constant pressure and the overall temperature rise in the compressor.

$$CW = WC_p \Delta T \quad (4-5)$$

Similarly, the turbine outlet temperature is obtained from the expression below

$$Tt_{out} = Tt_{in} - Tt_{in}\eta_t \left[1 - \left(\frac{Pt_{out}}{Pt_{in}} \right)^{\frac{\gamma-1}{\gamma}} \right] \quad (4-6)$$

The corrected turbine work (NDTW) is obtained from

$$NDTW = \left(\frac{TW}{\delta\sqrt{\theta}} \right) = f \left(\frac{Pt_{out}}{Pt_{in}}, CS \right) \quad (4-7)$$

Where TW is the turbine work, which is expressed as:

$$TW = WCp\Delta T \quad (4-8)$$

Considering system components pressure losses, the turbine pressure ratio is expressed as:

$$PR_t = \frac{Pt_{out}}{Pt_{in}} = PR_c \left[\frac{\sum(1 - \Delta P)_{HPS}}{\sum(1 + \Delta P)_{LPS}} \right] \quad (4-9)$$

The turbomachinery input data at the design point are the inlet conditions of the compressor and turbine such as mass flow rate, component efficiencies, and inlet temperatures and pressures

4.4.2 Heat Exchangers

The heat exchangers which include the recuperator, intercooler, gas heater and pre-cooler were modelled using the ϵ -NTU method and a counter-flow shell and tube configuration was assumed. The ϵ -NTU method was used since the inlet condition (temperature and pressure) of the fluid stream can be easily obtained and simplifies the iteration involved in predicting the performance of the flow arrangement. This method is fully described in references [114,115] and has been applied to complex counter flow heat exchanger by Navarro [116]. The approach also assumes that the heat exchanger effectiveness is known and the pressure losses were given.

Therefore, the effectiveness of the heat exchanger is the ratio of the actual heat transfer rate to the thermodynamically limited maximum heat transfer rate available in a counter flow arrangement.

$$\varepsilon = \frac{Q_{actual}}{Q_{max}} = \frac{C_{hot}(T_{hotin} - T_{hotout})}{C_{min}(T_{hotin} - T_{coldin})} = \frac{C_{cold}(T_{coldout} - T_{coldin})}{C_{min}(T_{hotin} - T_{coldin})} \quad (4-10)$$

Where C_{min} and C_{max} are the smaller and larger of the two magnitudes of C_{hot} and C_{cold}

$$C_{min} = \begin{cases} C_{hot} & \text{for } C_{hot} < C_{cold} \\ C_{cold} & \text{for } C_{cold} < C_{hot} \end{cases} \quad (4-11)$$

$$C_{hot} = (WC_p)_{hot \text{ fluid Stream}}, \quad C_{cold} = (WC_p)_{cold \text{ fluid Stream}} \quad (4-12)$$

The model assumed a counterflow shell and tube heat exchangers, hence, the number of the transfer unit (NTU) is obtained as shown in equation 4-13

$$NTU = \frac{LOG_e \left[\frac{2 - \varepsilon(1 + C^* - \eta_{Hex})}{2 - \varepsilon(1 + C^* + \eta_{Hex})} \right]}{\eta_{Hex}} \quad (4-13)$$

Whereas,

$$C^* = \text{Capacity rate ratio} = \frac{C_{min}}{C_{max}} \quad (4-14)$$

$$\eta_{Hex} = (C^{*2} + 1)^{0.5} \quad (4-15)$$

Considering the effect of pressure losses, then the exit pressure at design point for the heat exchangers is given as:

$$P_{out} = P_{in}(1 - \Delta P) \quad (4-16)$$

Where ΔP is the pressure losses specified by the user at input data of each component of the heat exchangers. It important to emphasize, that GT-ACYSS allows the user to specify whether the pre-cooler utilizes water cooling or dry cooling in order to be able to assess the cogeneration capability of the plant modelling in future applications. The code was modelled to have the working fluid temperature after pre-cooling process equal to the compressor entry

temperature; although in a real scenario the temperature may change and is dependent on the efficiency of the pre-cooler.

4.4.3 Heat Source

In GT-ACYSS, the energy input to the system is modelled an external heat source supplying thermal heat input at a specified temperature and combustion efficiency. The model allows the user to assume the type of heat source (nuclear, fossil or solar).

Therefore, heat gained is given by:

$$Q_g = WC_{p(gas)}\Delta T \quad (4-17)$$

4.4.4 Cycle Performance Calculation

The cycle of the engine at any point of operation is determined by the values of the thermodynamic properties of the working fluid at inlet and outlet stations of each component. Therefore, the overall plant cycle assessment is represented as shaft output power (SOP), specific output power (SP), and cycle thermal efficiency. Specifying auxiliary and generator efficiencies, the overall cycle performance characteristics were obtained by the following equations:

$$SOP = (TW - \frac{CW}{\eta_m})\eta_{aux}\eta_g \quad (4-18)$$

The specific power (SP) which defines the engine capacity is given by:

$$SP = SOP/W \quad (4-19)$$

The thermal efficiency of the cycle is calculated as:

$$\eta_{th} = SOP/Q_g \quad (4-20)$$

The mechanical shaft output power can be written as a product of torque (G) and shaft speed given by

$$SOP = G\omega = GN\left(\frac{2\pi}{60}\right) \quad (4-21)$$

Thus, load speed will influence the output torque for a particular power level delivered. At part-load performance analysis, the power output characteristic is obtained as a function of engine shaft speed and relevant control variables.

4.5 Component Matching

Component matching refers to the interactions between the gas turbine components which satisfies the engine matching conditions of mass and energy conservation to produce the system operating line. To be able to predict an accurate design and off-design point performance of the closed-cycle gas turbine would require an accurate assessment of the component performance, sizing and matching of both the turbomachinery and heat exchangers, which is accomplished through details of their maps or analytical models. These operating maps give detailed illustrations at a wide range of operating conditions for both design and off-design points. The interaction of the gas turbine components defines the operating restrictions to achieve satisfactory performance under different conditions. The procedure used in GT-ACYSS was based on references [23,86,110,113]. In this program, the components matching were analyzed to meet mass flow compatibility, speed compatibility and work compatibility.

Considering an intercooled-recuperated closed-cycle gas turbine engine model for typical illustrations as shown in fig 4-2, the matching requirements can be described using equations 4-21 – 4-25. A useful feature to note about GT-ACYSS is the level of flexibility it allows the user to make performance calculations with or without component maps. This option permits quick trade-off examinations.

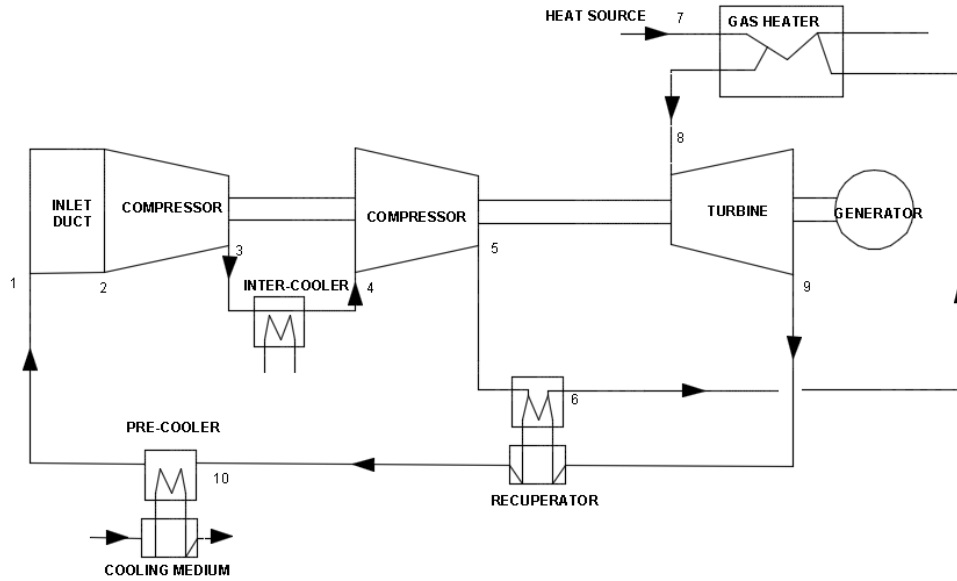


Figure 4-2 Schematic Diagram of Intercooled - Recuperated Closed - Cycle Gas Turbine Plant

From fig 4-2 above, mass flow compatibility between the turbine and HP compressor is expressed as:

$$\frac{W_8 \sqrt{T_8}}{P_8} = \frac{W_4 \sqrt{T_4}}{P_4} \times \frac{P_4}{P_5} \times \frac{P_5}{P_8} \times \sqrt{\frac{T_8}{T_4}} \times \frac{W_8}{W_4} \quad (4-22)$$

The HP compressor inlet temperature T_4 in fig. 4.-2 is controlled by the inter-cooler, and is assumed to remain approximately constant due to intercooling. Hence, the operating line on the HP compressor characteristics will tend towards surge along the line of constant non-dimensional speed as the load demand increases.

The flow compatibility between the LP compressor exit and the HP compressor inlet is given by:

$$\frac{W_4 \sqrt{T_4}}{P_4} = \frac{W_3 \sqrt{T_3}}{P_3} \times \frac{P_3}{P_4} \times \sqrt{\frac{T_4}{T_3}} \times \frac{W_4}{W_3} \quad (4-23)$$

In a similar manner, the flow compatibility between the LP compressor inlet and exit is given by:

$$\frac{W_3\sqrt{T_3}}{P_3} = \frac{W_2\sqrt{T_2}}{P_2} \times \frac{P_2}{P_3} \times \sqrt{\frac{T_3}{T_2}} \times \frac{W_3}{W_2} \quad (4-24)$$

The speed compatibility is expressed as:

$$\frac{N_8}{\sqrt{T_8}} = \frac{N_2}{\sqrt{T_2}} \times \sqrt{\frac{T_2}{T_8}} \quad (4-25)$$

The power balance, for which turbine work is greater than compressor work gives the useful work. This is expressed as:

$$UW = TW - (CW1 + CW2) \quad (4-26)$$

4.6 Multi-Fluid Component Scaling for Single Shaft Configuration

To accurately simulate the performance of any closed-cycle gas turbine power plant in combination with any heat source, often requires the availability component data in the form of characteristics map. However, this component characteristics maps for new entrant design or existing components are usually not accessible. Hence, theoretical maps obtained using scaling methods are often relied upon to adapt data from one component map into a new component map. The maps for different components used in this program were obtained using multi-fluid scaling methods which multiplies the scaling factors derived at the design point to the original component map at the off-design points [117].

The referenced map used in GT-ACYSS was adapted from TURBOMATCH; a Cranfield University in-house performance simulation tool [109]. Each Component operation is defined by an appropriate change of state equations which describes its thermodynamic behaviour, hence, a consideration of the selected working fluid properties is of high importance to the scaling method and simulation model accuracy. To accommodate working fluid flexibility, maps were scaled considering the influence of gamma and specific gas constants.

The scaling factor used in the simulation model were obtained using equations (4-26) – (4-30), and are documented in references [23,95,118–120].

4.6.1 Turbomachinery Component Map Scaling

The turbomachinery maps are usually represented with dimensionless parameters such as corrected mass flow, corrected speed, pressure ratio, component efficiencies and work functions. As previously mentioned, the GT-ACYSS have several component maps in its library adapted from TURBOMATCH using multi-fluid scaling process depending on the working fluid in use. Thus, the governing principle for the selection of an appropriate component map is keeping the scaling factor close to 1.

Figure 4-3 shows a flowchart of scaling technique for the turbomachinery component maps used in GT-ACYSS.

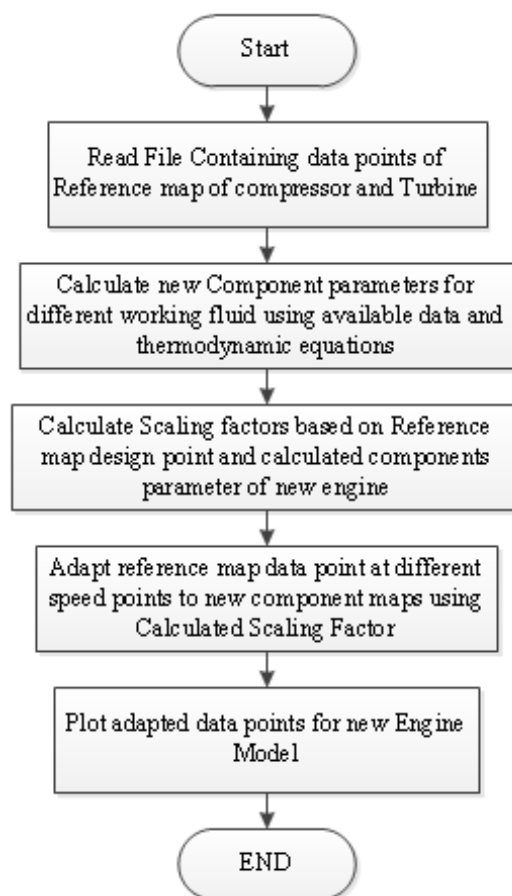


Figure 4-3 Flow chart of Multi-Fluid Scaling Method used for Turbomachinery Component Maps

From the flowchart shown in Fig-4-3, the first step is to obtain the design point characteristics of the new engine and that of the reference map in the library. Next, is the program (GT-ACYSS) calculates the scaling factors using equations (4-27) – (4-31). Once the scaling factor is obtained, it is multiplied with the reference map off-design points to obtain new scaled off-design points using equations (4-32) – (4-46).

The Corrected Mass flow scaling factor is expressed as:

$$CMSF = \frac{\left(\frac{W_{DP} \sqrt{\theta_{DP}}}{\delta_{DP}} \times \sqrt{\frac{R_{gas}}{\gamma_{gas}}} \right)_{DP}}{\left(\frac{W_{DP} \sqrt{\theta_{DP}}}{\delta_{DP}} \times \sqrt{\frac{R_{gas}}{\gamma_{gas}}} \right)_{DPrefmap}} \quad (4-27)$$

The Corrected Speed scaling factor is given by:

$$NSF = \frac{\left(\frac{N}{\sqrt{\theta_{DP} \gamma_{gas} R_{gas}}} \right)_{DP}}{\left(\frac{N}{\sqrt{\theta \gamma R}} \right)_{DPrefmap}} \quad (4-28)$$

The pressure ratio scaling factor is obtained from:

$$PRSF = \frac{(PR_{DP} - 1)}{(PR_{DPrefmap} - 1)} \quad (4-29)$$

The Isentropic efficiency scaling factor is expressed as:

$$\eta_{cSF} = \frac{(\eta_c)_{DP}}{(\eta_c)_{DPrefmap}} \quad (4-30)$$

The work function scaling factor is given by:

$$DHSF = \frac{\left(\frac{\Delta H}{\sqrt{\theta\gamma R}}\right)_{DP}}{\left(\frac{\Delta H}{\sqrt{\theta\gamma R}}\right)_{DPrefmap}} \quad (4-31)$$

The corresponding data points for the scaled map are obtained using the following equations:

$$Pressure\ ratio\ (PR) = \frac{(PR_{DP} - 1)}{(PR_{DPrefmap} - 1)} (PR_{refmap} - 1) + 1 \quad (4-32)$$

$$Mass\ flow\ (W) = CMSF * W_{refmap} \quad (4-33)$$

$$Component\ Efficiency\ (\eta_c) = \eta_{cSF} * \eta_{crefmap} \quad (4-34)$$

$$Work\ Function\ (DH) = DHSF * DH_{refmap} \quad (4-35)$$

The scaling factors are calculated at the design point, hence, there no changes at off-design conditions.

4.6.2 Heat Exchangers Scaling at Off-design Operation

For Pressure Loss Scaling, a simplified method used for obtaining the pressure drop due to friction for internal flow applicable to heat exchangers is the use the Darcy friction factor (f); a dimensionless parameter [114,115,121] that is defined as:

$$\Delta P = f \left(\frac{L\rho V^2}{2D} \right) \quad (4-36)$$

For a given heat exchanger, the hydraulic diameter (D) and Length (L) are constant. Hence, the pressure loss becomes proportional to the friction factor, fluid density and velocity, which can be expressed as:

$$\Delta P \propto f\rho V^2 \quad (4-37)$$

Expressing the fluid velocity in the heat exchanger in terms of mass flow rate becomes:

$$V = \left(\frac{W}{\rho A} \right) \quad (4-38)$$

Since the cross-sectional area of the flow passage in the heat exchanger will remain constant, therefore:

$$\Delta P \propto f\rho^{-1}W^2 \quad (4-39)$$

Implementing the simple Blasius correlation [121] for calculating the friction factor makes:

$$f = \frac{0.3164}{Re^{0.25}} \quad (4-40)$$

Where Reynolds Number (Re) is expressed as:

$$Re = \frac{\rho V D}{\mu} \quad (4-41)$$

Combining equations (4-37), (4-39), and (4-40) to calculate for friction factor scaling in terms of mass flow rate and fluid viscosity becomes:

$$f \propto W^{-0.25} \mu^{0.25} \quad (4-42)$$

Therefore, combining equations (4-41) and (4-38) will become:

$$\Delta P \propto W^{1.75} \mu^{0.25} \rho^{-1} \quad (4-43)$$

The simulation model assumed that the within the heat exchangers the fluid properties do not change significantly at off-design conditions, hence, the pressure loss for off-design operation is scaled with the mass flow rate, expressed as:

$$\Delta P_{OD} = \Delta P_{DP} \times \left(\frac{W_{OD}}{W_{DP}} \right)^{1.75} \quad (4-44)$$

Similarly, the heat exchanger effectiveness are scaled in terms of mass flow rate as described in reference [23]

For inter-cooler and pre-cooler

$$\varepsilon_{OD} = 1 - (1 - \varepsilon_{DP}) \times \left(\frac{NDMF_{OD}}{NDMF_{DP}} \right) \quad (4-45)$$

For recuperator and gas heater

$$\varepsilon_{OD} = 1 - (1 - \varepsilon_{DP}) \times \left(\frac{W_{OD}}{W_{DP}} \right) \quad (4-46)$$

4.7 Working Fluid Options

From the perspective of thermodynamic performance, all permanent gases can be utilised for closed cycle gas turbine working fluid [64,65]; however, there are important constraints which are considered when selecting a suitable fluid for closed-cycle application such as thermal stability, inflammability, chemical inertness and toxicity. GT-ACYSS is modelled to allow its user have some degree of flexibility in selecting their choice working fluid to be simulated from the listed in the program library namely; helium, air, nitrogen, and carbon dioxide. The fluid properties were provided by a series of gas properties subroutine which computes the thermodynamic and transport properties of the listed working fluid.

4.7.1 Modelling of Fluid Properties in GT-ACYSS

Correct estimation of working fluid thermodynamic and transport properties is an important aspect of developing an accurate performance prediction model

[23]. To this end, a variety of models for calculating fluid properties has been developed and could be applicable for closed-cycle gas turbine performance prediction code [23,77,95,122–124]. However, most of these models treated the fluid properties as a semi-perfect gas, typically which are only a function of temperature [23,77]. This is true at high temperatures; but at high pressures and low temperatures, which is common to closed-cycle gas turbine conditions, the fluid properties change rapidly.

An estimation of the properties of working fluid listed in GT-ACYSS was modelled using empirical correlations and coefficients. The empirical equations and coefficients are power expansions in terms of pressure and temperature. They were obtained experimentally by fitting the power series to measured isotherm and isobar from experimental data and tables of references [122–125]. A modification on the curve fitting equation by [95,126] was used to ensure that the coefficients approximations were very good. For CO₂, its properties change rapidly with pressure and temperature near its critical points, especially at the low-temperature region. Similarly, all working fluids were modelled as a function of pressure and temperature. The results of the curve-fitted data were compared against the NASA SP-273 [122], and gas tables of reference [123]. A general representation of polynomial for some of the gas properties is shown in equations (4-46) – (4-51)

a) Specific Heat Capacity at Constant Pressure C_p

$$C_p = \sum_{i=0}^{i=6} A_i T^i \text{ for } T < 400 \text{ K} \quad (4-47)$$

$$C_p = \sum_{i=0}^{i=6} i A_i T^{(i-1)} \text{ for } T \geq 400 \text{ K} \quad (4-48)$$

Whereas,

$$A_i = f(P)$$

b) Enthalpy H: The enthalpy of the working fluids were calculated using integration and averaging as shown in equation (4-3)

$$H = \int C_p dT \quad (4-49)$$

c) Entropy S

$$S = S_0 + A_0 \ln T + \sum_{i=1}^{i=6} A_i \frac{T^i}{i} \text{ for } T < 400 \text{ K} \quad (4-50)$$

$$S = S_0 + A_0 \ln T + \sum_{i=2}^{i=6} \frac{i}{i-1} A_i T^{(i-1)} \text{ for } \geq 400 \text{ K} \quad (4-51)$$

Whereas,

$$S_0, A_0, A_i = f(P)$$

d) Gamma γ

$$\gamma = \frac{C_p}{(C_p - R_{gas})} \quad (4-52)$$

Where

$$R_{gas} = \frac{R}{MW}, R = 8314.36, MW = \text{Molecular Weight of Individual selected gases.}$$

In Appendix A-2, other thermodynamic and empirical equation utilised to model the transport and certain thermodynamic properties of listed working fluid in GT-ACYSS were discussed.

Figure 4-4 to 4-6 shows how close the correlation approximation of fluid properties obtained compared to references [123,125,127]. In each case, the mean deviation from the reference tables of gas properties is less than 1%. The maximum deviation in each case occurred at temperatures below 300⁰K. Similar graphs have been produced for other fluid properties, with almost the same level of accuracy as shown in Appendix A-2.

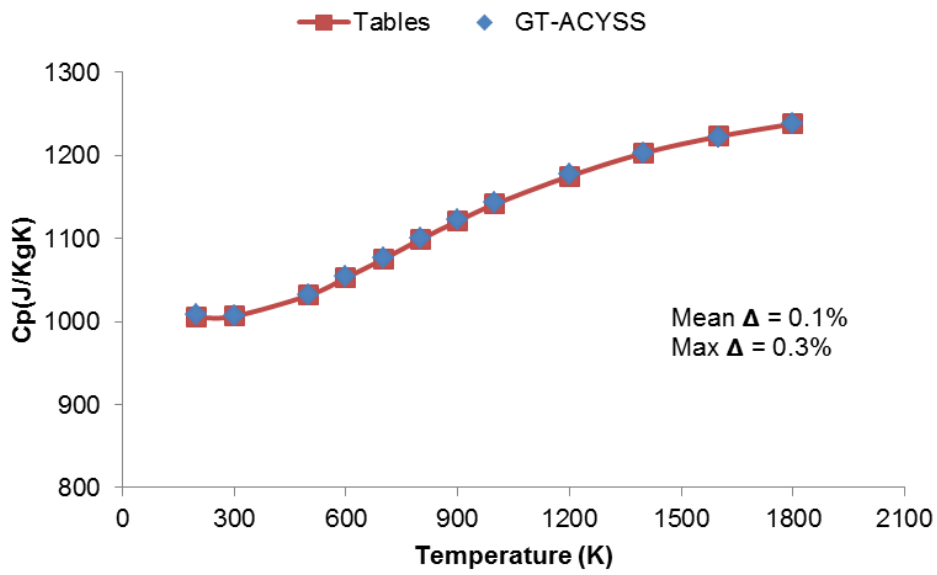


Figure 4-4 Comparison of GT-ACYSS Model for Air Specific Heat Capacity with Tables - Variation with Temperature at Pressure of 1atm

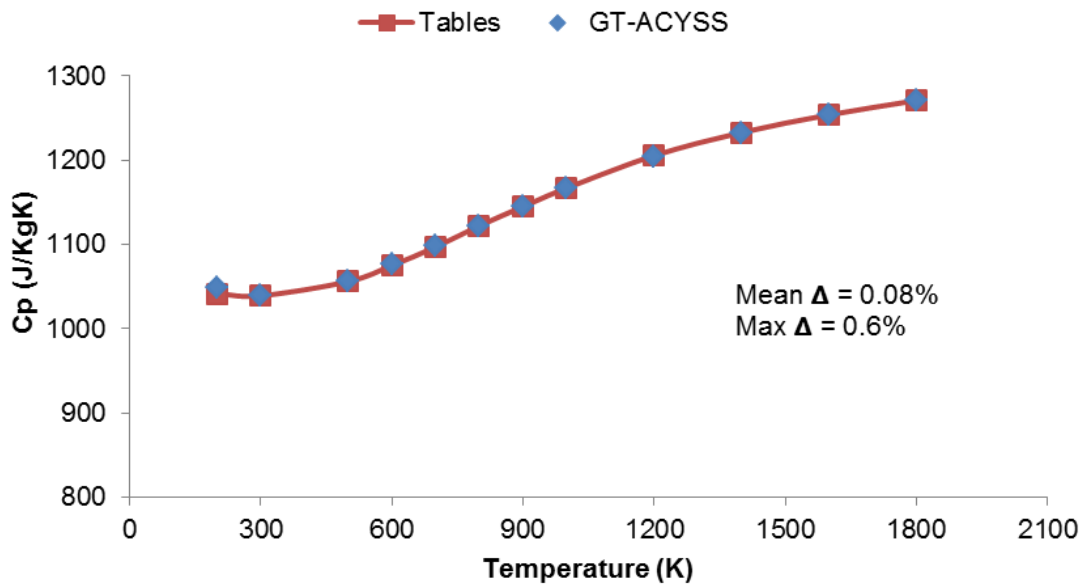


Figure 4-5 Comparison of GT-ACYSS Model for N2 Specific Heat Capacity with Tables - Variation with Temperature at Pressure of 1atm

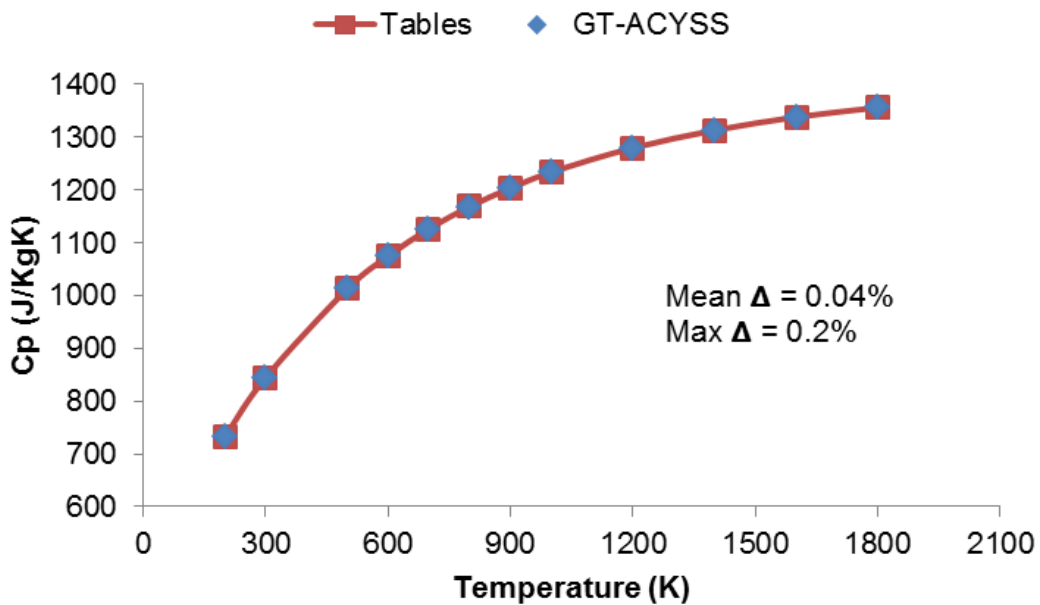


Figure 4-6 Comparison of GT-ACYSS Model for CO₂ Specific Heat Capacity with Tables - Variation with Temperature at Pressure of 1atm

4.8 Control Options and Strategy

Closed-cycle gas turbine offers a viable option for stable power conversion system due to its potential to relatively maintain high-performance characteristics under varying operating conditions if an understanding of its control strategy selections is properly implored. The central goal of any control strategy implemented in single-shaft closed-cycle GT operations should be for the power plant to quickly adjust to wide range of fluctuating load variation without significantly affecting the cycle thermal efficiency, also for prevention of thermal shocks on plant components during critical transients, and for providing automatic control manoeuvres during plant start up and shut down.

To this end, references [128,129] have discussed the different control strategies that are applicable to closed-cycle gas turbine operations. In an attempt to understand the modelling of the different control strategy in closed-cycle gas turbine operation, Covert et al., [130] analysed the effect of various control mode on the cycle efficiency at part-load operations. The work by reference [129] described other alternative control options and dynamic behaviour of a single-shaft closed-cycle operation using bypass control mode. Similarly,

reference [37,128,129] investigated the operational envelope of bypass control during transients. Other authors that attempted to provide an open source procedure are documented in [13,49,87,131].

However, to the best of my knowledge, none of the references cited so far provided a detailed description of a specific procedure for predicting closed-cycle gas turbine performance at various off-design conditions using different control strategy. In order to accommodate these requirements, a modelling procedure for the performance of a single-shaft gas turbine using a different control strategy is described.

The control methods developed in this section was based on parametric analysis of influencing cycle parameters like pressure ratio, heat source temperature, and mass flow on the plant performance. By maneuvering these parameters using appropriate control logic, the plant can be regulated to match any changes in load demand or sudden requirement for idling or shutdown.

At the moment, GT-ACYSS allows the user to select from a list of different control options according to the reference plant configuration and performance assessment to be carried out. The control options include Inventory control mode, Bypass control mode, Heat source temperature control mode and combined mode (integration of the listed control modes to achieve different control task). Each of these control methods has their benefits and trade-offs that will be addressed in the application of control option section. These four control strategies and their modelling procedures are discussed in this section using fig 4-7 to enhance understanding.

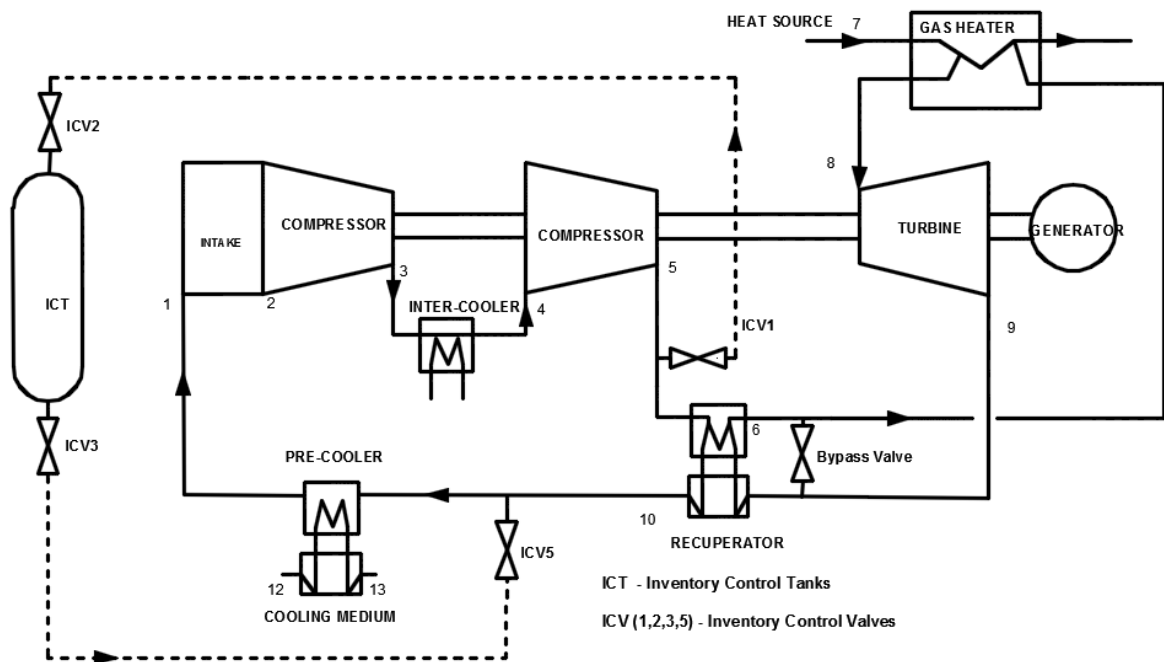


Figure 4-7 Scheme of Reference Plant Circuit with Different Control Options

4.8.1 Inventory Control (ICS)

This control option has been widely mentioned as an attractive possibility especially at part load [29,132] because it allows the power plant to operate within a wide range of load fluctuation at a good cycle thermal efficiency. The operating concept of the control logic is for the power plant to be able to store, or save energy during off-peak periods and replenish this energy during peak load demand via inventory control system (ICS). This means that the working fluid is either extracted or injected into the power conversion system, resulting in a related change in system pressure, change in density, change in mass flow rate and, therefore, also a change in power level ($W = \rho AV$).

During the plant operations, the daily fluctuations in power demand as a result of varying operating conditions are adjusted by means of the inventory control system (ICS), which comprises of the inventory control tank (ICT), and inventory control valves (ICV) as shown in Fig. 4-7. When a reduction in shaft power is required as result of a decrease in load demand, the ICV1 is opened so that the working fluid flows from the HPC into the ICT. The working fluid stored in the

ICT is injected back into the power conversion circuit by the opening of ICV3, if the output power is to be increased.

At part-load, the operation of the cycle at reduced mass flow rate allows operation with the same temperatures and pressure ratio. Since the mass flow rate is proportional to the system pressure and flow density, this implies that the power plant operates with the same thermodynamic cycle, resulting in approximately constant cycle efficiency and specific work. The fact that the temperatures remain invariant as the mass flow rate is reduced implies that the local speed of sound is constant [22].

Figure 4-8 shows the iteration modelling procedure using inventory control at a steady state condition. The inventory control system is regulated based on the pressure variation between the plant cycle and the inventory tank. This variation determines the power limit and the possibility of maintaining high part-load efficiency to which inventory control is achieved. Other restrictions to inventory control system include: (a) size and pressure of the inventory storage tank, (b) shaft rotational speed effect on blade tips (c) location of inventory valves in the cycle loop (d) availability of inventory transfer compressor, and (e) cost of implementing any of the options listed.

To this end, the possible locations of the inventory valves and how it affects the performance of the inventory control system have been discussed in the work of references [13,46]. Similarly, Bitsch et al., [132] have analysed the relationship between inventory control range, total control volume and total helium inventory in the helium coolant circuit.

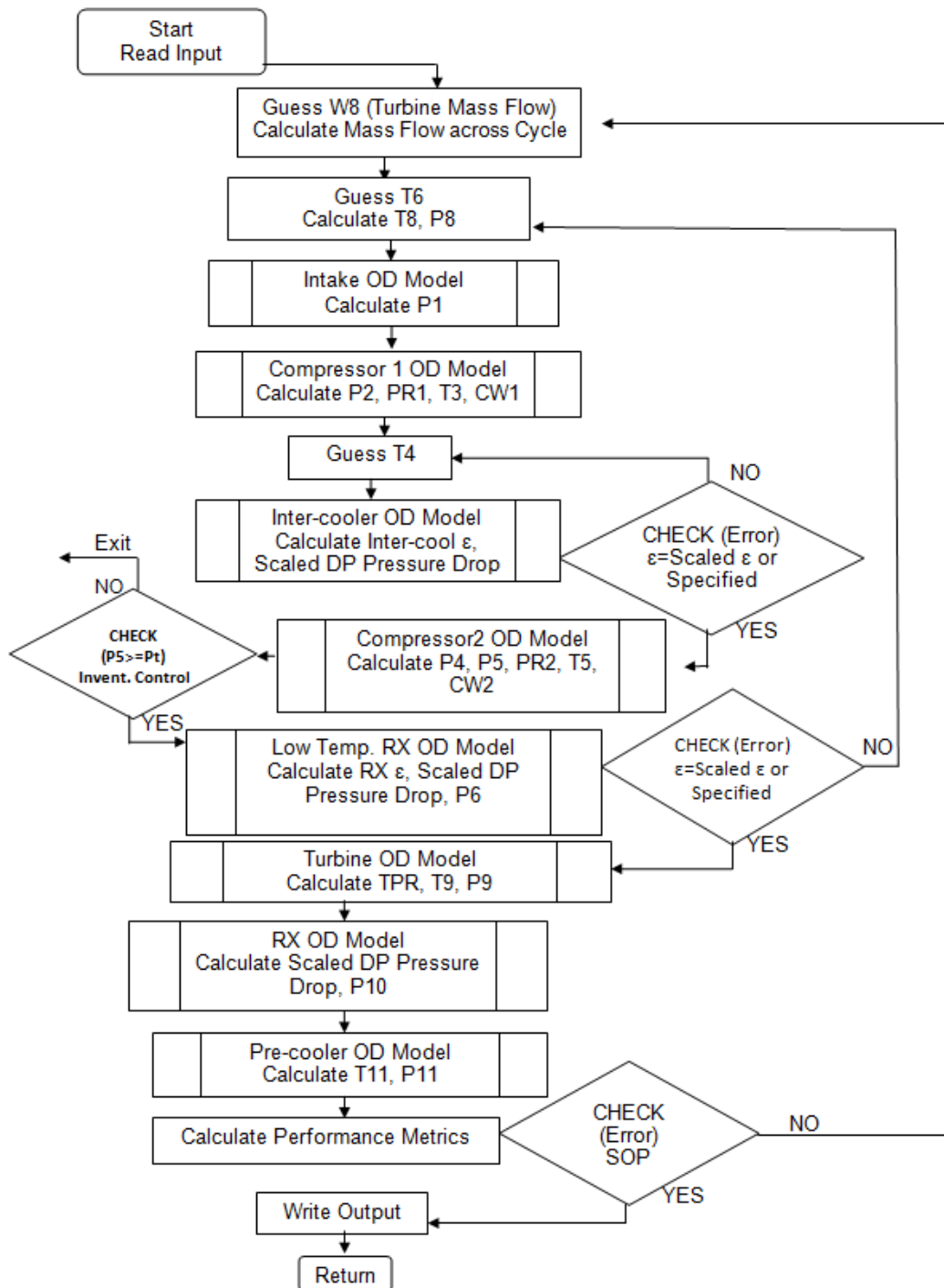


Figure 4-8 Iteration Procedure using Inventory Control Strategy at steady-state

In Bitsch et al., work, the power minimum range was predefined based on a reference design, at a constant tank temperature, while the volume of the tank was varied. The design and technical considerations for developing the storage tank for inventory control are documented in references [30,133–135].

A modified Bitsch et al., [132] model was implemented in GT-ACYSS to develop a physical procedure to represent the inventory load control limit.

1) Inventory Load Control Model

$$\Omega_{min} = \frac{1 + \frac{M_{T1}}{M_{GT5}}}{1 + \psi \left(\frac{M_{T1}}{M_{GT5}} \right)} \quad (4-53)$$

If case 3 option is considered where $n > 1$ then

$$\Omega_{min} = \Omega_{min}^{\frac{1}{n}} \quad (4-54)$$

$$\Omega_{max} = \frac{1 + \frac{M_{T1}}{M_{GT5}}}{1 + \left(\frac{\psi}{OPR} \right) \left(\frac{M_{T1}}{M_{GT5}} \right)} \quad (4-55)$$

Where,

Ω_{min} = Minimum Equilibrium Inventory – control Power Range

Ω_{max} = Maximum Equilibrium Inventory – control Power Range

$\psi = \frac{P_5}{P_{T1}}$, P_{T1} = Initial Pressure of storage tank, n = number of storage tank

M_{T1} & M_{GT5} = initial mass of tank and Cycle loop,

OPR = Overall Pressure ratio

2) Thermo-Fluid Model

To model the thermodynamic behaviour the plant using inventory control, the law of conservation of mass, conservation of momentum and conservation of energy was used to balance the fluid extraction and injection in the GT-cycle and storage tank relationship. Thus,

$$\Delta M_T = \Delta M_{GT} \quad (4-56)$$

Where,

$$\Delta M_T = \frac{\Delta P_T \times V_T}{RT_t} = \frac{\Delta P_{GT} \times V_{GT}}{RT_{GT}} = \Delta M_{GT} \quad (4-57)$$

Energy balance is given by

$$\delta Q - \delta W = \delta U + \delta PE + \delta KE \quad (4-58)$$

But $\delta W = 0, \delta KE = 0, \delta PE = 0$

A. Storage Tank and GT-Cycle Loop Model

During low power demand, the ICV1 is opened for extraction of working fluid into the tanks, the HPC discharge temperature is assumed to be constant. This was so because the HST is assumed constant and the large variation of the HPC temperature to the storage tank initial temperature. Similarly, during injection to the GT-cycle loop, the reverse is the case for the opening of ICV3.

If the process is Isothermal, then

$$\Delta M_T = (1 - \Omega_{min}) \times M_{GT5} \quad (4-59)$$

$$V_T = \left[\frac{(1 - \Omega_{min}) \times M_{GT5} \times RT_t}{(P_{t2} - P_{t1})} \right] \quad (4-60)$$

If the process is adiabatic then

$$V_T = \left[\frac{(1 - \Omega_{min}) \times M_{GT5} \times (RT_{t2} - RT_{t1})}{(P_{t2} - P_{t1})} \right] \quad (4-61)$$

From Equation 4-6 the tank final temperature is given thus

$$T_{t2} = \left[\frac{T_{t1} C_v M_{T1} + C_{pGT} (\Delta M_{GT}) T_{GT}}{C_v M_{T2}} \right] \quad (4-62)$$

To minimise the influence of adiabatic effect on the storage tank, reference [30,134,135] implemented a capacitance in the storage tank to absorb the heat from the GT-cycle loop fluid, thus lowering the tank temperature, thus

$$T_{t2} = T_{cap} + \Delta T_{lag}$$

B. Valve Model

Mass flow in the ducting during inventory change was determined according to reference [10,46]

$$W = \sqrt{\frac{\Delta P \times \rho}{2f \left(\frac{L}{D}\right)}} \quad (4-63)$$

Mass flow rate is given by

$$\frac{dW}{dt} = WA \quad (4-64)$$

4.8.2 Bypass Control (BCS)

In this case, the power level is controlled by regulating the bypass valve as shown in Fig. 4-7. The high-pressure gas is bled off to short-circuit the gas heater (GH) and turbine to the low-pressure side of the recuperator, and, as such, the mass flow, pressure ratio and efficiency of the turbine drop, causing a decrease in the output power. The redirected flow is circulated into the compressor at an unchanged gas inventory, thus, increasing the pressure level and compressor work. The LPC pressure decreases as the bypass valve opens. This decreases the turbine pressure ratio and adds to the reduction of the turbine power. The same effect takes place in the HPC. The cycle temperatures are held constant with just thermal power input matching the deficits required to maintain the cycle temperatures at reduced mass flow through the heat source. The advantage of this control option is that it can be initiated for rapid power changes to match load variation. Thus, this control option is usually implemented in closed-cycle gas turbines to achieve fast control response and to prevent the shaft from over-speed [50]. It is also important to note that the position of the bypass valve has some effect on the cycle performance [13,136]

The impact on the performance is readily calculated since the cycle temperature may be taken to remain fixed. The recuperator will process equal masses on both sides at all times, which means that the ideal design situation of $T_6 = T_9$ is maintained at part-load as shown in fig. 4-7. This is due to the fact that with constant T_8 and constant compressor pressure ratio, $T_6 = T_9$. A mixer is introduced to combine the hot gas stream the cold gas stream, which balances the system enthalpy, thus, yielding $T_6 = T_9$. The cycle analysis is merely a working accounting with the full mass flow processed by the compressor and less in the heater and turbine. An ideal cycle analysis gives

$$\eta_{th} = \left[1 + \frac{SP}{SP_{max}} \left(\frac{\theta_8}{\theta_2} - 1 \right) \right]^{-1} \quad (4-65)$$

Where,

$$SP_{max} = \left(\frac{\theta_8}{\theta_2} - 1 \right) (\theta_2 - 1), \quad \theta_8 = \frac{T_8}{T_{ref}}, \quad \theta_2 = \frac{T_2}{T_{ref}} \quad (4-66)$$

Figure 4-9 shows the iteration modelling procedure using bypass control at a steady state condition. In GT-ACYSS, to model for load rejection and emergency stop, bypass control was implemented in pseudo-transient mode. Thus,

$$I \frac{d\omega}{dt} = G_t - (G_{cT} + G_L) \quad (4-67)$$

Where,

I = moment of inertia

G_t = Turbine torque

G_{cT} = total compressor torque

$G_L = \text{Load}$

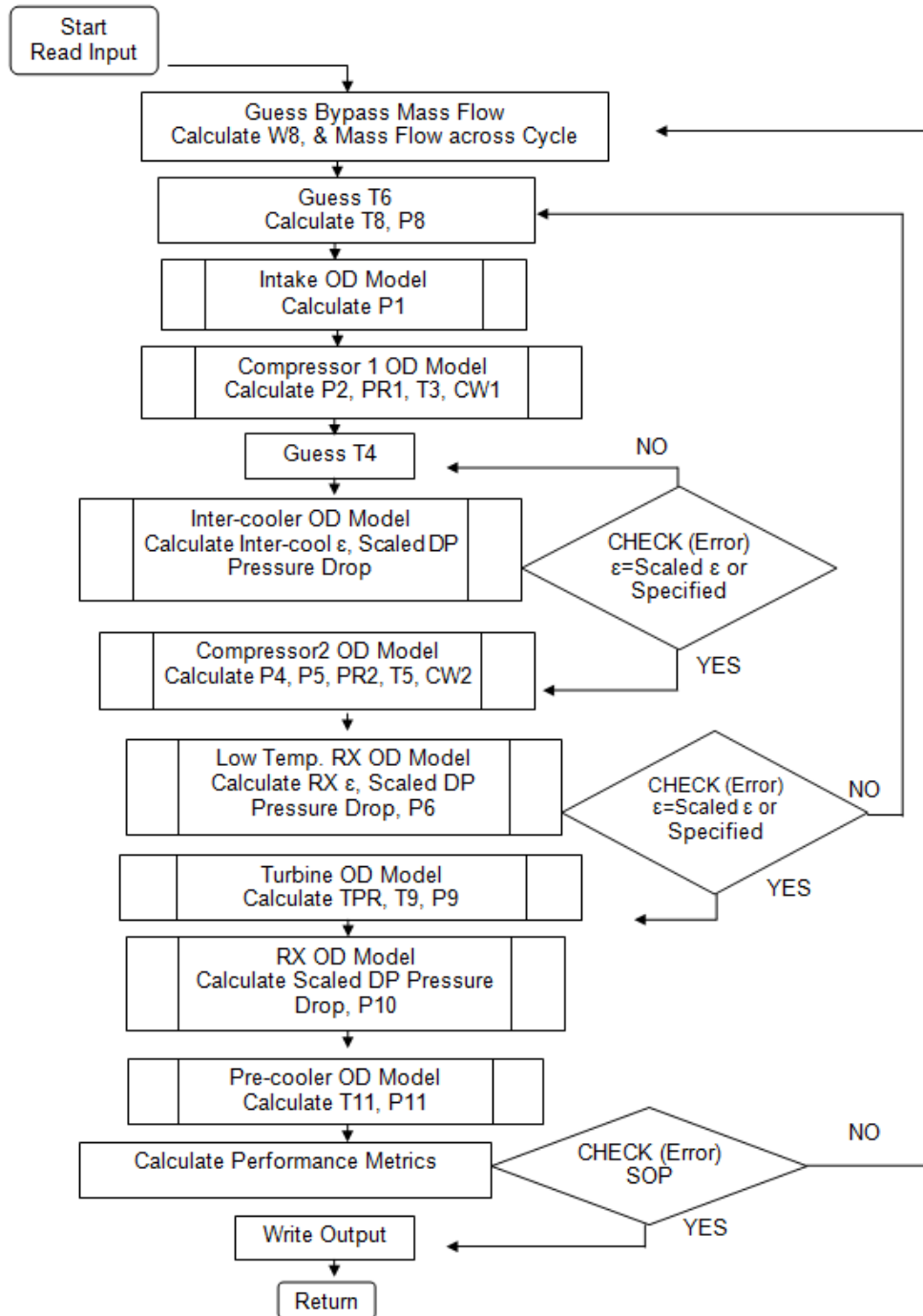


Figure 4-9 Iteration Procedure using Bypass Control Strategy at steady-state

4.8.3 Heat Source Temperature Control (HST)

The power level is altered by changing the temperature of the working fluid at the gas heater (GH) via changes in the heat source temperature. In this case,

the fluid inventory remains constant, and a drop in TET causes a decrease in the components cycle temperature and system pressure level, thus, a reduction in cycle efficiency. Figure 4-10 describes the iteration procedure with heat source temperature control.

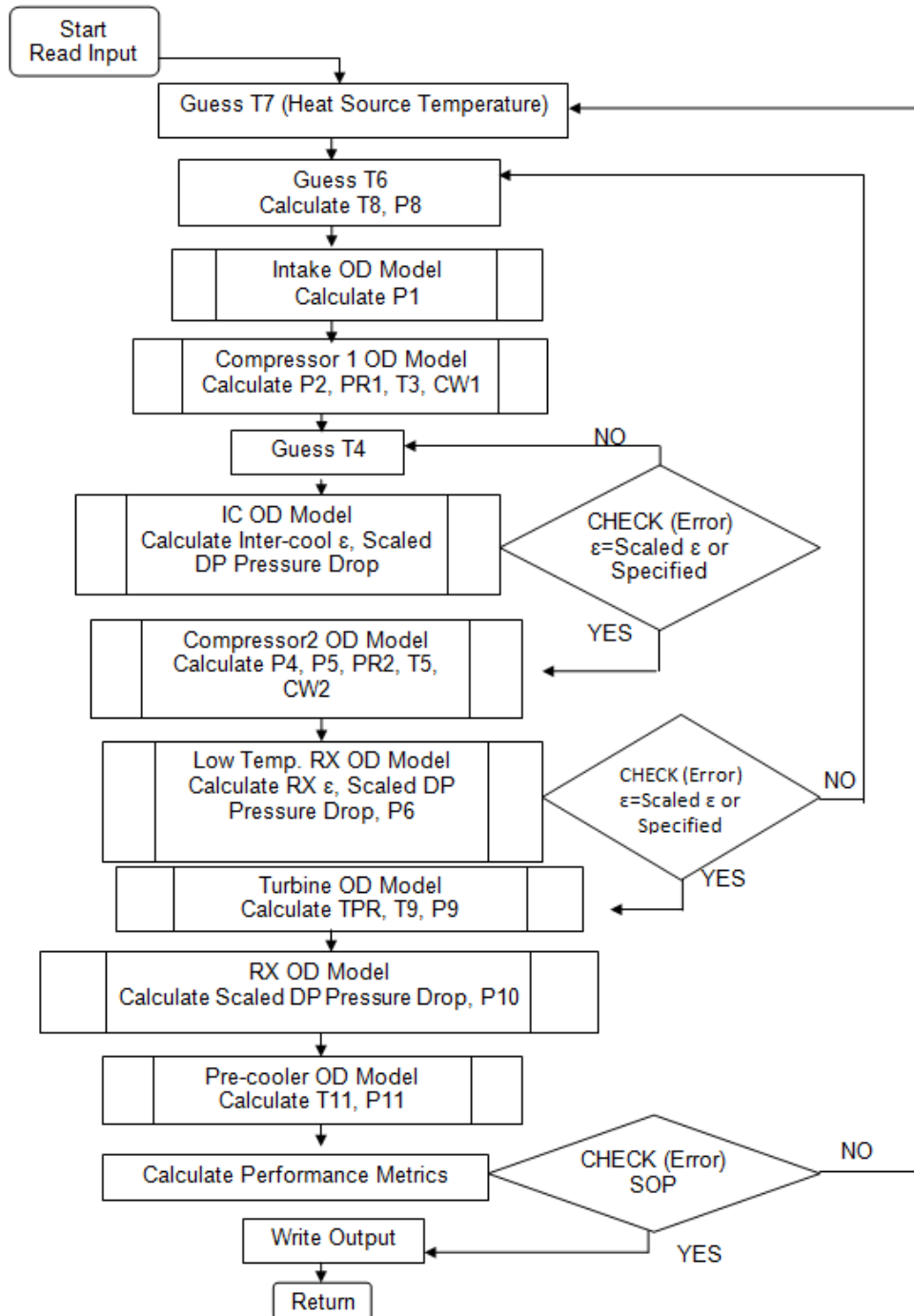


Figure 4-10 Iteration Procedure using HST Control Strategy at steady-state

4.8.4 Combined Control Mode

The combine control strategy utilizes integrated control actions of the options mentioned above to regulate the behaviour of the engine in order to avoid limitations in shaft speed or low cycle efficiencies. This approach consists of controllers which issue commanding signals to the control options subsystems to perform integrated control functions. The load demand acts as the primary input which determines the appropriate control subsystem to be initiated. For any closed-cycle gas turbine power plant, either all or part of these control methods discussed is simultaneously utilized to meet diverse control requirements during operation. Hence, a combined control system is usually integrated with several subsystems to allow the interactive control action as required. For example, a combined control mode can be designed to have an inventory control for slow load moderation, a bypass control for rapid load response, shaft speed control and emergency shut-down capability, and a heat source temperature control to regulate heat source power input as required by the system as shown in fig. 4-7.

During this operation certain percentage of power level changes triggers the control response for load-following or load-rejection.

4.9 Solution Convergence Method

The solution convergence technique requires the use of a control mechanism to satisfy mass flow, speed and power compatibility. The mathematical approach to this non-linear relationship between the dependent and independent variables required several iterations. The approach used in GT-ACYSS was essentially similar basic technique used in references [23,86,91,112,113] with minor modifications. The solution to the unknown independent variable which matches the computed value of the dependent variables to its required or estimated values was solved using a combination of the secant-bisection method. The derivation of the method has been extensively discussed in reference [137]. Basically, the iterative process begins with a first pass through the entire cycle configuration made with initial guesses for all unknown independent variables determined by the control option selected (for example

mass flow for inventory control and bypass, or TET for heat source temperature control, compressor pressure ratio, heat exchanger efficiencies etc). The results of the first pass are checked through the compatibility matching and the succeeding passes through the configuration are made changing each respective unknown by a small amount from the convergence solution technique. The convergence tolerance in GT-ACYSS is 10^{-5} . A typical illustration using engine shown in Fig. 4-7 to demonstrate the structure of simulation convergence in GT-ACYSS is described by fig. 4-11.

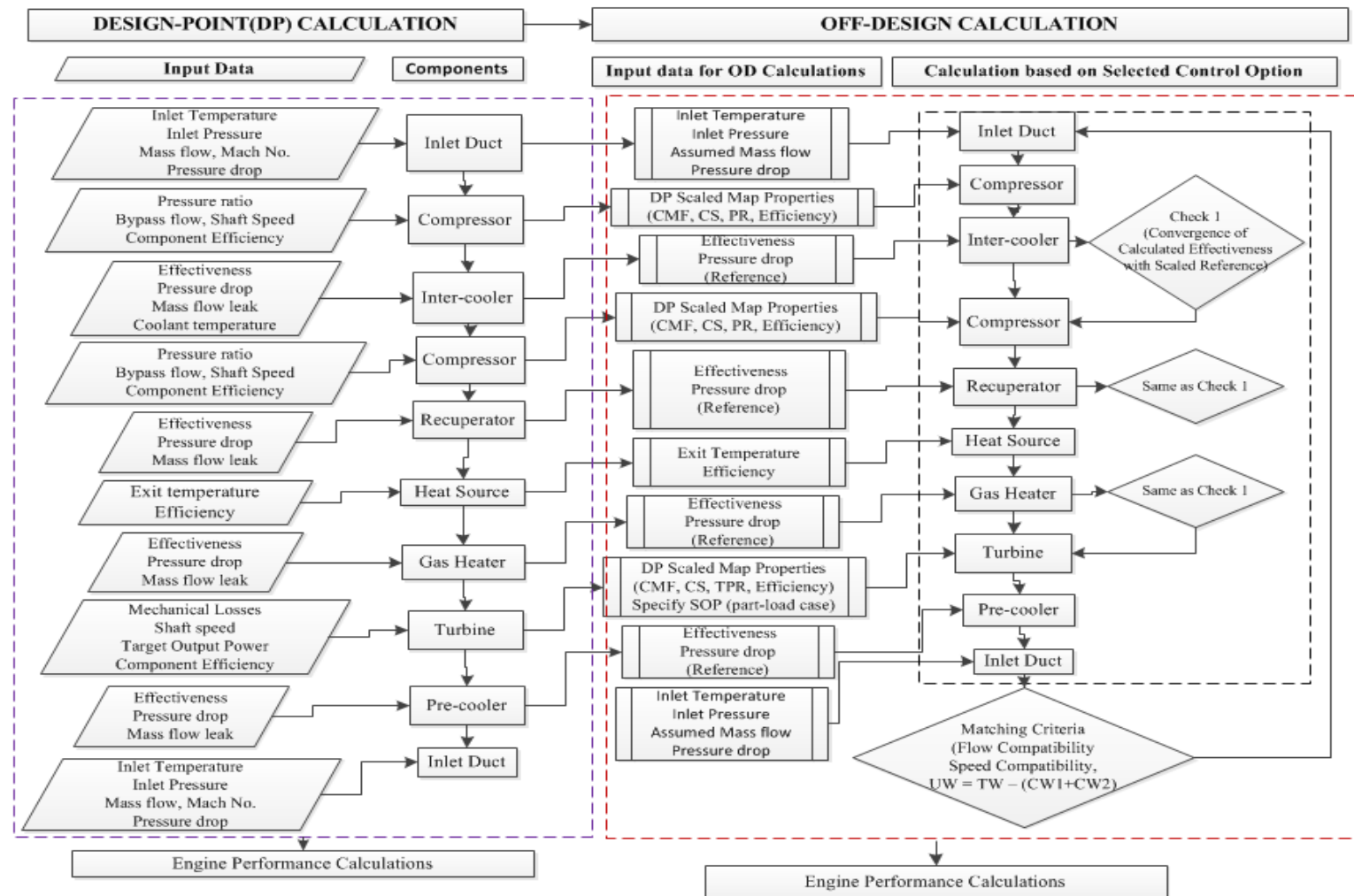


Figure 4-11: Structure of Simulation Convergence in GT-ACYSS

4.10 Application of GT-ACYSS Performance Code and Control Options

To verify the capability of the simulation tool, two applications were considered in this study. The first application was the simulation of three closed-cycle gas turbine plants with design point data obtained from the open literature and modelled in GT-ACYSS. The reference plants modelled to consist of two recuperated cycle plants and an intercooled-recuperated cycle plant. The design point modelling was based on published design specifications, and an optimal combination of both known and guessed parameters was utilized to obtain reasonable minimum mean deviations of performance and major gas path parameters. After the design point specifications were simulated, off-design performance variation was predicted and verified with available reference data using appropriate control handle discussed in section (4.10).

The second application is a performance comparison of the control options and load rejection simulation using bypass control. An intercooled-recuperated closed-cycle gas turbine plant was used for the second application.

4.11 Results and Discussions

This section presents the results and discussions on the application of the GT-ACYSS performance code and control options.

4.11.1 Application 1: Simulation of three closed-cycle gas turbine plant

A. Case 1

The reference plant modelled for case 1 is inspired on GTHTR300; a plant designed and under development by Japan Atomic Energy Agency. The plant is a single-shaft recuperated closed-cycle gas turbine with nuclear reactor supplying thermal energy and cooled with helium. The plant configuration is shown in fig. 4-12. It consists of a single turbomachinery set (turbine-compressor), recuperator, pre-cooler and the reactor. The

performance of the engine was simulated in GT-ACYSS and compared with results in [27,138–140].

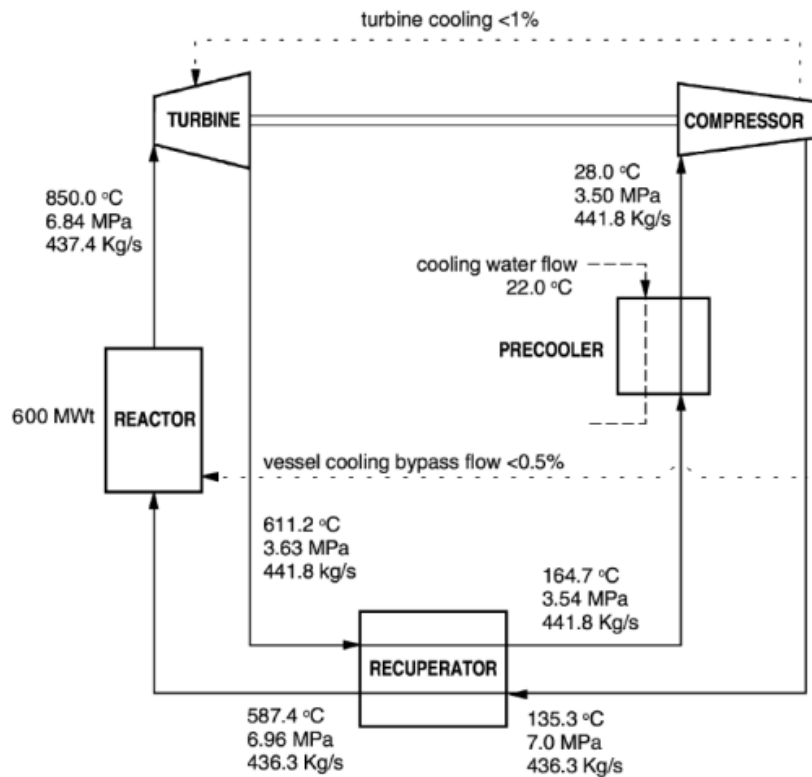


Figure 4-12 Schematic of reference plant modelled for case 1 [27,138–140]

During the simulation, the reactor was modelled as an external heat source and system pressure losses were accounted for, which include; 1.7% at both the high and low-pressure side of the recuperation, and 1.4% at the reactor. Bypass cooling of 0.5% and mass flow leakage of 1% were estimated based on knowledge of the main design parameters. Table 4-2 presents a comparison between the simulated engine performance results with published data in references [27,138–140]. From the results obtained, the component performance characteristics and gas path parameters predictions fell within close range compared with referenced information. Hence, this enabled a feasible simulation of the engine overall performance indicators such as power generated, cycle efficiency and exhaust gas temperature (EGT); which were in reasonable agreement with the reference data. In general, the average deviation of the simulated values from reference design point data was 0.39%.

This means that the aim of producing the engine performance parameters through accurate prediction of component characteristics parameters can be realized reasonably in GT-ACYSS.

Table 4-2 Comparison of Simulated results and Published Design Point Data for case 1

Description	Reference Plant DP (Published Data) [27,138–140]	GT-ACYSS (Simulated)	Deviations (%)
Turbine entry temp. (K)	1123	1123	-
Shaft Speed (rpm)	3600	3600	-
Compressor pressure ratio	2.0	2.0	-
Compressor inlet Pressure (MPa.)	3.5	3.5	-
Compressor inlet temp. (K)	301	301	-
Compressor polytropic efficiency (%)	90.5	89.9	-0.6
Reactor power (MW)	600	603	+0.5
Turbine polytropic efficiency (%)	93	91.8	-1.3
Turbine pressure ratio	1.88	1.90	+1.0
Turbine EGT (K)	884	886	+0.2
Flow rate at compressor (kg/s)	441.8	441	-0.2
Plant thermal efficiency (%)	46.8	46.9	+0.2
PC effectiveness (%)	95	95.0	-
RX effectiveness (%)	95	94	-1.0
Rated power (MW)	280	283.1	+1.1
Working Fluid		Helium	

Next, is to predict the engine compressor map and off-design condition at part-load. To achieve this, the reference map was digitized and replotted on the non-dimensional basis for easy comparison with simulated results as shown in fig. 4-10. The plot points in fig. 4-13 shows results of pressure ratio and corrected mass flow as a function of rotational speed. As the engine throttles from 0% to design capacity speed, both the pressure ratio and corrected mass flow moves to the right with an increase in their values. Similarly, the heat input at full load to part-load condition was predicted by varying the compressor inlet pressure at constant turbine entry temperature. Figure 4-14 describes the performance at part load using inventory control.

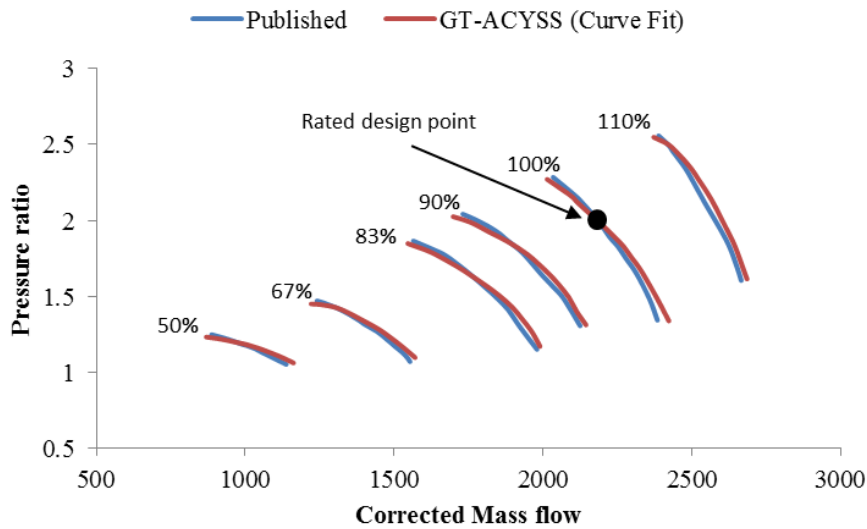


Figure 4-13 Compressor performance comparisons with GT-ACYSS at full speed

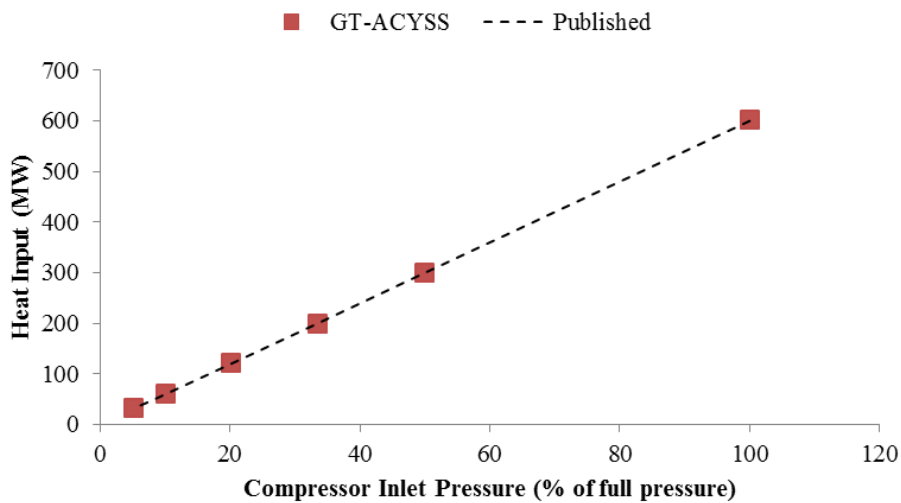


Figure 4-14 Heat power requirement comparisons from full to part-load

Comparing the simulated results to data in reference [138] showed quite a reasonable agreement, which confirms the validity of the program off-design simulation routine. For the compressor map, six-speed lines of the simulated result were analysed and their root-mean-square deviations calculated. The largest root mean square obtained was less than 0.5% which confirms that the results were quite in good agreement with reference data.

B. Case 2

The reference power plant simulated in case 2 is inspired by Escher Wyss Ravensburg power plant in Germany. Its main design characteristics were based on the cycle shown in reference [2]. The cycle consists of a low-pressure compressor (LPC), intercooler (IC), high-pressure compressor (HPC), recuperator heat exchanger (RX), gas-heater (GH), turbine, and a pre-cooler (PC). Both the LPC and HPC are driven on a single shaft.

Similar to case 1, total system pressure loss of 8%, mechanical losses to drive compressors at 10% and total flow leakage of 0.5% were considered during simulation. The design and operational data used for comparison were obtained from reference [2].

The result of simulation at the design point was compared with published data and the deviation calculated. A summary of the engine performance is presented in table 4-3. Again, the results of simulated performance parameters were in good agreement with the reference data with the largest deviation at 1.7%. In general, an average deviation of 0.45% was obtained from the predicted performance.

Figure 4-15 shows an off-design performance prediction at changes in compressor inlet temperature due to changes in the cooling temperature. To achieve the simulation goal, the compressor inlet temperature was used as an input. As the compressor inlet temperature increases at constant TET, the position of $N/\sqrt{T_1}$ changes, and the mass flow inventory is increased to compensate for the drop in power. Since the engine was designed to operate at constant power output, mass flow increase causes the system pressure to increase as shown in fig. 4-15. This change causes both the LPC and HPC pressure ratio to drop thereby reducing the cycle thermal efficiency. Although, there was no reference data to compare with the simulated result, however, the performance trend at varying condition seems to be in agreement with the behaviour of the closed-cycle gas turbine at changes in compressor inlet temperature.

Table 4-3 Comparison of Simulated results and Published Design Point Data for case 2

Description	Reference Plant DP (Published Data) [2,141]	GT-ACYSS (Simulated)	Deviations (%)
Turbine entry temp. (K)	935	936.0	+0.11
Shaft speed (rpm)	3000	3000	-
LPC pressure ratio	1.65	1.64	-0.60
LPC inlet pressure (MPa)	0.8	0.80	-
LPC inlet temp. (K)	290	290	-
HPC Pressure ratio	2.40	2.40	-
LPC & HPC Isentropic efficiency (%)	78.50	78.00	-0.60
Heat input (MW)	9.87	9.88	+0.10
Turbine Isentropic efficiency (%)	88	88.30	+0.30
Turbine pressure ratio	3.64	3.65	+0.20
Turbine EGT (K)	692.15	700.00	+1.10
Flow rate at Compressor (kg/s)	27.83	27.83	-
Plant thermal efficiency (%)	23.30	23.68	+1.63
IC effectiveness (%)	90.00	90.50	+0.50
PC, RX & GH effectiveness (%)	84.70	85.00	+0.35
Rated power (MW)	2.3	2.34	+1.74
Working Fluid		Air	

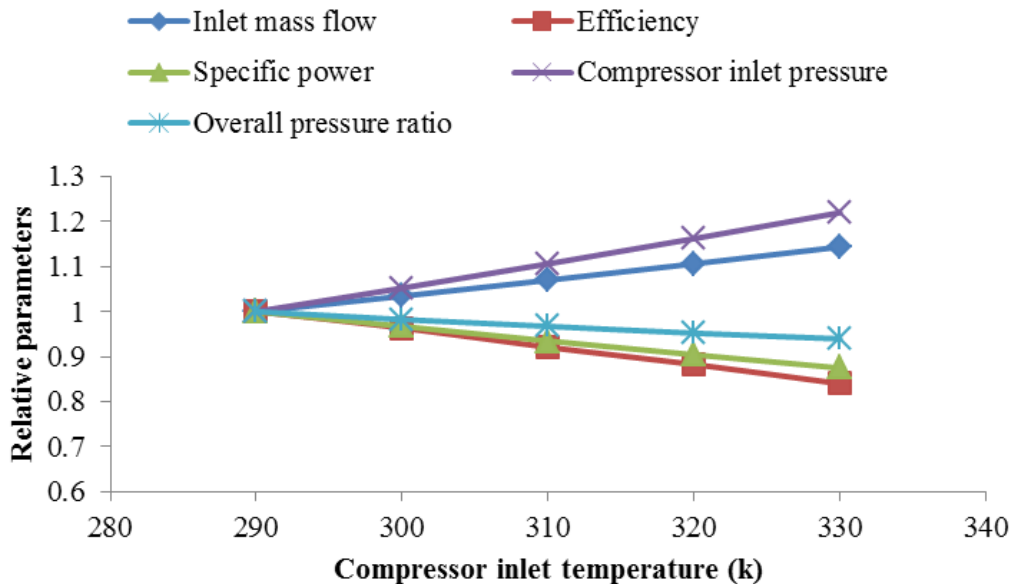


Figure 4-15 Variation in performance due to changes in compressor inlet temperature for fixed power operation

C. Case 3

The reference plant is a single-shaft recuperated closed-cycle configuration shown schematically in Figure 4-16. The major components of the plants consist of a turbine-compressor set, a recuperator, and a pre-cooler. The thermal energy is provided by the naturally-fired gas heater and nitrogen was used as a working fluid. The design point and off-design simulation of the reference engine were carried out in GT-ACYSS and compared with [110,142,143].

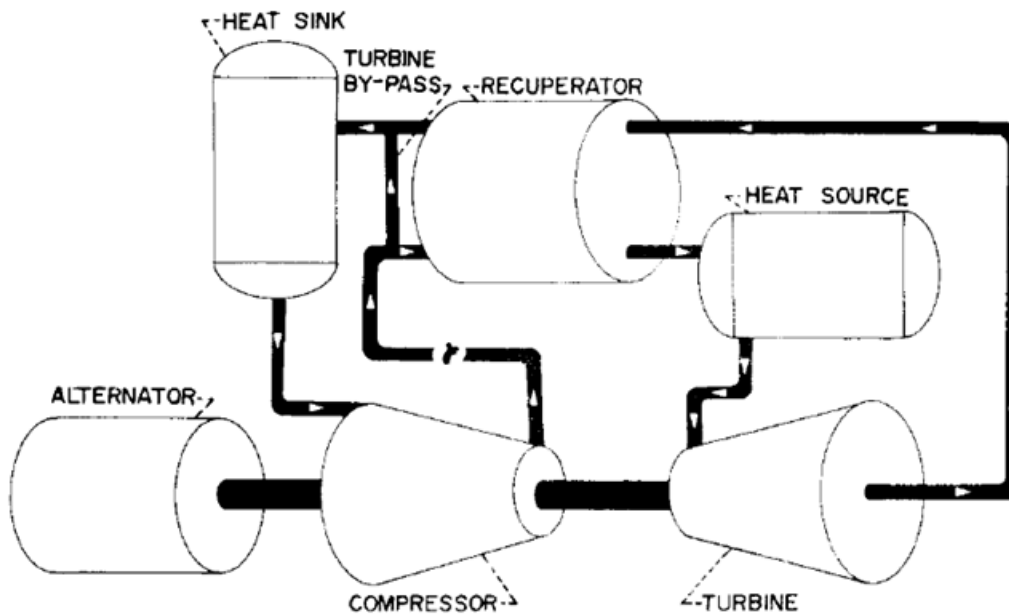


Figure 4-16 Schematic of reference plant modelled for case 3

Table 4 shows the performance comparison of simulated results with reference data at the design point. The simulated result its highest deviation of 2.5%. This may be due to modelling of the gas properties, however, the general results seem to be within reasonable limits an average deviation of 0.86%. Figures (4-17), (4-18) and (4-19) are the off-design performance of the engine compared with reference data. The off-design part-load presented in fig. 4-17 was simulated using bypass control. This means that the working fluid is bled off to short-circuit the gas heater (GH) and turbine into the low-pressure side of the recuperator, and, as such, the mass flow, pressure ratio and efficiency of the

turbine drop, causing a decrease in the output power. This control option is usually implemented in closed-cycle gas turbines to achieve fast control response on power drop and to prevent the shaft from over-speed.

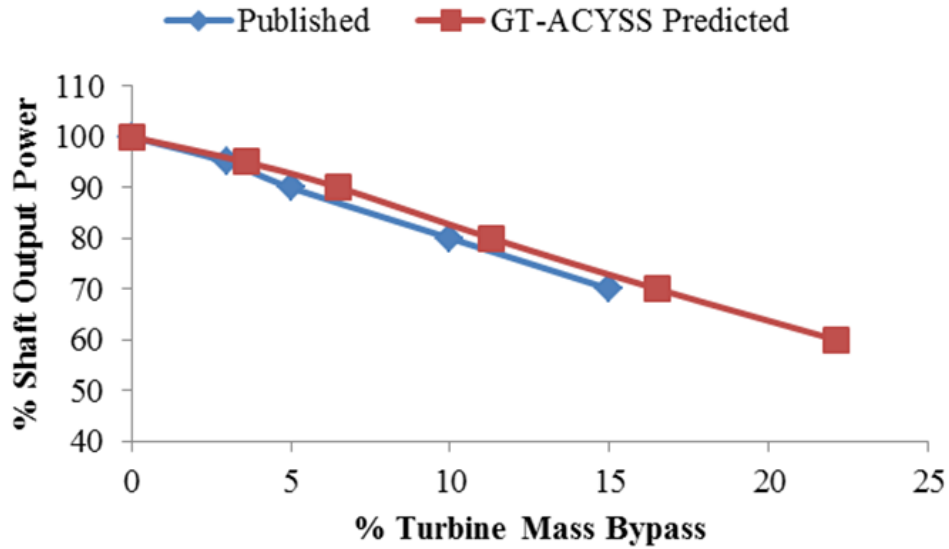


Figure 4-17 Part Load Performance Comparison

Table 4-4 Comparison of Simulated results and Published Design Point Data for case 3

Description	Reference Plant DP (Published Data) [110,142,143]	GT-ACYSS (Simulated)	Deviations (%)
Turbine entry temp. (K)	922	921.5	+0.05
Shaft speed (rpm)	22000	22000	-
Compressor pressure ratio	2.72	2.72	-
Compressor inlet pressure (MPa)	0.8	0.8	-
Compressor inlet temperature (K)	328	328	-
Compressor isen. efficiency (%)	82	80.40	-1.95
Heat input (MW)	3.058	3.133	+2.45
Turbine isen. efficiency (%)	86	84.70	-1.50
Turbine pressure ratio	2.38	2.36	-0.84
Flow rate at Compressor (kg/s)	11.8	11.10	-2.50
Plant thermal efficiency (%)	16.7	16.3	-2.40
PC effectiveness (%)	94	94.0	-
RX effectiveness (%)	79.0	78.8	-0.25
Rated power (MW)	0.510	0.511	+0.23
Working Fluid		Nitrogen	

The result in fig. 4-17 shows a close prediction of part-load performance compared to published data, with a root mean square deviation of 0.16%. In fig. 4-18 pressure ratio and corrected mass flow were plotted against engine rotational speed. As the engine speed is throttled from idle to synchronous idle at zero power an increase of pressure ratio and corrected mass flow is observed [144], which is consonance to the behaviour of closed-cycle gas turbines. This result demonstrates the capability of the code to simulate or monitor engine characteristics during idling.

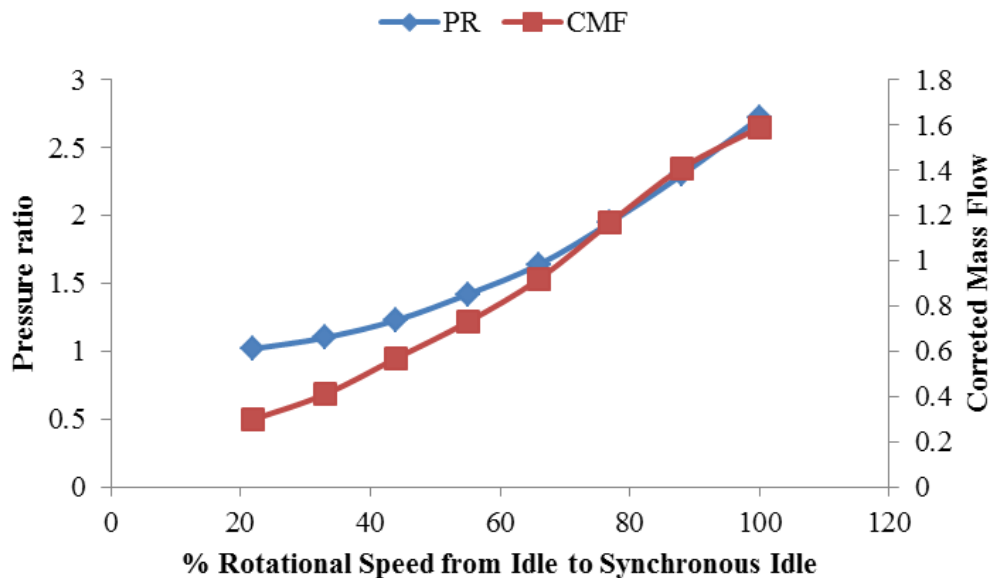


Figure 4-18 Engine rotational Speed as a function of pressure ratio and corrected mass flow

In fig. 4-19, the effect of changes in the compressor inlet temperature against the power output is presented. As expected, the power output followed a decreasing trend as ambient temperature increases due to a reduction in gas inventory and a decrease in $N/\sqrt{T_1}$. Comparing both simulated and obtained data results, a 0.3% mean deviation was obtained from the performance variations.

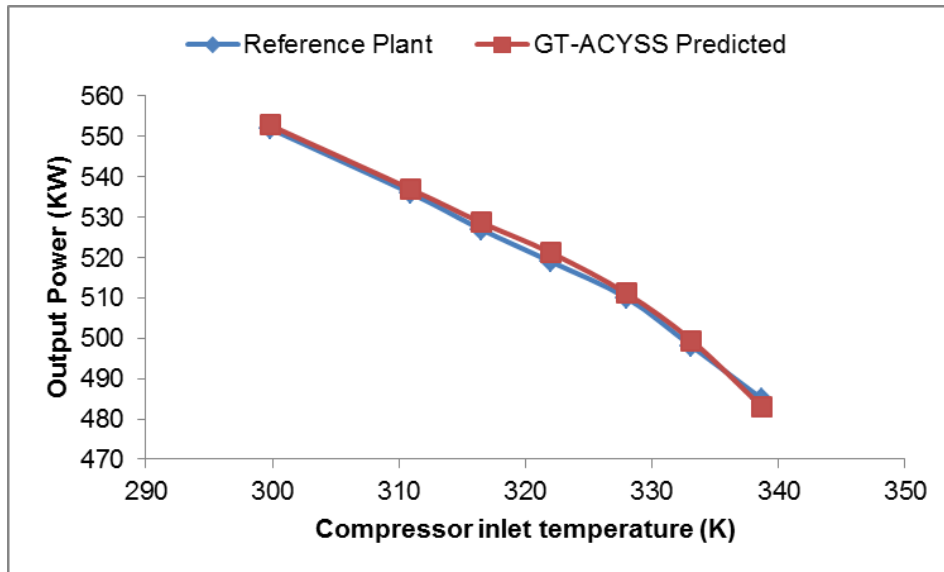


Figure 4-19: Effect of compressor inlet temperature

4.11.2 Application 2: Control Option performance analysis and Load Rejection

This section will present the results of performance simulation using GT-ACYSS control options. The reader is assumed to have read the preceding section on control options for background understanding of the control systems utilized in this research.

The following cases were simulated using different control options and the performance compared.

1. part-load operation
2. compressor inlet temperature variation
3. pseudo-transient load rejection

The main design characteristics of the reference plant used in this study were based on the cycle shown in fig (4-7). The cycle consists of a low-pressure compressor (LPC), intercooler (IC), high-pressure compressor (HPC), recuperator heat exchanger (RX), gas-heater (GH), turbine, and a precooler (PC). Both the LPC and HPC are driven on a single shaft. An example of the reference power plant is the Escher Wyss Ravensburg power plant in Germany. A summary of the plant characteristic is described in Table 4-5

Table 4-5 Summary of Power Plant Design Point Description

Description	Unit
Heat Source Temp. (K)	1100
LPC Pressure ratio	1.65
LPC Inlet Pressure (atm.)	8.2
LPC Inlet Temperature (K)	290
HPC Pressure ratio	2.40
LPC& HPC efficiency (%)	86
Turbine efficiency (%)	90
Flow rate at LPC (kg/s)	230
Plant Thermal Efficiency (%)	41.2
IC effectiveness (%)	90
RX & GH effectiveness (%)	90
Rated power (MW)	40.8
Working Fluid	Air

During the simulation analysis, the selected control options (inventory, bypass, and heat source temperature control) were assumed to operate independently at the same power level and the cooling medium was assumed to operate at constant temperature and flow. Cycle secondary effects were not considered throughout this analysis.

A. Part-load Operations

Generally, the primary goal of part-load operations using any control option is to maintain high efficiencies while keeping all components within their operating range. Theoretically, to achieve this will mean that overall temperature ratio and pressure ratio will be close to the steady state limits. However, this may not be easily satisfied using a single control option without making a compromise to certain practical constraints which will be discussed in this analysis. Fig.4-20 – 4-27 provides the part-load performance of the reference plant accomplished with the listed control strategies described in the preceding section. Each control option is assumed to operate independently at the same power level during the simulation analysis.

In the fig (4-20) – (4-21), part load operations were simulated with inventory control (ICS). During the operation mode of the ICS as shown in fig 4-7, circulating the mass flow of air is withdrawn from the power cycle almost proportional to the power output to keep the turbine entry temperature constant, whilst all temperature across the cycle remains constant for same LPC inlet conditions, which is controlled by the cooling medium. This withdrawal of mass flow reduces the density and pressures across the cycle as shown in Fig. 4-20. However, pressure ratios of LPC and HPC remain constant as can be seen in Fig.4-20, because the operating point N/\sqrt{T} and the non-dimensional mass flow, does not change significantly, hence, the cycle efficiency remains relatively constant as shown in Fig 4-21. At 50% output power, a cycle thermal efficiency of 40% was obtained. The slight drop in efficiency is a result small change in the working fluid properties. Nonetheless, this control option brings about a rapid acceleration of the shaft as the load is reduced which must be balanced.

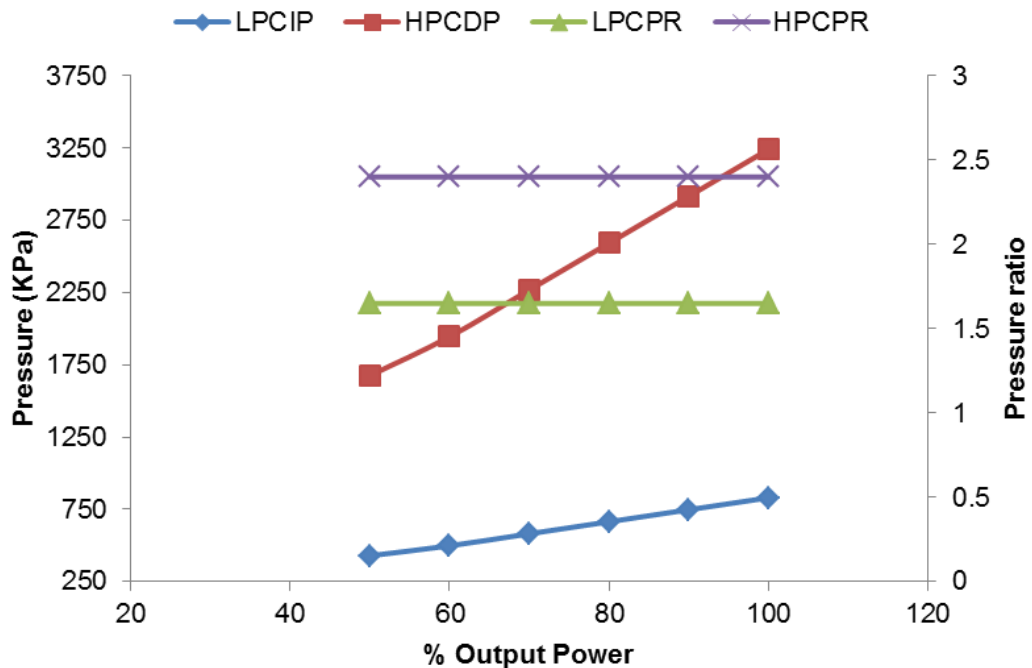


Figure 4-20 Effect of Part Load Performance on PR and Compressor Pressures using ICS

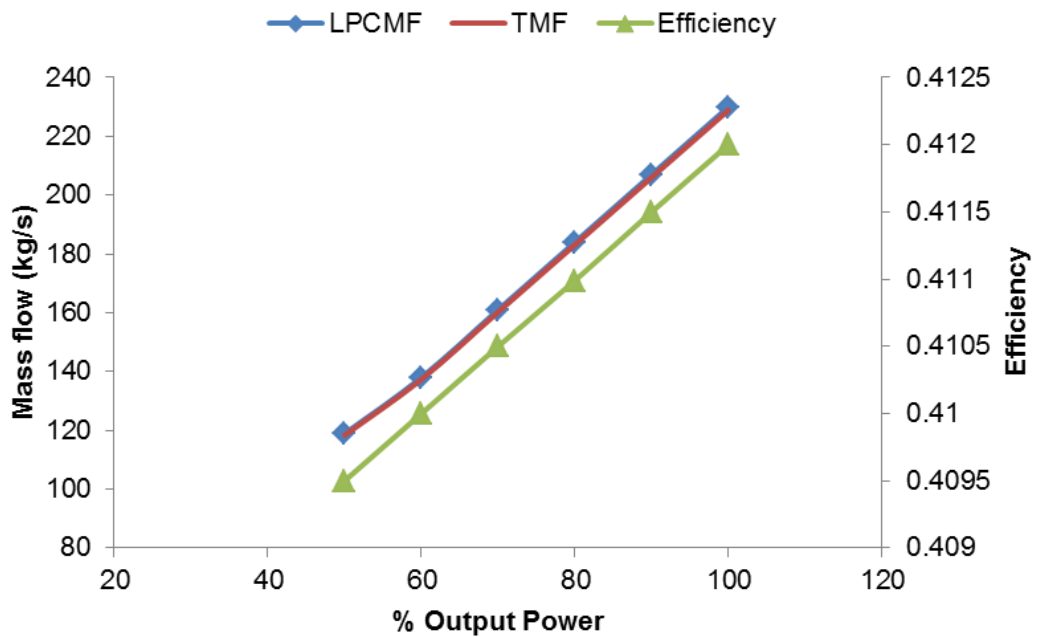


Figure 4-21 Effect of Part Load Performance on Mass Flow and Cycle Efficiency using ICS

In fig 4-21, it seems as though moving further low at part-load operation will be very beneficial with this control option since the efficiency is still reasonably high. However, the possibility of maintaining high part-load efficiency to any desired limit using the inventory control is restricted to the following: (a) the size and initial pressure of the tank, (b) centrifugal force on blade tip as a result of shaft rotational speed, (c) location of inventory valves in the cycle loop (d) availability of inventory transfer compressor, and (e) cost of implementing any of the listed options. A techno-economic study which addresses a, c, d, and e is presented in chapter 7 of the thesis.

Next, is to simulate the part-load operation using bypass control (BCS). In the bypass mode analysis, both the ICS and HST were kept constant. The performance of the BCS is presented in Fig. (4-22) – (4-23). As mass flow is bled off after the HPC to short- circuit the turbine, there is relative mass flow difference between the compressor and turbine which is translated in the reduction of the system operating pressure ratios and mass density. This reduction modifies the operating point to a new position (the new matching point

between the compressor and turbine) and reduces the turbine output power and cycle thermal efficiency as shown in Fig. (4-22) and (4-23). Both the LPC and HPC pressure ratio decreases with the dominant effect in the HPC. However, during this process, the LPC inlet pressure increases and the discharge pressure remain relatively the same as that of steady state when the fluid returns to the circuit as shown in Fig.4-7. From the results presented, using BCS for 50% output power drops the cycle thermal efficiency to 25.8%. This control option can be an effective means of part-load control from zero to full load rejection. However, its major drawback is the low efficiency obtained compared with other control options.

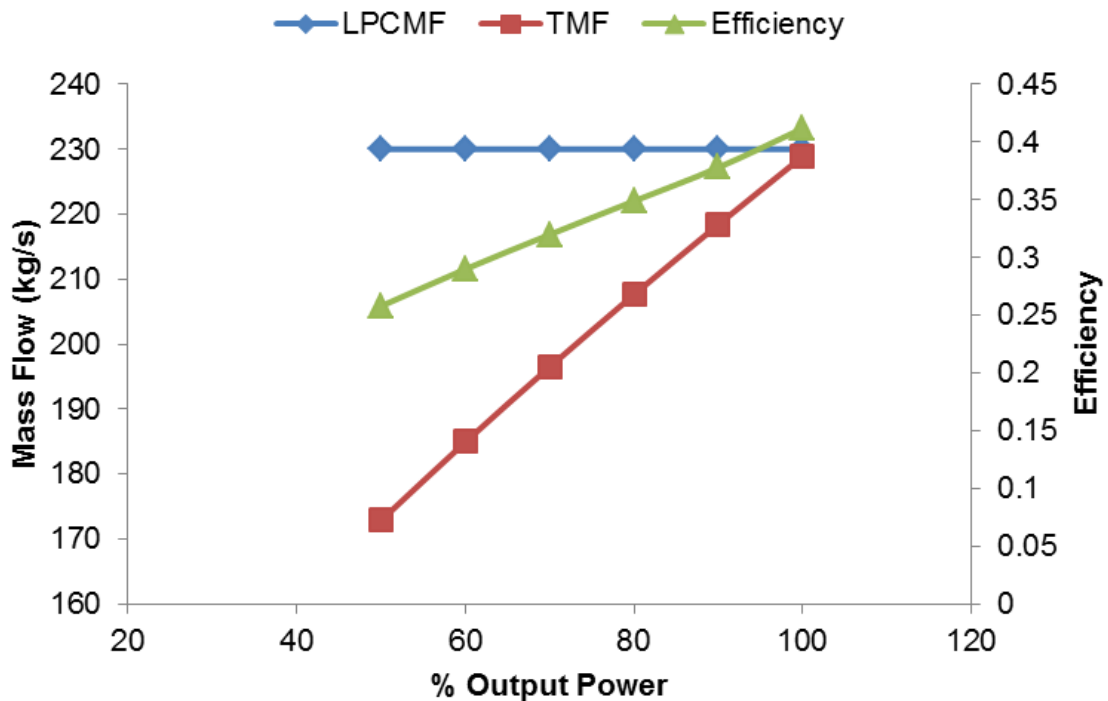


Figure 4-22: Effect of Part Load Performance on Mass Flow and Cycle Efficiency using BCS

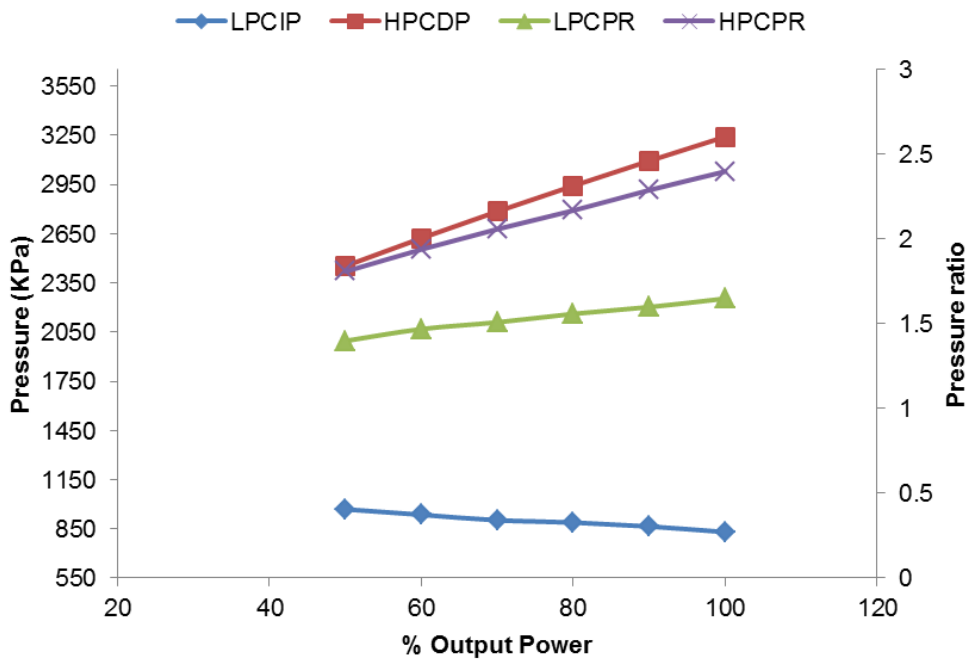


Figure 4-23: Effect of Part Load Performance on PR and Compressor Pressures using BCS

Another way part-load operation can be achieved is by decreasing the cycle highest temperature which achieved via the heat source temperature control (HST). With HST in active mode, both the ICS and BCS are assumed to remain constant. At part-load operation, the cycle temperature ratio decreases as result of a reduction in HST and changes the position of the pressure ratios downward thereby reducing the cycle thermal efficiency almost linearly from 41.2% to 31% at 50% output power as shown in Fig. 4-24 – 4-25. During the process, as the TET decreases, the density of the fluid entering the turbine increases and thus decreases the volumetric flow rate (for the same mass flow rate). This decreases the turbine pressure ratio. To alleviate this will require the fluid inventory to be increased. One drawback of the control option is that decreasing the system temperatures will require a slow rate of change to avoid thermal shock.

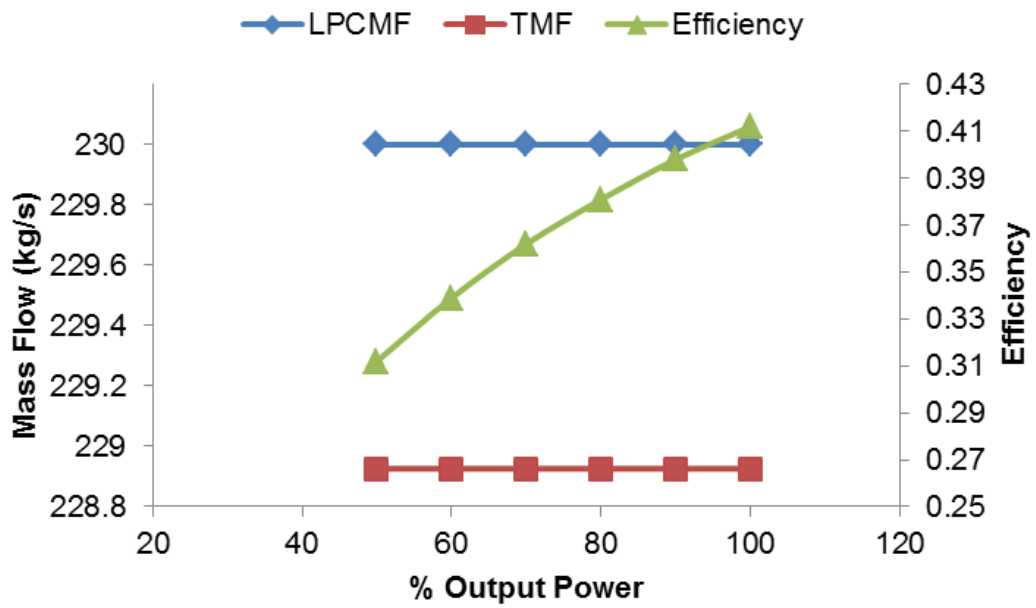


Figure 4-24 Effect of Part Load Performance on Mass Flow and Cycle Efficiency using HST

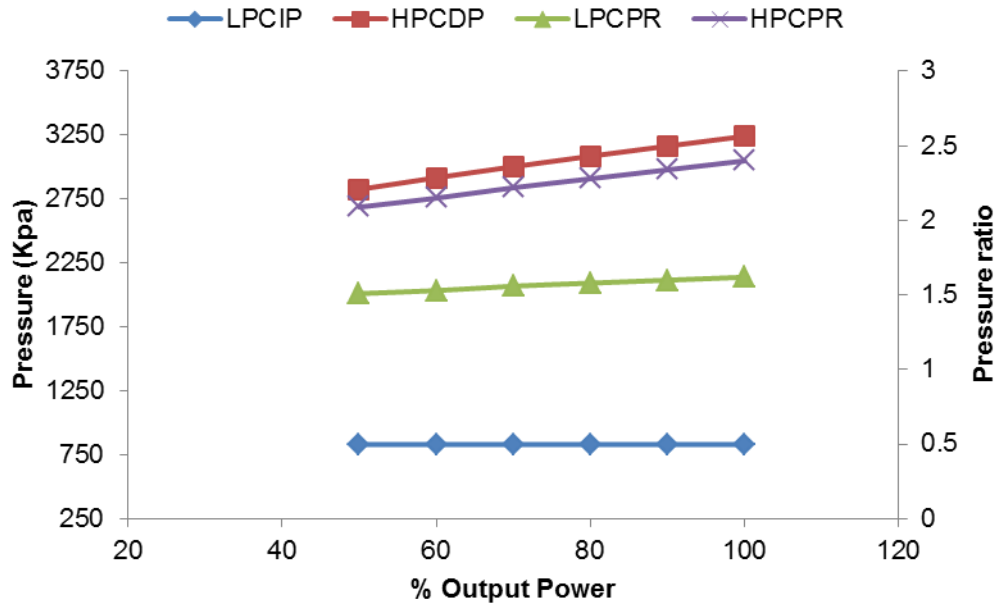


Figure 4-25 Effect of Part Load Performance on PR and Compressor Pressures using HST

Assuming some of the limitations of mentioned for each control option is neglected, Fig 4-26 shows performance comparison at part load in terms of overall cycle efficiency for each single control option and combination of two control options (second control option follows after the first control option). Simulating inventory followed by temperature control may not be feasible in practice without other control mechanisms since both strategies results to increase in shaft speed at part-load operations which could lead to mechanical failure of components. Inventory control followed by bypass is been mostly used for many closed-cycle power plant operations. This has been the most convenient method for stopping the engine if required. Another realistic control measure is the temperature and bypass control.

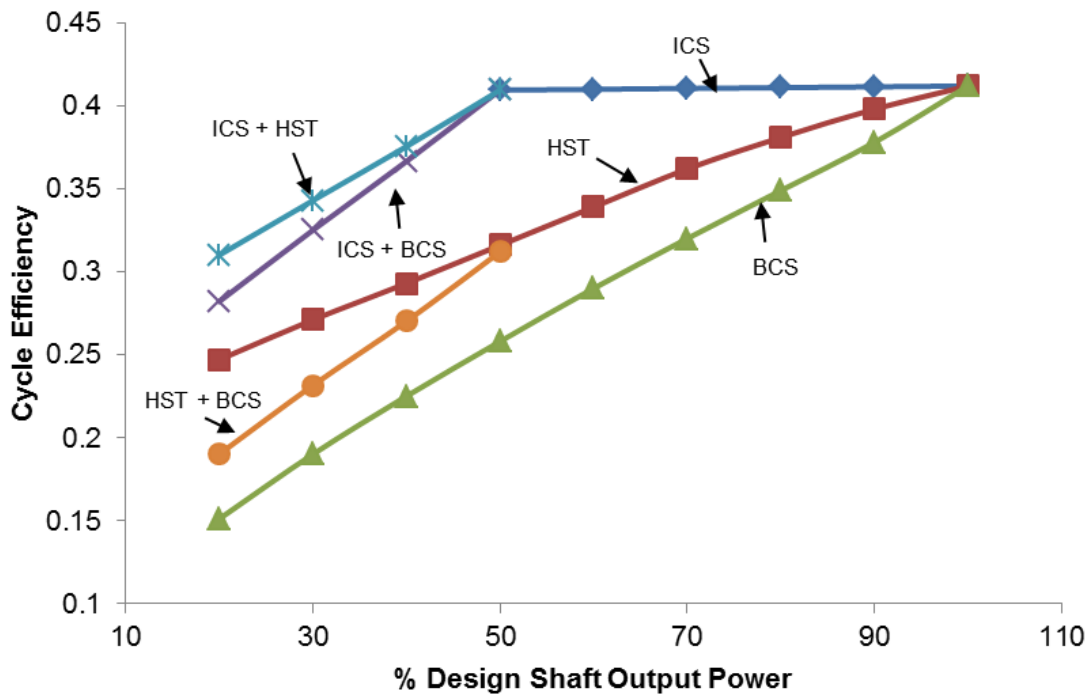


Figure 4-26 Comparison of Efficiency for Different Control Strategy at Part Load

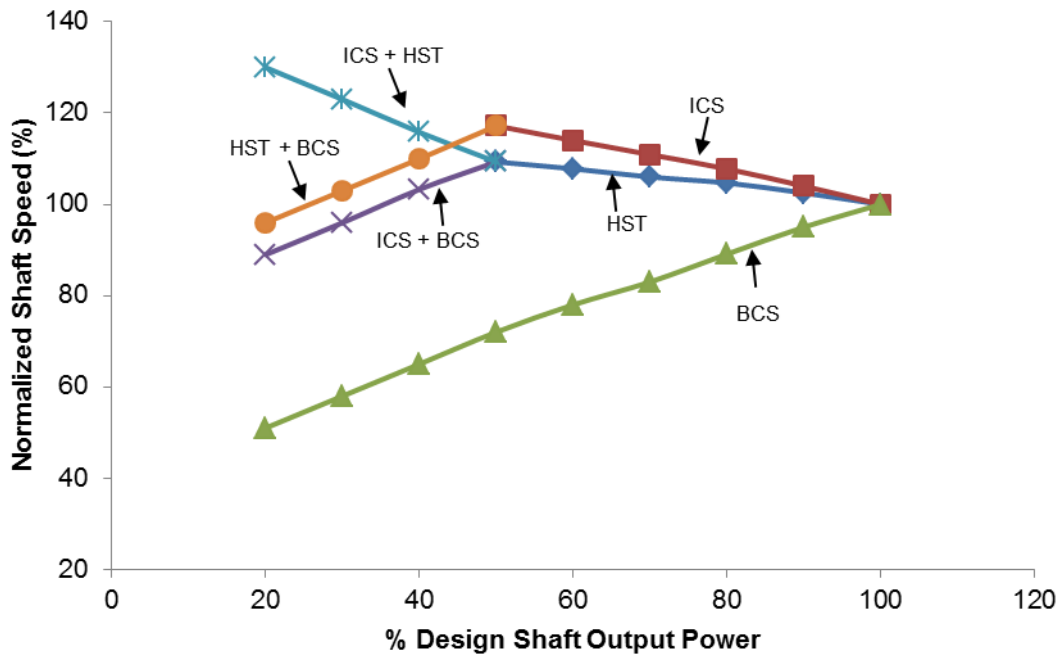


Figure 4-27 Comparison of shaft speed for Different Control Strategy at Part Load

B. Compressor inlet temperature variation

During this analysis, the intake inlet temperature was utilised as input. This was done as a representative of temperature to which the working gas is cooled before entering the compressor, which is dependent on ambient conditions, cooling medium and the design of the pre-cooler. In real closed-cycle power plant operation, once the compressor inlet temperature has been specified at the design point, any variation to this value will be as a result the cooling medium and ambient condition. In this analysis, the power plant is designed to operate always at fixed power conditions.

To this end, ICS and HST control were simulated independently, and their performance compared. Implementing the ICS during this off-design condition showed that a change in the LPC inlet temperature changes the temperature ratio, N/\sqrt{T} , mass density and pressure ratio at constant TET. These changes will result in a drop of shaft power and cycle thermal efficiency as shown in Fig. 4-28. Hence, to compensate for this drop at constant power operation mode

which is applicable to industrial power plant would require the opening of the ICS valves for injection of working fluid. This injection causes an increase in mass flow and pressure in the circuit as shown in Fig. 4-29.

Similarly, for HST control mode, an increase in intake temperature reduces the LPC and HPC pressure ratios thereby resulting in a low expansion in the turbine and drop in output power. Hence, to maintain constant output power settings, the HST control allows for an increase in turbine entry temperature, thereby increasing the heat rate as shown in Fig. 4-30 and 4-31

Apparently, implementing BCS for constant output power operation as intake temperature increases would require additional alternative control system because the mass flow has to be injected which cannot be handled by BCS alone.

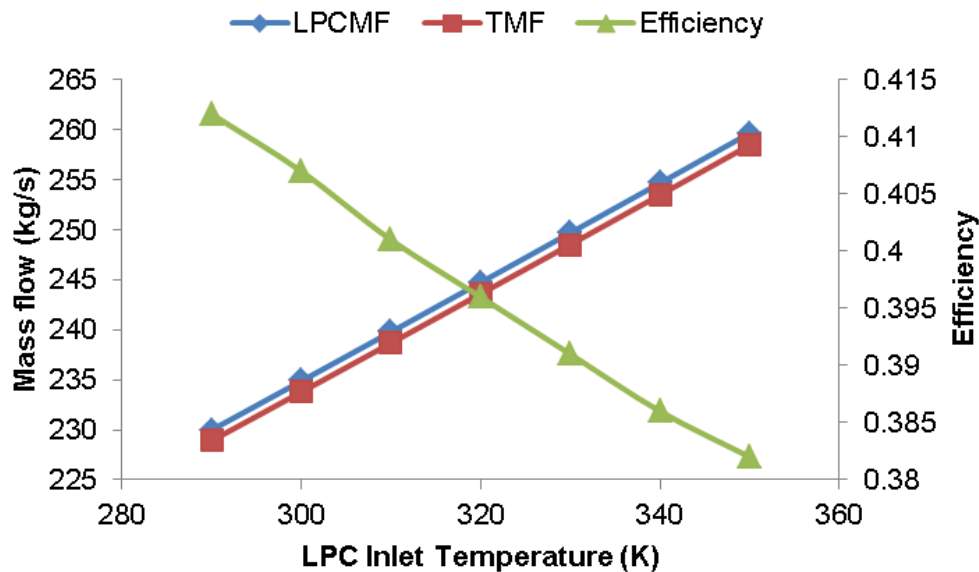


Figure 4-28 Effect of CIT on Mass Flow and Cycle Efficiency using ICS

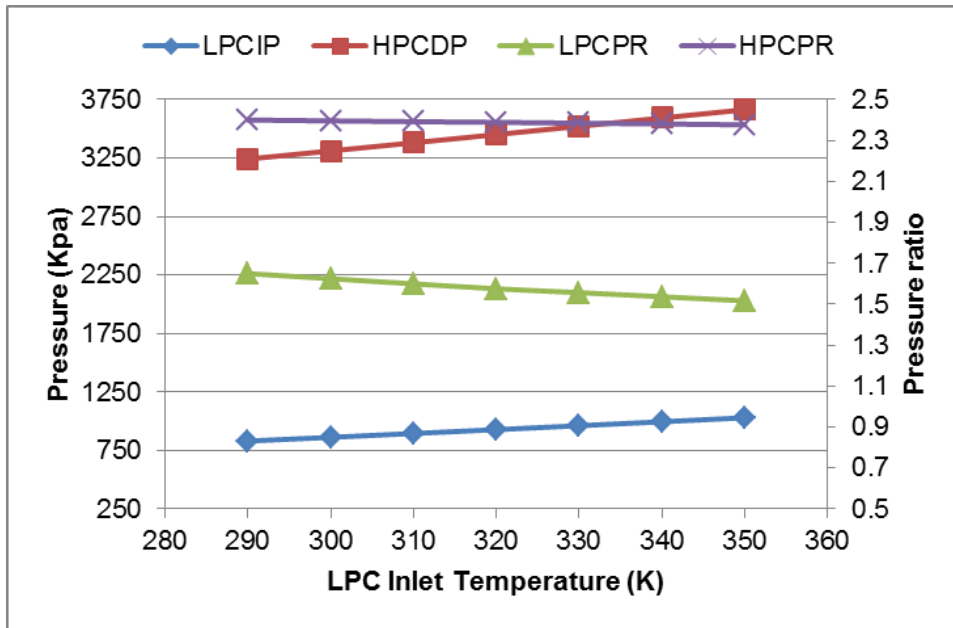


Figure 4-29 Effect of CIT on PR and Compressor Pressures using ICS

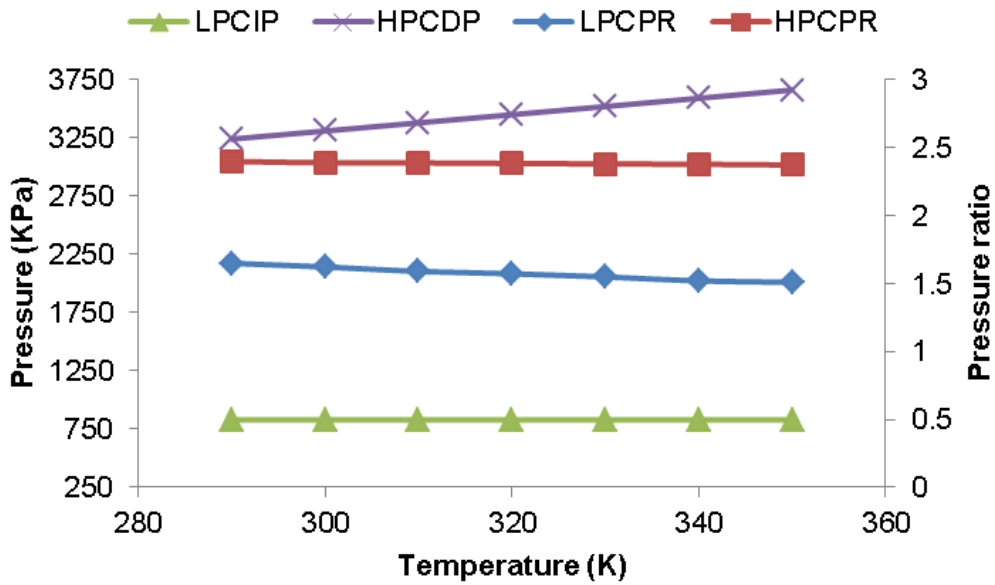


Figure 4-30 Effect of CIT on PR and Compressor Pressures using HST

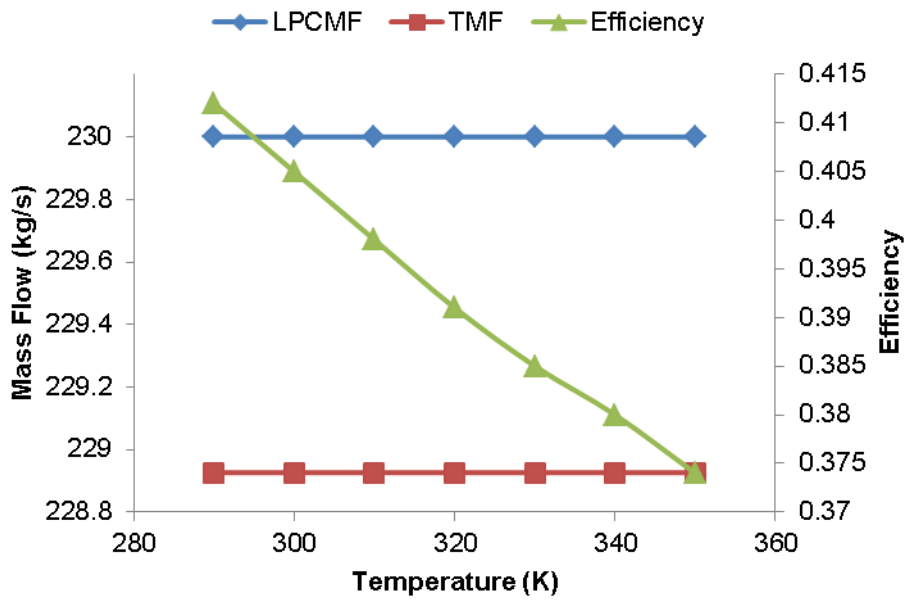


Figure 4-31 Effect of CIT on Mass Flow and Cycle Efficiency using HST

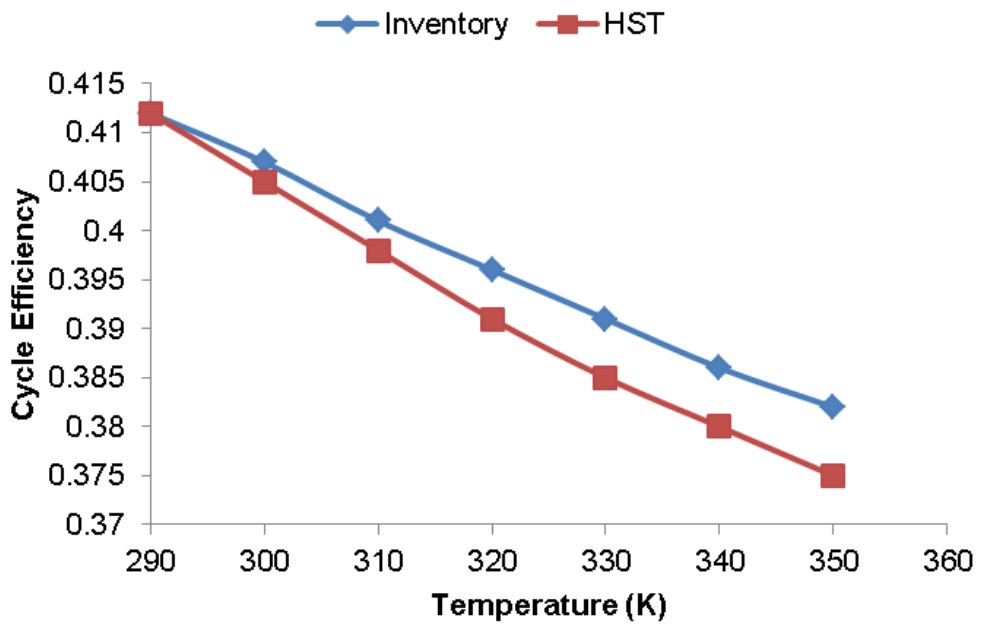


Figure 4-32 Comparison of Efficiency for Different Control Strategy at Changes in CIT

Fig. (4-26), (4-27), and 4-32 provides a performance comparison of the control strategies discussed at both part-load and varying intake temperature. At 50% load demand, inventory control maintained peak efficiency, while bypass control showed a rapid response to load change but produces the worst part load efficiency of 25.8% at same load demand. As changes in intake temperature increases, bypass control cannot compensate for such a drop in power, hence would require another control mode to be activated. The results also showed that HST control yielded fairly high efficiencies at both operating conditions; however, further reduction at part load using HST or ICS could lead to mechanical failure of rotating parts [31,89,136,145]

C. Load Rejection

It is essential for the closed-cycle power plant to operate in an efficient, safe, secure and reliable manner, hence, the use of different control options. The goal of each control mechanism is to maintain a symbiotic relationship with load demand or the electric grid, especially during instabilities, interruptions and emergency conditions. Stability is maintained by matching the power generated by the ever-changing load demand which can be triggered by environmental conditions, load-following mode, load rejection or emergency stop.

Load following is being able to increase or decrease the power plant output to balance changes in load demand, which is usually achieved by controlling the inventory level. In contrast to load following, load rejection is defined as a very rapid decrease in load demand (usually when the rate of change of power output is $>10\%$), which requires a rapid response via the control mechanism. Load rejection due to the loss of grid power is one of the most severe load control scenarios for a closed-cycle power plant which can be controlled with bypass valves (bypass valve rapidly opens to decrease the turbine work and increase compressor work to try to slow the accelerating shaft).

The focus of this section is to simulate in load rejection with bypass control mechanism for power plant shown in fig. 4-7 and table 4-5.

Simulation Setup

- Only bypass control was utilized for this simulation
- Load rejection was simulated in steady-state pseudo transient operation (load rejections was set at 20% per seconds)
- The bypass valve size was assumed
- Rotor inertia was assumed
- Rotational speed was set at 3600rpm
- ICS and HST were kept constant
- Secondary effect was neglected

Figures (4-33) – (4-35) clearly shows the behaviour of the power plant during load rejection. In the steady state operation of the plant, the torque developed must be balanced with the load torque determined by the required power. As the load torque changes, there is an imbalance resulting in a change in the rotational speed, system temperatures, and pressure ratios.

The bypass valve opens to prevent the turbomachine from over-speed and to keep the cycle operation ready for any load recovery. In reality, the bypass valve is designed to provide system shut down to an idle state as in the case of a load rejection, and completely stop as in the case of any turbomachinery failure. However, during the process of bypass system control, other control processes are activated for example HST control to prevent thermal overstressing of the recuperators.

During the simulation, the steady state full power operation is disturbed by the load reduction starting at $t = 0$. The electric load is reduced at 20% per sec for 5 secs when it has reached the nominal no-load level. Fig 4-33, shows the reduction of the engine power output in case of a load release or quick shut down within few seconds from 0% to 100% full load release by means of opening of the bypass valve and to maintain nominal engine speed. As can be seen, as the load release increases at BVC, the engine over-speed increases from 1% to 30% and the system pressure ratios also

increase. The over-speed triggers the bypass valve to open. When the bypass valve is opened, the working fluid flow bypasses the turbine thereby reducing the turbine torque and power by reducing turbine flow and pressure ratio as shown in fig 4-33 & 4-34. This BVO results in a rise in temperature at the turbine output which is caused by a drop in expansion ratio and therefore the enthalpy gradient in the machine. Thus, the efficiency of the turbine reduces rapidly to almost zero percent at full load rejection. The pre-cooler load increases as the major portion of the flow are circulated through it while the recuperator load decreases due to the lower mass flow through it as shown in fig 4-35.

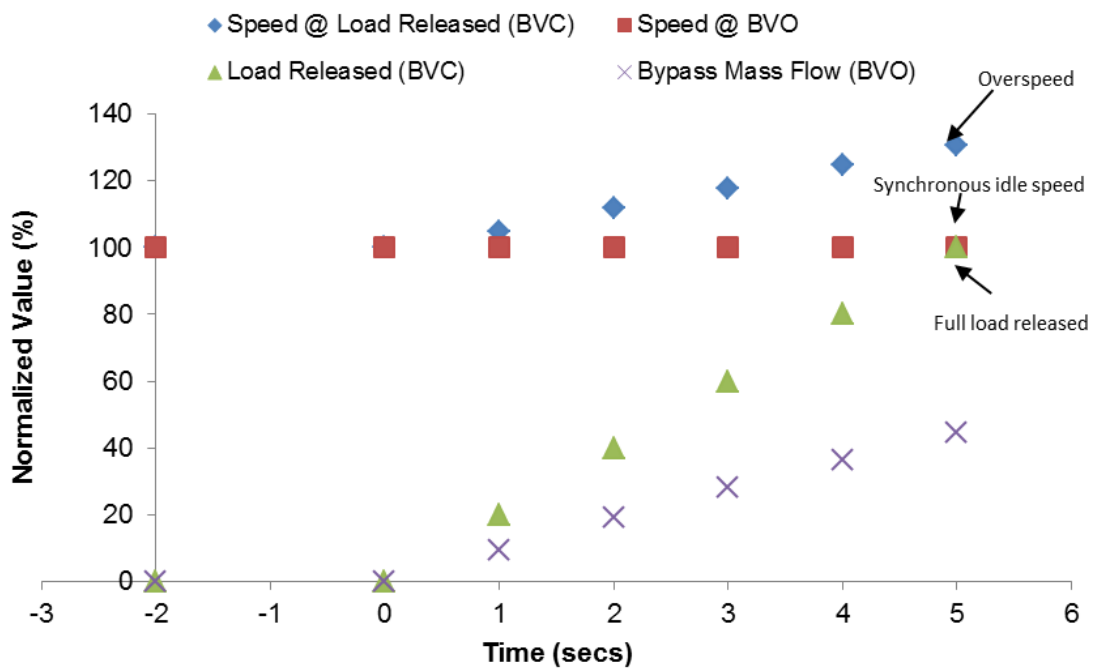


Figure 4-33 Estimation of Pseudo-Transient Behaviour with bypass control (speed & load released)

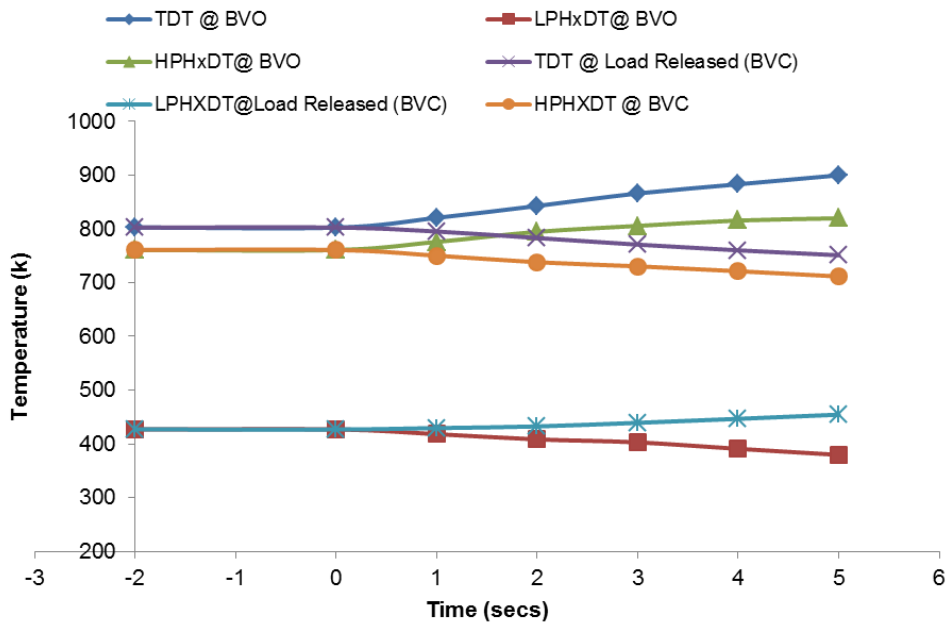


Figure 4-34 Estimation of Pseudo-Transient Behaviour with bypass control (system temperatures)

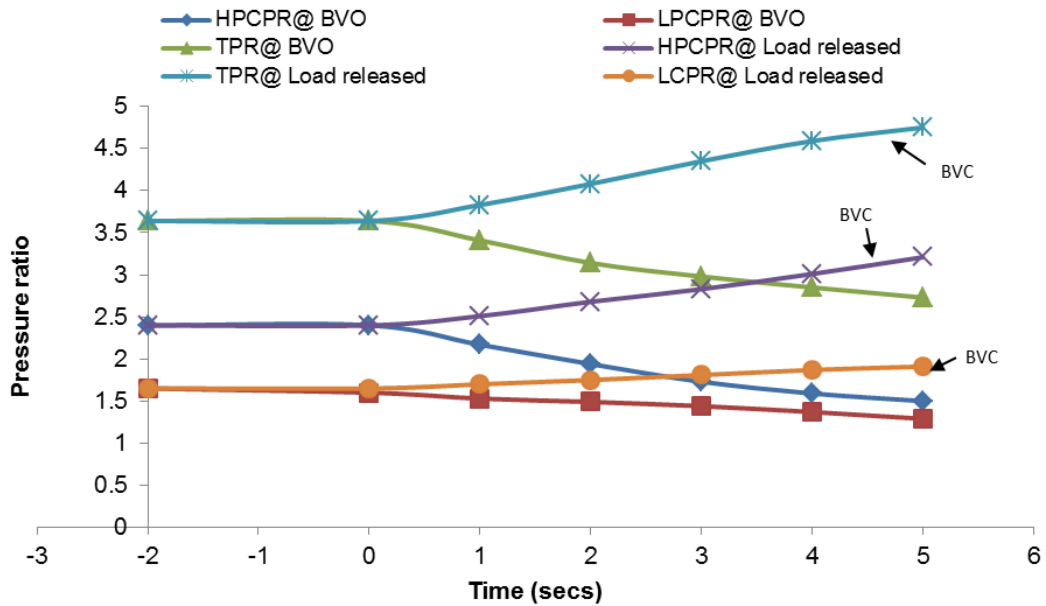


Figure 4-35 Estimation of Pseudo-Transient Behaviour with bypass control (system pressure ratios)

4.12 Technical studies on Inventory Control

Among the various control options in closed-cycle gas turbine operations discussed previously, the inventory control option has been widely mentioned as an attractive possibility because it allows the power plant to operate within a wide range of load fluctuation at a good cycle thermal efficiency. However, there are certain factors mentioned in section 4.8.1 that can limit the possibility of maintaining high cycle efficiency as the level of load control decreases such as (a) the size and initial pressure of the tank, (b) centrifugal force on blade tip as a result of shaft rotational speed, (c) location of inventory valves in the cycle loop (d) availability of inventory transfer compressor, and (e) cost of implementing any of the listed options. In this section, a technical study on the influence of initial tank pressure and size of the tank using pressure differential as the driving force of the inventory control is presented. The second part of this analysis is an economic cost comparison between using multiple inventory control tanks and using an additional transfer compressor for fluid extraction and injection in the system circuit. A single-shaft intercooled-recuperated closed-cycle gas turbine plant represented in Fig 4-7 is used for this study and its main characteristics are shown in Table 4-6.

Table 4-6 Summary of Power Plant Design Point Description

Description	Unit
Heat Source Temp.	1100 (K)
LPC Pressure ratio	1.65
LPC Inlet Pressure	8.2 (atm.)
LPC Inlet Temperature	290 (K)
HPC Pressure ratio	2.40
LPC& HPC efficiency	86 (%)
Turbine efficiency	90 (%)
Flow rate at LPC	230 (kg/s)
Plant Thermal Efficiency	41.2 (%)
IC effectiveness	90 (%)
RX & GH effectiveness	90 (%)
Rated power	40.8 (MW)
Working Fluid	Air

The scenario for the size of tank is represented as: (a) the working fluid flowing from the HPC into a single ICT by natural pressure differential, so that the extraction of the working fluid stops when the pressure at the ICT and the HPC

discharge pressure is at equilibrium, as shown in Fig 4-7 (b) further extraction via natural pressure differential is achieved by using multiple ICTs as shown in Fig 4-36. After the pressure equilibrium has been reached, further extraction into the ICT is achieved by means of transfer compressor TC, as shown in Fig 4-37. In this technical study, the results of influence mass transfer on tank temperature, design and weight analysis of the ICT were discussed. The principal goal of this study is to ascertain the technical and economic benefit for choosing any three options under consideration: a single ICT, multi-ICTs or inventory control with transfer compressor.

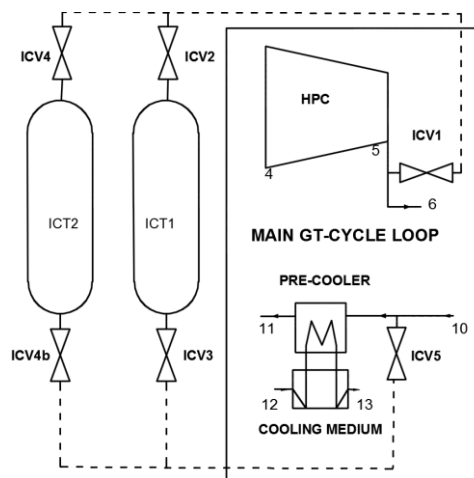


Figure 4-36 Inventory Control with Multi – Storage Tank using a Natural pressure differential

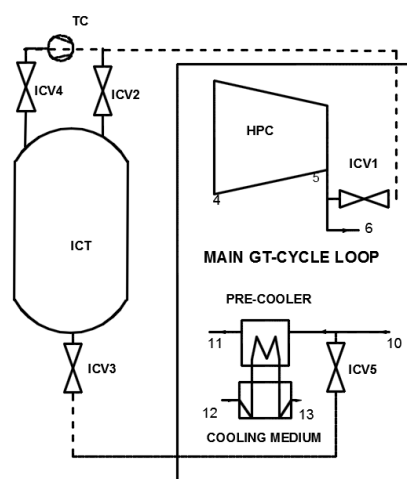


Figure 4-37 Inventory Control with Transfer Compressor (TC)

In this study, the minimum power range is not fixed but determined by the ratio of the HPC discharge pressure to tank pressure, and the number of the tanks.

4.12.1 Method of Analysis

A modified Bitsch et al [132] model was implemented in developing the physical procedure to represent the inventory load control system of the reference plant. The storage tank utilised for this purpose is an ASME standard pressure vessel. An overview of the procedure used for this analysis is described in figure 4-38

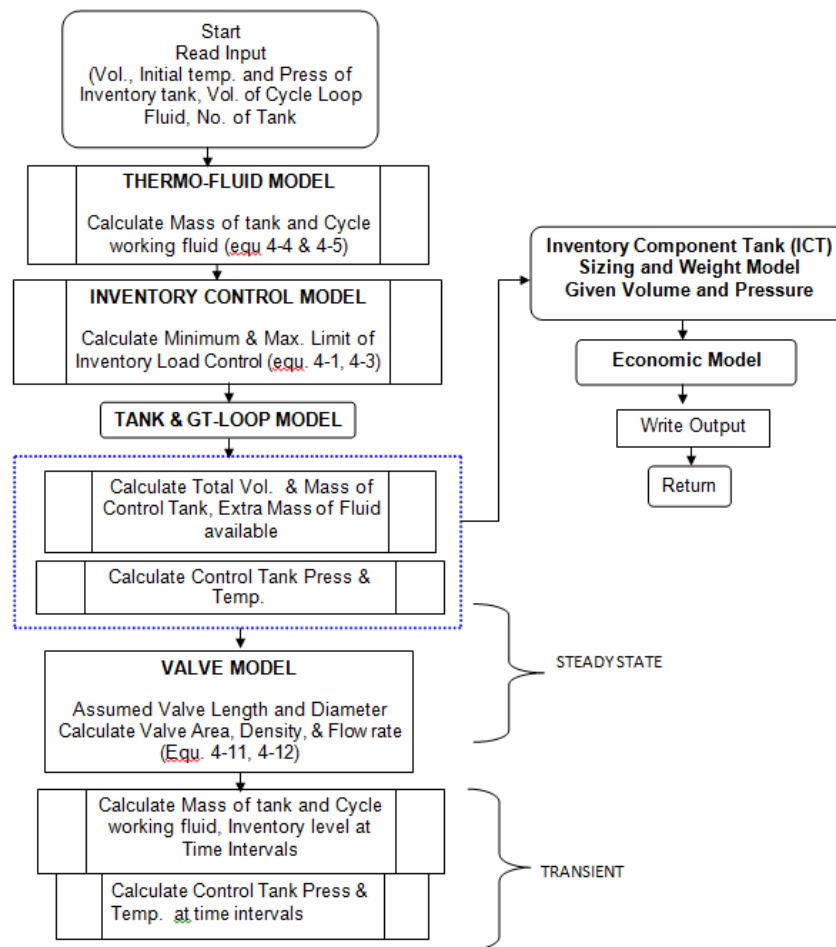


Figure 4-38 Procedure for Analysis

The modelling equations for the thermo-fluid model, inventory control model, storage tank & GT-loop model and valve model have been presented in Eqs. (4-53) – (4-64). The weight & sizing model is presented in Eqs.(5-27) – (5-39) and the economic model for the inventory control system is presented in Eqs. (6-10) – (6-12).

4.12.2 Results and Discussion

The analysis provides justification, on the importance of extracting the working fluid to its optimum minimum load requirement and returning the working fluid to 100% load capacity during load increase.

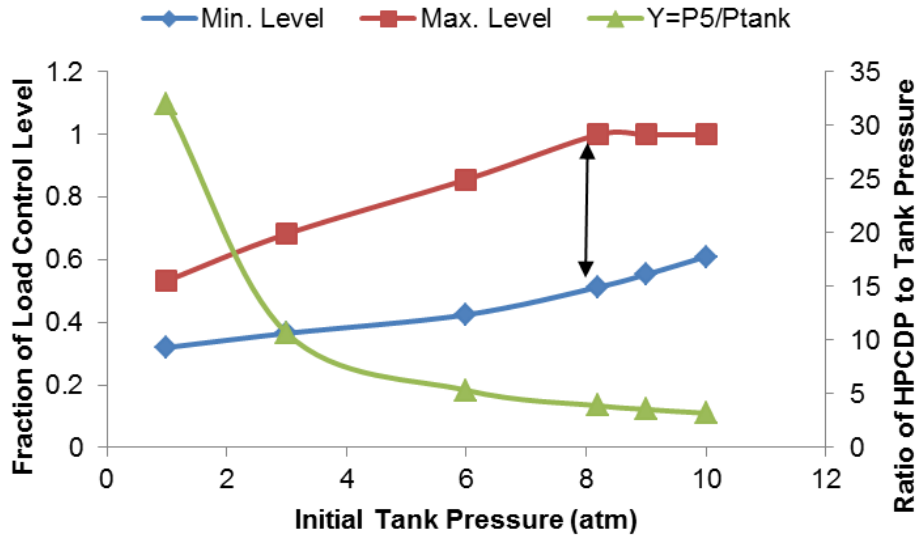


Figure 4-39 Effect of Tank Pressure on Inventory Control Level

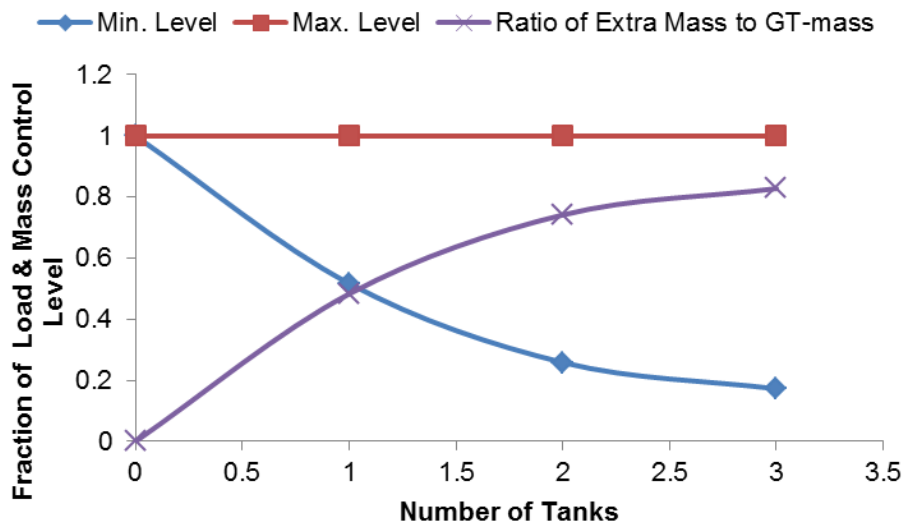


Figure 4-40 Effect of Number of Tanks

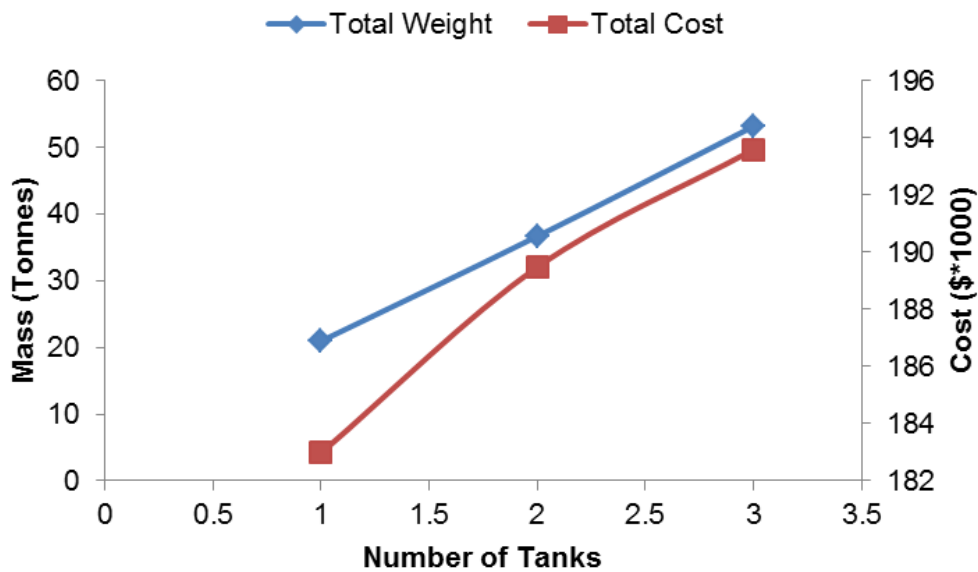


Figure 4-41 Weight and Cost Analysis of ICS

Figure 4-39 describes the influence of ICT initial pressure on the limit of load control by the ICS using a single ICT. The blue line represents working fluid transfer from the HPC exit into the ICT in the case of load decrease, while the red line represents a transfer from the ICT into cycle loop through the pre-cooler inlet in the case of load increase. At an initial ICT pressure of 1 atm., the load reduced at the optimum point of 32% by the natural pressure differential. However, during load increase (return of fluid from ICT to GT cycle loop), the maximum load levels that can be returned using pressure differential would be 53%. This is because at this point the ICT pressure and the cycle intake pressure becomes equilibrium, which implies that a transfer compressor will be required to return power to full capacity. As the initial tank pressure increases, the minimum load control decreases and the maximum return to full load increases. At an ICT initial pressure equal to or greater than the LPC inlet pressure, the nominal value of 100% load can be reached but at a minimum part load of 50%.

To obtain a reasonable wide range of load control would mean that either (a) the total volume of the ICT is increased by increasing the number of ICT or (b) an auxiliary transfer compressor is installed. For alternative (b), this would imply

that the ratio of the HPC discharge pressure to the ICT initial pressure determines the location of the auxiliary transfer compressor. For alternative (a), the increase in the total volume of ICT would be represented by increasing the number of ICTs.

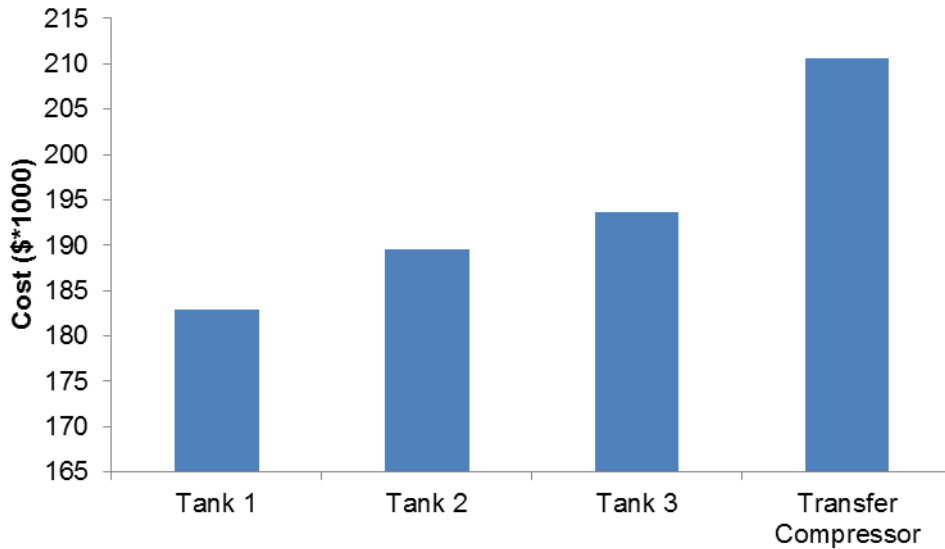


Figure 4-42 Cost Economics of Inventory Control Options

Figure 4-40 represents the influence of a number of tanks on the load control level. During this analysis, the initial pressure of the ICT was assumed to be equal to the LPC inlet pressure, so that at all point the 100% return load can be obtained. Therefore, as the number of tanks increases, the ICS reduces the load level and the ratio of extra mass to the cycle loop mass increases. Comparing the results for a different number of tanks shows that for a single ICT with an initial tank pressure equal to LPC inlet pressure, the minimum inventory load level obtained for the single ICT is 50% and for two (2) ICTs 26% minimum load level can be obtained.

Figure 4-41 represents a breakdown of the weight of ICT components and their respective cost. From the results, the cylindrical shell contributed over 70% of the total weight of the ICT. As the number of tanks increases, the weight per tank decreases, because of the decrease in volume per tank.

An economic trade-off on which approach to consider in terms of capital cost is described in Figure 4-42. The decision to take any particular approach may also require maintenance considerations, operations, and contingency cost. However, the results in represented in Figure 4-42 favors the increase in a number of tanks to cost of installing auxiliary transfer compressor by a factor of 0.08 at 17% load control level.

The main conclusions from this study are as follow:

- The initial tank pressure and the total volume of tanks influence the load control range.
- If the ICS is to be designed such that 100% inventory can be restored without the use of auxiliary transfer compressor, then the ratio of the cycle peak pressure to the ICT initial pressure should be relatively equal to the cycle overall pressure ratio.
- The ratio of the cycle peak pressure to the tank initial pressure determines the location of the auxiliary transfer compressor.
- The capital cost of implementing an increased ICT volume provides a better option compared with auxiliary transfer compressor cost.
- The pressure differential provides a preferred mechanism as it takes advantage of the existing pressure variation between the GT-cycle loop and ICT without reliance on additional turbomachinery, which is potentially expensive.

4.13 Chapter Conclusion

This chapter describes a procedure that has been used to develop GT-ACYSS; a performance simulation for closed-cycle gas turbines. The program was written in Fortran 90. The main features of the procedure are that components can be assembled to represent different engine configurations; therefore it should prove to be useful for exploratory studies at the design stage. Four different working fluids have been incorporated to give the user flexibility and the results from the verification of the fluid properties modelled show a mean

deviation between 0.04% and 0.1%. Another feature of the program is the flexibility to analysis the performance of different control options.

The performance of a single-shaft intercooled-recuperated closed-cycle gas turbine under three independent control strategies has been presented. The rationale behind this analysis was to explore the different control strategy and its independent iterative procedure for the closed-cycle gas turbine. The results presented showed that the inventory control strategy has a high efficiency at both part-load and design in ambient conditions compared with other control options presented. However, its limitation for a continuous discharge of gas inventory at reduced load depends on the rotational speed for which the centrifugal forces acting on the blade tips could become too high and on the size and pressure of the storage tank. Also, continuous increase by the HST can also lead to an increase in shaft speed.

To avoid as much as possible these limitations in shaft speed or low efficiencies at a further reduction in power would require, a combined control mode to be adopted. The bypass control would rather recommend for rapid load response and shaft speed control.

Also in this chapter, a technical study on the inventory control requirement options to maintain high cycle efficiency at part load is presented. The results show the initial tank pressure and the number of inventory tank have to influence on the load control level. As the number of inventory tanks increases, the load control level reduces and the system is still able to provide high part load efficiency.

5 EFFECT OF WORKING FLUID ON PERFORMANCE AND DESIGN OF CLOSED-CYCLE GAS TURBINE

5.1 Background

The degree of flexibility in using different working fluids is a unique characteristic of the closed-cycle gas turbine [2], which has recently contributed towards its adoption in several applications such as land-based power plants, space, and marine power supplies [4,45]. From the viewpoint of thermodynamic performance, all permanent gases can be utilized as working fluid for closed-cycle gas turbine operation, since fluid will be operated in the gaseous region beyond its critical temperature all through the cycle. However, selection of the appropriate working fluid depends on meeting several criteria, some of which are dictated by the special requirements of the existing conversion module. Any selected fluid should have an acceptable level of thermal stability at maximum cycle temperature dictated by the heat source temperature. It should not be corrosive to the materials of the machinery and should be readily available at modest cost. Other factors to consider include inflammability and toxicity.

Among these gases, air has been the most common working fluid utilized in land-based power plants, whereas for space power applications, where weight and size are important, monatomic gases like helium, argon, and mixtures of helium and xenon can be utilized [63–65]. For a nuclear heat source, helium and carbon dioxide have been successfully implemented in past for reactor cooling and steam generation [2].

The content of this chapter is principally to present analyses for the effect of selected working fluids on the components design and performance of the closed-cycle gas turbine. The purpose of the working fluid study is to identify

and compare the candidate fluids suitable for investment decisions from component design perspective, overall system performance and plant operations for working fluid switch which may not require major modification on the engine configuration. The analysis of both the performance and the component model was carried out using GT-ACYS; a tool which has been described in previous chapters. An overview of the component design model utilized for calculating the engine component sizing is also presented in this chapter.

5.2 Working Fluid and Material Compatibility

As previously mentioned, most gases are potentially viable for closed-cycle gas turbine operation. However, for the purpose of this study, the following gases were selected:

- Air
- Carbon Dioxide
- Helium
- Nitrogen

Air is the most readily available; therefore, the proposal for utilizing any other gas as working fluid should be as good as, or better than air to justify its use. The air was selected simply for performance comparison with other gases. Corrosion resistance is formed by creating a protective oxide layer on the metal surface which is a result of chemical interaction between chromium and oxygen. Carbon dioxide was selected because it has good critical properties for this application; it has good thermal stability at high cycle temperature; it has low corrosion levels to materials to be used and its thermodynamic and transport properties are fairly well known [64,65,81]. It has also been considered as a potential working fluid since it may have a positive environmental impact. Carbon dioxide has an oxidizing effect on most metals and easily forms a protective oxide surface layer. Impure carbon dioxide can cause a carburizing effect on the component materials. Helium has been a thermodynamically attractive choice due to its inert nature toward metallic components and its high heat properties to the overall performance of the engine. However, high-purity

helium is required to prevent carbide formation when it reacts with component materials. Nitrogen was used because of its availability and material compatibility. This has also been implemented in real operation of closed cycle gas turbine. However, nitrogen may create some difficulties due to nitriding.

Consequently, the gases selected have been successfully used for closed-cycle gas turbine units in operations [2,9,27,48,49,64]. A summary of remarks on these gases has been presented in Table 5-1.

Table 5-1 Remarks on Working Fluid

Fluid	Critical Temp.(K)	Critical Pres. (atm.)	General Remarks
Helium	5.19	2.24	Very good materials compatibility, very good heat and transport properties, expensive
Nitrogen	126.2	33.5	Satisfactory material compatibility, moderate heat, and transport properties, readily available
Carbon Dioxide	304.19	72.8	Satisfactory material compatibility, good heat, and transport properties, readily available
Dry Air	132.65	37.71	Poor material compatibility, moderate heat, and transport properties, readily available

5.2.1 Working Fluid Safety Issues

Safety is another important aspect of considerations on the choice of working fluid because there could be hazardous effect in any eventuality of leakage, or explosions of pressure parts as a result of metal embrittlement. Apart from nitrogen which can react with oxygen at high temperature, other fluids selected seem to be non-toxic, and non-embrittling. Another important aspect of safety and operational concern in the use of a working fluid is the nature of their chemical reactions [80,81] especially when the working fluid is different from the reactor coolant.

5.3 Performance Parametric Analysis

The aim of the parametric analysis is to understand the factors influencing the design point performance selections and working fluid considerations for the closed-cycle gas turbine power plant and to enhance decision-making process

of selecting the optimum cycle performance characteristics. This will assist in the identification of the characteristics requirements for different closed-cycle gas turbines applications and heat sources. For example, selecting appropriate working fluids (effect of their thermodynamic and transport properties) to be used, cycle configuration, heat source temperature, pressure ratio, compressor inlet conditions, and component efficiencies.

The selection of these cycle parameters and configuration has a pronounced effect on the cycle performance. Calculations with these cycle parameters were implemented in GT-ACYSS and their results analysed. When one parameter is studied, in most cases, other parameters of the cycle were assumed constant.

5.3.1 Influence of Cycle Configuration

The cycle configurations tend to have a governing effect on acquisition cost and performance of the power plant. Various configurations are possible, however, quantitative analysis was implemented for single-shaft configuration to evaluate the potential performance gains and justify the benefit for an additional cost of a more complex cycle. Cycle configurations considered in this analysis include simple cycle, intercooled, intercooled-recuperated and recuperated cycle. A typical diagrammatic representation of these configurations as shown in the appendix

An analytical evaluation of the listed power plant arrangements was done with baseline conditions shown in Table 2. The different configurations were compared for different working fluids (helium, air, carbon dioxide and nitrogen). The performance results are shown in figs 5-1 and 5-2.

Table 5-2 Baseline Parameter for Parametric study

Parameters	Values
Compressor mass flow rate (kg/s)	441
Compressor inlet temperature (K)	301
Compressor inlet pressure (MPa)	2.5
Compressor isentropic efficiency (%)	85
Turbine inlet temperature (K)	1023
Turbine exit pressure (MPa)	2.55
Turbine isentropic efficiency (%)	85
ReX, & PC (%)	85

The studies assumed that the heat source transfers a fixed heat rate to the working fluids at some specified temperature. During this simulation, component pressure losses were not taken into consideration. For each working fluid, the same values for the turbomachinery and heat exchangers component efficiencies have been assumed as shown in Table 5-2.

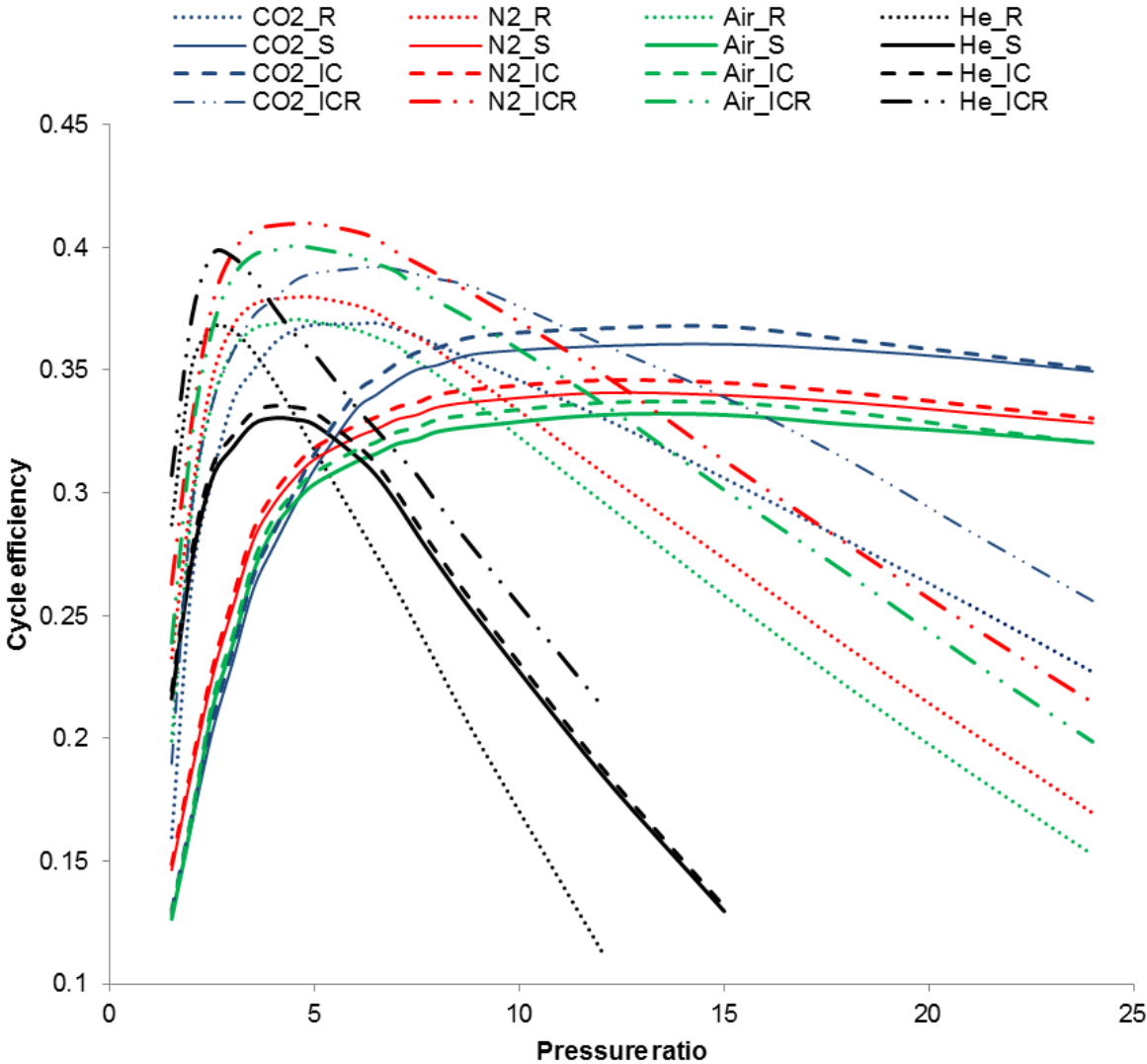


Figure 5-1 Effect of cycle configuration on cycle efficiency at different pressure ratios and working fluids

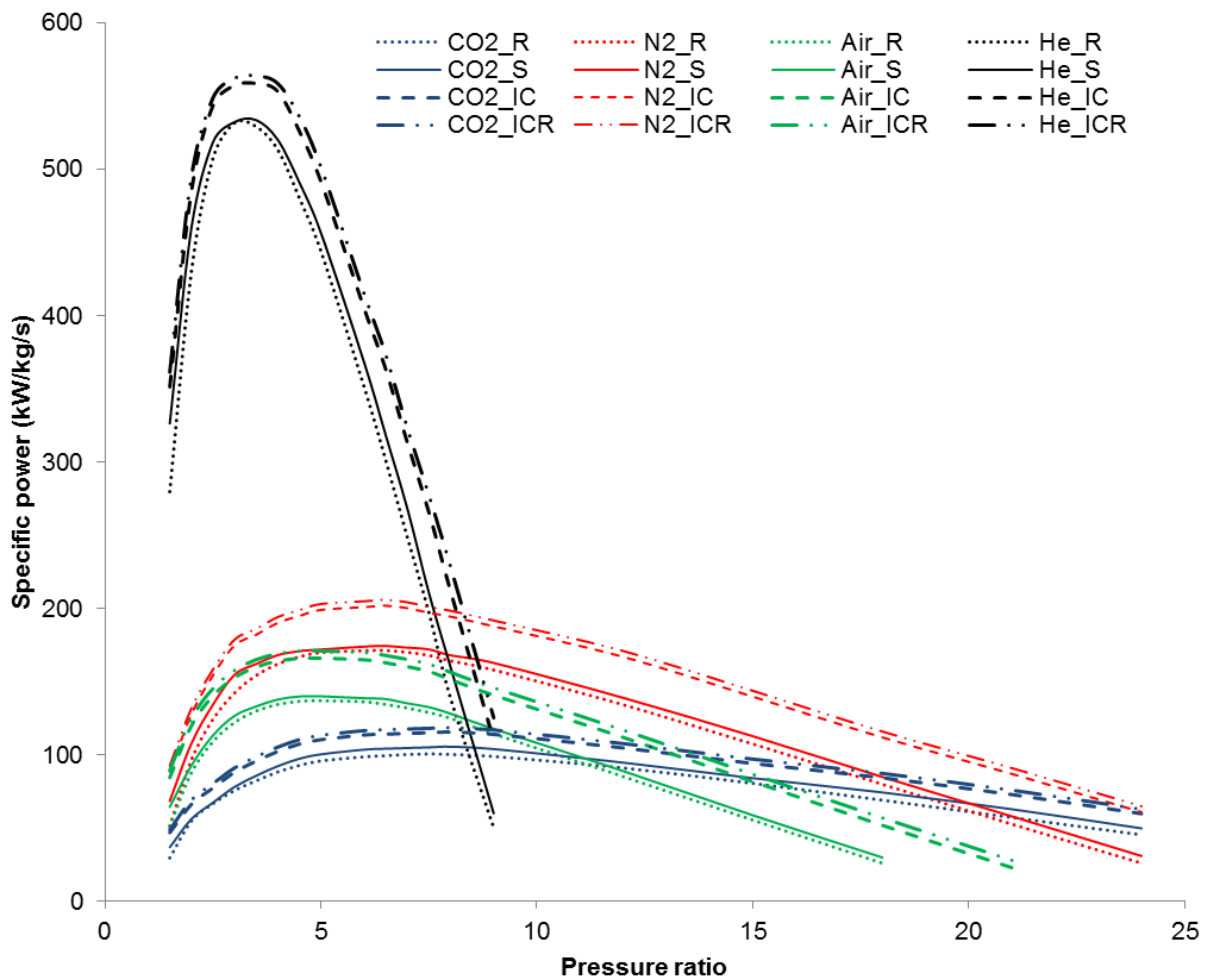


Figure 5-2 Effect of cycle configuration on specific power at different pressure ratios and working fluids

Figure 5-1 shows the effect of the selected cycle configurations on the overall cycle efficiency at different pressure ratios and for selected working fluids. The simple cycle is the most common form of closed-cycle configuration and offers the least efficiency at low-pressure ratios. For this cycle, the efficiency increases as the pressure ratio increases until it reaches a maximum at some pressure ratio for a fixed TET. The simulation results show that the simple cycle efficiencies for the different working fluids peaked at 36.05% for carbon dioxide at a pressure ratio of 15:1, 34.07% for nitrogen at pressure ratio of 12:1, 33.5% for air at pressure ratio of 12:1 and 33.2 for helium at pressure ratio of 4:1. To

achieve the above efficiencies at the specified optimum pressure ratios for a simple cycle would result in an excessive number of compressor and turbine stages. Similarly, the specific power peaks at pressure ratios of 9 for carbon dioxide at 105.5 kW/kgs, 7:1 for nitrogen at 174.32 kW/kgs, 7:1 for air at 138 kW/kgs, and 4:1 for helium at 533.5 kW/kgs.

Introducing a recuperator offered a better cycle efficiency at lower pressure ratios for all working fluids. This is because of the utilization of the waste heat extracted from the turbine discharge temperature to preheat the working fluid prior to entering the gas heater, thus allowing more working fluid to pass through and increasing the overall efficiency at every pressure ratio for which recuperation is possible. The recuperated cycle shows a maximum in cycle efficiency that occurred at a much lower pressure ratio than the simple cycle. The low-pressure ratio can be of benefit in the reduction of the turbo-set sizes which means a great reduction in the overall cost of turbo-set. Unlike the simple cycle as the pressure ratio increases beyond its maximum efficiency, the need for recuperation becomes irrelevant. This is because the temperature difference between the turbine exit and compressor discharge approaches zero. The simulated results of the recuperated cycle in fig. 5-2 show a maximum cycle efficiency of 38.2% for carbon dioxide at a pressure ratio of 6.5:1, 37.96% for nitrogen at a pressure ratio of 4.5:1, 37.06% for air at a pressure ratio of 4.5:1, and 36.74% for helium at a pressure ratio of 2.5:1. The specific power for the recuperated cycle was slightly lower than that of the simple cycle. This is due to a slight increase in the turbine discharge temperature, which reduces the turbine work. Similarly, for the recuperated cycle, the specific power peaked at pressure ratios of 9 for carbon dioxide at 101.6 kW/kgs, 7:1 for nitrogen at 171.22 kW/kgs, 7:1 for air at 136.97 kW/kgs, and 4:1 for helium at 531.5 kW/kgs. It is important to mention that the benefit of using recuperation will be at an additional initial cost incurred for the heat exchanger. However, this additional capital cost can be offset during plant operation.

The decision whether to incorporate an intercooler to the simple cycle is important to the thermodynamic cycle since it affects both the plant layout and

heat rejection characteristics. Introducing intercooler reduces the total compressor work and improves the net output work. To evaluate the intercooled cycle (IC), the component efficiencies and pressure ratios in both compressors were assumed to be the same and equal to \sqrt{PR} . The cycle produces between 15% and 25% increase in output power which is reflected in the specific power as shown fig. 5-2. Intercooling offers a slight advantage in cycle efficiency (between 1.5% and 2.5%) compared with the simple cycle configuration. This is because it gives a lower compressor discharge temperature for the same pressure ratio as the simple cycle. Hence, the pressure ratio at which the compressor discharge temperature will become equal to the turbine discharge temperature is higher than that of simple cycle arrangement, which increases cycle peak pressure ratio (the point where maximum efficiency is obtained) as shown in fig. 5-1. However, this efficiency gain must be weighed against power plant complexity and differing heat rejection temperature. An intercooled cycle has been shown to be well suited to district heating [2,14]

A combination of intercooling and recuperation offers an optimal cycle performance. This is because; each new component added improves key cycle performance indicators. In this case, the intercooler increases the output power, while the recuperation provides an increase in the cycle efficiency as indicated in figs 5-1 and 5-2. This also implies that the maximum cycle efficiency occurs at lower pressure ratios, as compared with the simple cycle. The intercooled-recuperated cycle (ICR) improves the cycle efficiency between 10% and 15%. However, this extra benefit comes with an extra capital cost for the additional components.

From design point view, the implication of this cycle configuration analysis on cycle efficiency and specific power set a reasonable compromise in terms of plant size, cost (capital and operational cost), and turbo-set design challenges. Working fluids to some certain extent contribute to design choice of cycle configuration. For fluid like carbon dioxide, its optimal performance is achieved above its critical points which will mean pressurizing the system or operating at a very high-pressure ratio for a simple cycle configuration. For this reason, a

configuration with intercooling which allows for recompression of carbon dioxide is proven to be reasonable. For fluid like helium with low molecular weight and high gas properties (γ and C_p), the simple cycle configuration may seem more realistic. Other factors that may influence the design choice of cycle configuration are application (land-based, sea-based, space-based), proven operation, reliability, maintainability, cooling medium, plant layout, the potential for energy utilisation and sustainability, and current status of technology. The intended application will give a reasonable justification for the configuration is most suitable. However, economic quantification has to be undertaken to provide substantiation on any design choice cycle configuration.

5.3.2 Influence of working fluid properties on cycle efficiency and specific power

From ideal thermodynamic considerations, the closed-cycle gas turbine theoretical cycle thermal efficiency should be independent of the working fluid and should be identical for all perfect gases when temperature levels are the same and variations in specific heat capacity with temperature are neglected [64]. However, this is not so because there are several indirect effects of the working fluids properties on the components temperature gain or drop, which impacts on the cycle overall performance.

The results in Figs. 5-1 and 5-2 give a general overview of the influence of the fluid properties on the cycle efficiency and specific power for different cycle configuration. However, to highlight some overarching points which describe the effect of the working fluid properties on the cycle performance, a recuperated closed-cycle was simulated for selected working fluids at different pressure ratios and TETs. Like the previous, pressure losses and secondary effects were not accounted for during this simulation. From the simulated results shown in Figs. 5-3 and 5-4, there is an optimum pressure ratio for which the cycle efficiency and specific power is maximum at different TETs for each working fluid. At TET 1023, the cycle maximum efficiencies at optimum pressure ratio are 38.2% for carbon dioxide at a pressure ratio of 6.5:1, 37.96% for nitrogen at a pressure ratio of 4.5:1, 37.06% for air at a pressure ratio of 4.5:1, and 36.74%

for helium at a pressure ratio of 2.5:1. Similarly, the maximum specific power peaked at pressure ratios of 9 for carbon dioxide at 101.6 kW/kgs, 7:1 for nitrogen at 171.22 kW/kgs, 7:1 for air at 136.97 kW/kgs, and 4:1 for helium at 531.5 kW/kgs. Comparing the cycle performance against each working fluid shows that at lower pressure ratios, the fluid with a high ratio of specific heat capacity such as helium tends to have better cycle efficiency. On the contrary, as the pressure ratio increases, working fluids with decreasing specific heat ratio and higher molecular weight tend to have better cycle efficiency. However, helium will be an excellent choice for large power plants, because of its high thermal conductivity and specific heat ratio, which would be relevant for small heat exchangers and low mass flow, while air, nitrogen or carbon dioxide can be substituted for helium when considering reduction of the turbomachinery stages. Hence, there is a need for a compromise between the cycle efficiency, turbomachinery design challenges and cost. In reality, a slightly lower pressure ratio has been proven to be easier in terms of design, mechanical stresses [45,65]

The simulation carried out at TET of 1023K was repeated for TET of 1123K and 1223K. In reality, increasing TET is limited to material technology level, cooling, and the heat source capability. Generally, as the TET increases, there is an improvement on the cycle performance. This is because both the cycle efficiency and specific power of a non-ideal cycle depends on the TET. Higher TET produces higher turbine work output and hence high network output. Thus for better cycle performance, it is desirable to have high TET. However, operating at high TET requires a compromise in capital cost, operational cost and life of the components (heat exchanger and turbine). The result in fig 5-4 shows that cycle efficiencies increased by an average of 13.8% for carbon dioxide, 14% for nitrogen and air, and 15.5% for helium, as TET increased from baseline to 1223K. Similarly, the specific power also increases with TET at any given pressure ratio for all working fluids and the optimum pressure ratio at which maximum specific power occur increases as well as shown in fig. 5-5. The variation in cycle efficiencies of the working fluid is due to the effect of temperature on the fluid properties. Helium had a dominant improvement in

shaft efficiency and power as TET increased from 1023K to 1223K due to its stable thermodynamic properties. At fixed pressure ratio, helium generated five times power per unit mass than air because the specific heat of helium is about five times larger than air and nitrogen. For carbon dioxide, which is greatly affected by temperature and pressure below its critical point would imply that operating at very temperature could be difficult for carbon dioxide because of the dissociation of CO and reaction with graphite and metallic structure of the system component. Hence, when selecting appropriate design-point TET the type of working fluid among other several factors should be significantly considered

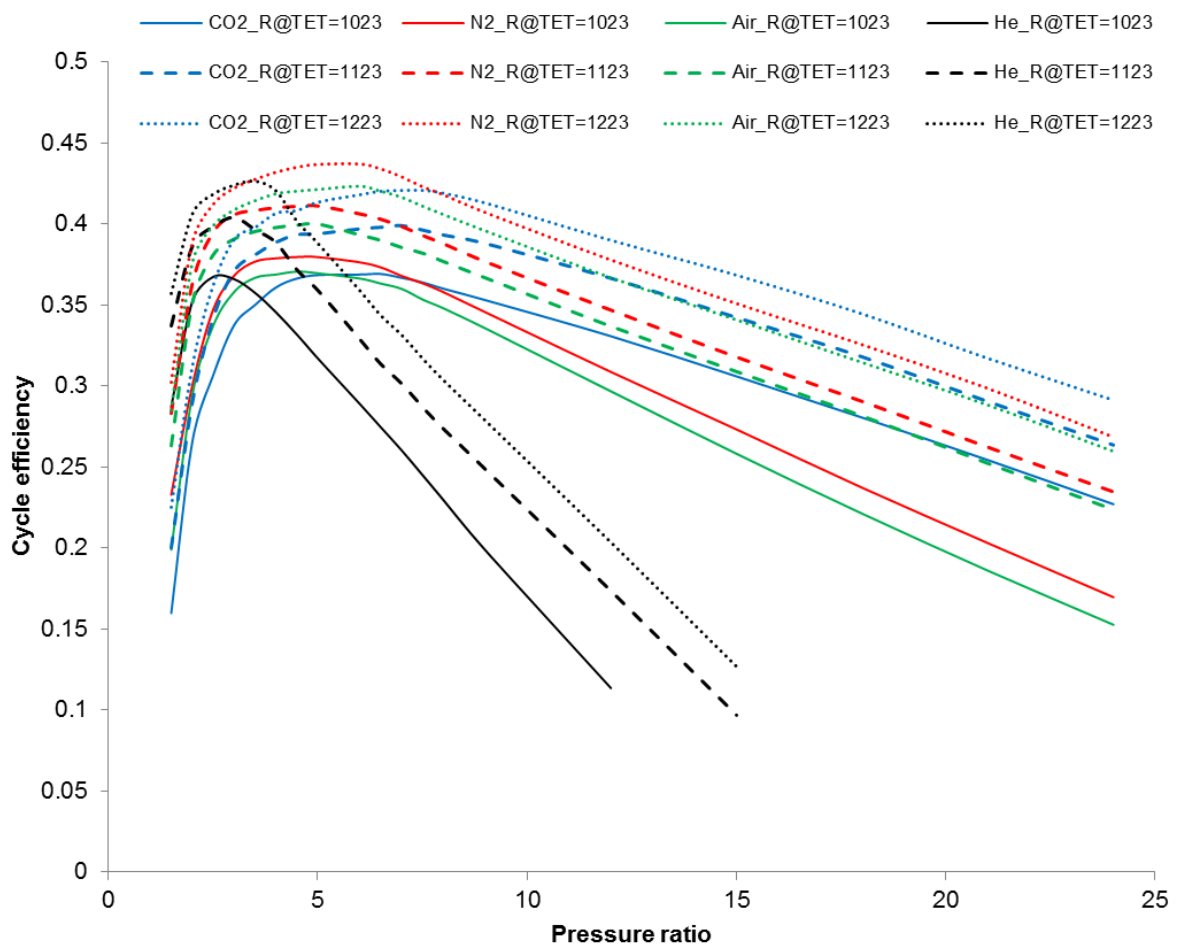


Figure 5-3 Effect of working fluid properties on cycle efficiency at different PR and TET

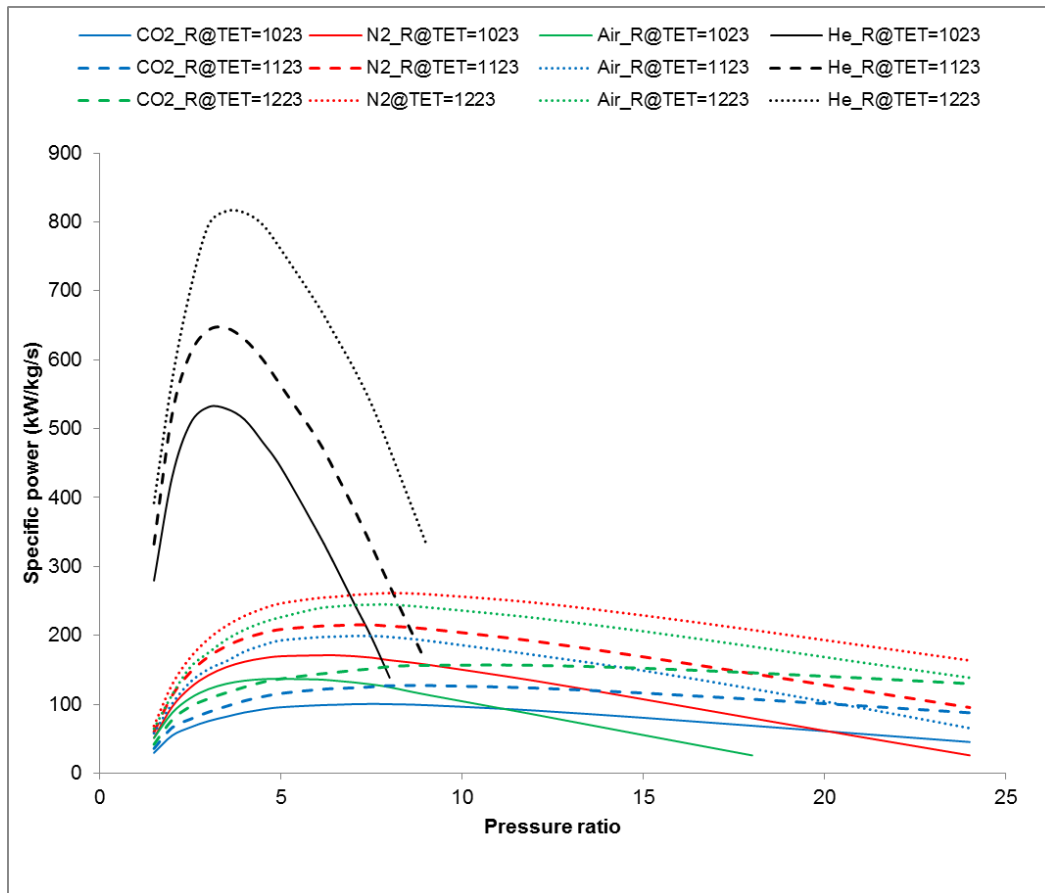


Figure 5-4 Effect of working fluid properties on specific power at different PR and TET

5.3.3 Influence of compressor entry conditions

One inherent advantage of the closed-cycle gas turbine is the possibility of controlling the working fluid entry condition (entry temperature and pressure). The compressor entry temperature (CET) for closed cycle gas turbine power plant is dictated by the environment to which the cycle waste heat is rejected. Hence, selecting the design point entry temperature is significant because it determines the cycle efficiency, the volume, and method of heat sink applicable.

To demonstrate the influence of compressor entry temperature on cycle efficiency and specific power, CET values ranging from 301K to 340K was

simulated for a fixed TET and PR, and results presented in Fig 5-5 and 5-6. The general trend from the result shows a decrease in shaft efficiency and power as compressor entry temperature increases. This is as a result of an increase in compressor work, which would require the turbine to do more work driving the compressor. With the increase in compressor entry temperature, the density of the working fluid decreases, consequently the mass flow into the turbine decreases. On the average, there was a 1.5% drop in efficiency with a corresponding increase in the entry temperature. Comparing the performance of the working fluid as a result of the changes in entry temperature shows that carbon dioxide was more impacted by the changes with cycle efficiency moving from 33.75% to 28.3% for 13% increase in compressor entry temperature. For nitrogen, air, and helium, their cycle efficiencies decreased by 10%, 11%, and 8% respectively. In a similar manner, the specific power of each simulated working fluid was impacted by the changes in compressor entry. These changes can have a direct impact on the operational cost of the system. However, one major reason for selecting a high compressor entry temperature for some working fluid such carbon dioxide is to quickly operate above the fluid critical temperature in order to achieve stability in the behaviour of the working fluid.

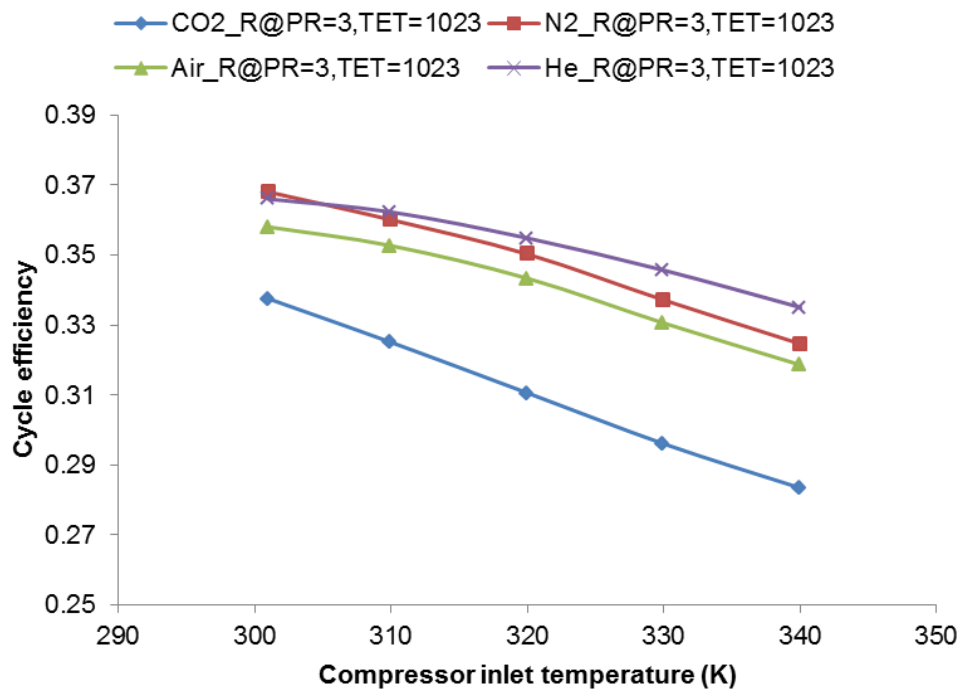


Figure 5-5: Influence of compressor entry temperature on cycle efficiency at fixed PR and TET

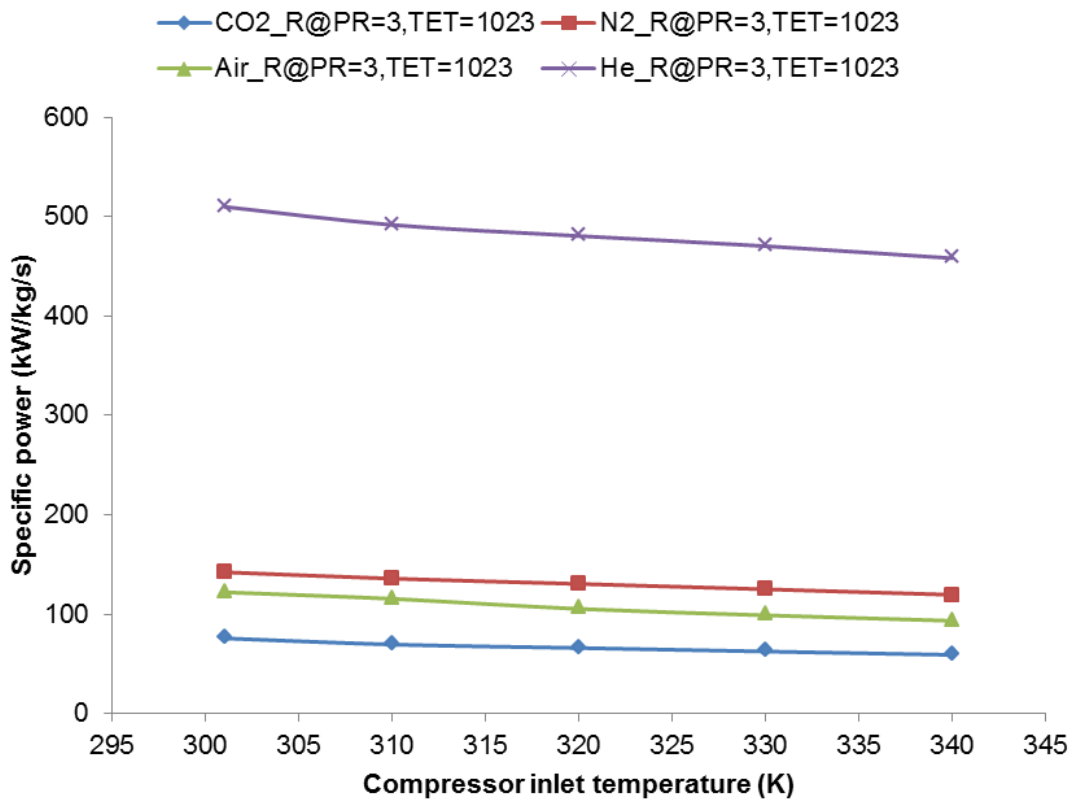


Figure 5-6 Influence of compressor entry temperature on specific power at fixed PR and TET

For ideal fluid, compressor entry pressure does not have any significant effect on the cycle performance. By pressurising the system, it becomes possible to significantly reduce the flow area and system weight within the turbomachinery, ducts and heat exchangers; however, there is an extent to which the system can be pressurized due to increase in stress level. For non-ideal situation, the property of the working fluid varies as a result of changes in the entry pressure; hence, it is important to simulate how changes in the system pressure impacts on the cycle performance. To demonstrate, the PR, TET, and CET were kept constant while the entry pressure was varied. Also, the effect of Reynolds number as a result of pressurizing the system was not taken into account during this simulation.

From the simulated results shown in Fig 5-7 and 5-8, there was an increase in the cycle efficiency for working fluid approaching its critical pressure such as

carbon dioxide, which gained about 0.15% in cycle efficiency. This is because pressure rise at constant PR reduces the compressor work to some extent and the thermodynamic properties approach stability especially when recompression system is introduced and also reduces the heat exchanger pressure drop. However as fluid approach stability and if Reynolds number is taken into consideration, the cycle efficiency will become negatively impacted. Other working fluid simulated showed almost flat efficiency curve with nitrogen and air having about 0.06% increase and helium had not significant changes. Also, the specific power is slightly impacted as explained above. Figure 5-8 gives an overview of the impact of compressor entry pressure on the cycle specific power.

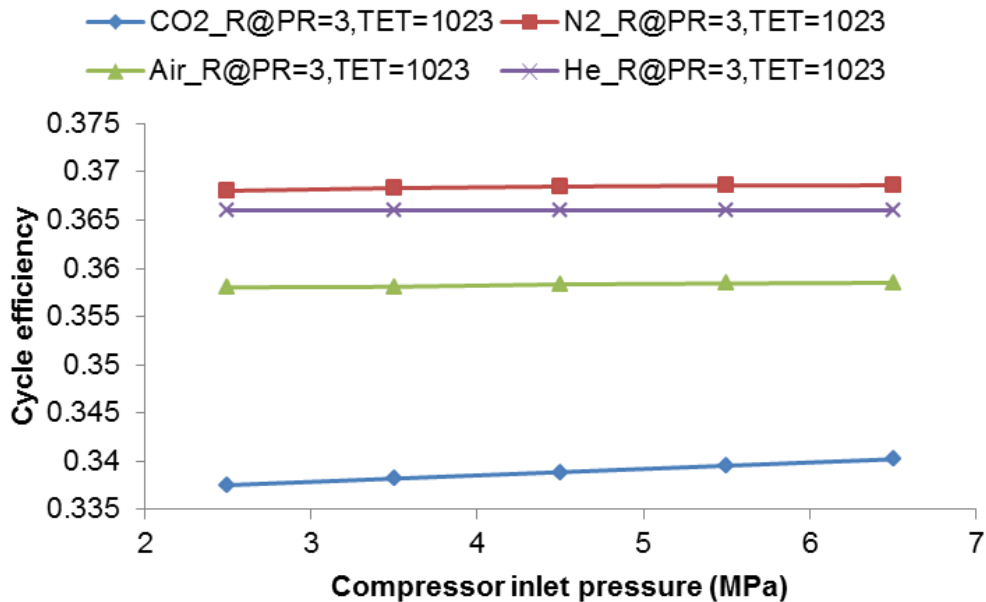


Figure 5-7 Influence of compressor entry pressure on cycle efficiency at fixed PR and TET

Similar to the compressor entry temperature, design for increased system pressure is aimed at achieving a reduction in component size and achieving a critical point of the working fluids.

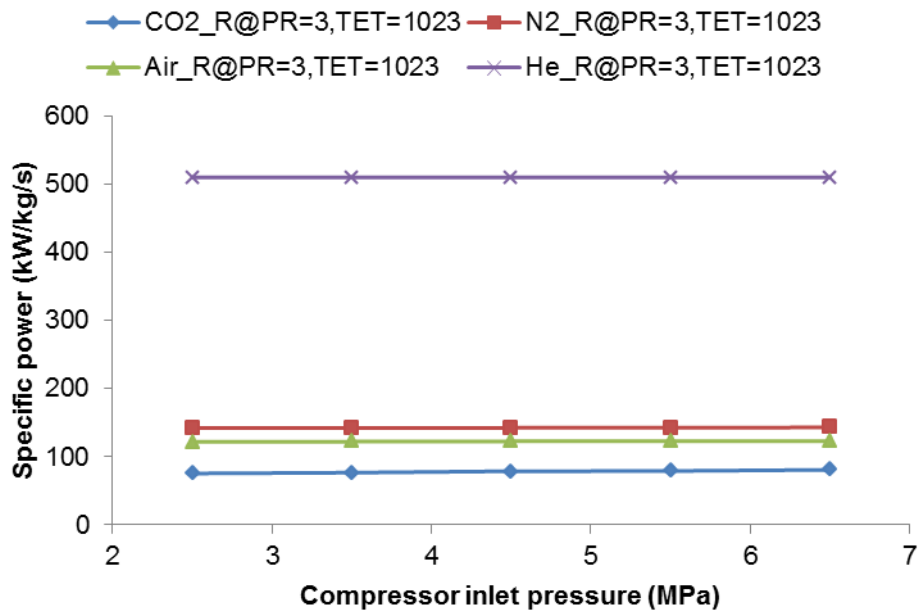


Figure 5-8 Influence of compressor entry pressure on specific power at fixed PR and TET

5.4 Sensitivity Analysis

In this section, the sensitivity of each component parameters on the cycle performance for selected working fluids is analysed. Sensitivity analysis is a technique which allows the analysis of changes from baseline component parameter on the overall performance of the closed cycle gas turbine. It reveals the importance of component parameters around the baseline condition. The aim of the sensitivity analysis is to understand the extent to which the selected working fluids performance is affected. It is important to note that the results presented in this section are based on simplified analysis, certain loss exist that were not considered (for example Reynolds number effect), since the purpose is to simply identify and quantify component parameters that affect the cycle performance, and to what extent the selected working fluids contribute to the changes in engine performance. To this end, the baseline condition selected for this analysis is shown in Table 5-2. The analysis was done for all working fluid at same pressure ratio (3:1), compressor entry condition and TET of 1023K.

The following component parameters were analysed in this section; effect of heat exchanger pressure losses, the effect of component efficiencies and heat exchanger effectiveness.

The results of the sensitivity analysis are presented in Fig. (5-9) – (5-18)

5.4.1 Effect of Pressure Drop

The closed cycle gas turbine plant utilizes several heat exchangers for any type of cycle configuration selected. The sizes and cost of these heat exchangers depend on the heat transfer coefficients of the working fluid and allowable pressure losses across the heat exchangers [64]. Hence, pressure losses could have an effect on cycle performances and it is desirable to select working fluids with high heat transfers and low flow resistance characteristics. In this parametric analysis, the overall system pressure losses were assumed at a constant rate for all the working fluid gases considered. However, the result shown below is the characteristic cycle performance as a result of the split of the overall fractional pressure drop between the various components. These losses would have a direct impact on the weight and performance of the components.

For a given compressor pressure ratio, the sum of the duct fractional and component pressure losses defines the turbine pressure ratio, hence the overall pressure ratio factor is defined as the ratio of the turbine and compressor pressure ratios. As the pressure losses increases, there is a corresponding decrease in the pressure ratio factor thereby reducing the turbine work output that can be extracted in the expansion process for the same heat supplied. Thus, the cycle thermal efficiency and power is reduced.

The pressure losses considered were varied within the range 1% to 7% for each heat exchanger. Each component pressure drop was simulated one at a time and results presented in Fig. (5-9) – (5-12). For the recuperator, the pressure drop was simulated for the low-pressure-side (LPS), high-pressure-side (HPS) and combined (LPS+HPS). The results show that the recuperator and gas heater pressure losses had a dominant effect on the cycle performance.

The pressure loss at the high-pressure-side of the recuperator significantly impacts on the cycle performance than the pressure loss at the low-pressure-side of the recuperator and the pre-cooler because of the lower density and high velocity in the matrix of the overall conserved volume. The pre-cooler has a dominant influence on the compressor entry conditions, hence a drop in the required entry pressure will significantly affect the efficiency and shaft power. However, the combined effect of the recuperator HPS and LPS showed the greatest influence on the cycle. Results comparing the effect of each component pressure drop are presented in the Appendix. Using nitrogen as an example, for 1% drop in pre-cooler pressure, there was 0.6% drop in cycle efficiency, similarly, 1% drop in pressure on recuperator low-pressure-side, recuperator HPS, gas heater and combined LPS and HPS, there was a corresponding 0.4%, 1.09%, 1.02% and 1.5% drop in efficiency respectively.

Analysing the contribution of the choice of working fluid to the changes in the cycle performance showed that helium had the least influence on the cycle performance as a result of pressure drop. This is due to its low molecular weight and high speed of sound compared with other fluid and the stability of its thermodynamic and transport properties. To this end, fig. 5-9 – 5-13 shows how each selected working fluid responded to pressure drop. For 1% drop in pre-cooler pressure drop, there was cycle efficiency deviation from baseline by 1.11% for carbon dioxide, 0.6% for nitrogen, 0.65% for air and 0.5% for helium. Carbon dioxide had the greatest shift from baseline cycle efficiency as the pressure drop increases. This is because of the behaviour of carbon dioxide (changes in properties) below its critical point and its molecular weight. Air and nitrogen were not too far away from each other in changes to cycle efficiency and specific power as a result of pressure drop.

To avoid repetition, the results of other component pressure losses presented in Fig (5-10) – (5-13) followed a similar trend. The working fluids showed a similar trend in losses on specific shaft power as a result of variation in pressure drop as shown in Appendix B.

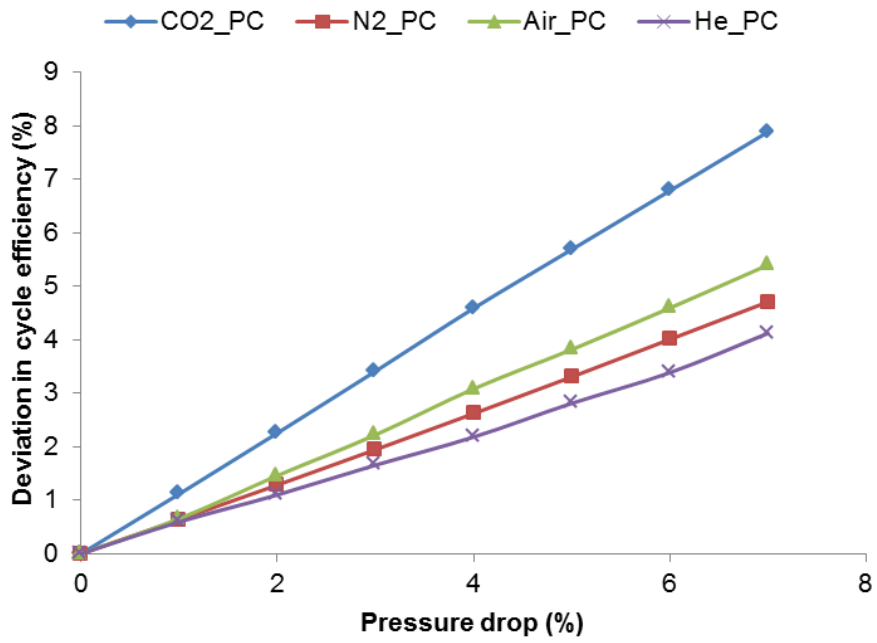


Figure 5-9 Effect of pre-cooler (PC) pressure drop on the cycle efficiency

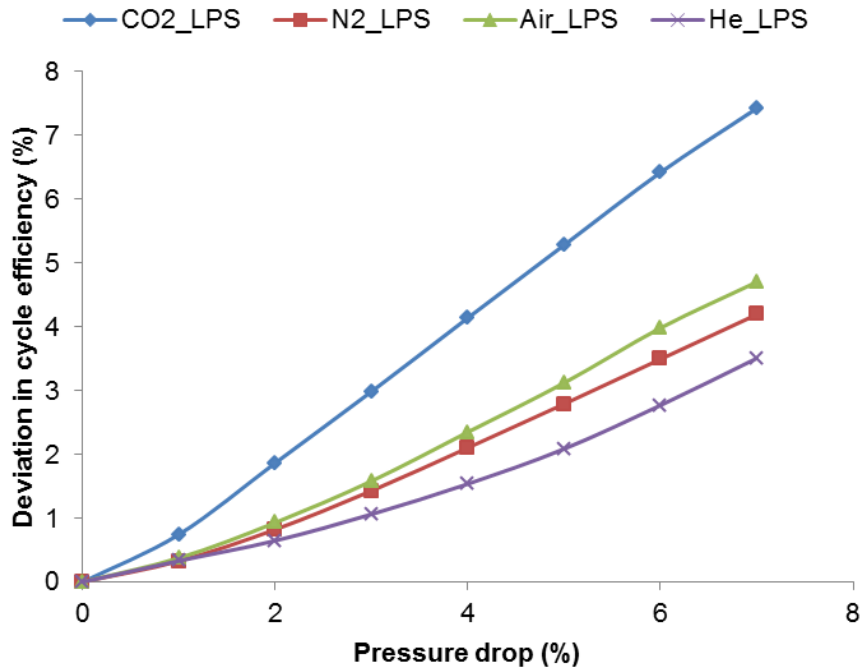


Figure 5-10 Effect of recuperator low-pressure-side (LPS) pressure drop on the cycle efficiency

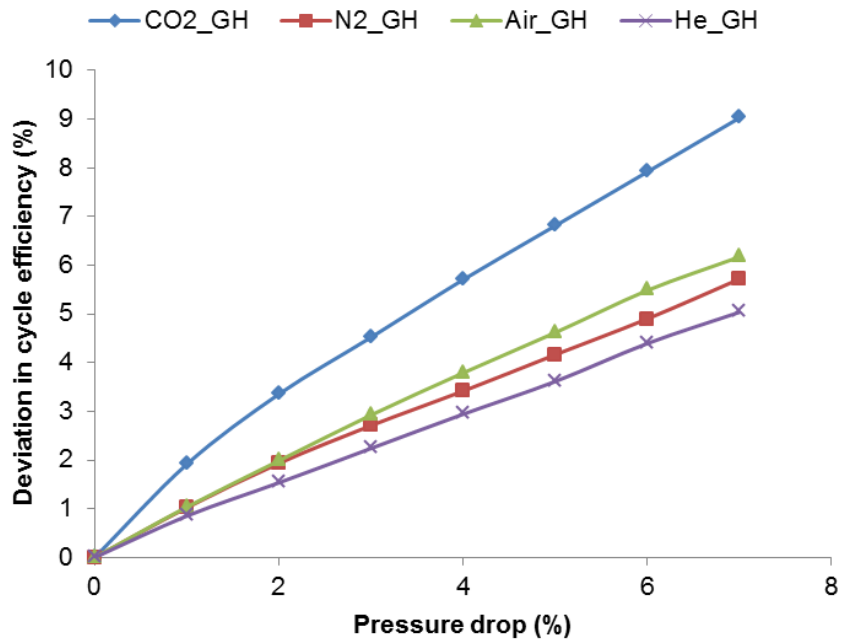


Figure 5-11 Effect of Gas Heater (GH) pressure drop on the cycle efficiency

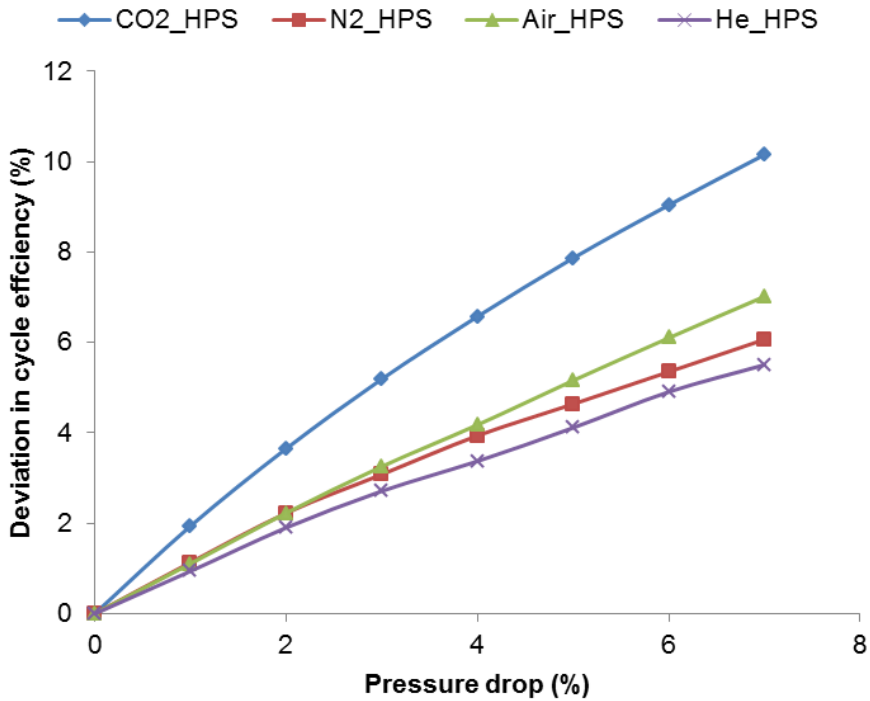


Figure 5-12 Effect of recuperator high-pressure-side (HPS) pressure drop on the cycle efficiency

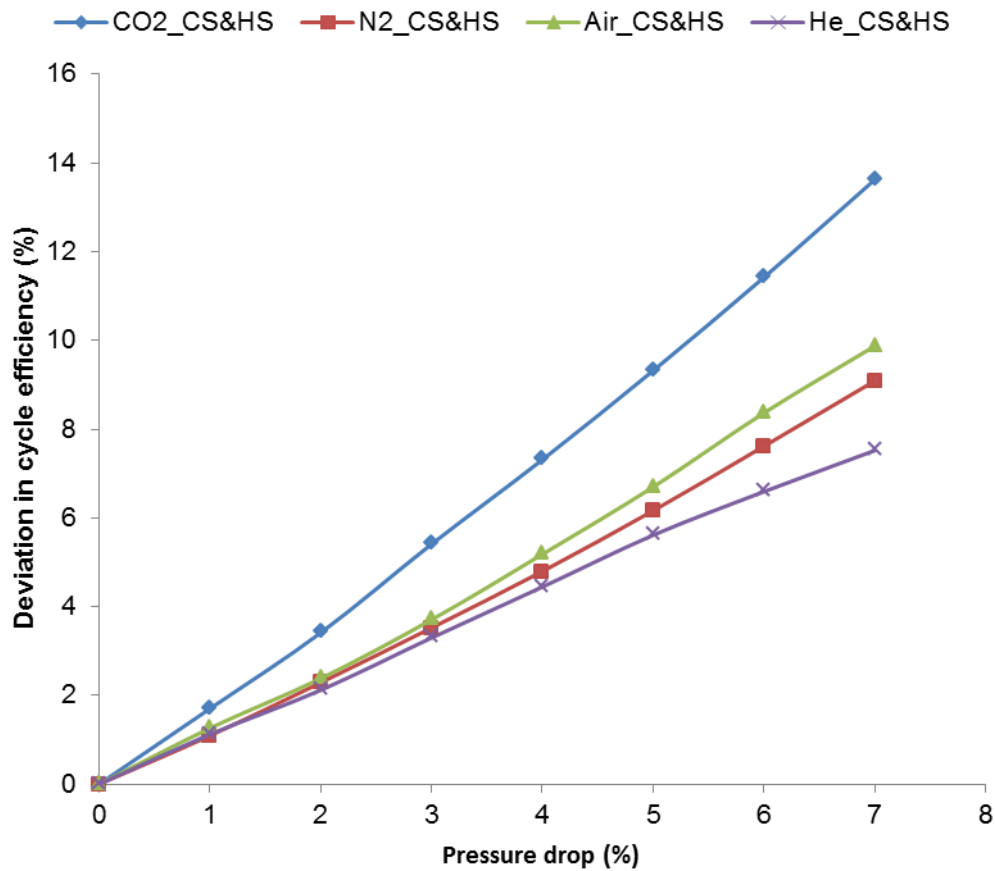


Figure 5-13 Effect of recuperator LPS & HPS pressure drop on the cycle efficiency

5.4.2 Effect of Component Efficiency

Compressor and turbine efficiencies play important roles in the cycle performance. However, these efficiencies are limited by the state-of-the-art design which is currently above 88% for industrial application [146]. For this reason, the sensitivity of compressor and turbine isentropic efficiencies on the closed cycle gas turbine was simulated with Table 5-2 as a baseline. The component performance losses have a nearly linear influence on cycle performance. This analysis reveals which component has the dominant influence on the shaft efficiency and power for efficiencies and which working

fluid contributed most to the variation in cycle performance. Changes in component efficiencies ranging from 70 to 100% were simulated for the selected working fluid considered. The results are presented in Fig 5-14 to 5-16.

As expected, the curve for variation in compressor and turbine efficiencies show similar trends. However, the result shows that the turbine efficiency has a greater influence on the thermal efficiency and specific power with approximate 1.8 times greater impact in thermal efficiency per every 1% drop in component efficiency for all working fluids utilized. This is because when turbine efficiency drops, the turbine power is reduced and the discharge temperature increases, hence the cycle efficiency is reduced. On the hand, when compressor efficiency decreases, more power is required for the compressor and the compressor discharge temperature increases. Thus, an increase in compressor power reduces the cycle efficiency by reducing the net power output. However, an increase in compressor discharge temperature partially offsets the increase in compressor power which make the changes in compressor efficiency less impactful compared with turbine isentropic efficiency. The result also shows a similar trend on the specific power

From the analysis, carbon dioxide has a dominant variation on cycle efficiency for both compressor and turbine. For every 1% drop in compressor efficiency, there was averagely 1.1% changes in cycle efficiency and 0.98% in specific power, and 1.3% for turbine isentropic efficiency. This may be due to the sharp variation of its thermodynamic properties as temperature and pressure changes, hence the difference in component work with baseline increased. Helium had the least changes with 0.5% changes in cycle efficiency for every 1% change in compressor isentropic efficiency and 0.6% for every 1% change in turbine isentropic efficiency.

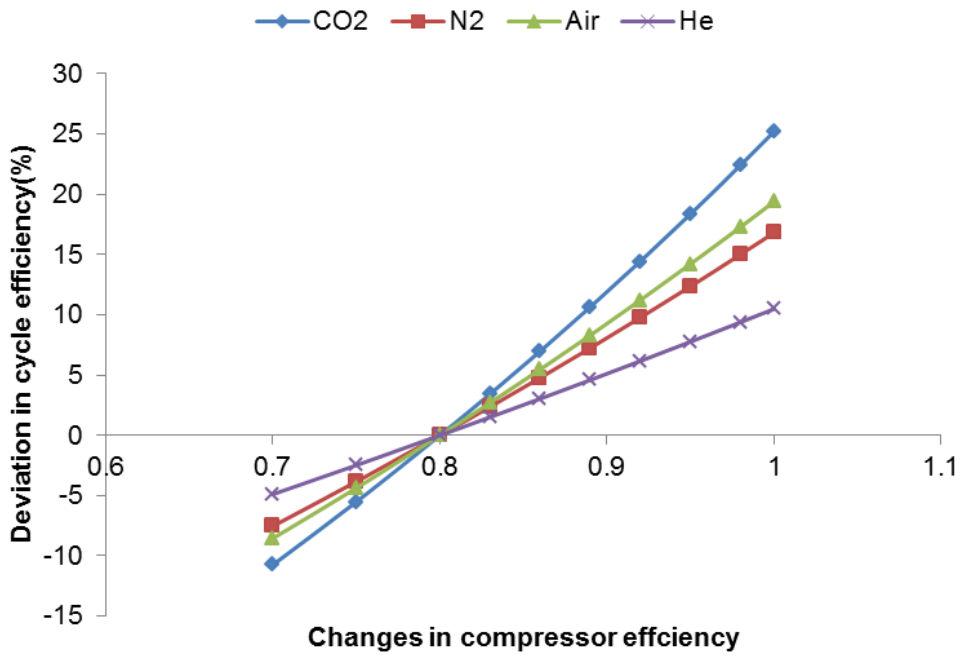


Figure 5-14 Sensitivity of compressor efficiency on cycle efficiency

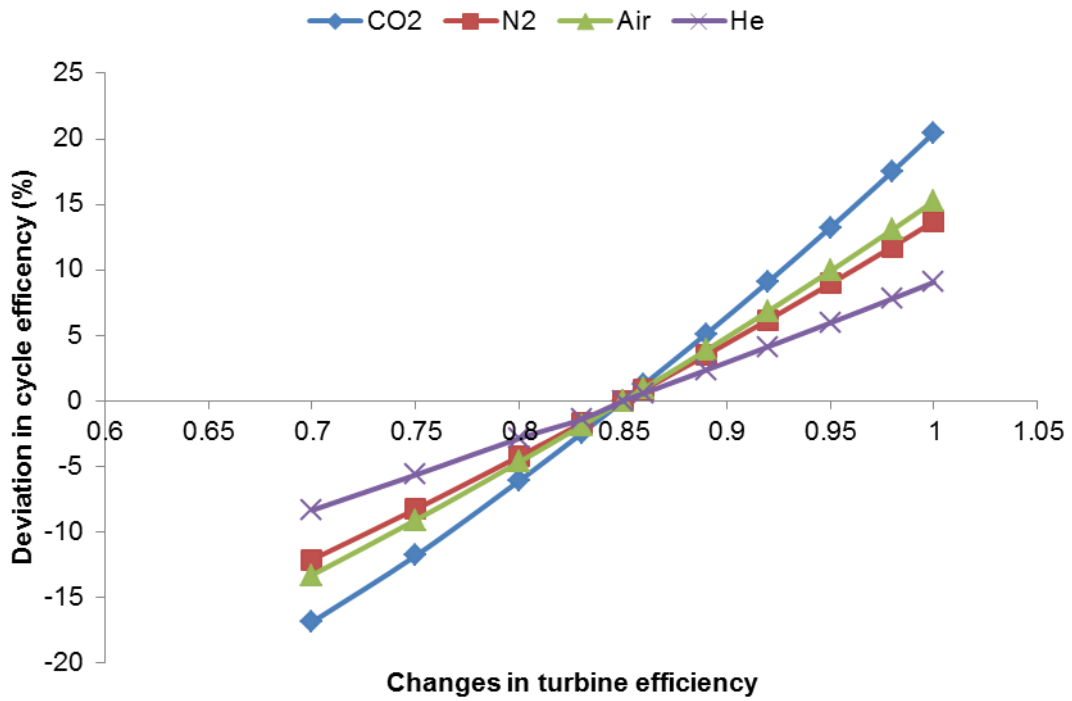


Figure 5-15 Sensitivity of turbine efficiency on cycle efficiency

5.4.3 Effect of Heat Exchanger Effectiveness

The heat exchangers analysed include the recuperator, gas heater and the precooler. The recuperator recovers some waste from the turbine, thus increasing the cycle efficiency. The extent to which the heat recovered can be utilized depends on the effectiveness of the recuperator. Similarly, the gas heater interfaces with the heat source indirectly coupled to the closed-cycle gas turbine. The amount of heat received from the heat source is the exchanger by the gas heater onto the turbine. Thus, the effectiveness of these heat exchangers utilized in the closed cycle gas turbine plays an important role in the cycle performance. To demonstrate this, the effectiveness of the listed heat exchangers were varied between 70% and 100%, and their sensitivity to cycle performance compared with different working fluids used in this analysis.

This analysis was carried out at a fixed pressure ratio 3:1 for all working fluids and TET of 1023K. Other baseline characteristics used during the analysis are as recorded in Table 5-2.

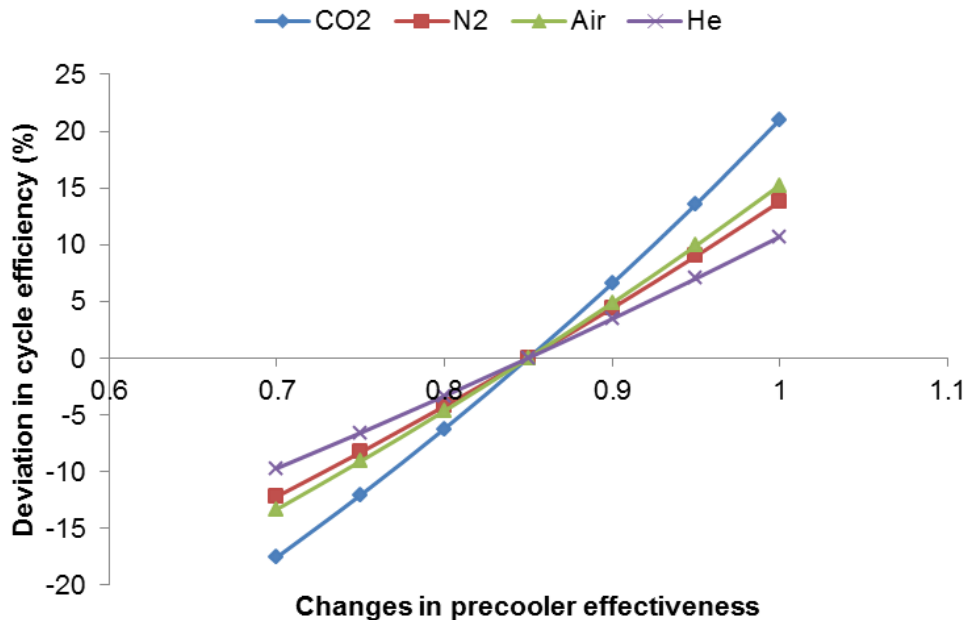


Figure 5-16 Sensitivity of pre-cooler effectiveness on cycle efficiency

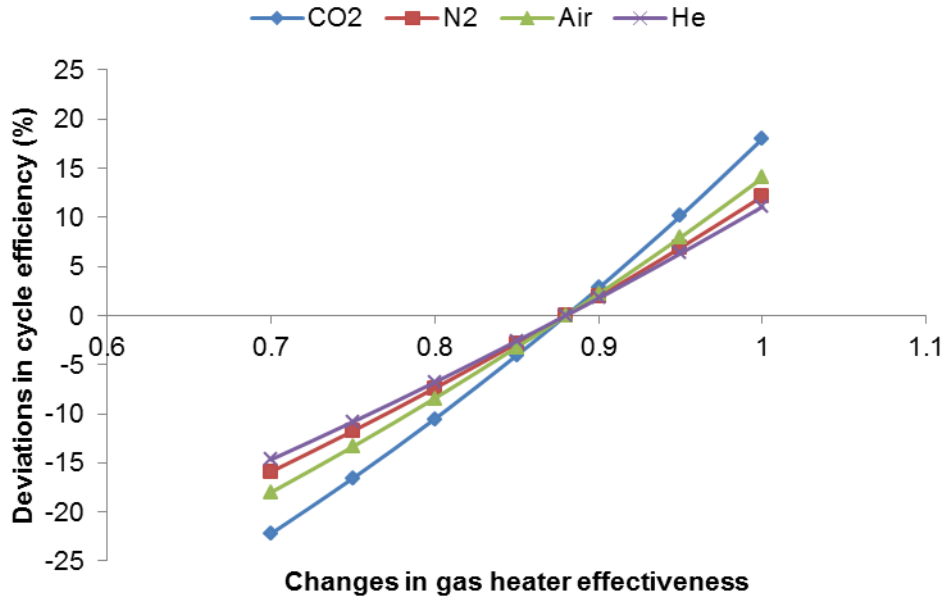


Figure 5-17 Sensitivity of gas heater effectiveness on cycle efficiency

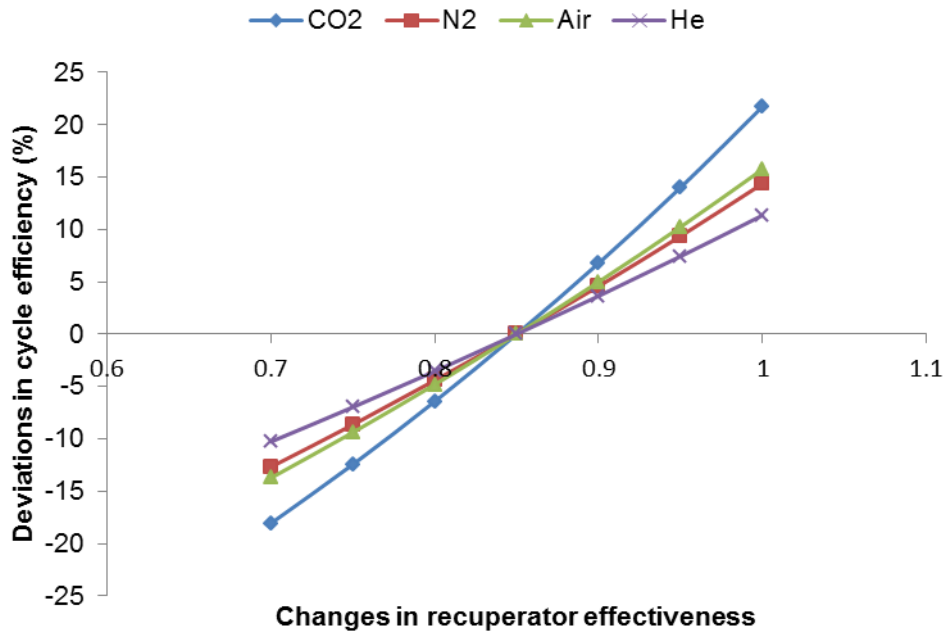


Figure 5-18 Sensitivity of recuperator effectiveness on cycle efficiency

Selecting heat exchangers with high effectiveness have the ability to drastically raise the cycle efficiency. However, achieving such design is largely influenced by the working fluid to be used. The pressure drop, weight and surface area of the heat exchangers are dependent on the thermodynamic and transport properties of the working fluid to be used. The results from the sensitivity analysis are shown in Figs. (5-16), (5-17) and (5-18). The analysis shows that changes in the effectiveness of the gas heater had a more significant sensitivity to the cycle efficiency compared with other heat exchangers. This is because changes from the baseline gas heater effectiveness have a direct effect on the value of TET. However, the type of fluid in use does some contribution to the extent to which the cycle performance is impacted. Next to the gas heater is the recuperator in terms of the level of sensitivity to cycle efficiency.

Comparing the behaviour of each working fluid used in the analysis, the results presented show that for every 1% variation in pre-cooler, recuperator or gas heater effectiveness, helium demonstrated 0.68%, 0.72% and 0.88% variation in cycle efficiency. Similarly, nitrogen gave 0.865%, 0.9% and 1% respectively, carbon dioxide gave 1.28%, 1.32% and 1.43% variation in cycle efficiency, while for air, 0.95%, 0.98% 1.11% was obtained. For helium, the heat exchangers effectiveness does not have any significant sensitivity to the specific power since the fluid properties are relatively stable. Minor changes in specific power for carbon dioxide was observed which comes from the fact that its gas properties

5.5 Effect on Inventory Control Systems

As previously mentioned the inventory control offers a unique characteristics feature when modulating output power to match the required load demand. The unique opportunities it offers have made it to be widely used in most closed-cycle gas turbine plant design and operations. In this section, a technical study on how the different working fluid affects the design and performance characteristics of the inventory control system using a part-load operation as a case study. The aim of this analysis is to demonstrate how the selected working

fluid affects the weight, volume of the inventory tank, valve response time and the effect of Reynolds number of the cycle performance.

As previously described, the inventory control systems consist of the inventory tank, and valves as shown in Fig 4-7

5.5.1 Case Study

To demonstrate the set objective, an intercooled-recuperated closed-cycle gas turbine plant inspired by the Escher Wyss Ravensburg power plant was utilized for this study. The plant arrangement is similar to the diagram described in Fig. 4-7. The design characteristics of the plant are outlined in Table 5-3. The initial volume of the inventory tank and the GT cycle was assumed before the part-load operation and opening of the inventory control valves.

Table 5-3 Summary of Power Plant Design Point Description

Description	Unit
Heat Source Temp.	1100 (K)
LPC Pressure ratio	1.65
LPC Inlet Pressure	8.2 (atm.)
LPC Inlet Temperature	290 (K)
HPC Pressure ratio	2.40
LPC& HPC efficiency	86 (%)
Turbine efficiency	90 (%)
Flow rate at LPC	230 (kg/s)
IC effectiveness	90 (%)
RX & GH effectiveness	90 (%)
Tank pressure	8.2 (atm.)
Initial tank volume	2100m ³
GT cycle volume	1500m ³

Table 5-4 Simulated cycle performance at constant mass flow

Working fluid	Simulated Power (MW)	Efficiency (%)
Air	40.8	41.2
Carbon dioxide	27.50	39.8
Helium	170.14	41.98
Nitrogen	43.28	41.5

The rated power and plant efficiency for the different working fluids used in this analysis was obtained from simulations in GT-ACYSS for the mass flow as shown in Table 5-4 based on characteristics shown in Table 5-3. The part-load operation was simulated to understand the impact of the different working fluids on the cycle performance taking into account the effect of Reynolds number. Also, during the part-load operation, there is a transfer of mass from the main gas turbine system to the inventory tank. Using the Eqs (4-53) to (4-65) modelled in GT-ACYSS, to analyse the effect of the selected working fluids on the inventory control level in terms of mass of the inventory tank, volume of the inventory and response rate of the valves, as the selected working fluid is transferred from the main cycle system to the inventory tank under part-load operations.

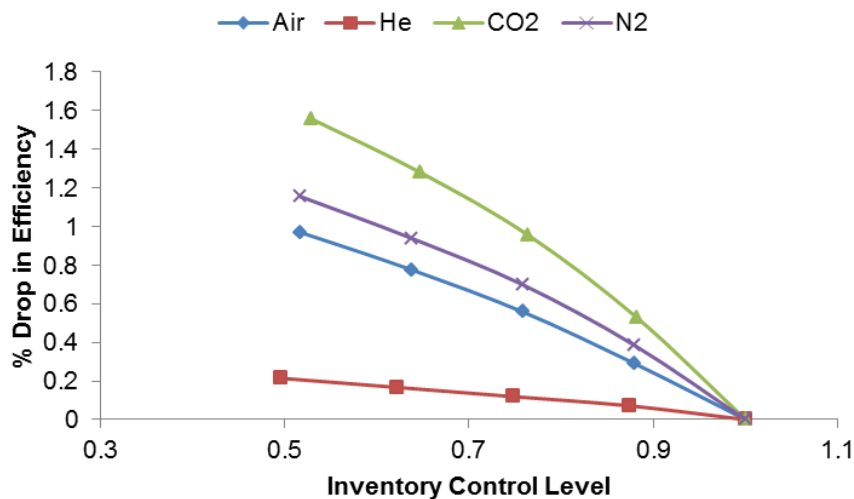


Figure 5-19 Effect of Reynolds number on cycle efficiency at part-load operation

At first, the effect of Reynolds number on the cycle performance was analysed. Reynolds number describes the relative importance of fluid resistance to flow. For any flow gas condition, this is reflected as the ratio of body forces (reflecting velocity and momentum effects) to viscous forces (causing frictional pressure losses) [147,148].

Thus, the turbomachinery component efficiency correction is given by:

$$1 - \eta_{fluid} = K[Re_{fluid}]^{-n} \quad (5-1)$$

$$n = 0.2 \text{ for } Re > 0.45 * 10^5, n = 0.5 \text{ for } Re < 0.45 * 10^5$$

Where Reynolds number is expressed as

$$Re = \frac{\rho U_m L}{\mu} \quad (5-2)$$

As shown in Fig 5-19, the effect of Reynolds number on the cycle performance is almost un-noticed for helium fluid with 0.2% drop in efficiency, while air had 0.9% drop, nitrogen 1.1% and carbon dioxide 1.5% drop in cycle efficiency at 50% part-load. These changes can be traced to the molecular weight and properties of the fluid.

Based on the assumptions made for the initial volume of the inventory tank and GT cycle, the initial masses of the inventory tank and the GT cycle before the start of part-load operation were obtained using Equ. 4-57. The result of the initial mass is shown in Fig. 20. Due to the molecular weight of helium, it puts it at an advantage to having a compact inventory tank and GT cycle system. Thus, this will have a direct effect on the capital cost. Also, assuming the size of inventory tank is kept constant for all working fluids, it implies that utilising helium will accommodate more fluid volume compared with other working fluids used in this study.

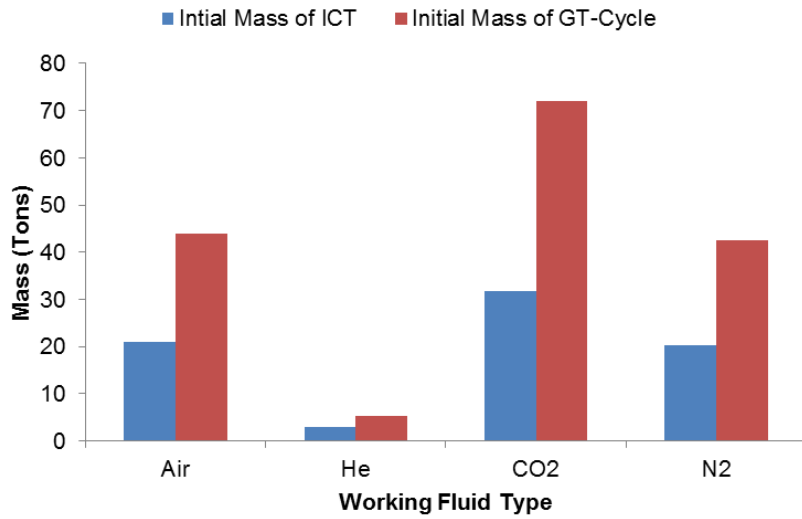


Figure 5-20 Mass of Inventory tank and GT cycle before part-load operations

During part-load operation, the working fluid in the GT cycle is transfer into the inventory control tank. Figure 21 shows the mass of fluid taken out from the GT cycle at the opening of inventory valves from 100% load to 50% load. Similarly, Fig. 22 describes the total mass of the inventory tank as the load requirement moves from full load to 50%.

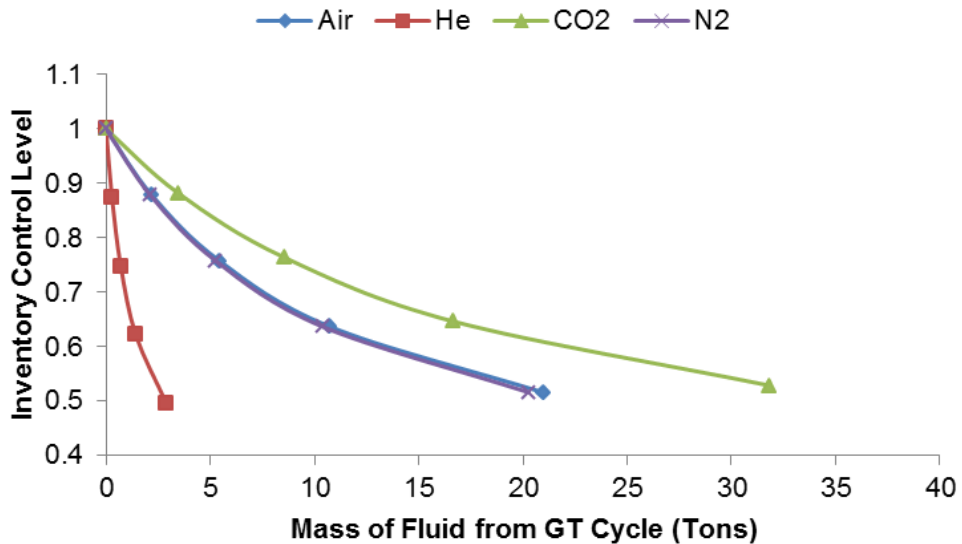


Figure 5-21 Mass of working fluid leaving the GT cycle during part-load operation

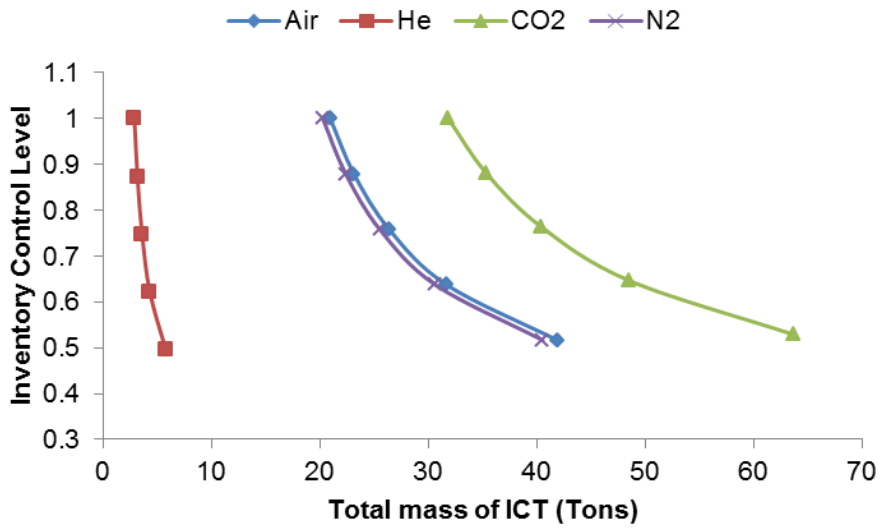


Figure 5-22 Total mass of ICT during part-load operation

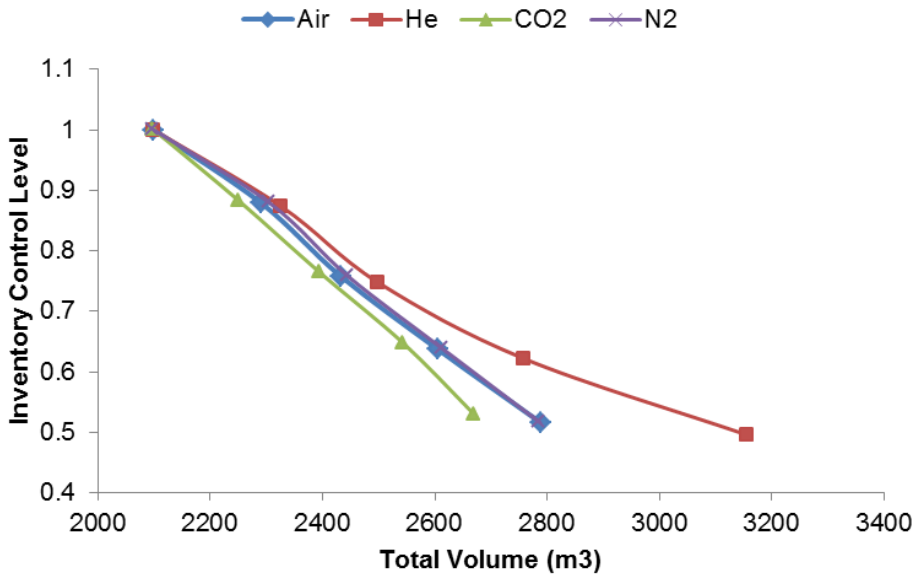


Figure 5-23 Total volume of inventory tank during part-load operation

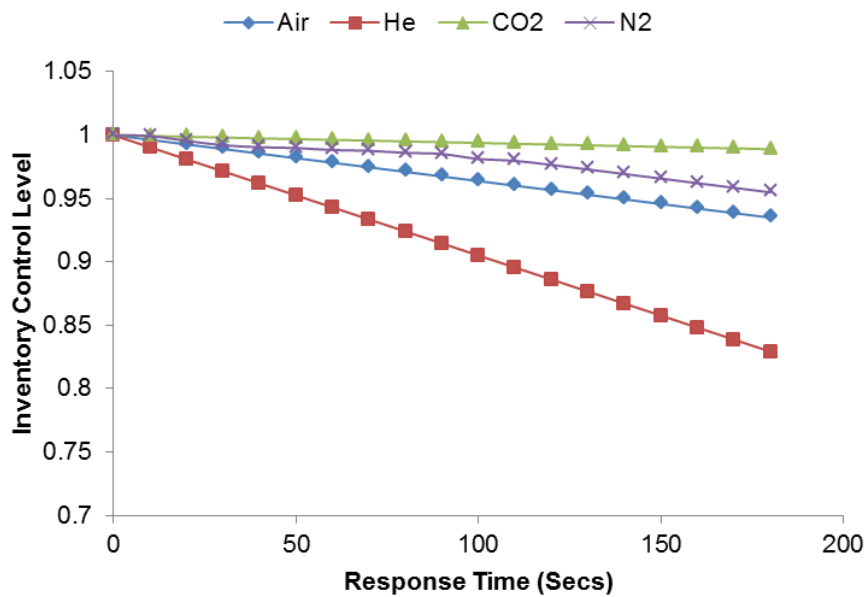


Figure 5-24 Working fluid response to part-load operation

Similarly, Fig.5-23 shows the total volume of the inventory tank at full load to 50% load. This implies that the level of the inventory control at part-load can be influenced by the working fluid for a fixed inventory tank size. In figure 5-24, for a fixed valve diameter, the response rate of carbon dioxide was the least, as a result of its molecular weight. To increase the rate of response for carbon dioxide will require a larger valve size diameter, which means, an additional cost. Although helium seems to show some reasonable advantage over other fluids, it is, however, necessary for a full economic assessment to be done to validate its viability.

5.6 Effect on Component Design, Sizing, and Operational Performance

The size of the gas turbine cycle equipment is greatly influenced by the type of working fluid to be used. In this section, the plant thermodynamic model; turbomachinery and heat exchanger models developed in the work are used to evaluate the effect of different working fluid on the performance of a closed-cycle power plant and on the preliminary design and sizing of its components. The aim of this section is to present a comparison of the selected working fluids on the preliminary component designs and sizing of the closed-cycle gas

turbine. Secondly, this section also presented a comparison of the working fluids from an operational performance point of view, for an existing plant original designed to work with a specified working fluid. The study identifies candidate working fluids that may be suitable for the plant operations without major modifications on the engine configurations and discusses the potential challenges that may be encountered.

The models presented were incorporated into the GT-ACYSS plant performance model. The size of the equipment is of interest since it has an influence on the cost of the plant.

5.6.1 Turbomachinery Preliminary Design and Sizing Model

The preliminary design and sizing process of the turbo-set is basically set-off with design assumptions and initial value specifications. Next, is to carry out the overall configuration of the annulus, followed by the aerodynamic design of each stage. The outcome of each process is checked with the reasonable rule of thumb standard values. These standard values are obtained from turbomachinery design experiences.

For the purpose of this study, the compressor and turbine design model implemented were based on mean-line analysis of free vortex flow along the blades and a constant axial flow velocity V_a span-wise [146]. The inlet angle was assumed to be zero. The model also assumed a constant pressure and temperature ratio per stage and both components were designed for subsonic flow, in the stages. The input requirements are obtained from the thermodynamic cycle calculation results and specifications for the compressor and turbine design such as the component pressure ratio, mass flow, component efficiency, inlet temperature and pressure. In this model, the user can select the annulus configuration of choice.

For the compressor, the temperature or pressure rise through the whole component is obtained from the performance calculation; hence, a simple assumption of the temperature rise per stage can be used to obtain the number

of stages. The following relationships were used to carry out the turbomachinery preliminary design and sizing.

Compressor annulus area (A_c) for inlet or outlet geometry is given as:

$$A_c = \frac{W_c \sqrt{T_c}}{Q_0 K_b P_c} = \frac{\pi (D_m)^2}{4} \quad (5-3)$$

Where,

K_b = blockage factor

Q_0 = Non-dimensional mass flow for a given inlet Mach number

$$D_m = \frac{D_h + D_t}{2} \quad (5-4)$$

The hub-to-tip ratio is obtained is given as:

$$\text{hub - to - tip ratio} = \frac{D_h}{D_t} \quad (5-5)$$

The relationship between the rotational speed and mean blade speed is given as:

$$rpm = \frac{U_m * 60}{\pi D_m} \quad (5-6)$$

Stage efficiency η_{stage} is given as

$$\eta_{stage} = \frac{\ln PR^{\frac{\gamma-1}{\gamma}}}{\ln \left[T_3 \left[1 + \frac{\left(PR^{\frac{\gamma-1}{\gamma}} - 1 \right)}{\eta_c} \right] \right]} \quad (5-7)$$

Similarly, stage pressure ratio is obtained from,

$$R_{stage} = \left[\eta_{stage} \frac{\Delta T_{stage}}{T_2} + 1 \right]^{\left(\frac{\gamma}{\gamma-1} \right)} \quad (5-8)$$

Number of stages is given as:

$$\text{Number of Stages} = \frac{C_p \Delta T}{\Delta h} \quad (5-9)$$

Rotor inlet velocity is given as

$$V_1 = \frac{V_{a1}}{\cos \alpha_1} \quad (5-10)$$

Where,

$$\alpha_1 = \tan^{-1} \frac{U_m}{V_{a1}} \quad (5-11)$$

The stage out outlet velocity is given as

$$V_3 = \sqrt{V_{a3m}^2 + V_{w3m}^2} \quad (5-12)$$

Where,

$$V_{w3m} = \frac{C_p * \Delta T_{stage}}{U_{2m}} \quad (5-13)$$

The stage and blade load coefficient is obtained by

$$\text{Load Coefficient} = \frac{\Delta h}{U_m^2} = \frac{V_{w3m}}{U_{2m}} \quad (5-14)$$

$$\text{Flow Coefficient} = \frac{V_a}{U_m} \quad (5-15)$$

De Haller number is given as

$$\text{Rotor De Haller no.} = \frac{V_2}{V_1} = \frac{V_{a2m}}{V_{a1m}} * \frac{\cos \alpha_1}{\cos \alpha_2} \quad (5-16)$$

$$\text{Stator De Haller no.} = \frac{V_4}{V_3} = \frac{V_{a1m}}{V_{a2m}} * \frac{\cos \alpha_3}{\cos \alpha_4}$$

The process for calculating the turbine sizing is similar to that of the compressor, but instead of pressure or temperature rise, the pressure or temperature drop is calculated

$$\text{Turbine temperature drop} = \frac{\text{Power}}{W * C_p} \quad (5-17)$$

The annulus area is calculated using thermodynamic inputs from the design point. However, a slightly different approach is utilised to estimate the inter stage annulus area. A work done factor is used instead of a blockage factor to take into account boundary layer build-up

The length of the turbomachinery components was estimated using Sagerser et al., empirical model [107]

The compressor length is given by:

$$L_c = D_m * [(0.2 + [(0.234 - (0.218 * \text{hub_tip_ratio}))] * N_s)] \quad (5-18)$$

The turbine length is given by:

$$L_T = N_s \left[\left(\frac{\bar{D}_t - \bar{D}_h}{0.96 * \text{hub_tip}} \right)_{rotor} + \left(\frac{\bar{D}_t - \bar{D}_h}{0.96 * \text{hub_tip}} \right)_{stator} + (2N_s - 1) \left(0.4 * \frac{\bar{D}_t - \bar{D}_h}{0.96 * \text{hub_tip}} \right)_{rotor} \right] \quad (5-19)$$

5.6.2 Heat Exchanger Preliminary Design and Sizing Model

The purpose of the heat exchangers in a closed-cycle gas turbine is to transfer heat energy from one fluid medium to another for heating or cooling purposes. Thus, the heat exchangers play important roles in the cycle performance and there is a need for reliable heat exchangers that are able to withstand high temperature and pressure as required in closed-cycle power plants [149].

To this end, the choice of working fluid greatly influences the selection and design of heat exchangers. In this subsection, preliminary design and sizing were carried out for the recuperator. In complement to this, thermodynamic characteristics of the heat exchanger compactness for the different working fluid are also compared. The effectiveness-NTU method was used in the cycle

calculation to determine key design parameters for sizing the heat exchangers. Straight flow channels with counterflow arrangement were assumed in the design.

In the previous chapter, a method for calculating the NTU has been described. Consequently, the step to the estimation of heat exchanger sizing is a continuation.

Recall that NTU was obtained from,

$$NTU = \frac{LOG_e \left[\frac{2 - \varepsilon(1 + C^* - \eta_{Hex})}{2 - \varepsilon(1 + C^* + \eta_{Hex})} \right]}{\eta_{Hex}} \quad (5-20)$$

Where,

$$\eta_{Hex} = (C^{*2} + 1)^{0.5}$$

Next, is to calculate the maximum effectiveness

$$\varepsilon_{max} = \frac{2}{(1 + C^* + \eta_{Hex})}$$

If $\varepsilon > \varepsilon_{max}$, then the number of multiple shell is given by

$$Sn = \frac{LOG_e \left(\frac{1 - \varepsilon}{1 - \varepsilon \times C^*} \right)}{LOG_e C^*} \quad (5-21)$$

Sn , was approximated to the nearest whole number, hence, the effectiveness per shell is calculated as

$$\varepsilon_{Sn} = \frac{\left(\frac{1 - \varepsilon}{1 - \varepsilon \times C^*} \right)^{\frac{1}{Sn}}}{1 - C^* \times \left(\frac{1 - \varepsilon}{1 - \varepsilon \times C^*} \right)^{\frac{1}{Sn}}} \quad (5-22)$$

Having established the Heat Exchanger Effectiveness per shell, the number of transfer unit is calculated,

$$NTU_{Sn} = \frac{LOG_e \left[\frac{2 - \epsilon_{Sn}(1 + C^* - \eta_{Hex})}{2 - \epsilon_{Sn}(1 + C^* + \eta_{Hex})} \right]}{\eta_{Hex}} \quad (5-23)$$

Therefore, $\frac{Q}{\Delta T_m}$ is obtained by

$$\left(\frac{Q}{\Delta T_m} \right)_{Sn} = C_{min} \times NTU_{Sn} \quad (5-24)$$

The Surface area for each shell is obtained from

$$A_{Sn} = \left(\frac{Q}{\Delta T_m} \right)_{Sn} \times U^{-1} \quad (5-25)$$

Where,

U = overall heat transfer coefficient

The heat exchanger length is given by

$$Heat\ Exchanger\ Length = \frac{DA}{4} \quad (5-26)$$

Where D = Diameter, A = Area

5.6.3 Inventory Tank Design Sizing and Weight Model

As previously mentioned, the inventory control systems consist of the storage tank and valves. For the purpose of this study, a cylindrical pressure vessel was selected for the inventory storage tank. This type of pressure vessels is generally preferred because they present a simple manufacturing problem and better use of available space. To design the pressure vessels, ASME VIII code was used as a reference guide [150,151]. The ASME code design criteria consist of basic rules specifying the design method, load, allowable stress, acceptable materials, and fabrication.

The pressure vessel consists of cylindrical shells, two ellipsoidal head, saddle supports, valves and reinforcement, and an insulator perforated on the walls of the cylindrical shell [135,152].

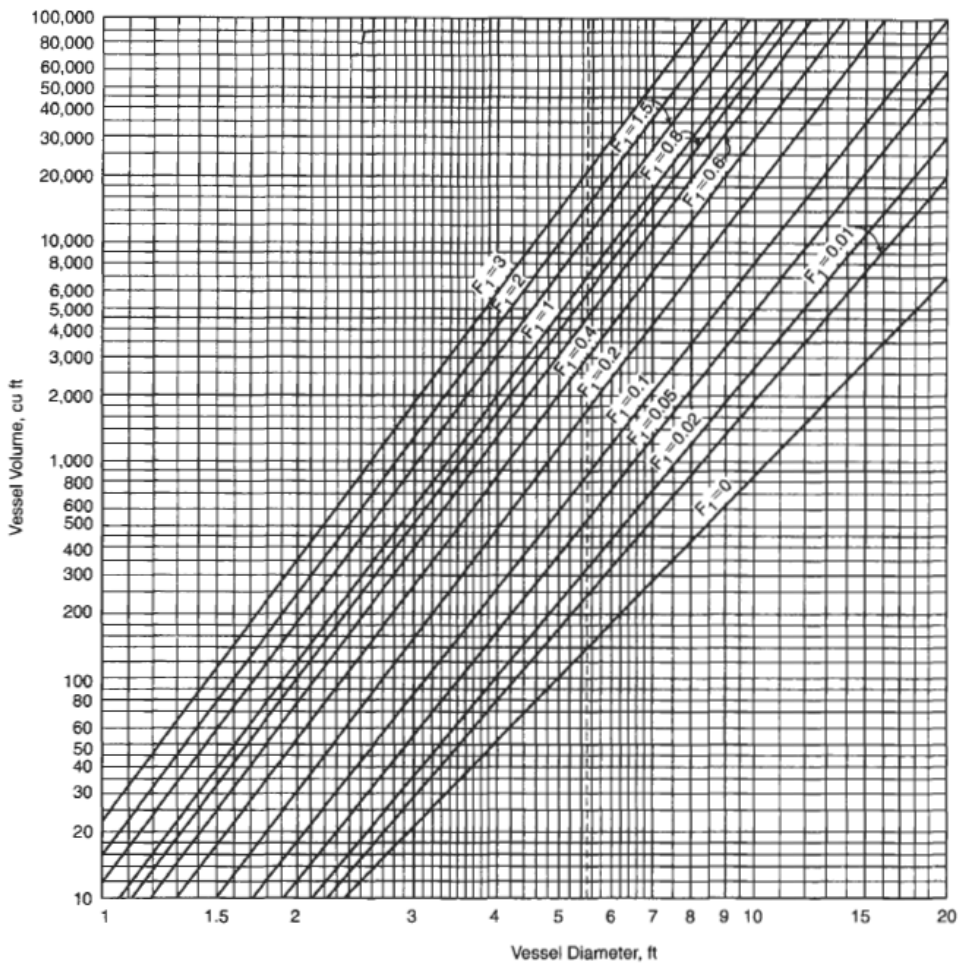


Figure 5-25 Chart for Determining Optimum Diameter of Pressure Vessel Storage Tank [153,154]

The procedure for determining the optimum size and weight of the storage tank pressure vessels based on reference [153,154] is as follows

First, the tank capacity factor F is determined by:

$$F = \frac{P_{tDesign}}{C \times S_a \times E}, \quad 0 \leq C \leq 0.125, \quad 0.85 \leq E \leq 1 \quad (5-27)$$

Where,

$$P_{tDesign} = (P_5 + P_{t1}) \times J \quad (5-28)$$

S_a = stress value of material

E = joint efficiency

J = factor of safety

C = corrosion allowance

Using the Value of F and Total Volume of Fluid in storage tank, the diameter D is obtained from Fig (5-25), and total length L of pressure vessel storage tank is given by:

$$L = \frac{4V_T}{\pi D^2} \quad (5-29)$$

The thickness of the cylindrical shell (CST_T) is obtained as follow

$$CST_T = \frac{P_{tDesign} \times r_i}{[S_a E - 0.6P_{tDesign}]} + C \quad (5-30)$$

Where,

r_i = internal radius

Next, is to calculate the internal volume of the cylindrical shell (V_{cs}), which is given by

$$V_{cs} = \pi r_i^2 h \quad (5-31)$$

The maximum allowable stress used to determine the minimum vessel wall thickness was based on material properties from references [150,153,154]

Similarly, the required thickness of the dished head ellipsoidal (EH_T) was obtained from,

$$EH_T = \frac{P_{tDesign} \times D \times K}{[2S_a E - 0.2P_{tDesign}]} + C, \quad K = \frac{[2 + (D/2h)^2]}{6} \quad (5-32)$$

Where,

D = internal diameter

K = stress intensification factor

Volume of the ellipsoidal (V_e) is calculated as

$$V_e = \frac{2\pi r_i^2}{3} \quad (5-33)$$

Hence, total internal volume of tank is given by

$$V_T = V_{CS} + V_e \quad (5-34)$$

Therefore, the insulator volume (V_c) was obtained, since the internal volume is occupied by the perforated insulator

$$V_c = V_T - \frac{W_c}{\rho_c} \quad (5-35)$$

Having obtained the volume, the weight of the cylindrical shell was obtained from,

$$W_{CS} = \pi \times D \times CST_T \times L \times \rho \quad (5-36)$$

Weight of the ellipsoidal head (W_{EH}) is given as

$$W_{EH} = 1.084D^2 \times EH_T \times \rho \quad (5-37)$$

Weight of insulator (W_c) is given as

$$W_c = V_T \times HC_{ratio} \times \rho \quad (5-38)$$

$$HC_{ratio} = \text{insulator packing ratio}$$

Therefore, the total weight of the Pressure vessel storage tank is given as

$$Total\ Weight_{ICS} = (W_{CS} + W_{EH} + W_c) \quad (5-39)$$

Where n = number of tanks

5.6.4 Case Studies

In this subsection, the effect of selected working fluids (carbon dioxide, nitrogen, helium, and air) on the component design and sizing of a recuperated closed-cycle gas turbine coupled with a Gen-IV nuclear reactor is analysed. The design point characteristics of the reference plant are shown in Table 5-5 and a

schematic representation of the plant is also shown in Fig.5-26. The reference plant had nitrogen as working fluid.

The plant thermodynamic and turbomachinery models developed in GT-ACYSS was used to evaluate the effect of changing working fluid on the performance and component design of the reference plant. The study was carried out assuming a constant overall temperature ratio and isentropic temperature ratios for all working fluid. This is to give the same reasonable condition for the analysis of the turbo-set, in order to have similar temperature and pressure at the inlet and outlet of the compressor, turbine, and recuperator.

To this end, obtaining the pressure ratios for other working fluids based on Table 5-5 becomes:

$$PR_c = (X_c)^{\left(\frac{\gamma_c-1}{\gamma_c}\right)} \quad (5-40)$$

$$X_t = \left(\frac{P_7}{P_6}\right)^{\left(\frac{\gamma_t-1}{\gamma_t}\right)}, \quad X_c = \left(\frac{P_3}{P_2}\right)^{\left(\frac{\gamma_c-1}{\gamma_c}\right)}$$

Where X_c = compressor isentropic temperature ratio

X_t = turbine isentropic temperature ratio

In analysing the effect of the different gases, it was essential to set-up another common basis for comparison. Hence, the following cases were studied;

- Case 1 – Same output power for all working fluid design
- Case 2 – Constant rotational speed
- Case 3 – Fixed geometry – Same Non-Dimensional Point

For the first case, the aim was to give an analytical support to decision making from OEMs or procurement point of view, on the effect of using the aforementioned working fluids on the performance and component design of the reference power plant. To achieve this, the shaft output power was kept constant as the basis for comparison and the corresponding mass flows for each working fluid were obtained. The components were designed with limiting

value of mean speed U_m (constant U_{mean} for all working fluids) and axial velocity V_a been assumed. Constant outer diameter annulus configuration was assumed in this study. The effects of the working fluids based on these assumptions are described in Fig 5-27 and 5-28.

In the second case, the rotational speed was assumed to be constant, and the operating point of each fluid on the nitrogen compressor characteristics was obtained.

In the third case, the component inlet area and Mach number were assumed to be constant. Obtaining the required mass flow for each case was achieved using equation 5-40.

$$W = \rho AV = \rho AM \sqrt{\gamma RT} \quad (5-41)$$

Therefore, for constant Mach number, compressor inlet area and compressor isentropic temperature ratio T_c , the changes in mass flow will be influenced by changes in gas properties of each working fluid.

The following procedures were taken:

- a. Analyse design and performance characteristics of actual plant cycle using nitrogen as working fluid
- b. Analyse the cycle performance and component design point sizing using different working fluid based on the case scenarios presented above.

Table 5-5 Summary of reference plant design point description

Description	Unit
Heat Source Temp.	1100 (K)
Compressor isentropic temp. ratio	1.350
Compressor Inlet Pressure	4.7 (atm.)
Compressor Inlet Temperature	311 (K)
GH, RX, PC Pressure drops	2%, 1.5%, 1%
Compressor efficiency	85 (%)
Turbine efficiency	86 (%)
Flow rate at Compressor	230 (kg/s)
Plant Thermal Efficiency	40.0 (%)
PC & GH effectiveness	95 (%)
RX effectiveness	86 (%)
Rated power	38.2 (MW)
Working Fluid	Nitrogen

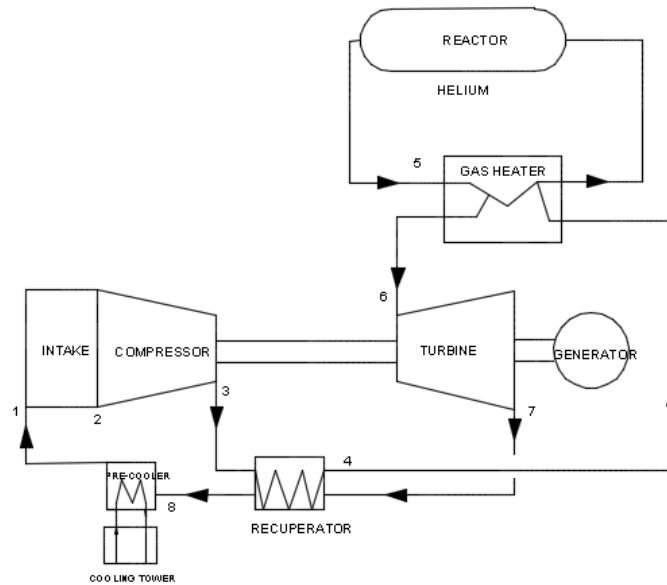


Figure 5-26 Schematic representation of the Gen-IV reactor indirectly coupled with a recuperated closed-cycle gas turbine

As previously mentioned, all working fluid in the case1 were designed to give an output power of 38.2MW, with fixed temperature ratio and isentropic temperature ratio. The thermodynamic performance results are shown in Appendix B. Thus, there was a reduction in helium mass flow by 71% (65.2kg/s) to compensate for its high thermodynamic properties. Similarly, the mass of CO₂ was raised by 30% (300.2kg/s) to obtain the same output power conditions. Nitrogen and air share close properties which explain why their mass flow remained almost the same. The mass flow of air was set at 235kg/s which is 2% higher than that of nitrogen as shown in Table 5-5. The pressure ratios obtained are as follow – 2.91for nitrogen, 2.13 for helium, 2.92 for air and 3.923 for carbon dioxide.

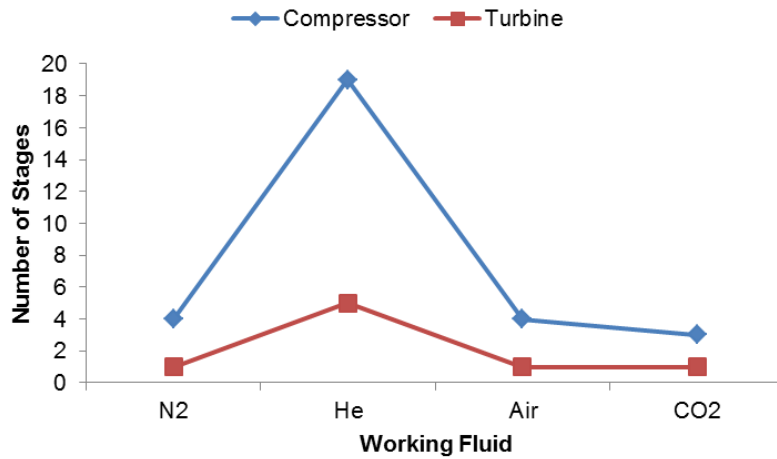


Figure 5-27 Case1 – Turbomachinery number of stages (same output power for all working fluids)

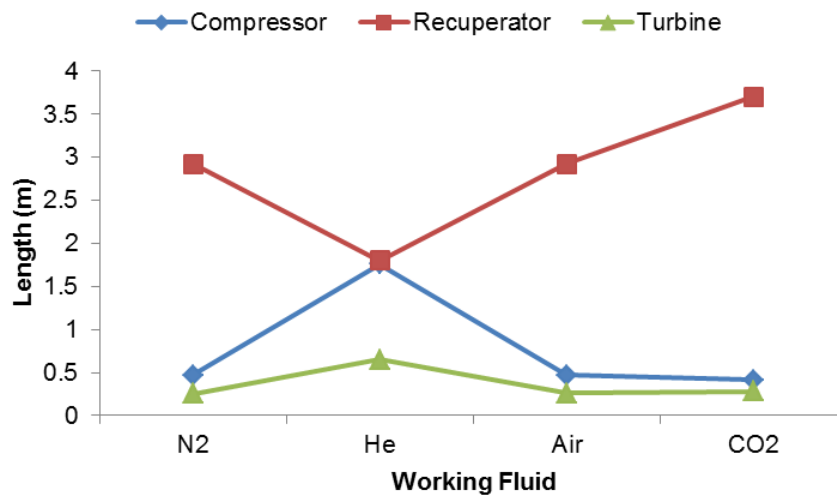


Figure 5-28 Case1 – Length of the compressor, turbine, and recuperator (same output power for all working fluids)

The choice of working fluid affects the number of stages for the attainment of the required compressor pressure ratio and high efficiency. It also affects the machine size for a high-pressure closed-cycle system. The specific heat of helium is about five times that of nitrogen or air, and since the stage temperature rise is inversely proportional to the specific heat for a given limiting blade speed [6,12], it follows that the temperature rise available per stage when

running with helium will be about one fifth that of nitrogen, which of course, results in more stages being required for a helium compressor.

Figure 5-27, describes the number of stages required to achieve the same overall temperature rise or drop for the compressor and turbine respectively for nitrogen, helium, carbon dioxide and air when designing at constant mean speed U_m . For helium, the number achievable compressor stages were obtained as 19, nitrogen and air at 4 stages while carbon dioxide gave 3 stages. Similarly, the model obtained 5 stages for the helium turbine and 1 stage for carbon dioxide, air, and nitrogen. The number of stages for the turbine is greatly influenced by the specific capacity as can be seen in Eq. 5-9. Also, it is important to note that the axial inlet Mach number for helium was set so low at 0.19 whereas nitrogen had 0.57, air 0.59 and carbon dioxide 0.640 due to the thermodynamic properties of each working fluid used in this study to obtain same conditions set at the beginning. The analysis shows that the properties of gamma and low molecular weight, which makes a gas particularly advantageous from the viewpoint of heat transfer, result in a very low attainable pressure ratio per stage for turbomachinery if it is considered that the work input per stage is limited by mechanical considerations. However, if the number of stages for the helium were to be reduced, which will probably be the case for a specific rather than comparative design, careful attention will have to be given to the rotational speed and stress level. The turbo-set shaft speed obtained for the comparative design was set at 7616rpm, 6764rpm, 7613rpm, and 6745rpm for nitrogen, helium, air and carbon dioxide respectively.

Figure 5-28, gives an overview of the length of each component for the different working fluids. The surface area of the heat exchangers in a closed-cycle gas turbine is greatly influenced by the type of working fluid. It can be seen that the ratio of working fluid heat transfer and pressure loss is proportional to the ratio of gas pressure multiply by specific heat to the fluid molecular weight [15]. The thermodynamic properties of helium tend to favor its usage for a compact heat exchanger design compared with other fluids. A typical overview of the case 1 result obtained is shown in Table (5-6), (5-7), and (5-8).

Table 5-6 Case1 – Compressor Characteristics (same output power for all working fluids)

Reference Plant Component	Compressor Characteristics			
	Nitrogen	Helium	Air	Carbon dioxide
Working Fluid	Nitrogen	Helium	Air	Carbon dioxide
Compressor Inlet Temperature (K)	311	311	311	311
Compressor Inlet Pressure (Atm.)	4.7	6.4	4.68	3.49
Mass Flow (Kg/s)	230	65.20	235	300.2
Non-Dimensional Mass Flow	0.124	0.068	0.126	0.176
Rotational Speed (rpm)	7616	6764	7613	6745
Non-Dimensional Speed	21.20	6.520	21.55	24.58
Inlet Flow Axial Mach Number	0.57	0.19	0.590	0.640
Relative Tip Mach Number	0.98	0.34	0.996	1.28
Pressure Ratio	2.91	2.13	2.92	3.923
Compressor Temperature Ratio	1.351	1.351	1.351	1.351
Compressor Exit Temperature (K)	439.4	439.4	439.4	439.4
Compressor Exit Pressure (Atm.)	13.70	13.70	13.70	13.70
Umean	275	275	275	275
Number of Stages	4	19	4	3
Temperature Rise per Stage	31.6	6.78	31.9	39.1
First Stage Characteristics				
First Stage Tip Diameter (m)	0.81	0.91	0.81	0.91
First Stage Hub Diameter (m)	0.57	0.72	0.58	0.64
Hub to Tip Ratio	0.7	0.7	0.7	0.7
Tip Speed (m/s)	323.5	323.5	323.5	323.5
Axial Velocity (m/s)	200	200	200	200
De Haller No.	0.72	0.73	0.72	0.74
Stage Flow Coefficient	0.65	0.70	0.64	0.58
Stage Loading	0.45	0.45	0.45	0.45
Inlet Area (m ²)	0.264	0.33	0.264	0.34
Last Stage Characteristics				
Last Stage Tip Diameter (m)	0.81	0.91	0.81	0.91
Last Stage Hub Diameter (m)	0.69	0.72	0.70	0.82
Hub to Tip Ratio	0.86	0.79	0.86	0.89
Tip Speed (m/s)	323.5	323.5	323.5	323.5
Axial Velocity (m/s)	242	202	244	246
De Haller No	0.85	0.76	0.85	0.87
Stage Flow Coefficient	0.81	0.70	0.82	0.83
Stage Loading	0.39	0.40	0.39	0.37
Exit Mach Number	0.35	0.16	0.48	0.53
Exit Area (m ²)	0.134	0.24	0.134	0.126
Isentropic Efficiency (%)	85	85	85	85
Reynolds Number (10 ⁻⁶)	4.431	0.258	3.594	2.568
Overall Compressor Length (m)	0.47	1.76	0.47	0.41

Table 5-7 Case1 – Recuperator Characteristics (same output power for all working fluids)

Reference Plant Component	Recuperator Characteristics			
	Nitrogen	Helium	Air	Carbon dioxide
Working Fluid	Nitrogen	Helium	Air	Carbon dioxide
Inlet Temperature (K) LP	874.7	853.9	876.2	908.5
Inlet Temperature (K) HP	439.4	439.4	439.4	439.4

Inlet Pressure (Atm.) LP	4.83	6.58	4.81	3.55
Inlet Pressure (Atm.) HP	13.78	13.78	13.78	13.78
Mass Flow (Actual)	224	63.2	229	292
Total Pressure Loss	3.5	3.5	3.5	3.5
Inlet Flow Mach Number	0.35	0.16	0.48	0.53
Effectiveness (%)	86	86	86	86
UA (MW/K)	1.69	2.35	1.68	1.1
Overall Recuperator Length (m)	2.92	1.8	2.93	3.7

Table 5-8 Case1 – Turbine Characteristics (same output power for all working fluids)

Reference Plant Component	Turbine Characteristics			
	Nitrogen	Helium	Air	Carbon dioxide
Working Fluid	Nitrogen	Helium	Air	Carbon dioxide
Turbine Inlet Temperature (K)	1100	1100	1100	1100
Turbine Inlet Pressure (Atm.)	13.23	13.23	13.23	13.230
Mass Flow	224	63.200	229	292
Non-Dimensional Mass Flow	0.025	0.055	0.083	0.092
Rotational Speed	7616	6764	7613	6745
Non-Dimensional Speed	11.541	3.467	11.733	13.639
Inlet Flow Mach Number	0.300	0.110	0.313	0.400
Pressure Ratio	2.780	2.030	2.79	3.760
Turbine TR	1.292	1.327	1.288	1.220
Number of Stages	1	5	1	1
Umean	330	293	331	293
First Stage Tip Diameter (m)	0.94	1.052	0.939	0.922
First Stage Hub Diameter (m)	0.720	0.614	0.720	0.737
Hub to Tip Ratio	0.765	0.581	0.766	0.798
Tip Speed (m/s)	374	372	374	325
Axial Velocity (m/s)	200	200	200	200
Stage Flow Coefficient	0.600	0.680	0.604	0.682
Stage Loading	2.66	2.77	2.565	2.95
Inlet area (m ²)	0.29	0.58	0.286	2.95
Last Stage Tip Diameter (m)	-	1.091	-	-
Last Stage Hub Diameter (m)	-	0.564	-	-
Hub to Tip Ratio	-	0.517	-	-
Tip Speed (m/s)	-	388	-	-
Axial Velocity (m/s)	-	200	-	-
Exit Area (m ²)	-	1.00	-	-
Isentropic Efficiency	86	86	86	86
Reynolds Number (10 ⁻⁶)	12.183	0.530	11.072	6.938
Overall Turbine Length (m)	0.25	0.65	0.26	0.28

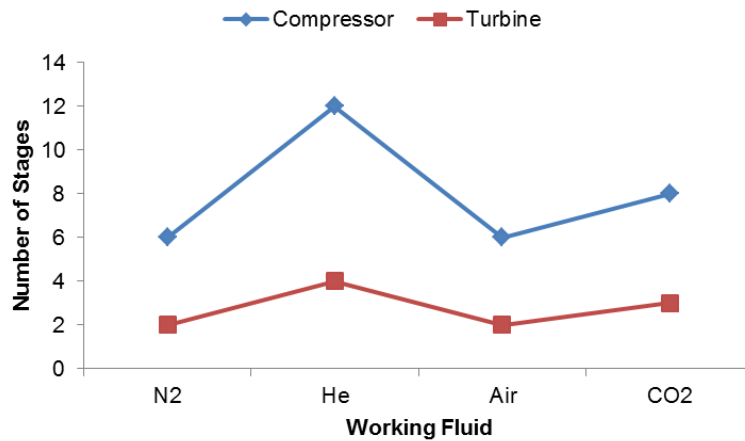


Figure 5-29 Case2 – Turbomachinery Number of stages (same rotational speed for all working fluids)

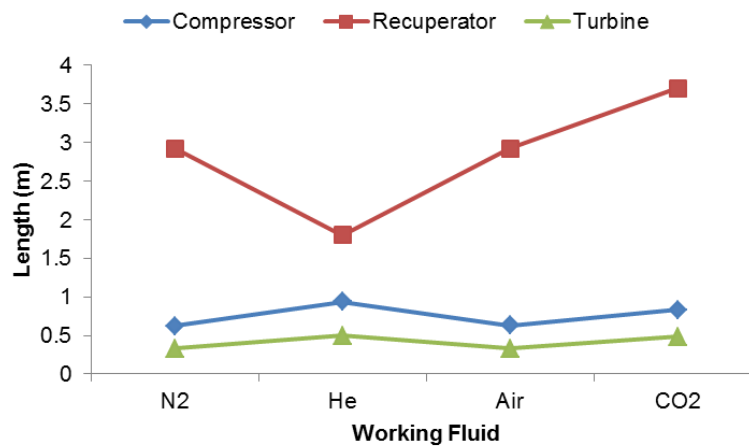


Figure 5-30 Case2 - Length of the compressor, turbine, and recuperator (same rotational speed for all working fluids)

In case 2, at the constant rotational speed of 5800rpm, the non-dimensional speed and mass flow rise by 25% (20.28) and 11% (255kg/s) respectively, when switching from nitrogen to CO₂. This increase moves the Speedline operating point above the surge margin; hence, this massive change cannot be accommodated without physical modification on the compressor and turbine geometry as shown in Figure 5-29, 5-30 and 5-31. The power output drops by a factor of 0.21. Similarly, switching to helium moves the operating point to surge

line at 62% (6.117) reduction in non-dimensional speed, and at a pressure ratio of 2.13. However, due to the thermodynamic properties of helium, the realisable number of compressor stages would be 12, which implies that the compressor and turbine would need to be modified. Also, there is an increase in the output power by a factor of 1.02. Air and Nitrogen showed similar behaviour; hence, switching the fluid to air would not require modification of the turbomachinery component. For both fluids, 6 number of compressor stages. The turbine results showed 2, 4, 2 and 3 stages for nitrogen, helium, air and carbon dioxide.

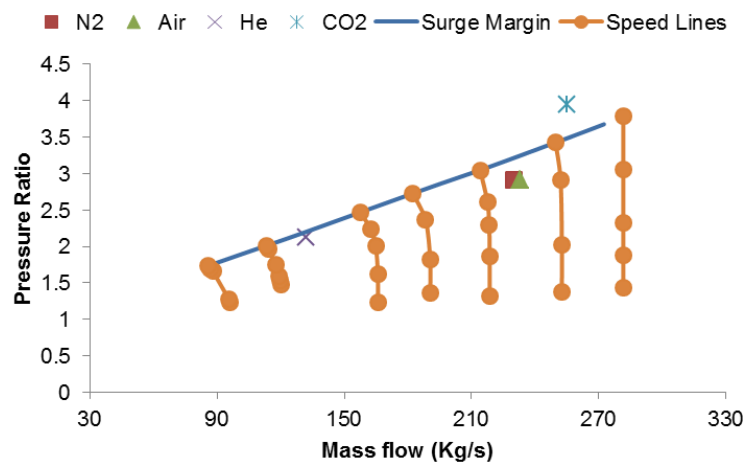


Figure 5-31 Case2 – compressor characteristics (same rotational speed for all working fluids)

It is important to observe that changing the working fluid from nitrogen to helium or carbon dioxide greatly modified the aerodynamic requirements by removing Mach number constraints [7,35,146]. The challenge then becomes to possibly induce the gas velocities within the allowable blade stress threshold. Since the rotational speed for all the fluid is the same, then, the size of the compressor is thus dictated by the choice of the blade speed, since the stage loading factor is inversely proportional to the square of the blade speed [12,79]. These also affect the turbine in a similar manner as described for the compressors.

The cycle performance for case 2 followed a similar trend as reported in case 1. Detailed results for the first and last stages of the compressor of case2 can be

found in Table 5-9. The recuperator characteristics remain the same as case1.
The turbine characteristic is shown in Appendix

Table 5-9 Case2 – Compressor Characteristics (same rotational speed for all working fluids)

Reference Plant Component	Compressor Characteristics			
	Nitrogen	Helium	Air	Carbon dioxide
Working Fluid				
Compressor Inlet Temperature (K)	311	311	311	311
Compressor Inlet Pressure (Atm.)	4.7	6.4	4.68	3.46
Mass Flow (Kg/s)	230	132	232.8	255
Non-Dimensional Mass Flow	0.124	0.139	0.124	0.149
Rotational Speed (rpm)	5800	5800	5800	5800
Non-Dimensional Speed	16.18	6.117	16.45	20.28
Inlet Flow Axial Mach Number	0.3	0.28	0.3	0.35
Relative Tip Mach Number	0.82	0.82	0.82	0.82
Pressure Ratio	2.91	2.13	2.92	3.94
Temperature Ratio	1.351	1.351	1.351	1.351
Compressor Exit Temperature (K)	439.4	439.4	439.4	439.4
Compressor Exit Pressure (Atm.)	13.78	13.78	13.78	13.78
Umean	275	285	260.87	260
Number of Stages	6	12	6	8
Temperature per stage	21.4	10.8	21.9	16.01
First Stage Characteristics				
First Stage Tip Diameter (m)	1.05	1.08	1.05	1.04
First Stage Hub Diameter (m)	0.73	0.73	0.72	0.73
Hub to Tip Ratio	0.7	0.7	0.7	0.7
Tip Speed	323.5	335	307	305.8
Axial Velocity	108	270	110	105
De Haller No.	0.739	0.723	0.74	0.83
Stage Flow Coefficient	0.35	0.9	0.38	0.35
Stage Loading	0.31	0.71	0.31	0.33
Inlet Area	0,444	0.47	0.438	0.441
Last Stage Characteristics				
Last Stage Tip Diameter (m)	1.05	1.08	1.04	1.04
Last Stage Hub Diameter (m)	0.9	0.83	0.9	0.93
Hub to Tip Ratio	0.85	0.79	0.856	0.89
Tip Speed	323.5	335	307	305.8
Axial Velocity	116	255	119	122
De Haller No	0.78	0.75	0.79	0.79
Stage Flow Coefficient	0.4	0.836	0.42	0.42
Stage Loading	0.27	0.51	0.28	0.28
Exit Mach Number	0.254	0.28	0.26	0.26
Exit Area	0.233	0.35	0.228	0.20
Isentropic Efficiency (%)	85	85	85	85
Reynolds Number (10^{-6})	4.431	0.25	3.594	2.568
Overall Compressor Length	0.625	0.936	0.628	0.83

In the comparison of case 3, all the working fluid was designed on the basis of constant Mach number and constant non-dimensional points. Hence, Figure 5-32 shows that switching to helium would require an increase in the rotational speed by a factor of 2.89 in order to maintain the same number of stages. Also the blade tip speed increases by a factor of 2.83, which exceeds the maximum limit expected. This also affects the component efficiency. For CO₂, there is a reduction in speed by a factor of 1.3. Figure 5-33 describes the length of the turbomachinery and recuperator for each working fluid.

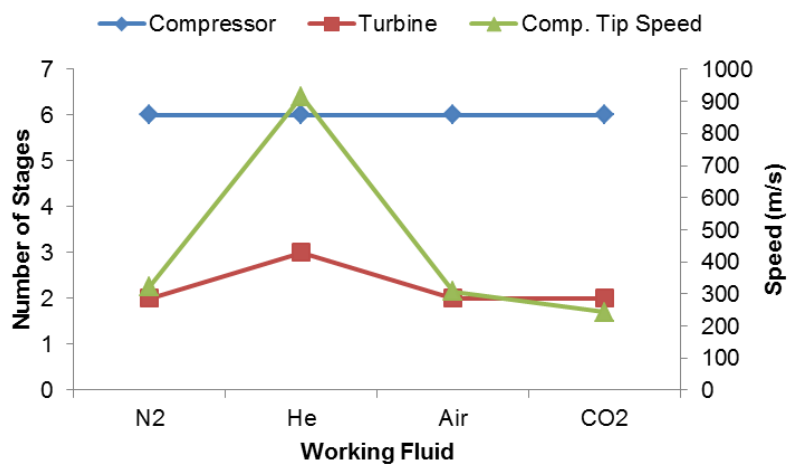


Figure 5-32 Case3 – Turbomachinery Number of stages (same geometry)

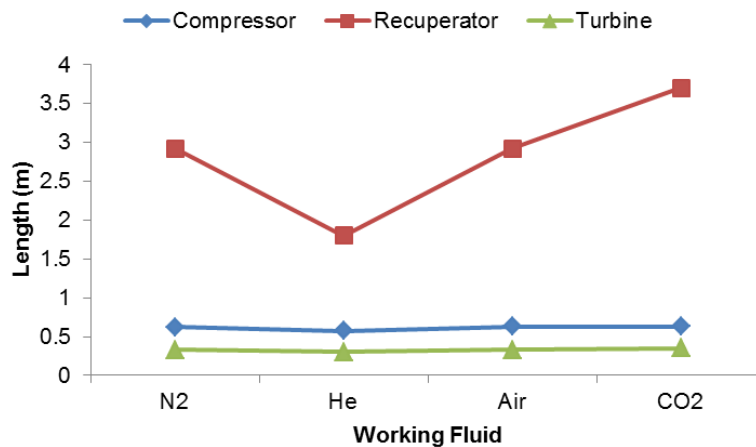


Figure 5-33 Case3 - Length of the compressor, turbine and recuperator (same geometry for all working fluids)

Table 5-10 Case3 - Compressor Characteristics (same geometry for all working fluids)

Reference Plant Component	Compressor Characteristics			
	Nitrogen	Helium	Air	Carbon dioxide
Working Fluid	Nitrogen	Helium	Air	Carbon dioxide
Compressor Inlet Temperature (K)	311	311	311	311
Compressor Inlet Pressure (Atm.)	4.7	6.4	4.68	3.49
Mass Flow (kg/s)	230	129.5	232.8	205.4
Non-Dimensional Mass Flow	0.124	0.124	0.124	0.124
Rotational Speed (rpm)	5800	16784	5704	4441
Non-Dimensional Speed	16.18	16.18	16.18	16.18
Inlet Flow Axial Mach Number	0.3	0.3	0.3	0.3
Relative Tip Mach Number	0.82	0.82	0.82	0.82
Pressure Ratio	2.91	2.13	2.92	3.923
Temperature Ratio	1.351	1.351	1.351	1.351
Compressor Exit Temperature (K)	439.4	439.4	439.4	439.4
Compressor Exit Pressure (Atm.)	13.70	13.70	13.70	13.70
Umean	275	770.0	260.9	205.8
Number of Stages	6	6	6	6
Temperature per stage	21.4	21.45	21.4	16.1
First Stage Characteristics				
First Stage Tip Diameter (m)	1.05	1.04	1.05	1.04
First Stage Hub Diameter (m)	0.73	0.72	0.72	0.73
Hub to Tip Ratio	0.7	0.7	0.7	0.7
Tip Speed (m/s)	323.5	915	307	242.1
Axial Velocity (m/s)	108	305	110	100
De Haller No.	0.739	0.75	0.74	0.83
Stage Flow Coefficient	0.35	0.37	0.38	0.43
Stage Loading	0.31	0.29	0.31	0.27
Inlet Area (m ²)	0.444	0.435	0.438	0.441
Last Stage Characteristics				
Last Stage Tip Diameter (m)	1.05	1.04	1.05	1.04
Last Stage Hub Diameter (m)	0.9	0.83	0.9	0.93
Hub to Tip Ratio	0.85	0.83	0.856	0.89
Tip Speed (m/s)	323.5	915	307	242.1
Axial Velocity (m/s)	116	326	119	114
De Haller No	0.78	0.82	0.79	0.88
Stage Flow Coefficient	0.4	0.48	0.42	0.47
Stage Loading	0.27	0.25	0.269	0.23
Exit Mach Number	0.254	0.257	0.26	0.26
Exit Area (m ²)	0.233	0.238	0.228	0.238
Isentropic Efficiency (%)	85	85	85	85
Reynolds Number (10 ⁻⁶)	4.431	0.25	3.594	2.568
Overall Compressor Length (m)	0.625	0.623	0.628	0.630

The overarching results from the effect of working fluid on component design study showed that:

- At constant output power, the relative number of stages required to achieve a given temperature ratio for nitrogen, helium, carbon dioxide and air were 1, 4.8, 0.86 and 1 respectively, when designing at constant mean speed U_m .
- Increasing the shaft rotational speed of helium considerable decreases the number of stages and length of turbomachinery, while decreasing the rotational speed of carbon dioxide increases the number of stages and length.
- The pressure ratio and mass flow for helium decreases, carbon dioxide increases and the air were relatively similar compared with nitrogen fluid.
- Switching fluid at constant rotational speed moves the operating points above surge margin for carbon dioxide and on surge margin for helium, which imply the utilising both fluids will require modification of the turbomachinery components.
- At constant Mach number, the tip speed of helium increase by a factor of 2.83 which exceeds design consideration, hence, the components would need to be redesigned.

5.7 Chapter Conclusion

In this chapter, the effect of thermodynamic and transport properties of the selected working fluids (nitrogen, carbon dioxide, air and helium) on the thermodynamic performance and preliminary component sizing of a closed-cycle gas turbine have been presented. The results presented herein, shows that selecting of any design choice working fluid has its positive and negative effect on investment decision in terms of the cycle configuration, design and sizing of turbomachinery and heat exchangers, optimum cycle efficiency, optimum pressure ratio, optimum TET, availability and cost of working fluid, working fluid compatibility with component materials and safety.

The overall analyses in this chapter provide insight to cycle parameters influencing the performance of the closed-cycle gas turbine and this provides guidance for selection of design choice. The analysis also identified and compared candidate working fluids suitable for investment decisions from

component design perspective, overall system performance and plant operations for working fluid switch which may not require major modification on the engine configuration.

The following remarks highlight the conclusion of this chapter.

- The choice of working fluid to a reasonable extent affects the design choice cycle configuration. It set a reasonable compromise in terms of plant size, cost (capital and operational cost), and turbo-set design challenges. For fluid like carbon dioxide, its optimal performance is achieved above it critical points which will mean pressurizing the system or operating at a very high-pressure ratio for a simple cycle configuration. However high-pressure ratios tend to pose component design challenges, especially when used for simple cycle configuration. For this reason, a configuration with intercooling which allows for recompression of carbon dioxide is proven to be reasonable. For fluid like helium with low molecular weight and high gas properties (gamma and C_p), the simple cycle configuration may seem more realistic. Other factors that may influence the design choice selection of cycle configuration are an application (land-based, sea-based, space-based), proven operation, reliability, maintainability, cooling medium, plant layout, the potential for energy utilization and sustainability, and current status of technology. The intended application will give a reasonable justification for the configuration is most suitable.
- Cycle efficiency is greatest for working fluid with a higher ratio of specific heat at low-pressure ratio and least ratio of specific heat at higher pressure ratio. Since the specific heat ratio of helium is larger than, air, nitrogen and carbon dioxide the optimum efficiency for helium occur at the lowest pressure ratio compared with other fluids.
- Selecting an optimum pressure ratio should be a reasonable compromise between cycle configuration choice, optimum cycle efficiency, specific power, component design constraints, and cost. The

optimum pressure ratio selected has a great influence on the working fluid turbomachinery design and sizing.

- Both compressor inlet temperature and pressure have an effect of the fluid performance since changes in these parameters have a slight impact on their thermodynamic properties of the working fluid. The limit to which the system is pressurized is dependent on the mechanical structural integrity of the system.
- Selecting a design choice TET has a significant influence on the cycle efficiency and specific power. However, the limit to which this can be achieved is dependent on the material technology and design constraints. Current material technology puts TET at 1123K for closed cycle gas turbine operation coupled indirectly to any heat source.
- For a closed-cycle gas turbine, the sensitivity of the heat exchangers to the overall cycle performance compared with other cycle parameters implies that the success the energy conversion system in the future application will depend on technology advancement of the heat exchangers design.
- Although helium gas showed good cycle performance compared with other fluids are low-pressure ratio, the overarching turbomachinery design constraint and other economical assessment will be needed to narrow any design choice considerations.
- The preliminary design assessment of the working fluid showed as expected that it is more difficult to compress or expand helium, hence, the more number of stages is required to achieve its design goal. The specific heat of helium is about five times that of nitrogen or air, and since the stage temperature rise is inversely proportional to the specific heat for a given limiting blade speed, it follows that the temperature rise available per stage when running with helium will be about one fifth that of nitrogen, which of course, results in more stages being required for a helium compressor.
- A full evaluation of the cycle with these gases will need detailed design calculations for the turbomachines and the heat exchangers, and

consequently an economic assessment. This will be hopefully addressed in the subsequent study.

6 TECHNO-ECONOMIC ANALYSIS ON DESIGN AND OPERATIONAL PERFORMANCE WITH DIFFERENT WORKING FLUID

6.1 Background

To date, the closed-cycle gas turbine provides very attractive benefits, and the key to its acceptance is the operational flexibility and low maintenance cost it offers due to the isolation of the working fluid from the environment. However, for the full potential of the closed-cycle gas turbine power plant to be realised, more competitive cost information needs to be generated, correlated and compared in terms of design, performance, and operations.

To this end, in the modern economic aware environment, it is critical to understand the economies associated with the purchase or product development of technology such as this, comparing the effect of the selected working fluids. The comparison on a performance basis only is not enough to decide design choice of working fluids for the closed-cycle gas turbine, thus, the need for techno-economic analysis. The economic assessment provides reasonable information for making good investment decisions, with the goal of ensuring that an investment is “worthwhile”, that is, the expected future profits justify the initial investment expenditures [98,100,103].

However, assessing the economic potentials of any design choice working fluid of the closed-cycle gas turbine plant is a difficult task that may require one to build on previous research opinions. It is arduous to give comprehensive economic assessment comparison for the effect of working fluids on cost profile due to several considerable uncertainties and the absence of a standard framework. Nonetheless, the study had to rely on comparisons from the preliminary assessment of several research opinions.

Consequently, the work of Dostal [13] considered the economic assessment of supercritical carbon dioxide comparing direct and indirect coupling to the heat source. The FOM (figure of merit) approach was utilised in his work to develop an economic appraisal of the plant. Similarly, Doulgeris et al., [155] presented

an approach for economic assessment of the carbon dioxide cycle for new generation nuclear power plants using component thermodynamic relationship for cost analysis and comparing two cycle configuration. Also, economic assessment of plant utilising helium as a working fluid has been documented in past works such as reference [47,84]. Nonetheless, from the literature review, it appears so far that an economic assessment on closed-cycle gas turbine comparing the effect of different working fluids such as air, nitrogen, helium, and carbon dioxide have not been explored.

For this reason, this chapter presents an economic assessment of the influence of different working on a selected closed cycle gas turbine. The aim of this chapter is to present the economic assessment tool developed in this research within the TERA framework for assessing both economic attractiveness and risk using the selected working fluids. This would involve carrying out a detailed economic description of all factors including machinery costs, efficiencies, operational cost and availability that would support decision making for any investment on this energy conversion system for different working fluids. This technical and economic data developed, then becomes an important investment decision reference bank for look-up on factors that affect the design and operational performance of a closed-cycle gas turbine with different working fluids. The assessment is carried out using typical economic performance indicators such as net present value (NPV), internal rate of return (IRR), discounted pay-back-period (DPBP) and levelized cost of electricity (LCOE) as shown in Fig. 6-1.

6.2 Working Fluid Economics and Availability

The availability and cost of the selected working fluids will have great influence on the design choice for application in the real system under considerations. Although air, nitrogen and carbon dioxide are readily available at modest cost, helium which is one of the noble gases is limited in supply and at an expensive price. Table 6-1 shows a break-down of the cost of each working fluid selected based on references [156,157]. It should be understood that air will not be free in that it will require careful processing to remove moisture and particulate

matter for it to be used in a closed system. Hence, in Table 6-1, the cost affixed to air is to cover for the processing of moisture and impurities.

Based on available data in reference [65,86] and implementing the law of economy of scale [71,79], it studies assumed that the total volumetric capacity of the reference plant (38.2MW) is 52972ft³, at an average pressure of 13.7atm and maximum cycle temperature of 1100K. Thus, the average volume of fluid in the system is assumed at 800,000ft³ which is recharged yearly.

Table 6-1 Cost of Working Fluid [156,157]

Working Fluid	Cost
Helium	\$104 per 1000 ft ³
Nitrogen	\$27.5 per 1000 ft ³
Carbon Dioxide	\$18 per 1000 ft ³
Air (Process to remove impurities)	\$8 per 1000 ft ³

6.3 Method of Analysis

Surveys from the literature show that there various techniques for developing an economic model for existing or new technology in closed-cycle gas turbine [96,98,100,103,155,158–160]. However, the most important item to consider is that the model should give a detailed description of the assessment flow process and underlying assumptions. Thus, an overview of the economic model developed for this research purpose is described in Figure 6-1.

The model presented describes the approach used for the initial investment cost, the cash flow process and measure of economic performance. The initial investment cost consists of the equipment cost, fluid cost, operation and maintenance cost. The bottom-to-top approach which adds the cost of the individual component of the entire system was used for the gas turbine equipment cost. This is to be able to reflect the impact of the selected working fluids on the component cost which adds-up to give the overall equipment cost. The input for this model is the thermodynamic performance and design sizing results obtained from reference plant. Another critical aspect of the model is the sets of economic assumption utilized for the assessment such as discount rate,

capacity factor, tariffs, and others. The approach presented has its strength and weaknesses, however, the cost trends give a precise understanding of the economic effect of different design choice working fluids. As previously mentioned the economic performance assessment was done using net present value (NPV), internal rate of return (IRR), discounted pay-back-period (DPBP) and levelized cost of electricity (LCOE).

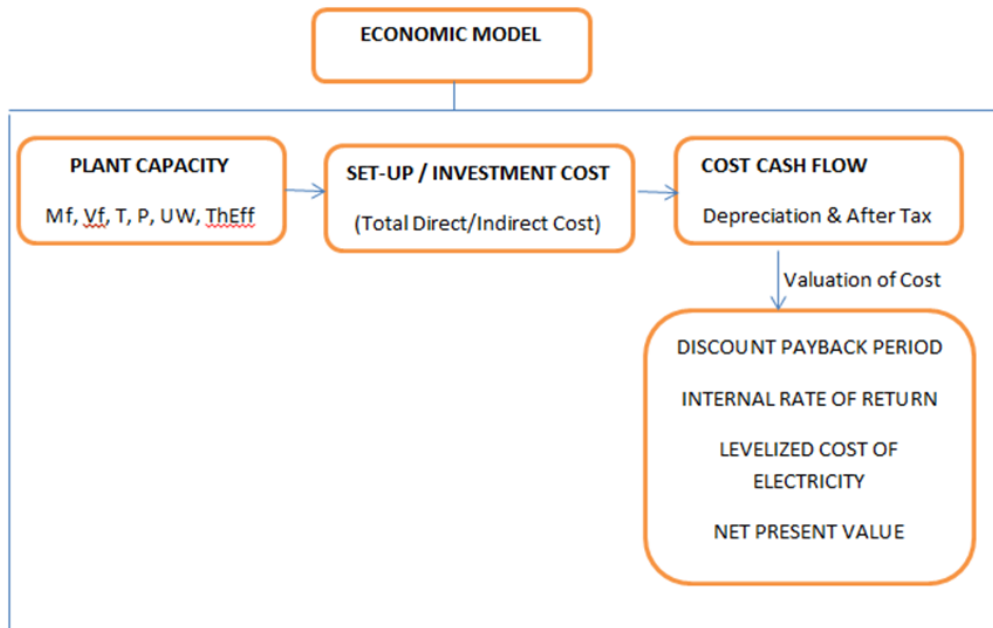


Figure 6-1 Scheme of economic analysis

6.4 Equipment Component Cost

The equipment component cost refers to the cost for purchase of equipment, which was estimated using the bottom-to-top approach. It depends on the components comprising the system and its particular specifications. The major closed-cycle gas turbine components cost includes; the turbomachinery sets, heat exchangers, generator, heat source and working fluid. Cost estimation for each component was obtained based on preliminary component sizing done in the previous chapter. The method of estimation is based on functional relationship to principal thermodynamic parameters obtained from performance results.

6.4.1 Turbomachinery

The turbo-set cost is driven by both the size and number of stages required to achieve pressure ratio change. The cost of turbomachinery was obtained based on models in reference [155]

$$\text{Compressor Cost} = UF * 39(1 - \eta_c)^{-1} * W_{ceq.} * PR_{ceq.} * LOG (PR_{ceq.}). \quad (6-1)$$

$$\begin{aligned} \text{Turbine Cost} = UF * 927(1 - \eta_T)^{-1} * W_{ceq.} * PR_{Teq.} * LOG (PR_{Teq.}). \quad (6-2) \\ * [1 + \exp(0.036 * TET - 31.86)] \end{aligned}$$

$$PR_{ceq.} = (PR_{stage}^n)_{ref} \quad (6-3)$$

Where

$$n = \text{number of stages} = \frac{LOG(PR_c)}{LOG(PR_{stage})}$$

Similarly, the equivalent mass flow is obtained as follows

$$\left(\frac{W\sqrt{T}}{AP} \times \sqrt{\frac{R}{\gamma}} \right)_{fluid} = \left(\frac{W\sqrt{T}}{AP} \times \sqrt{\frac{R}{\gamma}} \right)_{ref} \quad (6-4)$$

6.4.2 Heat Exchangers

An approximate costing of the heat exchangers was done using the C-value method [149]. This method reduces the difficulties in defining the area and overall coefficient. Steps to sizing estimation of the heat exchangers using the ϵ -NTU method have been described in the previous chapter.

The next stage was to evaluate the cost of the heat exchanger per unit $\frac{Q}{\Delta T_m}$, using logarithmic interpolation of the costing data [149] in Appendix D. The cost of the heat exchangers are obtained from the product of C_{value} and $\frac{Q}{\Delta T_m}$

$$C_{cs} = Exp \left\{ LOG_e C_1 + \frac{LOG_e \left(\frac{C_1}{C_2} \right) \times LOG_e \left[\frac{\left(\frac{Q}{\Delta T_m} \right)_{Sn}}{\left(\frac{Q}{\Delta T_m} \right)_1} \right]}{LOG_e \left[\frac{\left(\frac{Q}{\Delta T_m} \right)_1}{\left(\frac{Q}{\Delta T_m} \right)_2} \right]} \right\} \quad (6-5)$$

The cost factors were obtained from

$$CR = a + b LOG_{10} A_{Sn} \quad (6-6)$$

Where a and b are read from Appendix E

Therefore,

$$C_{value} = C_{cs} \left[CR_{tube} + CR_{shell} + CR_{L/D} + \left(0.5 + (0.5 \times CR_p) \right) \times (1 + CR_s) + CR_t - 5 \right] \quad (6-7)$$

The Total Cost of the Heat Exchanger assembly is calculated from

$$Hexcost = C_{value} \times \left(\frac{Q}{\Delta T_m} \right)_{Sn} \times Sn \quad (6-8)$$

6.4.3 Generator

Cost of the generator was obtained using the equations from reference [155]

$$Gencost = UF * 70 * (P_{elect})^{0.95} \quad (6-9)$$

6.5 Economic Model of Inventory Control System

Developing the inventory control component sizing and weight was necessary to estimate the capital cost model. The cost of each the inventory control system was estimated based on Turton et al., [160] module costing model with

reference to the weight, length, and material used. Carbon steel material was utilised in this study.

Therefore, the Total Cost of Inventory Control System was estimated thus;

$$Total\ Cost_{ICS} = F_M C_b + C_a + \text{Cost of Valves} \quad (6-10)$$

Where $F_M = \text{Material cost factor}$

$$C_b = \exp[9.100 - 0.2889(\ln Total\ Weight_{ICS}) + 0.04333(\ln Total\ Weight_{ICS})^2]$$

$$C_a = 246D^{0.7396}L^{0.7068}$$

The cost valve was estimated based on the diameter of the valve using reference [161]

6.5.1 Cost of Transfer compressor

To estimate the cost of the extra compressor, the transfer compressor was sized based on the rate of change of power required after the natural pressure differential the GT-cycle loop and storage tank is at equilibrium for 50% load.

$$EC\ Power\ Capacity = (P - P_E) - P_{lmin} \quad (6-11)$$

Where

$EC = \text{extra compressor,}$

$P = \text{Design Point Power, } P_E = \text{Power at equilibrium pressure differential,}$

$P_{lmin} = \text{Minmium required part – load Power}$

Therefor cost of transfer compressor is given using power law scaling factor

$$Cost = KA_a^n \quad (6-12)$$

Where $K = \frac{C_b}{A_b^n}, n = \text{cost exponent, } A_a = \text{EC Power Capacity, } A_b =$

$\text{reference compressor power capacity, } C_b = \text{Reference compressor cost}$

6.6 Cash Flows

This study assumes that the economic period starts in the year the plant is going to be installed and end in the end year the plant is taken out of service. The starting point of the assessment is represented by the estimation of the capital cost based on different working fluids. The total investment capital cost is as expressed as the sum of closed-cycle gas turbine capital cost, operating and maintenance cost, heat source fuel cost, depreciation cost, and various estimated indirect cost. The indirect cost represents general facility costs which include engineering, overhead, buildings, and contingencies. The contingency cost covers cost incurred due to more detailed design, additional equipment technology, and other exigencies.

The cash flow described in this section is applicable yearly over the investment period. In addition, payment of taxes and depreciation was included in the cash flow calculations.

6.6.1 Revenue and Expenses

The revenue is defined as the money generated as a result of the sales of electricity during the cash flow year. The revenue depends on the plant capacity and electricity pricing. This study assumed that tax rate remains constant throughout the lifetime of the investment. Thus, the revenue after taxes is given as:

$$R = EP * P * G * 8760 * (1 - tax\ rate) \quad (6-13)$$

Where

$EP = electricity\ pricing\ (\$/kWh)$

$P = unit\ capacity\ (kW)$

$G = Unit\ capacity\ factor$

The expense is defined as the overall costs incurred annually which include the initial closed-cycle gas turbine unit. Other components of the expenses include the operating cost and plant depreciation cost given as,

$$Exp = CGT \text{ cost} + Fuel \text{ Cost} + Operating \text{ Cost} + Depreciation \text{ Cost} \quad (6-14)$$

The closed-cycle gas turbine cost is calculated as,

$$CGT \text{ cost} = turboset \text{ cost} + heat \text{ exchanger cost} + fluid \text{ cost} + indirect \text{ cost} \quad (6-15)$$

The operation and maintenance cost comprises of fixed O&M cost and variable O&M cost. Variable O&M cost includes auxiliary equipment maintenance. Typical rates of variable and fixed O&M cost for closed-cycle gas turbine application was obtained from references [162].

The fuel cost for closed-cycle gas turbine coupled indirectly was estimated using as an assumed fuel tariff factor which is used to represent the heat source fuel given by;

$$Fuel \text{ Cost} = fuel \text{ tariff} * kWh \text{ of power generated} \quad (6-16)$$

Depreciation simply refers to the decline in value of an asset due to physical, technological, functional deterioration and other factors that may lead to the asset end of service. Accounting for depreciation reduces the taxes during the plant operation [98,159] as shown in Eq. 6-15. There are different methods for calculating depreciation discussed in references [159,160], however, the “straight-line depreciation” method was adopted since it assumes a linear decrease with time in the value of the asset.

$$Taxable \text{ Income} = annual \text{ operating profit} - depreciation \quad (6-17)$$

$$Depreciation = \frac{aquisition \text{ cost}}{book \text{ life}} \quad (6-18)$$

6.6.2 Operating Income and Annual Net Cash Flow

The operating income is obtained by deducting all investment cost that is reflected in the expenses from the revenue. Thus, the operating income is given as;

$$OI = R - Exp \quad (6-19)$$

The annual earnings also referred to as the profit is given by the operating income less than the annual investment payback. This is expressed as:

$$E = OI - Interest \quad (6-20)$$

Converting the expenses into streams of equal annual payment within the lifespan of the project, then, the annual net cash flow becomes:

$$NCF = E - \left[ICC * \left(\frac{i * (1 + i)^n}{(1 + i)^n - 1} \right) \right] \quad (6-21)$$

The net cash flow is used to determine the overall investment cash flow in a particular year. It includes all costs and investment returns within the year of analysis.

6.7 Measure of Economic Assessment

Economic return is a major driver for any investment. Hence, measures or indexes of economic assessment are performance indicators used to ascertain the viability of an investment and can be used as the basis for comparison among alternative investment options

6.7.1 Levelized Annual Revenue

The Levelised Annual Revenue Requirement is also known as the annual levelised cost of electricity. This is defined as the sales of electricity produced that would make the present value sum of discounted revenue and expenses equal. This implies that the power plant will be profitable in the absence of technology or market risk if the electricity generated were sold at price higher than the levelized cost. Thus, this is calculated as follow

$$LARR = CGT \text{ cost} * LFCR + OC * LF \quad (6-22)$$

Where

$$LFCR = \text{Levelised fixed charge rate} = \frac{1}{n} + i * \left(1 - \frac{1}{n * a} + \frac{SFF}{a}\right) \quad (6-23)$$

$$SFF = \text{Sinking fund factor} = \frac{i}{(1 + i)^n - 1} \quad (6-24)$$

The SFF describes how much money that must be put into savings account each year in order to have a given amount

$$LF = \text{Levelised factor} = PWCF * CRF \quad (6-25)$$

$$CRF = \frac{i * (1 + i)^n}{(1 + i)^n - 1}$$

$$PWCF = \frac{1 - \left(\frac{1 + a}{1 + i}\right)^n}{1 - a}$$

a = inflation rate

i = interest rate

$PWCF$ = present worth cost factor

OC = operating cost

6.7.2 Net Present Value

The net present value is commonly used to quantify the value of an investment and decide if it is worth undertaking. It represents an estimate of wealth generated by a project. It is defined by the discounted sum of all cash flows over the lifetime of the plant, including initial cash flows (fixed investment).

$$NPV = NCF \left[\frac{1 - (1 - i)^{-n}}{i} \right] \quad (6-26)$$

The investment is worthwhile only if the NPV is greater than zero. If NPV equals to zero, it means that the investor precisely breaks even on the project. For competing for NPV with values greater than zero, the project which offers the highest NPV should be preferred. This is because; higher NPV means higher net profit to be achieved, so the investment will have favorable economic performance.

6.7.3 Internal Rate of Return (IRR)

The internal rate of return is used to determine the profitability of an investment. It corresponds to the interest rate or discount rate that makes the NPV equal to zero. At this discount rate, the net present value of the project expenses is equal to the present value of the revenues. It represents the average periodic rate of return earned on funds while they are invested in a project. The higher the internal rate of return, the more profitable the project.

$$IRR = d = 0 \geq \sum_{t=1}^n \frac{NCF}{(1+d)^t} - ICC \quad (6-27)$$

6.7.4 Discounted Pay-back Period

This is defined as the length of the period required to recover the investment cost and the desirable discount rate from the net cash flow produced by the investment. Hence, an investment with high positive NPV and long payback period may be potentially risky. The discounted payback period is equal to the smallest value of n which satisfies the expression,

$$DPBP = n = 0 \leq \sum_{t=1}^n \frac{NCF}{(1+d)^t} - ICC \quad (6-28)$$

6.8 Case Studies

To demonstrate the techno-economic effect of the selected working fluids a single-shaft recuperated closed-cycle gas turbine with an output power of 38.2MW as described in Table 5-5 and Figure 5-26 of the previous chapter. The basis of comparison for the different working fluids is as described in case 1 (constant output power for all working fluid) of section 5.6.4 in the previous chapter. The design configuration as a result of the different working fluids effect has been presented in figure 5-27 and 5-28 based on the conditions described in section 5.6.4 of chapter five.

To this end, first, a cost assessment of the closed-cycle gas turbine component was carried out. The cost for each component was estimated based on functional relationship to principal thermodynamic parameters shown in Eqs (6-1) – (6-9). This approach was used to enable a precise assessment of the effect of the working fluid on the component cost and gives a quick comparison of each fluid. Next, is to give a detailed analysis of the discounted annual cash flow based on several assumptions presented in Table 6-2. This step involved recording the cash inflow and outflow over the operating life cycle of the power plant. The approach takes into account the time value for money. Based on the cash flows obtained, an economic performance assessment using NPV, IRR, DPBP, and LCOE is analysed and results discussed.

Table 6-2 General assumptions for economic analysis

Parameter	Nitrogen	Helium	Air	Carbon dioxide
Nominal Power (kW)	38,200	38,200	38,200	38,200
Availability of Plant (%)	93	93	93	93
Capacity factor	0.9	0.9	0.9	0.9
Tax rate (%)	30	30	30	30
Plant Operating period (years)	30	30	30	30
Economic analysis Period (years)	30	30	30	30
Discount rate (%)	8	8	8	8
Interest rate (%)	8	8	8	8
Inflation rate (%)	3	3	3	3
Electricity pricing	0.12	0.12	0.12	0.12
Fuel tariff	0.033	0.033	0.033	0.033

Table 6-3 Estimated closed cycle gas turbine capital cost for different working fluids

Component	Cost (\$/kW)			
	Nitrogen	Air	Helium	Carbon dioxide
Compressor	30	30	50	38
Turbine	28	28	43	35
Recuperator	82	83	71	86
Gas Heater	92	93	81	96
Pre-cooler	78	78	68	84
Generator	41	41	41	41
Heat source	154	154	154	154
Indirect cost (a, b, c)	40	40	40	40
Working fluid	0.576	0.168	2.18	0.377
Closed GT Cost (\$/kW)	545.576	547.168	553.18	574.377
			Overall cost (\$K)	
Closed GT Cost (\$*10 ³)	20,841	20,902	21,131	21,941

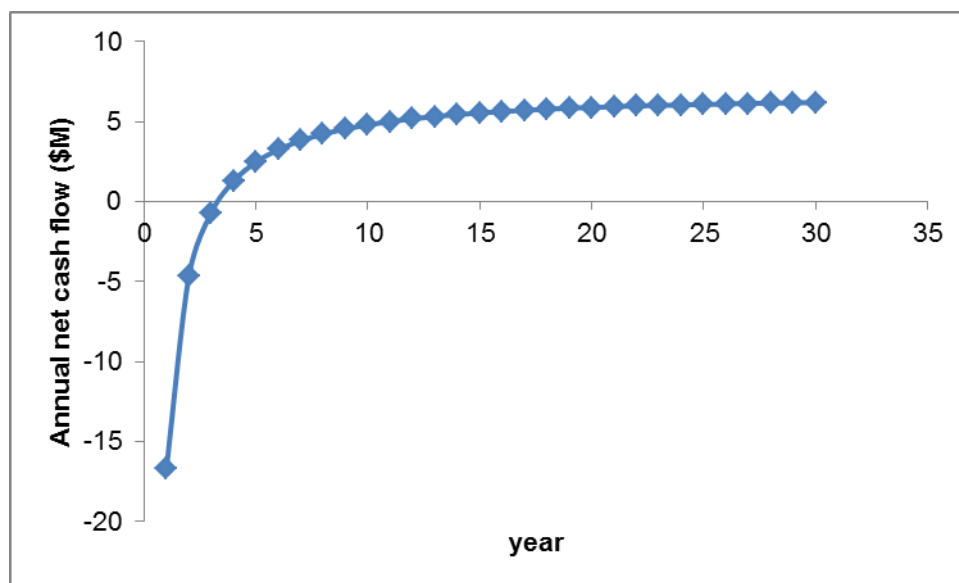


Figure 6-2 present annual net cash flow comparison for nitrogen

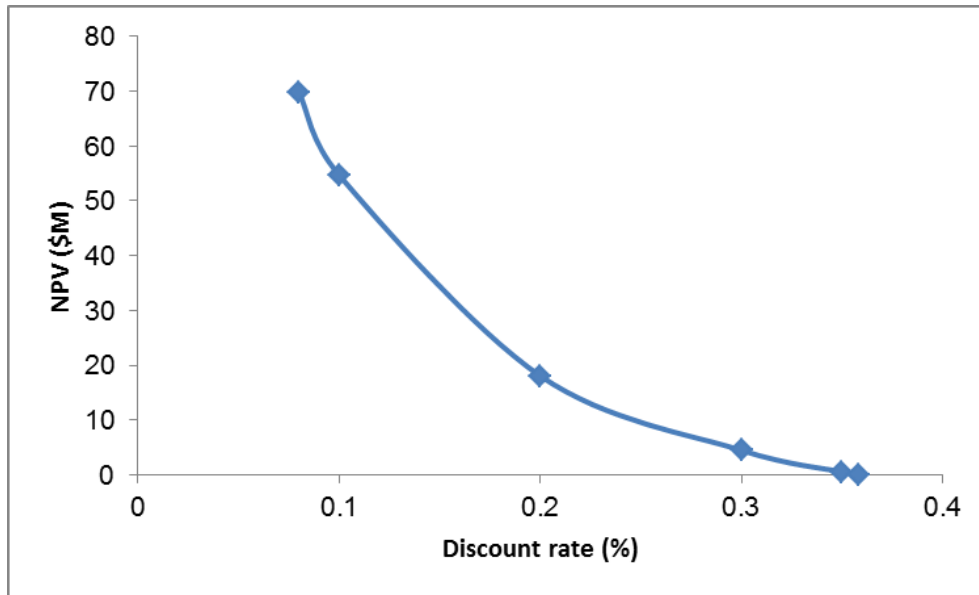


Figure 6-3 Internal rate of return for nitrogen

Table 6-4: Economic performance results

Parameter	Nitrogen	Helium	Air	Carbon dioxide
NCF (M\$)	6199	6118	6199	6081
IRR (%)	35.84	35.84	35.84	35.84
DPBP (year)	4	4	4	4
LCOE (\$/MWh)	58.3	58.23	58.26	58.5
NPV (M\$)	69793	68882	69796	68462

6.9 Results and Discussions

Table 6-3 showed results of total component cost for each working fluid. During the estimation of the total component, the heat source and pressure storage tank were assumed to be constant, hence it was not considered in the analysis. Comparing the result of Table 6-3 showed that the initial capital cost of using carbon dioxide was higher by 5.28% \$/kW using nitrogen as a baseline. This means that a design choice with carbon dioxide as working fluid will be more expensive to purchase than a system using nitrogen. This is because of the influence of the ratio of heat transfer to mean temperature ($\frac{Q}{\Delta T_m} = UA$) and the high molecular weight of carbon dioxide which affects the heat exchanger

surface area and length as well as the turbo-set number of stages and length as shown in Table (5-6) – (5-8), which implies that the recuperator size will be bigger, compared to other fluids. In terms of cost the advantage which carbon dioxide offer over nitrogen is the annual cost of working which is less by 34% \$/kW and may have a minor benefit on the system, in terms of operating cost. Similarly, the capital cost for helium is 1.4% \$/kW more than nitrogen. This is as result a of the effect of low molecular weight and high specific heat capacity of the turboset sizing for a given pressure ratio. The cost of the heat exchangers \$/kW for helium is the least compared with other fluids which can be attributed to its thermodynamic properties. However, a major disadvantage which helium could pose is the cost of the working fluid. The cost of helium for the required output power is averagely over 250% higher than the cost of other fluids, which makes it very expensive. This would imply that the operational cost of utilizing helium maybe the largest compared with other fluids. Air and nitrogen have similar properties effect on turbo-set cost and minor increase for the heat exchanger cost.

The result of Table 6-4 describes the measures of economic assessment for each working fluid. Generally, the cumulative yearly net cash flow of each working fluid followed the same trend as shown in Fig.6-2 using nitrogen as working fluid. The first four years had a negative cash flow which means that within these years the project had a negative profit margin. However, from the fourth year, the business became profitable shifting the curve upward. The net cash flow curve for other fluids is described in appendix C. The results presented in Table 6-4 shows that the overall present net cash flow of carbon dioxide was the least due to the cost of its initial capital. Recall that the analysis assumed equal fuel cost and O&M cost for each fluid. Hence, the variation in net cash flow will be influenced mainly by the capital cost and cost of working fluid. Nonetheless, the net cash flow of helium followed closely to carbon dioxide. This is because of the yearly cost of helium working fluid. Further, the economics of the plant operation for the different working fluids have been quantified in terms of NPV. The reduction in cash flow for helium and carbon dioxide is reflected in the NPV obtained each fluid respectively. Projects with

highest NPV show that the project has a possibility for more profit. The NPV technique normalizes the value of the investments in years to come and one can see how the NPV varies for a given discount rate as shown in Fig.6-3. An increase in the discount rate means greater risk. The trend shows that as the discount rate increases the NPV drops in an inverse proportion. For each working fluid, the IRR occurred at a discount rate of 35.84%. At this discount rate, the NPV is equal to zero. The variation of IRR comparing each fluid was insignificant; this may be due to the assumptions considered in the study. Similarly, the discounted payback period is approximately year 4 for each fluid. The reason for this is similar to that of IRR. The LCOE obtained for each working fluid seemed to be attractive when compared with the current cost of electricity in the USA (\$120/MWh). The reason for the low value is connected to assumptions taken. However, further analysis would be required to establish the preliminary evaluation of economic performance assessment.

It is worth noting that the economic performance assessment presented are very preliminary, due to several variabilities and assumptions surrounding the study and the author's aim is mainly to show how the various fluid affects the closed-cycle gas turbine cost estimation for the given output power.

Despite the efforts of the author, no direct validation can be provided for the economic figures reported here. To the best of the author's knowledge, no data regarding the financial indices considered in the present study are available in the public domain.

6.10 Chapter Conclusion

Preliminary economic assessments of the closed-cycle gas turbine have been presented with a focus on the total component cost for different working fluid. The cost of nitrogen and air components appears to be attractive. The measures of economic performance for nitrogen and air also appeared to be favourable based on the study assumptions. The cost of helium which is five times higher than the cost of nitrogen increases its operational cost compared with other working fluids. Further result analysis would be required to establish the preliminary evaluation of the economic performance.

7 RISK ANALYSIS

7.1 Background

Unfortunately, technical risk and mitigation are often addressed late in the project development process, resulting in less optimal technology procurement decisions and higher costs for risk mitigation. The incorporation of risk analysis from the outset of any project can assist in the early decision-making process.

There are many parameters that affect both the design choices and operating problems characteristics of a closed-cycle gas turbine system. These range from items peculiar to the particular application through fundamentals of mechanical component design. This chapter presents a risk component model for closed-cycle gas turbine technology considering the effect of different working fluids. The risk module provides an assessment of uncertainties and operational challenges of the closed cycle gas turbine plant for selected working fluids. Most significantly, the risk module will be a representative of trade-offs in the plant thermodynamic performance characteristics and its impact on the closed-cycle gas turbine technology. An overview of the structure of the risk model is presented in Fig 7-1. Each block on the structure presented is defined as an integrated unit based on input values from performance, component design, and economic model.

The risk module presented is made of two parts: financial and technological risk. The technological risk gives an assessment on the effect of the working fluid on material technology, the influence of operating high TET for each working fluid, the working fluid management system and the technology maturity level of the turbo-sets and heat exchanges for the selected working fluids. The financial risk aspect gives an assessment on the influence of pressure ratio and mass flow on the capital cost for each working fluid, the sensitivity of the cost of helium and impact of legislation on investment decision.

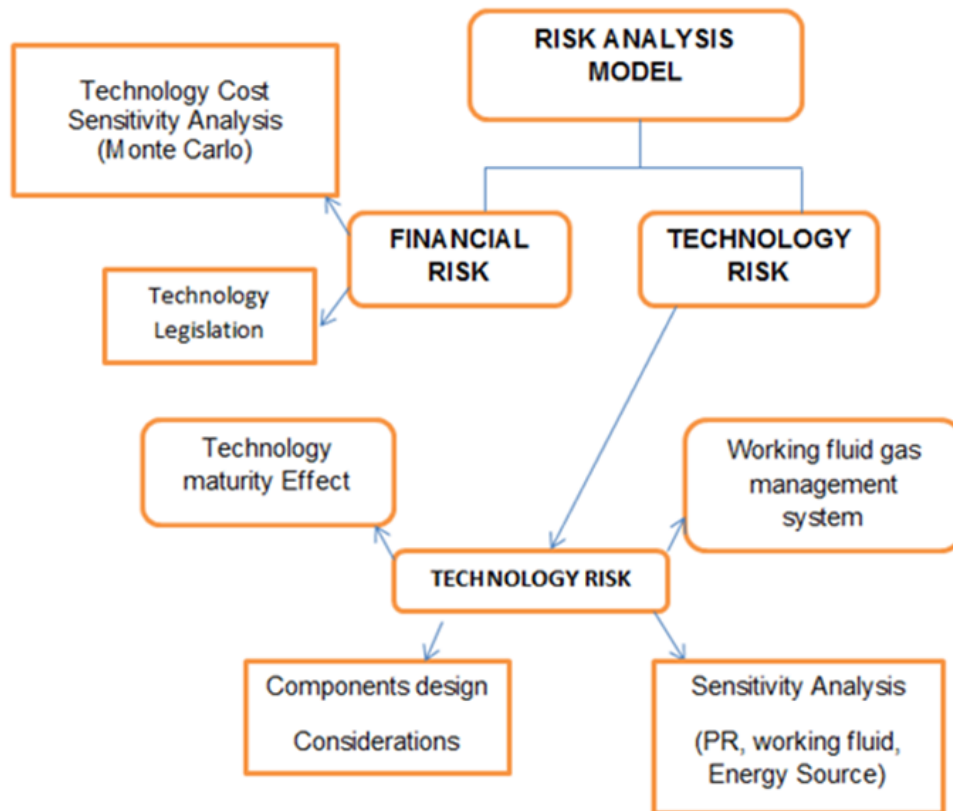


Figure 7-1: Scheme for Risk Analysis

7.2 Technology Risk

The success of the closed-cycle gas turbine is dependent on the technology level available for the design and production of its constituent parts. Thus, the technology maturity and operational challenges of the closed-cycle gas turbine components differ in terms of application for different working fluids considered in this study: some component technologies are very near state-of-the-art, whereas others tend to be more innovative but less developed. Hence, this can pose an investment risk especially for technologies with TRL (technology readiness level) below 4.

This section gives a wholistic assessment of the technological risk associated with the working fluids capability for the closed-cycle components. To the best of the author's knowledge, an attempt to discuss technological risk for different fluid selected in this study is another important novelty of this research. There has not been a comprehensive attempt to present potential technological risk that may be associated

with the working fluids design choice in open literature. The following technological risk is presented:

7.2.1 Material technology for high temperature and pressure

The key design drivers for the closed-cycle gas turbine are the level of cycle peak temperature into the turbine and the system pressure level that can be achieved compared with current technology. As indicated in Fig.5-3 and 5-4, an increase in cycle peak temperature to a possible maximum increases the cycle efficiency reasonably. However, this is limited by the material technology and the working fluid characteristics at this temperature. Currently, maximum cycle temperature for the closed-cycle gas turbine is at 1123K in a real application. Similarly, pressurising the system allows for compactness of machine and component, thereby reducing cost and allows for stability of the working fluid properties above their critical pressure and temperature. As the system pressure is increased, the size of the components for the closed-cycle gas turbines is reduced. This results in a reduction in cost up to the point where the thickness of the component casings and shells becomes awkwardly great and the thickness of heat exchanger tubes becomes sufficient so that temperature drop through the tube wall becomes a major factor. In practice, a peak system pressure of 20 to 30 atmospheres is usually favoured except for large fission or fusion reactor heat sources, in which case pressures of 30 to 50 atmospheres are commonly chosen.

To this end, the critical components that will be at potential risk are the heat source, heat exchanger and the turbine based on current material technology level applicable to the closed-cycle gas turbine. The turbine section is usually made of nickel-based alloy with varying amount of aluminum and titanium, while the heat exchangers and heat source are made of ferritic-martensitic steel, alloyed with chromium, aluminum and molybdenum. Thus, raising the system peak pressure and temperature to achieve competitive cycle performance compared with other conventional energy conversion systems will pose possible risk to the material and working fluid characteristics, expect new materials laced in ceramics for the heat exchanger and heat source are considered, and

adequate cooling technology is introduced for the turbine; which may lead to significant decrease in cycle efficiency.

However, the increased pressure and temperature will increase the stress level and mechanical integrity of the components. Apart from the impact on the mechanical impact, the working fluids are also prone to system risk. For helium, operating at very high temperature could induce a welding effect, as it passes through the metallic surfaces of the components. This could have a hazardous effect on sensitive equipment such as the control valves guide vanes, support bearings, and bushes. Shaft seal materials can also be affected especially with helium at high temperature and pressure. For carbon dioxide, at temperatures above 1000°K, there can be small pickups of carbon which could lead to decarburization, thus at this elevated temperature, the material used have to be coated to prevent decarburization. For air, the possibility for oxidation attack is increased; however, air will have a more favourable outcome than helium at high temperature if an iron-chrome-nickel alloys material is used. The behaviour of nitrogen in terms of oxidation capability at high temperature is similar to air. Nitrogen also has great chances of nitriding and embrittlement of material at high temperature. All these will have an effect on the life of the components. The consequence of any component failure could lead to ingress, especially for the heat exchangers.

7.2.2 Working fluid gas management

Handling of the working fluids is another potential technological risk for the closed-cycle gas turbine investment plan. This is important because the working fluid in the closed-cycle gas turbine usually remain in the cycle until it is renewed yearly. The decision for a design choice working fluid will also be influenced by how the fluid can be effectively managed without causing a system safety or environmental concerns when there is sudden leakage or interaction with the component materials.

Air is a readily available fluid and is easy to manage because it does not have any detrimental effect when exposed to the environment expect of the metal surfaces. With this in mind, it becomes easy to handle or stored in the inventory

tank over a period of time. As previously mentioned, the only main concern for the use of air is the oxidation of the gas turbine components. Although helium is an inert gas, the limitation for its use is that its supply is controlled by the US government hence, storage concerns can be factored in, as a possible risk to helium being selected for design choice working fluid. Storage is particularly important in helium because of the nature of its supply, thus, the issue of seal leakage associated with helium could limit its operational use or to be selected as design choice working fluid.

Chemical interaction between the heat source cooling medium and the system working fluid is controlled to prevent potential ingress into the system or chemical reaction with the gas turbine component. Helium is chemically inert and neutrally transparent and minimizes the problem of system corrosion and greatly reduce build-up. The decision to use any selected working fluid has to incorporate the working fluid gas management, especially in a nuclear-powered application where a high factor of safety similar to the aerospace industry is required.

7.2.3 Technology maturity level

Technology maturity or readiness level is a disciplined independent programmatic figure of merit that allows for effective assessment of, and communication regarding the maturity of new technologies [98]. Each technology project is evaluated against the parameters for each technology level and is then assigned a TRL rating based on the progress of the project. As shown in Fig 7-2, there are ratings of technology readiness level. This involves the progression of technology from a scientific principle and technological concept to laboratory-scale, bench scale, full-scale prototypes, and finally full deployment.

Technology Readiness Levels (TRLs)

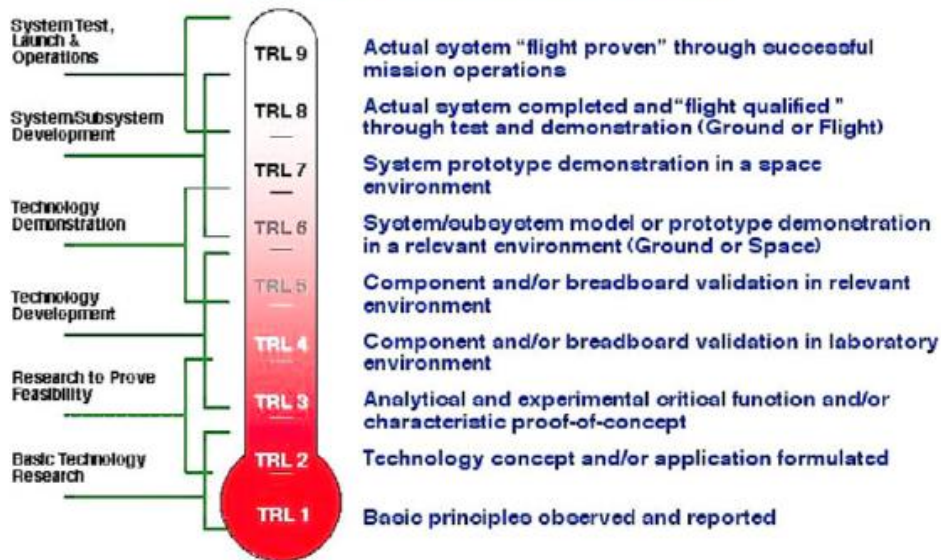


Figure 7-2 NASA Technology Readiness Level (TRL)

Considering the working fluids selected in this study, the use of components designed for specific fluids are at the various level of technology readiness. While some are still theoretical, some have been proven and deployed in several applications. Therefore, the TRL of the closed-cycle gas turbine component is a technological risk for any investment decision and needs to be incorporated into cost directly or indirectly. In this study, the technology readiness level was assign according to the stage of development and deployment of components (number of projects) that allow the use of each selected working fluids in closed-cycle gas turbine application. Although the author may not be able to give precise judgment on the number of projects this study relies on assessments from open literature for components that use each selected working fluid.

7.2.3.1 Working fluid TRL for turbomachinery component

The aerodynamic and mechanical design for turbo-components that use air as working fluid is widely proven and its configuration for any application whether axial, centrifugal or radial can be easily implemented. This makes the use of air as working fluid for closed-cycle gas turbine design less risk because its technology readiness level (TRL) can be put at 9 and many designer or

operator is very familiar with the design and operational challenges of air turbo-set. Thus, further, improvement to suit any design specification or optimum decision indicators can be initiated.

Although the basic aerodynamic design principles used for air turbo-set are applicable to helium, carbon dioxide, nitrogen and any selected fluid, it is important to recognize that the drastically different thermodynamic properties of the working fluids from those of air will require unique design considerations and operational challenges.

For helium, its high specific heat and low molecular weight make its aerodynamic design complex. Going with plants that operated with helium documented in references [2,4], it becomes obvious that there is still limited design and operational experience in the use of helium turbo-sets for closed-cycle gas turbine application. Although in the last one (1) decade there have been a growing number of researches and development in use of helium for high temperature and very high-temperature closed-cycle gas turbine application, this does not still put the TRL of helium turbo-sets above level 7. Thus, the technology risk for helium turbo-sets will be higher than air.

For carbon dioxide turbo-set, not until the 1990s when supercritical carbon dioxide power cycles started to gain relevance, there has not been any closed-cycle gas turbine power plant project in operation that uses carbon dioxide turbo-sets, apart from the Feher module in 1976 which was experimental [48]. Most application of the carbon dioxide turbo-set design is still at the preliminary or laboratory test stage [4,163]. Thus, the risk level for carbon dioxide turbo-set will be higher compared with helium or air because of its limited design and operational experience in closed-cycle gas turbine application. This would have the additional effect of investment decision for a closed-cycle gas turbine with carbon dioxide as a design choice. The carbon dioxide TRL can be put at below 5 which put it at great risk.

For nitrogen, its thermodynamic behaviour at different temperature and pressure is similar to that of air, which makes its aerodynamic and mechanical design easy to adapt and implement for the closed-cycle gas turbine power

plant application. Also, there have been some experimented and built power plant operating with nitrogen turbo-set, although this is not as popular as the use of air or helium. From the author's view, adapting nitrogen turbo-set for closed-cycle gas turbine application may pose less risk compared with helium, and carbon dioxide. This is because of its unique similarity with air, hence, the possibility of having similar or familiar operational challenges.

7.2.3.2 Working fluid TRL for heat exchangers

The heat exchanger is one of the main components of the closed-cycle gas turbine that influences its performance, hence, the technology readiness level for the heat exchangers plays a vital role to the success of power plant application. The TRL level is assessed in terms of effectiveness and ability to operate at high temperatures and pressures for different working fluids. Although material technology capabilities have been discussed in the previous section, this part will only focus on the TRL of heat exchangers for the different working fluids selected in this study.

Heat exchangers are usually complex, expensive and large in size; hence, it represents a significant driver in the capital cost and technical viability of the closed-cycle gas turbine plants. Thus, the development of highly reliable, highly compact, and fewer losses in pressure remain an active area of research, especially for high-temperature applications. Also, the effect of working fluid's chemical interaction on the heat exchanger materials, thermal stress under extreme operating conditions and thermal-hydraulic performance are still at the research and development stage. However, the TRL of the heat exchanger will be influenced by the working fluid in use.

Similar to the turbomachinery TRL discussed earlier, there are several projects and application of heat exchangers with air as working fluid, which puts its TRL at high levels. However, the decision challenge will be on the ability to cope with operating conditions parameters such as reliability, maintainability, corrosion, compactness, and cost. The use of air will give a larger heat exchanger compared with helium.

On the other hand, one advantage the use of helium has enjoyed is the compactness of its heat exchangers due to its thermodynamic properties. The helium exchangers have also been widely used and will not be incorrect to for the author to say that it is ahead of its time. The considerations listed for a high performing heat exchanger can be easily achieved with helium at relatively less cost compared to any other fluid used in this study. However, the low side to the use of helium is its tendency to leakage at high temperature and pressure which could pose as a risk factor unless an appropriate solution to seals and bearings are updated. Again, for carbon dioxide, the TRL with regards, to closed-cycle gas turbine application is low. This is because its technology is currently in its development stage. Another concern that may be raised for carbon dioxide its thermodynamic negative influence on the size of heat exchangers.

7.3 Financial Risk

The financial risk assessment is an important component of the risk analysis. The section is to provide understanding on certain factors that direct potential risk to the initial capital investment and cash flow. There so many factors that would have been analysed, but due to constraint during the research, only the influence of working fluid, constant pressure ratio and mass flow, and the effect of legislation are considered.

7.3.1 Cost of working fluid

Although the initial cost of working fluid may not significantly effect on the capital cost but it will affect the operational cost of the power plant. In Table 6-1, the cost of each working fluid was presented based on the time of this research. The cost of helium is about five (5) times more than nitrogen, eight (8) times more than carbon dioxide and twelves time more than air.

However, looking at each fluid, helium poses the greatest risk for analysis investment decision. This is because the supply of helium is largely controlled by the US government; hence, there is limited supply to the market which put the longer term operation of plants with helium at potential risk. The helium

market is based on a comprehensive framework which includes features such as geological uncertainty, depleatability, and multistage processing [164].

Helium is a non-renewable, finite resource which complicates its optimal allocation. Thus, scarcity and the variation in resource quality mean the future sources of helium will cost more to exploit [156,160]. From economies point of view, the present consumption from any given source thus forgoes its future profits, and the value of the resource is this forgone profit.

Theoretically, in a perfectly competitive market, the cost value of any working fluid will appreciate over time at the discount rate minus the cost escalation rate. However, due to the limited access to helium, its escalation rate maybe 10 to 15 percent more than the other working fluids if the demand for helium plants increases [164]. Also, as previously mentioned, storage is particularly important in the helium market because of the nature of its supply, hence, events such as maintenance on storage facilities can significantly put the additional cost to the use of helium.

Nitrogen is another fluid that can be of potential financial risk due to the cost of processing nitrogen from ammonia. This will also influence its future use for the closed-cycle gas turbine. For carbon dioxide, many western countries are putting tax incentives for carbon sequestration; hence, the cost of carbon dioxide may remain relatively stable over a longer period of time. This will also be the same experience for air.

7.3.2 Sensitivity to pressure ratio and mass flow

In this section, the influence of compressor pressure ratio and mass flow on the capital cost is discussed. The design choice for any closed-cycle gas turbine depends on the maximum cycle efficiency that can be obtained from a given pressure ratio. The choice of cycle pressure ratio determines the size of the turbo-sets in terms of a number of stages and length of the turbo-set. Thus, this will have a direct effect on the cost of the turbo-set based on the component cost analysis presented in chapter five (5). As the pressure ratio increases, the number of stages of the turbo-set is increased. However, this may seem to

favour the heat exchangers in terms of size, but made also show detrimental effects when the system is over pressurized. The cost implication is that the helium turbo-sets increases in cost rapidly compared to other selected working fluid as a result of the increase in pressure ratio. Similarly, the mass flow affects the component surface area and the output power of the plant. For fluid like helium with its specific heat capacity five times greater than air and nitrogen, it implies that for a given mass flow its specific power will be five times greater than air or nitrogen fluid. This means that helium will be more compact and give larger output power at a reasonable cost. In terms of size, carbon dioxide will be the largest because of its thermodynamic properties

7.3.3 Legislation

The legislation also plays an important role in the potential financial risk of any investment in closed-cycle gas turbine especially with regards to its heat source and working fluid options. The experiences of Chernobyl and Fukushima nuclear power plant have placed this technology in a negative perception and put more legislative bureaucracy on closed-cycle gas turbine projects. This also has a direct implication on the financial risk associated with such projects.

From the working fluid perspective, as previously mentioned, fluids like helium is government controlled. This means that the supply and sales can be politicised; which could have cost implication on investment. Also, carbon dioxide cost in different countries may greatly vary because of the legislation on tax incentive for technology that uses this working fluid. This means if there is a change in this incentive, the cost of investment may be affected.

7.4 Chapter Conclusion

In this chapter, a risk assessment of selected working fluid has been presented. The technology risk discussed includes working fluid gas management, material technology for high temperature and pressure, and technology maturity level for the selected working fluids. Similarly, financial risk was also presented. A major disadvantage of helium is its cost as a result of limited supply, hence, one has

to make room for cost exigencies if helium is selected as working fluid design choice for the closed-cycle gas turbine.

8 CONCLUSION AND RECOMMENDATIONS

8.1 Summary of a research study

As discussed in this thesis, the closed-cycle gas turbine provides very attractive benefits which make it a viable energy conversion system. It has the potential to complement the conventional power plants with little environmental impact. To this end, its viability and features are hinged on selecting the most appropriate working fluid, operating and design conditions which satisfy external regulatory constraints, high cycle performance, minimum overall size of components, minimum investment cost and maximum return on investment. Designing a system that would meet any one of these criteria as a decision-making tool can be exceedingly complex. Thus, the aim of the research was to analyse and compare the effects of selected working fluids on the closed-cycle gas turbine design, performance, economics, and risk, as a decision support tool for any future investment. A framework with data which describe the performance, costs, structural characteristics and design choices was developed in form of multidisciplinary tool.

The TERA method has been utilised in this research as a multidisciplinary framework for strategic decision making in closed-cycle gas turbine technology investments. The governing principles of TERA arise from different module integration, which allows for design considerations and/or operating areas such as performance, component design, economics and risk analysis.

The following offsetting objectives were implemented in the research:

- State-of-the-art review on closed cycle gas turbine technology, working fluid options, and its management system
- Cycle performance and closed-cycle gas turbine control options
- Components design characteristics based on working fluid options selected in the study
- Economics and risk analysis based on the effects of working fluids used in the study (helium, air, carbon dioxide, nitrogen)

In accomplishing the first objective, the research presented a historical development of the closed-cycle gas turbine technology, major concepts and important research and development in the use of different working fluids. Based on the reviews and previous operating experiences, the challenges that have hindered its large scale and the future prospect of the closed-cycle gas turbine was also presented such as limited design and operational experience of turbo components and heat exchangers. Also, from the research review, it was clear that although design and performance assessment has been performed for certain fluids, there has not been a detailed comparison of working fluids used in this study in terms of its economic assessment, risk and influence on component design, cycle performance and inventory control system of the closed-cycle gas turbine. This gap presented an opportunity for this research.

Based on the TERA methodology developed in the research, a simulation tool called GT-ACYSS was developed for closed-cycle gas turbine simulations with extended features such as flexibility in working fluid options, different cycle configuration, design, off-design and pseudo transient simulation for varying conditions, control option performance analysis and preliminary component design. The simulation tool was validated with data from the open literature. In the performance model, the effect of helium, carbon dioxide, air, and nitrogen was simulated and different sensitivity analyses were carried out. The sensitivity analysis involves the behaviour of model variables over predetermined bounds to determine their relative effect on the model outcome. Through this process, one can identify some subset variables that exert significant influence on the model results and determine the break-even points that alter the ranking of considered options. Each of these goals provides important insight to decision-makers who are rightly skeptical of fixed values.

Another important component of the research presented was the effect of the selected working fluids on the engine component design and performance. The reason for this was to show what fluid can be used to meet the goal of minimum overall engine size. Next, was an economic assessment of the plant based on

the working fluid impact on engine components designs using the same power output for all selected working fluid as a baseline during the analysis. Finally, one other novelty of the research was presented in the risk analysis especially on the economics of the working fluids. Section 8-2 presents a conclusion of the overarching results of case studies conducted to support the research arguments.

8.2 Conclusion of results

The first part of the results presented in this research resulted in validating the simulation tool developed using different cycle configurations. The results presented demonstrated that the scaling method of component maps and the algorithm of the simulation were reasonable for closed-cycle gas turbine performance analysis with mean deviations for different case studies between 0.1 and 1%. Also, the control option analysis showed that the inventory control strategy has a high efficiency at both part-load and design in ambient conditions compared with other control options presented. However, its limitation for a continuous discharge of gas inventory at reduced load depends on the rotational speed for which the centrifugal forces acting on the blade tips could become too high and on the size and pressure of the storage tank. Also, continuous increase by the HST can also lead to an increase in shaft speed. To avoid as much as possible these limitations in shaft speed or low efficiencies at a further reduction in power would require, a combined control mode to be adopted. The bypass control would rather recommend for rapid load response and shaft speed control.

The second sets of results were obtained during simulation of the effect of the selected workings and sensitivity analysis. The results show that choice of working fluid to a reasonable extent affects the design choice cycle configuration. The closed cycle performance can be enhanced by using additional components; however, their implementation would raise additional issues and complexity. Also, the closed-cycle gas turbine cycle efficiency is greatest for working fluid with a higher ratio of specific heat at low-pressure ratio and least ratio of specific heat at higher pressure ratio. Since the specific heat

ratio of helium is larger than, air, nitrogen and carbon dioxide the optimum efficiency for helium occur at the lowest pressure ratio compared with other fluids. The preliminary design assessment of the working fluid showed as expected that it is more difficult to compress or expand helium, hence, the more number of stages is required to achieve its design goal. The specific heat of helium is about five times that of nitrogen or air, and since the stage temperature rise is inversely proportional to the specific heat for a given limiting blade speed, it follows that the temperature rise available per stage when running with helium will be about one fifth that of nitrogen, which of course, results in more stages being required for a helium compressor.

The next set of results presented are the economic and risk assessment. It is obvious the performance only cannot be the base for investment decision on the closed-cycle gas turbine. Although helium showed competitive cycle performance, its economic and risk assessment put it on the low scale for possible design choice as shown in results of chapter 6 and 7.

8.3 Concluding Discussions

Among the fluids used in this research, helium is commonly chosen in design studies as working fluid for closed-cycle gas turbine systems. This is mainly because of its high thermal conductivity coupled with its high specific heat, make it better heat transfer fluid than any other gas used in this study. Hydrogen has sometimes been considered but has never been used as a working fluid in a closed-cycle gas turbine because of the explosion hazard. A major disadvantage of helium is its cost as discussed in the risk assessment. Also, helium poses a requirement challenge for the exceptionally high degree of leak tightness throughout the closed system, particularly with respect to the shaft seal. Carbon dioxide and nitrogen are also often candidates, primarily because they on the surface at least appear to reduce the oxidation and corrosion problems. However, it is has been found that iron-chrome-nickel alloys owe their high-temperature oxidation resistance to the formation of a dense, protective oxide film much like that of the oxide film on the anodized aluminum. For these iron-chrome-nickel alloys, strongly oxidizing conditions are

required not only to form this film initially but also to maintain it in the face of tendencies to form minute cracks with thermal strain cycling. As a consequence, it has been found that at temperatures above about 873K, ordinarily, air is a more favourable environment for the iron-chrome-nickel alloys than is helium; hence there is really no incentive from the structural materials standpoint to use helium rather than air.

The output of a closed-cycle gas turbine system is normally controlled by varying the system pressure. The most difficult control condition that must be met is the abrupt loss of load as a consequence of a circuit breaker trip. For this condition, the control problem is greatly eased if the working fluid can simply be vented to atmosphere, a step that presents no problem with air but would represent an important expense if helium were employed.

Helium has the advantage that it makes possible smaller turbine and compressor units, but the number of stages of these units is increased. If an appreciable number of machines were produced, there would undoubtedly be important cost savings. However, no such machines are in production and hence there is a strong incentive to employ air as a working fluid so that existing gas turbine machinery can be employed without carrying out a substantial design and development effort.

8.4 Limitation of Studies

As models created offer representation and simplifications of real engines, there will inevitably be errors that mean they do not represent fully the real equipment. This is compounded by not having a complete set of data for the engine, mostly because this data is proprietary and not released into the public domain for competitive reasons. It is important, however, to look at the limitations of the models to see where they can be improved

The engine model, although it shows good correlation with the performance data and behaves realistically, suffers from a lack of available data. Firstly, the component maps are from within the GT-ACYSS libraries, which are very unlikely to be the same as the original engine. Secondly, the overall pressure

ratio in the open literature, but not how this is distributed amongst each shaft, for which assumptions and judgment have to be made. Finally, the TETs were chosen so that the required output characteristics are met, however, the real TET may be different, which could slightly affect the overall efficiency.

8.5 Recommendations for Future Work

The experience gained during the research and case studies suggest that a lot of useful areas could have been covered in this thesis to give broad perspective to the closed-cycle gas technology, but due to time constraint, it could not be accomplished. Some of the areas identified for further work include:

- Total energy utilization implemented as Combined Closed-Cycle Gas Turbine Systems (Power and Heat Production with Closed-Cycle Gas Turbines). The objective is to analyze the influence of the top cycle TET and pressure on the selected waste heat utilization performance, analysis the economic benefit as compared with other conventional combined cycle plant
- Heat source alternative can be explored especially solar power closed-cycle gas turbine. Solar energy is an inexhaustible heat source that can be utilized to power a closed-cycle gas turbine.
- Modelling of transient behaviour of the closed-cycle gas turbine can be incorporated into the cycle performance simulation tool developed in this research. Also, further modification in cycle configuration and component maps can be implemented into the GT-ACYSS model
- The technology risk assessment module can be further enhanced to reflect the state of development in closed-cycle gas turbine component. Also, using Monte Carlo simulation, detailed sensitivity analysis studies on the effect of working fluid on the closed-cycle technology can be explored especially in terms of fluid availability and TET improvement using advanced materials.

REFERENCES

1. IEA. Energy and Climate Change Energy. Paris; 2015.
2. Frutschi HU. Closed-Cycle Gas Turbines: Operating Experience and Future Potential. 1st edition. New York: ASME; 2005.
3. Abram T., Ion S. Generation-IV nuclear power: A review of the state of the science. Energy Policy. 2008; 36: 4323–4330. Available at: DOI:10.1016/j.enpol.2008.09.059
4. Olumayegun O., Wang M., Kelsall G. Closed-Cycle Gas Turbine for Power Generation: A State-of-the-art Review. Fuel. 2016; 180: 694–717. Available at: DOI:10.1016/j.fuel.2016.04.074
5. Gosden E. New Era of UK Nuclear Power as Hinkley Point Finally gets go-ahead. The Telegraph. London; 15 September 2016; Available at: <http://www.telegraph.co.uk/business/2016/09/15/new-era-of-uk-nuclear-power-as-hinkley-point-finally-gets-go-ahe/>
6. El-Genk MS., Tournier J. On the use of Noble Gases and Binary Mixtures as Reactor Coolant and CBC Working Fluids. Energy Conversion Management. 2008; 49: 1882–1891.
7. Ulizar I., Pilidis P. Design of a Semi closed-Cycle Gas Turbine with Carbon Dioxide-Argon as Working Fluid. ASME Journal of Engineering for Gas Turbines and Power. 1998; 120: 330–335.
8. Gad-Briggs A., Pilidis P. Analyses of Off-Design Point Performances of Simple and Intercooled Brayton Helium Recuperated Gas Turbine Cycles. Proceedings of the 2017 25th International Conference on Nuclear Engineering ICONE25. Shanghai: ASME; 2017. p. ICONE25-67714.
9. Wang J., Gu Y. Parametric Studies on different Gas Turbine Cycles for a High-Temperature Gas-cooled Reactor. 2005; 235: 1761–1772. Available at: DOI:10.1016/j.nucengdes.2005.02.007
10. Staudt JE. Design Study of An MGR Direct Brayton-Cycle Power Plant.

Massachusetts Institute of Technology; 1987.

11. Ainley DG., Barnes JF. An Assessment of the Component Sizes of Nuclear Closed-Cycle Gas Turbines Using Argon and Helium. Proceedings of IMechE. Pyestock, Farnborough: IMechE; 1966. pp. 156–162.
12. El-Genk MS., Tournier J. Effects of Working Fluid and shaft Rotation Speed on the Performance of HTR Plants and the Size of CBC Turbo-Machine. Nuclear Engineering and Design. 2009; 239: 1811–1827.
13. Dostal V. A Supercritical Carbon Dioxide Cycle for Next Generation Nuclear Reactors. Massachusetts Institute of Technology; 2004.
14. McDonald CF. Large Closed Cycle Gas Turbine Plants. Sawyer's Gas Turbine Engineering Handbook, Vol. II. 3rd Editio. Norwalk, Con., USA: Sawyer, J.W Turbomachinery International Publications; 1985.
15. McDonald CF. Component Design Considerations for Gas Turbine HTGR Power Plant. Gas Turbine Conference and Products Show. New York: ASME; 1975.
16. Wohlgemuth JS. Comparison of Open and Closed Brayton Engines for Recuperated and Simple Cycles. Maryland; 1978.
17. Eames IW., Evans K., Pickering S. A Comparative Study of Open and Closed Heat-Engines for Small-Scale CHP Application. Energies. 2016; 9(130): 1–12.
18. McDonald CF. Gas turbine power plant possibilities with a nuclear heat source. Closed and open cycles. American Society of Mechanical Engineers (Paper). 1990; (New York, NY, United States). Available at: <http://www.scopus.com/inward/record.url?eid=2-s2.0-0025257997&partnerID=40&md5=386ba7cf52fcd800a0b63b884532e1e0>
19. Gad-Briggs A., Pilidis P. Analyses of Simple and Intercooled Recuperated Direct Brayton Helium Gas Turbine Cycles for Generation IV Reactor Power Plants. ASME Journal of Nuclear Engineering and Radiation

- Science. 2016; 3: 11017-1-011017-7. Available at: DOI:10.1115/1.4033398
20. David Doty F., Dewey Jones J. A New Look at the Closed Brayton Cycle. IECEC. 1990; Vol. 2: 166–172.
 21. Noblis CW. Analysis of Brayton Cycles Utilizing Supercritical Carbon Dioxide. New York; 2014.
 22. Decher R. Energy Conversion: Systems, Flow Physics, and Engineering. New York: Oxford University Press; 1994. 595-598 p.
 23. Walsh PP., Fletcher P. Gas Turbine Performance. 2nd edition. Oxford: Blackwell Science; 1998.
 24. Kuo SC., Shu HT. Alternative Closed-Cycle Gas Turbine System Design Considerations for Ship Propulsion Applications. ASME. 1979; : 1–11.
 25. Hodge J. Cycles and Performance Estimation. New York: Academic Press; 1955.
 26. Ishiyama S., Muto Y., Kato Y., Nishio S., Hayashi T., Nomoto Y. Study of steam, helium, and supercritical CO₂ turbine power generations in a prototype fusion power reactor. Nuclear Energy. 2008; 50: 325–332.
 27. Yan X., Kunitomi K., Nakata T., Shiozawa S. GTHT300 Design, and Development. Nuclear Engineering and Design. 2003; 222: 247–262.
 28. Siorek MP. Design of a Technology Demonstration Closed Brayton Cycle Engine for Small Electrical Power Generation Application. Carleton University; 2004.
 29. Pradeepkumar KN. Analysis of a 115MW, 3- Shaft, Helium Brayton Cycle Using Nuclear Heat Source. Cranfield University; 2002. Available at: DOI:10.1115/2001-GT-0523
 30. Matimba TAD. A Thermo-hydraulic Model of the Inventory Control System for Load Following in the PMBR. North-West University, Potchefstroom; 2004.

31. Botha BW., Rousseau PG. Control options for Load Rejection in a Three-Shaft Closed Cycle Gas Turbine Power Plant. Transactions of the ASME. 2007; 129: 806–813.
32. Olumayegun O., Wang M., Kelsall G. Thermodynamic Analysis and Preliminary Design of Closed Brayton Cycle using nitrogen as Working fluid and Coupled to Small Modular Sodium-cooled Fast Reactor (SM-SFR). Applied Energy. 2017; 191: 436–453.
33. El-genk MS., Tournier J. Performance Analyses of VHTR Plants with Direct and Indirect Closed Brayton Cycles and Different Working Fluids. Progress in Nuclear Energy. 2009; 51: 556–572. Available at: DOI:10.1016/j.pnucene.2008.11.004
34. Curt K. The Escher Wyss-AK Closed Cycle Turbine its Present Development and Future Prospect. Journal of the American Society of Naval Engineers. 1946; 58(3): 508–522.
35. Kelly C. The Escher Wyss-AK Closed-Cycle Turbine its Present Development and Future Prospect. Journal of the American Society of Naval Engineers. 1946; 58(3): 508–522.
36. Keller C., Schmidt D. Industrial Closed-Cycle Turbines for Conventional and Nuclear Fuel. ASME Gas Turbine Conference. Houston, Texas: Transactions of the ASME; 1967.
37. Bammert K., Krey G., Krapp R. Operation and Control of the 50-Mw Closed-Cycle Helium Turbine Oberhausen. ASME. 1974; (74-NaN-13): 1–8.
38. Harmon R. The Closed-Cycle Gas Turbine for Central and Dispersed Cogeneration and Central Power Application. National Closed Cycle Gas Turbine Seminar. Los Angeles; 1981.
39. Strumpf H. Conceptual Design of a Pulverized Coal Furnace for a Utility Size Closed-Cycle Gas Turbine Plant. ASME. 1979; (79-NaN-158).

40. Keller C. Gas Turbines for and Conventional Nuclear Fuel f Closed-Cycle Industrial Gas Turbines for Conventional and fuel. ASME. 1968; (67-NaN-10).
41. Duvall G., Taylor D. Operational Evaluation of a Closed Brayton Cycle Laboratory Engine. 11th IECEC Meeting. Lake Tahoe: ASME; 1976.
42. Gathy B. A Marine Nuclear Power Plant Design Utilizing the Direct Brayton Cycle. ASME. 1970; (70-NaN-3).
43. Bammert K., Burik J., Griepentrog H. Highlights and Future Development of Closed-Cycle Gas Turbines. Transactions of the ASME. 1974; (October 1974): 342–348.
44. Bammert, K, Groschup G. Status Report on Closed-Cycle Power Plants in the Federal Republic of Germany. Transactions of ASME, Journal of Engineering Power. 1977; (January): 76-NaN-54.
45. Pietsch A. Closed Cycle Gas Turbines 50MW and Smaller. Sawyer's Gas Turbine Engineering Handbook, Vol. III. 3rd Editio. Norwalk, Con., USA: Sawyer, J.W Turbomachinery International Publications; 1985.
46. Yan X. Dynamic Analysis and Control System Design for an Advanced Nuclear Gas Turbine Power Plant. Massachusetts Institute of Technology; 1990.
47. Francois E. Technical-Economic Analysis of a New Generation Nuclear Power Plant: The Very High-Temperature Reactor coupled with a Combined Cycle. Cranfield University; 2010.
48. Hoffmann JR., Feher EG. 150 KWe Supercritical Closed-Cycle System. Transactions of the ASME. 1971; 93(1): 70–80.
49. Dyreby JJ. Modelling the Supercritical Carbon Dioxide Brayton Cycle with Recompression. University of Wisconsin-Madison; 2014.
50. Li X., Yang X., Zhang Y., Wang J. HTR-10GT Dual Bypass Valve Control Features and Decoupling Strategy for Power Regulation. Hindawi Science

- and Technology of Nuclear Installations. 2017; : 1–12.
51. Griepentrog H., Sackarendt P. Vaporization of LNG with Closed-Cycle Gas Turbines. ASME. 1976; (76-NaN-38).
 52. Wheeler A. A Brief History of Nuclear Airplanes. mentalfloss. 2013. Available at: <http://mentalfloss.com/article/53184/brief-history-nuclear-airplanes> (Accessed: 26 October 2015)
 53. Narayanan K., Brendan D. Brayton Cycle Conversion for Space Solar Power. 48th AIAA/ASME/ASEE Joint Propulsion Conference and Exhibit, Atlanta. Atlanta, Georgia: AIAA; 2012. pp. 1–11.
 54. Colon R. Soviet Experimentation with Nuclear Powered Bombers. 2015. pp. 1–5. Available at: <http://www.aviation-history.com/articles/nuke-bombers.htm> (Accessed: 26 October 2015)
 55. Hays TC., Arena AS. Feasibility Study of Closed Cycle Propulsion for Unmanned Aerial Systems. AIAA. 2015; (June): 1–16.
 56. Baggenstoss W., Ashe T. Mission Design Drivers for Closed Brayton Cycle Space Power Conversion Configuration. Transactions of ASME, Journal of Engineering Power. 1992; (91-NaN-139).
 57. Klann J., Wintucky W. Status of the 2- to 15-KWe Brayton over System and Potential Gains from Component Improvements. Proceedings of IECEC. Boston, Massachusetts; 1971.
 58. Ribeiro GB., Francisco BF., Lamartine N. G. Thermodynamic Analysis and Optimization of a Closed Regenerative Brayton Cycle for Nuclear Space Power Systems. Applied Thermal Engineering. 2015; Available at: DOI:10.1016/j.applthermaleng.2015.06.093.This
 59. McDonald CF. The Closed-Cycle Turbine — Present and Future Prospectives for Fossil and Nuclear Heat Sources. ASME. 1978; : 1–28.
 60. Fayrweather D., et al. Advanced Marine Closed Brayton Engine. Proceeding of the Eleventh Intersociety Energy Conversion Conference.

- Nevada: American Institute of Chemical Engineers; 1976.
61. Resnick B. Technical Considerations in the development of a Maritime Gas-Cooled Reactor System. ASME. 1961; (61-NaN-14).
 62. McDonald CF. Closed-Cycle Gas Turbine Potential for Submarine Propulsion. ASME. 1988; (88-NaN-126).
 63. Harper AD., Jansen JS. Closed Brayton Cycle Engine Application to Emerging Unmanned Underwater Vehicle Missions. ASME. 1990; (90-NaN-307).
 64. Lee JC., J. Campbell J., Wright DE. Closed-Cycle Gas Turbine Working Fluids. Transactions of the ASME. 1981; Vol. 103: 220–228.
 65. Robinson S. Influence of Working-Fluid Characteristics on the Design of the Closed-Cycle gas Turbine. ASME. 1957; 95(2469): 427–428. Available at: DOI:10.1126/science.95.2469.427-b
 66. Forum Generation IV International. Technology Roadmap Update for Generation IV Nuclear Energy Systems. Washington D.C; 2014.
 67. Locatelli G., Mancini M., Todeschini N. Generation IV Nuclear Reactors: Current Status and Future Prospects. Energy Policy. 2013; 61: 1503–1520.
 68. Kuo SC. The prospects for Solar-Powered Closed-Cycle Gas Turbines. ASME. 1980; (80-NaN-26).
 69. Horton TL. Conceptual Design of a Solar Powered Closed-Cycle Gas Turbine Electric Power Generation System. ASME. 1979; (79-NaN-43).
 70. Schwarzbözl P., Buck R., Sugarmen C., Ring A., Marcos Crespo MJ., Altwegg P., et al. Solar gas turbine systems: Design, cost, and perspectives. Solar Energy. 2006; 80(10): 1231–1240. Available at: DOI:10.1016/j.solener.2005.09.007
 71. McDonald CF. A Hybrid Solar Closed-Cycle Gas Turbine Combined Heat and Power Plant Concept to Meet the Continuous Total Energy Needs of

- Small Community. *Journal of Heat Recovery Systems*. 1986; 6(5): 399–419.
72. Frutschi HU. The Relationship of Power and Heat Production with Closed Cycle Gas Turbines. *Journal of Engineering for Gas Turbines and Power*. Vol. 102: 288–291.
73. McDonald CF., Van Hagan TH., Kapich D. Performance Potential of an Advanced Nuclear Gas Turbine/Cogeneration System (HTGR-GT/C). *ASME Journal of Engineering for Gas Turbines and Power*. 1983; : 101–121.
74. Meyer L., Holland JW. Gas Turbine HTGR as a Thermal Energy Source for Desalination and District Heating. *Proceedings of International Energy Congress*. Copenhagen: IEC; 1976.
75. Mock TEA., Daudet H. Advanced Technology Cogeneration System Conceptual Design Study Closed Cycle Gas Turbines. Cleveland, Ohio; 1983.
76. Grochowina F. Performance Evaluation of Gas Turbines for Nuclear Power Plants. Cranfield University; 2011.
77. Yousef SH., Zaaout MS. Comparative performance of closed cycle gas turbine engine with heat recovery using different gases. *Heat Recovery Systems and CHP*. 1992; 12(6). Available at: DOI:10.1016/0890-4332(92)90017-C
78. Kato Y., Nitawaki T., Muto Y. Medium Temperature carbon dioxide Gas Turbine Reactor. *Nuclear Engineering and Design*. 2004; 230: 195–207.
79. Ulizar I., Pilidis P. Handling of Semiclosed Cycle Gas Turbine with a Carbon Dioxide-Argon Working Fluid. *ASME*. 2000; 122: 437–441.
80. Alpy N., Cachon L., Haubensack D., Floyd J., Simon N., Gicquel L., et al. Gas Cycle testing opportunity with ASTRID, the French SFR prototype. *Proceedings of supercritical CO₂ power cycle symposium*. Boulder,

Colorado; 2011. pp. 42–51.

81. Invernizzi CM. Prospects of Mixtures as Working Fluids in Real-Gas Brayton Cycles. *Energies*. 2017; 10: 1–15. Available at: DOI:10.3390/en10101649
82. RTO. Performance Prediction and Simulation of Gas Turbine Engine Operation. Paris; 2007.
83. Korakianitis T., Vlachopoulos NE., Zou D. Models for the Prediction of Transients in Closed Regenerative Gas Turbine Cycles With Centrifugal Impellers. *ASME Journal of Engineering for Gas Turbines and Power*. 2005; 127: 505–513. Available at: DOI:10.1115/1.1806450
84. Kikstra J. F., Verkooijen AHM. Dynamic Modeling of a Cogenerating Nuclear Gas Turbine Plant—Part I: Modeling and Validation. *ASME Journal of Engineering for Gas Turbines and Power*. 2002; 124(3): 725–733. Available at: DOI:10.1115/1.1426086
85. Visser WPJ., Broomhead MJ. GSP, a Generic Object-Oriented Gas Turbine Simulation Environment. *ASME Turbo Expo 2000: Power for Land, Sea, and Air*. Munich: ASME; 2000. pp. 2000-NaN-2. Available at: DOI:10.1115/2000-GT-0002
86. Vavra ME. A Graphical Solution to Matching Problem in Closed-Cycle Gas Turbine Plant. Washington; 1965.
87. Bardia A. Dynamics and Control Modelling of the Closed-Cycle Gas Turbine (GT-HTGR) Power Plant. Fourth Power Plant Dynamics, Control and Testing Symposium. Gatlinburg, Tennessee: General Atomic Company; 1980. p. GA-A15677 (1-28).
88. Dupont J., Jeanmonod R., Frutschi HU. Tugsim-10, a Computer Code for Transient Analysis of Closed-Cycle Gas Turbine Cycles and Specific Applications. *Nuclear Engineering Design*. 1977; 40: 421–430. Available at: DOI:10.1016/0029-5493(77)90050-4

89. Sanchez D., Chacartegui R., Munoz de Escalona JM., Sanchez T. Performance Analysis of an MCFC & Supercritical Carbon Dioxide Hybrid Cycle under Part-Load Operation. *International Journal of Hydrogen Energy*. 2011; 36: 10327–10336.
90. Vilim RB., Cahalan J. E., Mertzyurek U. GAS-PASS/H: A Simulation Code for Gas Reactor Plant Systems. ANL; 2004.
91. Al-Hamdan Q., Ebaid M. Modelling, and Simulation of a Gas Turbine Engine for Power Generation. *Transactions of the ASME*. 2006; 128: 302–311.
92. Sankar B., Shah B., Thennavarajan S. On Gas Turbine Simulation Modelling Development. National Conference on Condition Monitoring. Bangalore; 2013. pp. 1–17.
93. Korakianitis T., Wilson DG. Models for Predicting the Performance of Brayton-Cycle Engines. *ASME*. 1992; : 361–371.
94. Knauss DT. A Method of Predicting the Off-Design Performance of Closed-Brayton-Cycle Engines. 1978.
95. Ulizar Alvarez. JI. Simulation of Multi Fluid Gas Turbines. Cranfield University; 1998. Available at: <http://hdl.handle.net/1826/3537>
96. Khan RSR. TERA for Rotating Equipment Selection. Cranfield University; 2012.
97. Kyprianidis KG., Colmenares Quintero R., Pascovici DS., Ogaji SOT., Pilidis P., Kalfas A. EVA- A Tool for Environmental Assessment of Novel Propulsion Cycles. ASME TURBO EXPO. Berlin, Germany: ASME; 2008.
98. Di Lorenzo G. Advanced Low-Carbon Power Plants: The T.E.R.A Approach. Cranfield University; 2010.
99. Sirag A. A TERA Approach to Aero Engine Performance Assessment. Cranfield University; 2011.
100. Wanis M. Techno-Economic, Environmental and Risk Analysis (TERA) for

- Power Generation. Cranfield University; 2013.
101. Vicente E. Effect of Bypass Ratio on Long-Range Subsonic Engine. Cranfield University; 1994.
 102. Ogaji SOT., Pilidis P., Hales R. TERA- A Tool for Aero-engine Modelling and Mangement. Second World Congress on Engineering Asset Management and the Fourth International Conference on Condition Monitoring. Harrogate, United Kingdom; 2007.
 103. Gayraud. Technical and Economical Assessment for Industrial gas Turbine Selection. Cranfield University; 1996.
 104. Lagana MC. TERA for LNG Applications. Cranfield University; 2008. Available at: DOI:10.1260/0957456042880200
 105. Nind A. A Techno-economic Risk Assessment of Conventional Aero-Gas Turbine: Technological Limits and Future Directions. Cranfield University; 2016.
 106. Spindler PM. Environmental Design Space Model Assessment. Massachusetts Institue of Technology; 2007.
 107. Sagerser DA., Lieblein S., Krebs RP. Empirical Expressions for Estimating Length and Weight of Axial-Flow Components of VTOL PowerPlants. Cleveland, Ohio; 1971.
 108. Shapiro SR., Caddy M. NEPCOMP- The Navy Engine Performance Program. ASME Gas Turbine Conference. Zurich, Switzerland: ASME; 1995.
 109. Nikolaidis T. TURBOMATCH Scheme for Aero/Industrial Gas Turbine Engine. Cranfield: Cranfield University; 2015.
 110. W. M Crim J., Hoffmann JR., Manning GB. The Compact AK Process Nuclear System. Journal of Power and Energy. 1966; (April 1966): 127–138.
 111. Shirakura T., Awano S. Thermodynamical Performances of Closed-Cycle

- Gas-Turbine. Tokyo Joint Gas Turbine Congress. Tokyo: JSME, ASME; 1977. pp. 260–270.
112. Saravanamuttoo H., Rogers G., Cohen H. Gas Turbine Theory. 5th Editio. Harlow: Prentice Hall; 2001.
 113. Razak AMY. Industrial Gas Turbines - Performance and Operability. 1st edition. Cambridge: Woodhead Publishing Limited; 2007. 174-240 p.
 114. Kakac S., Liu H. Heat Exchangers Selection, Rating and Thermal Design. 2nd edition. New York: CPC Press; 2002.
 115. Shah RK., Sekulic D. Fundamentals of Heat Exchanger Design. New Jersey: John Wiley & Sons, Inc.; 2003.
 116. Navarro HA., Cabezas-Gomez LC. Effectiveness-NTU Computation with a Mathematical Model for Cross-Flow Heat Exchangers. Brazilian Journal of Chemical Engineering. 2007; 24(4): 509–521.
 117. Osigwe EO., Gad-Briggs A., Nikolaidis T., Pilidis P., Sampath S. Multi-Fluid Gas Turbine Components Scaling for a Generation IV Nuclear Power Plant Performance Simulation. Cranfield; 2018.
 118. Kurzke J. Correlations Hidden in Compressor Maps. Proceedings of ASME Turbo Expo. Vancouver: ASME; 2011. pp. 1–10.
 119. Rademaker ER. Scaling of Compressor and Turbine maps on the Basis of Equal flow Mach numbers and Static flow Parameters. Amsterdam; 2012.
 120. Kong C., Ki J., Kang M. A New Scaling Method for Component Maps of Gas Turbine Using System Identification. ASME Journal of Engineering for Gas Turbines and Power. 2003; 125: 979–985.
 121. Fox RW., Pritchard PJ., McDonald AJ., Leylegian JC. Introduction to Fluid Mechanics. 8th edn. Danvers: Wiley & Sons; 2011.
 122. Gordon S., McBride BJ. Computer Program for Calculation of Complex Chemical Equilibriim and Applications: Prt II. 1996.

123. Irvine, T. F. and Liley P. Steam and Gas Tables with Computer Equations. Orlando: Academic Press; 1984.
124. Hilsenrath J et al. Tables of Thermodynamic and Transport Properties of Air, Argon, Carbon Dioxide, Carbon Monoxide, Hydrogen, Nitrogen, Oxygen and Steam. Oxford: Pergamon Press; 1960.
125. Hendricks RC., Baron AK., Peller IC. GASP - A Computer Code for Calculating the Thermodynamic and Transport Properties for Ten Fluids: Parahydrogen, Helium, Neon, Methane, Nitrogen, Carbon Monoxide, Oxygen, Flourine, Argon and Carbon Dioxide. Ohio; 1975.
126. Ouyang L. New Correlations for Predicting the Thrmodynamic Properties of Supercritical Carbon Dioxide. The Open Petroleum Engineering Journal. 2012; 5: 42–52.
127. Keenan J., Kaye J., Chao J. Gas Tables. 2nd edn. 1983.
128. Bammert K., Krey G. Dynamic Behavior and Control of Single-Shaft Closed-Cycle Gas Turbines. Gas Turbine Conference and Products Show. Houston, Texas: Transactions of ASME, Journal of Engineering Power; 1971. pp. 447–453.
129. Openshaw F., Estrine E., Croft M. Control of a Gas Turbine HTGR. ASME. 1976; (76-NaN-97): 1–12.
130. Covert RE., Krase G., Morse DC. Effect of Various Contol Modes on the Steady-State Full and Part Load Performance of a Direct-Cycle Nuclear Gas Turbine Power Plant. ASME. 1974; (74-NaN-7): 1–9.
131. Dyreby JJ. Development of a Flexible Modelling Tool for Prediciting Optimal Off-Design Performance of Simple and Recompression Brayton Cycles. The 4th International Symposium - Supercritical CO2 Power Cycles. Pittsburgh; 2014.
132. Bitsch D., Chaboseau J. Power Level Control of a Closed Loop gas Turbine by Natural Transfer of Gas between the Loop and Auxilliary

- Tanks. BNES-Conference. London: BNES; 1970.
133. Berchtold M. 3220191: Varying the Pressure Level of a Closed-Cycle Gas Turbine Plant. Switzerland: US Patent Office; 1962.
 134. Berchtold M., Keller C. 3218807: Transfer of the Working Medium in the Working Medium Exchange between a Closed-Cycle Gas Turbine Plant and a Reservoir. Switzerland: US Patent Office; 1962.
 135. Nieuwoudt C. Helium Tank Management Model - A Report to Determine tank Sizes. Pretoria, South Africa; 2003.
 136. Carstens N. Control Strategies for Supercritical Carbon Dioxide Power Conversion Systems. Massachusetts Institute of Technology; 2007.
 137. Chapra S., Canale R. Numerical Methods for Engineers. 7th edn. New York: McGraw-Hill; 2015. chap. 5-7 p.
 138. Kunitomi K., Katanishi S., Takada S., Takizuka T., Yan X. Japan's Future HTR - the GTHTR300. Nuclear Engineering and Design. 2004; 233: 309–327. Available at: DOI:10.1016/j.nucengdes.2004.08.026
 139. Yan X., Sat0 H., Kamiji Y., Imai Y., Terada A., Tachibana Y., et al. GTHTR300 Cost Reduction through Design Upgrade and Cogeneration. Nuclear Engineering and Design. 2016; 306: 215–220.
 140. Yan X., Takizuka T., Takada S., Kunitomi K., Minatsuki I., Mizokami Y. Cost and Performance Design Approach for GTHTR300 Power Conversion System. Nuclear Engineering and Design. 2003; 226: 351–373. Available at: DOI:10.1016/S0029-5493(03)00212-7
 141. Keller C. The Coal-Burning Closed-Cycle Gas Turbine. Gas Turbine Power Conference. Washington D.C: ASME; 1961. pp. 1–7.
 142. Jordan FD. An Analog Computer Simulation of a Closed Brayton Cycle System. ASME. 1969; (69-NaN-50): 1–15.
 143. Janis J., Braun G., Ryan R. Performance Testing of the Compact APCSE Closed Brayton-Cycle System. Gas Turbine Conference and Products

- Show. Houston, Texas: ASME; 1967. pp. 1–16.
144. Osigwe EO., Li YG., Sampath S., Jombo G., Indarti D. Integrated Gas Turbine System Diagnostics: Components and Sensor Fault Quantification using Artificial Neural Network. 23rd ISABE Conference Proceedings. Manchester, UK: ISABE; 2017. p. ISABE-2017-2605. Available at: <https://isabe2017.org/>
 145. Munoz de Escalona JM., Sanchez D., Chacartegui R., Sanchez T. Performance Analysis of Hybrid Systems Incorporating High temperature Fuel cells and Closed Cycle Heat Engines at Part Load Operations. International Journal of Hydrogen Energy. 2013; 38: 570–578.
 146. Wilson DG., Korakianitis T. The Design of High-Efficiency Turbomachinery and Gas Turbine. 2nd edn. New Jersey: Prentice Hall; 1998.
 147. Bullock RO. Analysis of Reynolds Number and Scale Effects on Performance of Turbomachinery. Journal of Engineering for Gas Turbines and Power. 1964; : 247–255.
 148. Wassel AB. Reynolds Number Effects in Axial Compressors. ASME Journal of Engineering for Gas Turbines and Power. 1968; : 149–156.
 149. ESDU92013. Selection and Costing of Heat Exchangers. London; 2013.
 150. PDHOnline Course. ASME Section I & Section VIII Fundamentals. 2012.
 151. Thakkar BS., Thakkar SA. DESIGN OF PRESSURE VESSEL USING ASME CODE , SECTION VIII , DIVISION 1. IJAERS. 2012; 1(II).
 152. Frutschi HU. 4148191: Method for Regulating the Power Output of a Thermodynamic System Operating on a Closed Gas Cycle and Apparatus for Carrying out the Method. Sweden: US Patent Office; 1979.
 153. Moss D. Pressure Vessel Design Manual. 3rd edn. Oxford: Gulf Professional Publishing; 2004.
 154. Megyesy EF. Pressure Vessel Handbook. 12th edn. Tulsa, Oklahoma:

- Pressure Vessel Publishing; 1973.
155. Doulgeris G., Benjelloun M., Singh R. A Method for Techno-Economic Analysis of Supercritical Carbon Dioxide for New Generation Nuclear Power Plants. Proceedings of IMechE. 2011; 226(A): 372–383.
 156. Kimball S. ., Jewell S. Mineral Commodity Summaries 2016. Virginia; 2016. Available at: <https://minerals.usgs.gov/minerals/pubs/mcs/2016/mcs2016.pdf>
 157. BOC. BOC Gas price list. Gas price list. 2016. Available at: https://www.boconlineshop.com/shop/SearchDisplay?storeId=715839134&catalogId=3074457345616677919&langId=101&pageSize=10&beginIndex=0&searchSource=Q&sType=SimpleSearch&resultCatEntryType=2&showResultsPage=true&pageView=product_list&actualItem=nitrogen&isPu (Accessed: 29 December 2016)
 158. Phung DL. Theory and Evidence for Using the Economy-of-Scale-Law in Power Plant Economics. Tennessee; 1987.
 159. Dhillon BS. Life Cycle Costing for Engineers. Florida: CRC press Taylor & Francis; 2010.
 160. Gerrard AM. Guide to Capital Cost Estimating. 4th edn. Rugby: IChemE; 2007.
 161. Corporation F., Falls G. Automatic Control Valves Price List. 2014. Available at: https://flomatic.com/assets/pdf_files/Control-Valve-Price-List.pdf (Accessed: 8 January 2017)
 162. DECC. Installed Cost and Maintenance Cost. 2013.
 163. Wright SA., Radel RF., Vemon ME., Rochau GE., Pickard PS. Operation and Analysis of Supercritical CO₂ Brayton Cycle. New York; 2010.
 164. TNAP. The Impact of Selling the Federal Helium Reserve. Washington; 2000. Available at: <https://www.nap.edu/read/9860/chapter/8>

APPENDICES

Appendix A GT – ACYSS: Additional Information

A.1 Engine Configurations

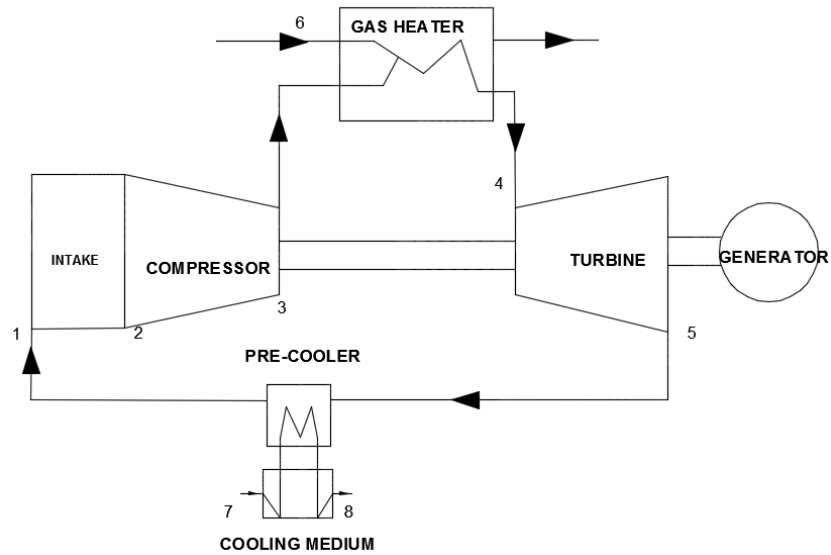


Figure A1 1 Simple Closed-Cycle Gas Turbine Configuration

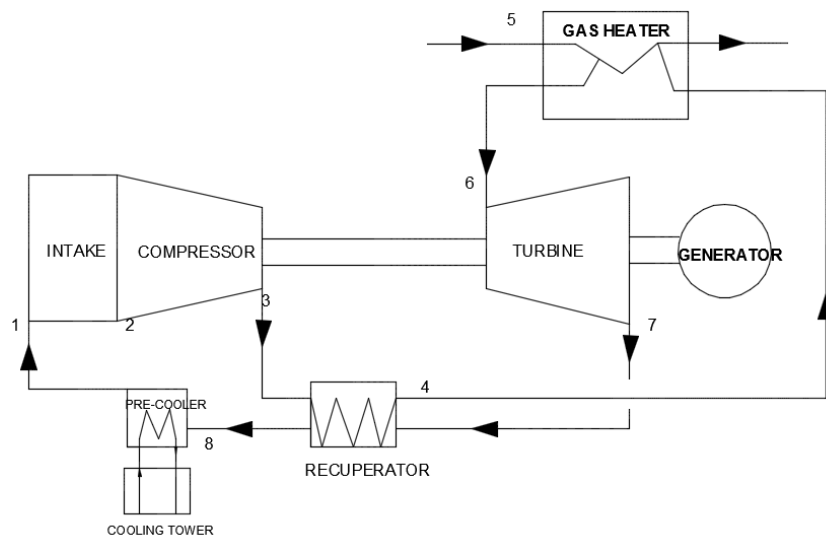


Figure A1 2 Closed-Cycle Configuration Recuperated

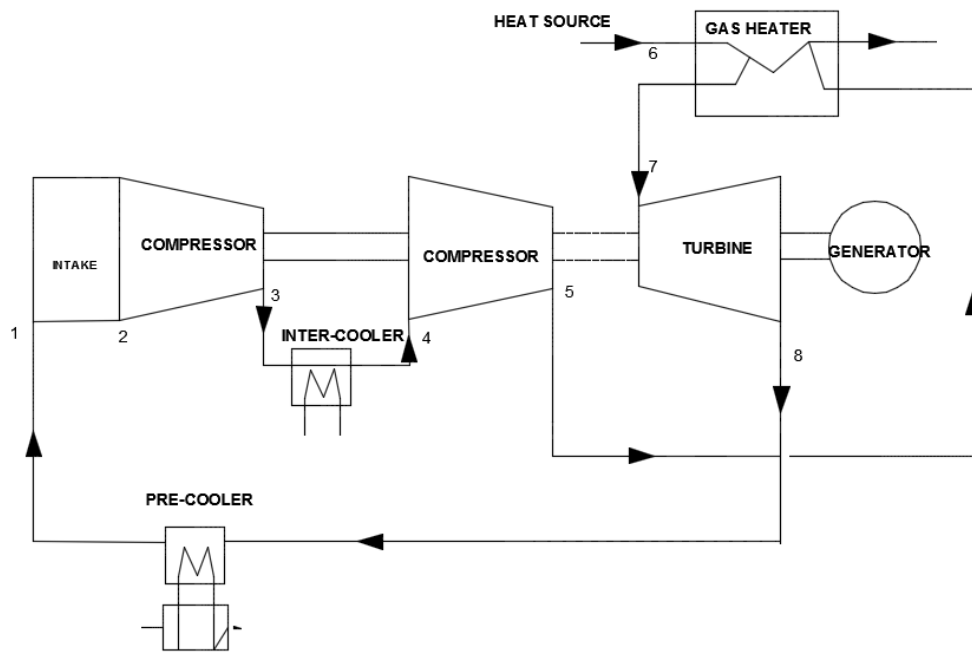


Figure A1 3 Closed-Cycle Configuration with Inter-cooler

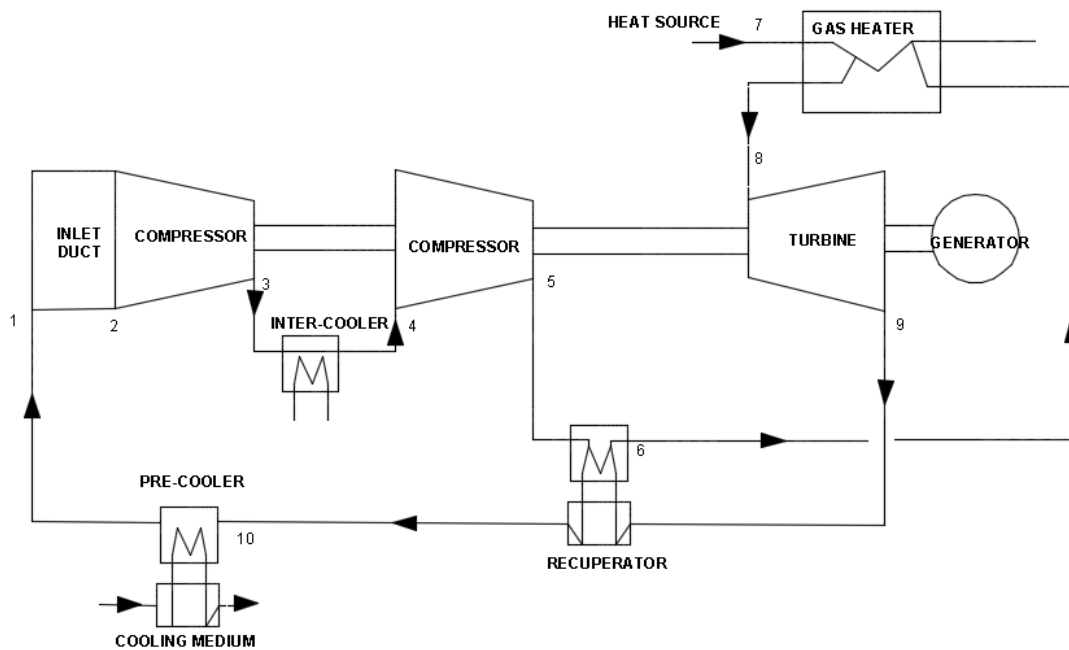


Figure A1 4 Closed-Cycle Configuration with Inter-cooler and Recuperated

A.2 Fluid Properties Modelling – Additional Information

$$C_V = C_P - R \quad (\text{A2-1})$$

$$\text{Gamma}(\gamma) = \frac{C_P}{1 - C_P} \quad (\text{A2-2})$$

Correlation formula for other properties of Helium

- Compressibility factor

$$Z = 1 + \frac{0.4446 * \frac{P}{101325}}{T^{1.2}} \quad (\text{A2-3})$$

- Coefficient of Dynamic Viscosity

$$\mu = 3.674E - 07 * T^{0.7} \left(\frac{Kg}{mS} \right) \quad (\text{A2-4})$$

- Coefficient of Thermal Conductivity

$$\lambda = 2.682E - 03 * \left(1 + \left(1.123E - 03 * \frac{P}{101325} \right) \right) * T^{\{0.71(1 - (2.10E - 04 * \frac{P}{101325}))\}} \left(\frac{W}{mK} \right) \quad (\text{A2-5})$$

- Prandtl Number Pr

$$Pr = \left(\frac{0.7117}{1 + (1.123E - 03 * \frac{P}{101325})} \right) * T^{-\{0.01 - (1.42E - 04 * P)\}} \quad (\text{A2-6})$$

Correlation formula for other properties of Air

- Compressibility factor

$$\begin{aligned} Z = A_0 + & \left(A_1 \frac{P}{101325} \right) + (A_2(9.8692E - 06 * P)^2) + (A_3(T - 273.16)) \\ & + \left(A_4 \left(\frac{P}{101325} \right) (T - 273.16) \right) \\ & + \{A_5(9.8692E - 06 * P)^2(T - 273.16)\} + (A_6(T - 273.16)^2) \\ & + \{A_7(9.8692E - 06 * P)(T - 273.16)^2\} \\ & + \{A_8(9.8692E - 06 * P)^2(T - 273.16)^2\} \end{aligned} \quad (\text{A2-7})$$

- Viscosity

$$\mu(T_r, \rho_r) = \Lambda * [\mu_0(T_r) + \Delta\mu(\rho_r)] \quad (\text{A2-8})$$

Where

$$\mu_0(T_r) = [A_0 T_r + A_1 T_r^{0.5} + (A_2 + A_3 T_r^{-1} + A_4 T_r^{-2} + A_5 T_r^{-3} + A_6 T_r^{-4})]$$

$$\Delta\mu(\rho_r) = A_7 \rho_r^1 + A_8 \rho_r^2 + A_9 \rho_r^3 + A_{10} \rho_r^4$$

$$T_r = \frac{T}{T^*}, \rho_r = \frac{\rho}{\rho^*}, T^* = 132.5 \text{ (K)}, \rho^* = 314.3 \left(\frac{\text{Kg}}{\text{m}^3}\right)$$

- Thermal Conductivity

$$\lambda(T_r, \rho_r) = \Lambda * [\lambda_0(T_r) + \Delta\lambda(\rho_r)] \quad (\text{A2-9})$$

Where

$$\lambda_0(T_r) = [A_0 T_r + A_1 T_r^{0.5} + (A_2 + A_3 T_r^{-1} + A_4 T_r^{-2} + A_5 T_r^{-3} + A_6 T_r^{-4})]$$

$$\Delta\lambda(\rho_r) = A_7 \rho_r^1 + A_8 \rho_r^2 + A_9 \rho_r^3 + A_{10} \rho_r^4 + A_{11} \rho_r^5$$

$$T_r = \frac{T}{T^*}, \rho_r = \frac{\rho}{\rho^*}, T^* = 132.5 \text{ (K)}, \rho^* = 314.3 \left(\frac{\text{Kg}}{\text{m}^3}\right)$$

Correlation formula for other properties of Nitrogen and Carbon dioxide

- Viscosity

$$\mu = A_1 \ln(T) + \frac{A_2}{T} + \frac{A_3}{T^2} + A_4 \quad (\text{A2-10})$$

- Thermal Conductivity

$$\lambda = A_1 \ln(T) + \frac{A_2}{T} + \frac{A_3}{T^2} + A_4 \quad (\text{A2-11})$$

Correlation Coefficient for Thermodynamic Properties of Air

Coefficient	Viscosity (Equ. 7)	Thermal Conductivity (Equ. 8)	Compres. Factor	C _p @ P<10atm (Equ. 9)	C _p @ 10<P≤70atm Equ. 10
Λ	6.1609E-06	25.9778E-03	-	-	-
A ₀	0.1285170	0.239503	1.00001	1.0598E+03	-
A ₁	2.6066100	0.006498	-5.8826E-04	-4.9712E-01	1.0687E+03
A ₂	-1.000000	1.000000	2.7106E-06	1.3360E-03	-1.9415E-01
A ₃	-0.709661	-1.926150	-3.3297E-07	-1.1073E-06	3.0254E-04
A ₄	0.6625340	2.0038300	1.2585E-05	4.0472E-10	-1.4040E-07
A ₅	-0.197846	-1.075530	-2.0659E-08	-5.5330E-14	2.3730E-11
A ₆	0.0077015	0.2294140	2.4925E-09	-9.8539E-20	4.0032E-16
A ₇	0.4656010	0.402287	-6.3706E-08	-	-
A ₈	1.2646900	0.356603	5.5619E-11	-	-
A ₉	-0.511425	-0.163159	-	-	-
A ₁₀	0.2746000	0.138059	-	-	-
A ₁₁	-	-0.0201725	-	-	-

Correlation Coefficient for Thermodynamic Properties of CO₂

Coefficient	Viscosity	Thermal Conductivity	Compres. Factor	C _p @ P<10atm	C _p @ 10<P≤70atm
Λ	-	-	-	-	-
A ₀	-	-	-	4.2360E+02	-
A ₁	0.54330318	0.53726173	-	1.8618E-00	6.1387E+02
A ₂	-0.1882389E03	-0.49928331E03	-	-1.8068E-03	5.8227E-01
A ₃	0.8872656E04	0.3739750E05	-	1.0375E-06	- 2.5931E-04
A ₄	0.2449936E01	0.32903619E01	-	-3.2606E-10	6.9978E-08
A ₅	-	-	-	4.3032E-14	-9.6851E-12
A ₆	-	-	-	- 1.5604E-19	3.8926E-16
A ₇	-	-	-	-	-

Correlation Coefficient for Thermodynamic Properties of N₂

Coefficient	Viscosity	Thermal Conductivity	Compres. Factor	C _p @ P<10atm	C _p @ 10<P≤70atm
Λ	-	-	-	-	-
A ₀	-	-	-	1.1263E03	-
A ₁	0.60443938	0.9430638	-	-6.5335E-01	1.1439E03
A ₂	-0.43632E02	0.1227989E03	-	1.5330E-03	-2.9284E-01
A ₃	-0.8844194E03	-0.1183943E05	-	-1.2095E-06	3.8508E-04
A ₄	0.18972150E01	-0.10668773	-	4.2833E-10	-1.7118E-07
A ₅	-	-	-	-5.7791E-14	2.8171E-11
A ₆	-	-	-	8.6364E-20	-4.5288E-16
A ₇	-	-	-	-	-

Correlation Coefficient for Thermodynamic Properties of He		
Coefficient	C_p @ $P < 10 \text{ atm}$ (Equ. 9)	C_p @ $10 < P \leq 70 \text{ atm}$ Equ. 10
Λ	-	-
A_0	5.1931E+03	-
A_1	0.0000	5.1931E+03
A_2	0.0000	0.0000
A_3	0.0000	-1.4040E-07
A_4	0.0000	0.0000
A_5	0.0000	0.0000
A_6	0.0000	0.0000
A_7	-	-

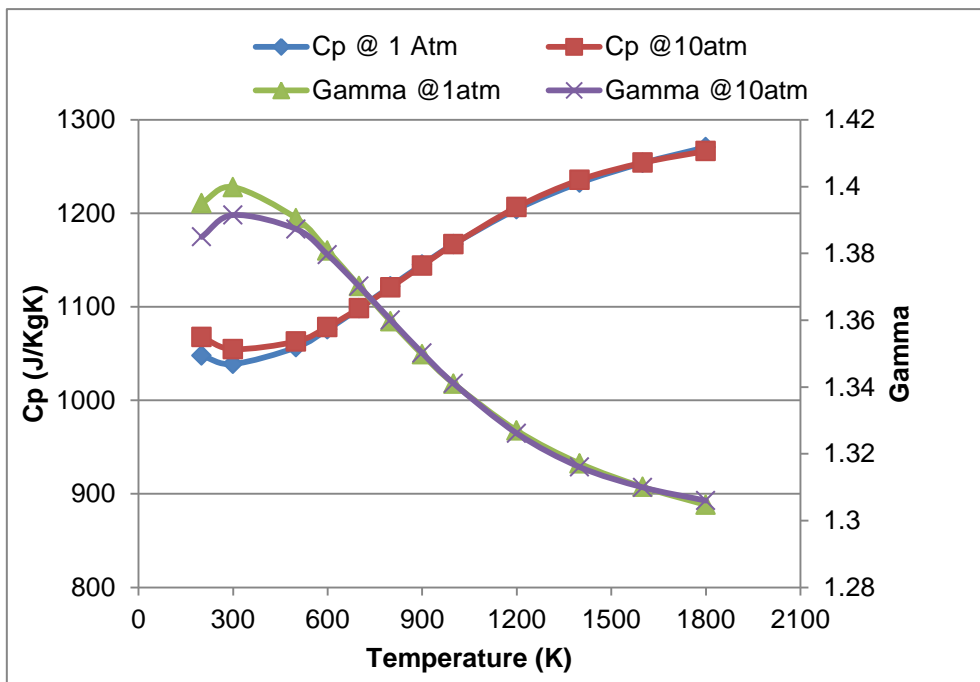


Figure A2.1 C_p and Γ of N_2 at 1 & 10 atm

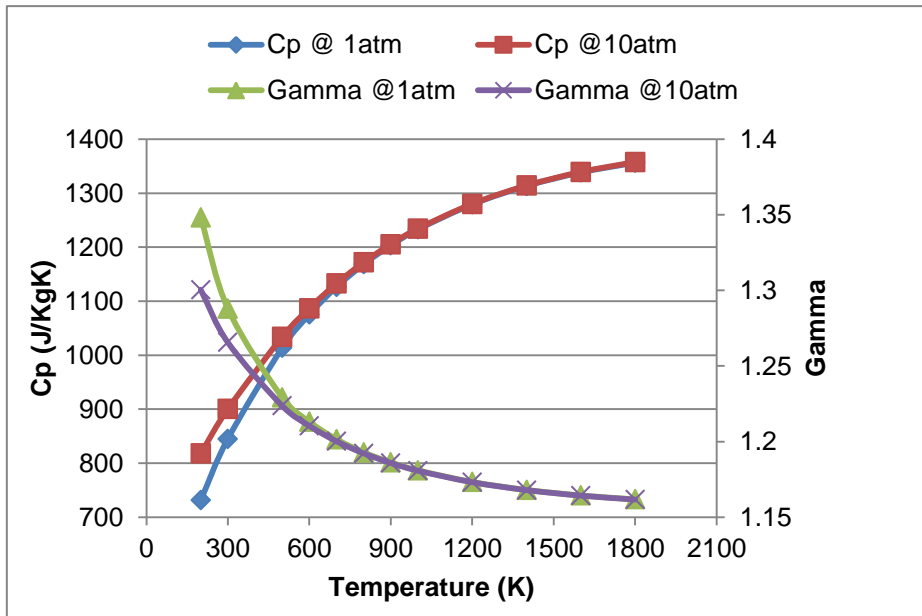


Figure A2 2 Cp and Gamma of CO2 at 1 & 10 atm

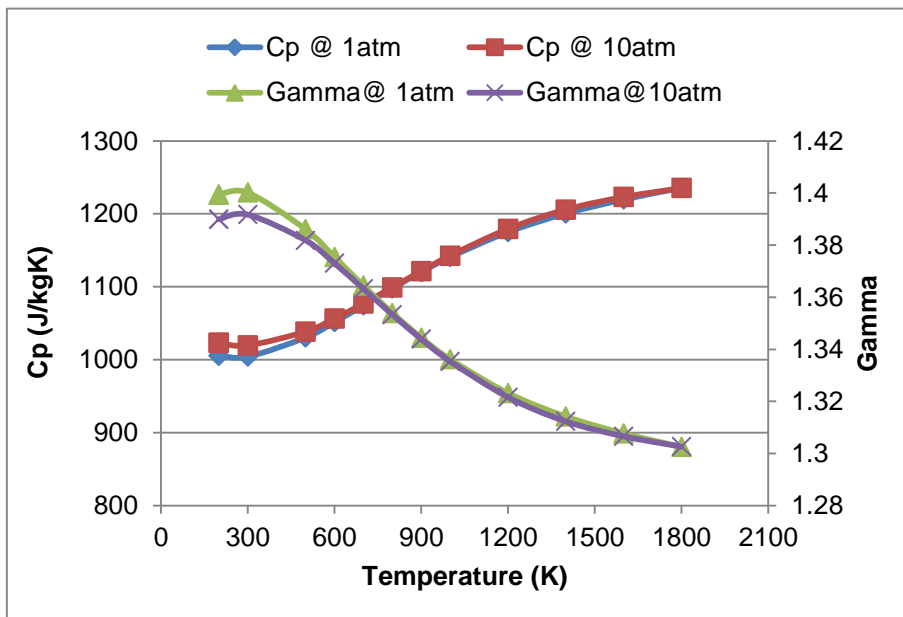


Figure A2 3 Cp and Gamma of Dry Air at 1 & 10 atm

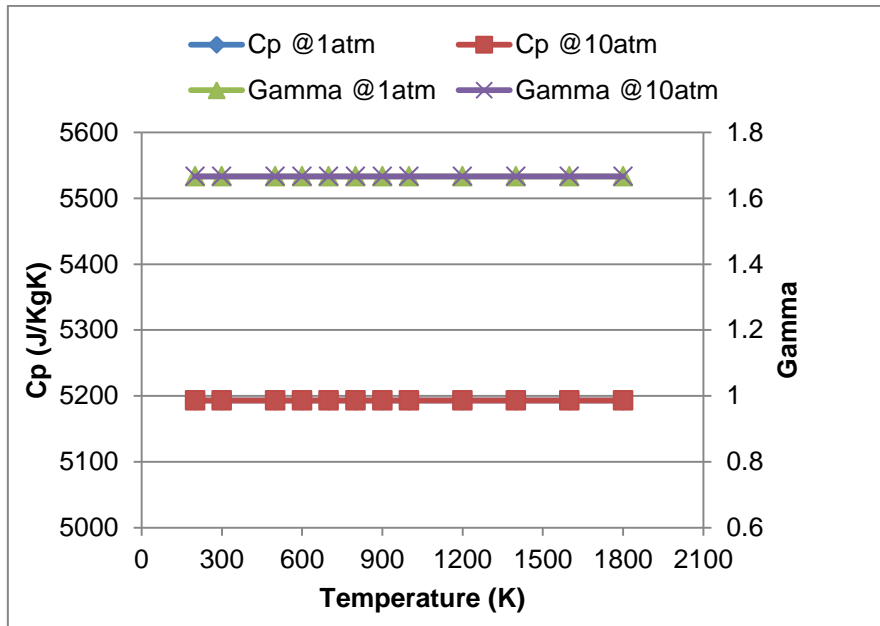


Figure A2 4 Cp and Gamma of Helium at 1 & 10 atm

```

!Closed Gas Turbine for Power Generation
!Modelled by Emmanuel Ozioma Osigwe January, 2017
!Design Point Simulation

!BRICK DATA ITEMS

!Cycle Calculation Type
1 ! Enter 1 for Design Point Calculations or 2 for off-Design Calculations

!Control/Handle
1 !Enter 1=Inventory control, 2=Heat source control, 3=Bypass control, 4=Combined control

!Reynolds Effect at offdesign
1 !Assume Pressure loss and Component Eff. at offdesign constant

!Heat Source
1 !Enter 1 for Natural gas, 2 for Solar powered, or 3 for Nuclear Powered

!Gas Properties Selection
1 !Enter 1=He, 2=CO2, 3=Air, 4=flare_gas, 5=Nitrogen

!Cycle Configurations
2 !Enter 1=simple cycle, 2=recuper, 3=intercooled-recuper or 4=intercooled cycle

!INTAKE
438 !Inlet Mass Flow (Kg/s) 230
0.0 !% Pressure Loss at the Intake
0.35 !Inlet Mach Number
301 !Inlet Temperature (K)
3500000 !Intake Inlet Pressure (Pa)

! COMPRESSOR CONDITIONS
2 !Enter 1 for isentropic or Enter 2 for polytropic efficiency
0.905 !Enter value between 0.0 to 1 for Compressor Isentropic or Polytropic Eff.
2.0 !Compressor Pressure ratio
4.0 !Compressor map type
1.0 !Enter value between 0 and 100 for % of Mass Flow required for bleed
0.0 !compressor geometry sizing calculation 1=calculate, 0.0 = Dont calculate

! RECUPERATOR CONDITIONS TUBE SIDE
0.94 !Enter value between 0.0 to 1 for Recuperator Effectiveness
0.5 ! Enter value btw 0.0 to 100 to account for any % mass flow loss (Leakage)
0.0 !Enter value between 0.0 to 1 for Recuperator Conductance if known, else enter 0.0 if unknown
1.0 !Enter value between 0 to 100 for % Recuperator Pressure at Loss Tube Side

! EXTERNAL HEAT SOURCE
0.95 !Enter value between 0.0 to 1 for external heat source combustion eff.
1123.0 !Heat Source Exit Temperature (K)

! GAS HEATER CONDITIONS TUBE SIDE
0.96 !Enter value between 0.0 to 1 for Gas Heater Effectiveness
0.5 ! Enter value between 0.0 to 100 to account for any % mass flow loss (Leakage)
0.0 !Enter value between 0.0 to 1 for Gas Heater Conductance if known, else enter 0 if unknown
1.3 !Enter value between 0 to 100 for Gas Heater % Pressure Loss Tube Side
0.0 !GH geometry sizing calculation 1=calculate, 0.0 = Dont calculate

! TURBINE CONDITIONS
-1 !Enter -1 if SOP unknown, 0.0 if Tw = cw and > 0.0 if known
2 !Enter 1 for Turbine isentropic or Enter 2 for polytropic efficiency
0.918 !Enter value between 0.0 to 1 for Turbine Isentropic or Polytropic Eff.
1.0 !Turbine map type
0.0 !Mechanical loss required to drive auxillary component
0.987 !Mechanical loss required to drive Electric Generator
0.0 !Mechanical loss required to drive Compressors
1 !Number of compressor on turbine shaft
0.0 !Turbine geometry sizing calculation 1=calculate, 0.0 = Dont calculate

! RECUPERATOR CONDITION SHELL SIDE (Utilizes same Recuperator Effectiveness)
0.0 ! Enter value btw 0.0 to 100 to account for any % mass flow loss (Leakage)
0.7 !Enter value between 0 to 100 for Recuperator % Pressure Loss Shell Side
0.0 !RX geometry sizing calculation 1=calculate, 0.0 = Dont calculate

! PRECOOLER CONDITIONS
0.95 !Enter value between 0.0 to 1 for Precooler Effectiveness
0.0 !Enter value btw 0.0 to 100 to account for any % mass flow loss (Leakage)
0.0 !Enter value between 0.0 to 1 for Precooler Conductance if Known, else enter 0 if unknown
0.0 !Enter value between 0 to 100 for Precooler % Pressure Loss Shell Side
295 !Enter value for cooling medium and temperature(Tcool<T1)
0.0 !PX geometry sizing calculation 1=calculate, 0.0 = Dont calculate

!off-Design Condition
6 1 1
0.5

```

Figure A2 5 Case 1 input file

Design Point Simulation Result

1 Table of Results for Components Thermodynamic Characteristics with Helium as working Fluid

Stn.No.	Gamma	w(Kg/s)	Pres. (Pa)	Temp. (K)	Enth. (J/Kg)	Cp(J/KgK)
1	1.666	440.000	3500000.000	301.000	1563123.125	5193.100
2	1.666	440.000	3500000.000	301.000	1563123.125	5193.100
3	1.666	435.620	7000000.000	408.889	2123400.000	5193.100
4	1.666	433.452	6930000.000	843.846	4382178.500	5193.100
5	1.344	0.000	0.000	1123.000	1411918.125	1430.669
6	1.666	435.675	6839910.000	1111.834	5773864.500	5193.100
7	1.666	435.675	3524672.750	871.610	4526355.500	5193.100
8	1.666	435.675	3500000.000	436.652	2267577.500	5193.100
9	1.666	440.000	3500000.000	301.000	1563123.125	5193.100
10	0.000	0.000	0.000	295.000	91752.540	4182.850
11	0.000	0.000	0.000	429.569	645261.538	4322.123

3 Table of Results for Cycle Performance

Converged at = 6 Iterations

Compressor work = 236100736.00 watts

Turbine work = 541013056.00 watts

Shaft Power = 283112320.00 watts

Electric Power = 300948448.00 watts

Heat Input = 602367376.00 watts

cycle_Ther_Eff = 0.47

Sp. Shaft Power = 643.44 Kws/Kg

A.3 Simulation Results for different control strategy

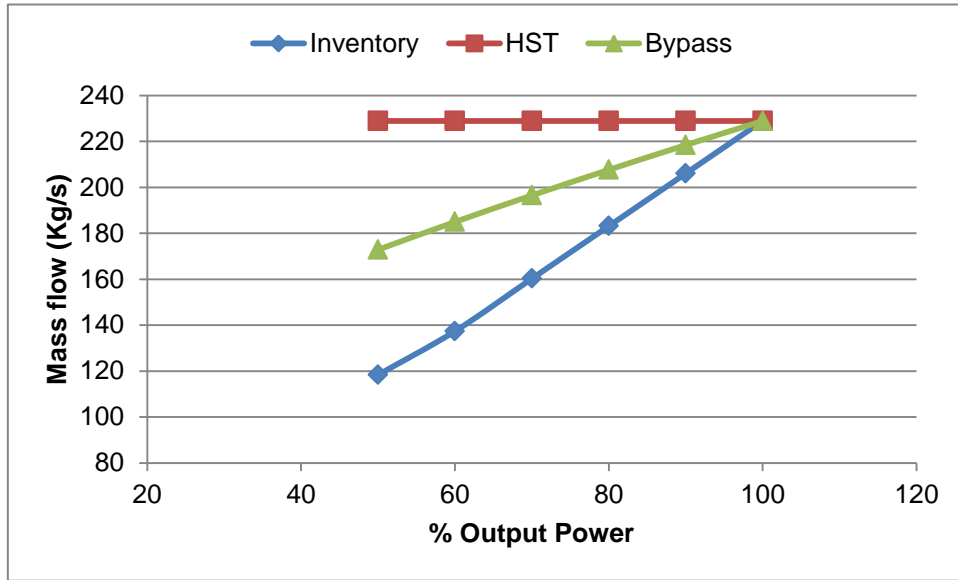


Figure A3 1 Comparison of Control Strategy during Part Load Operations (Mass Flow)

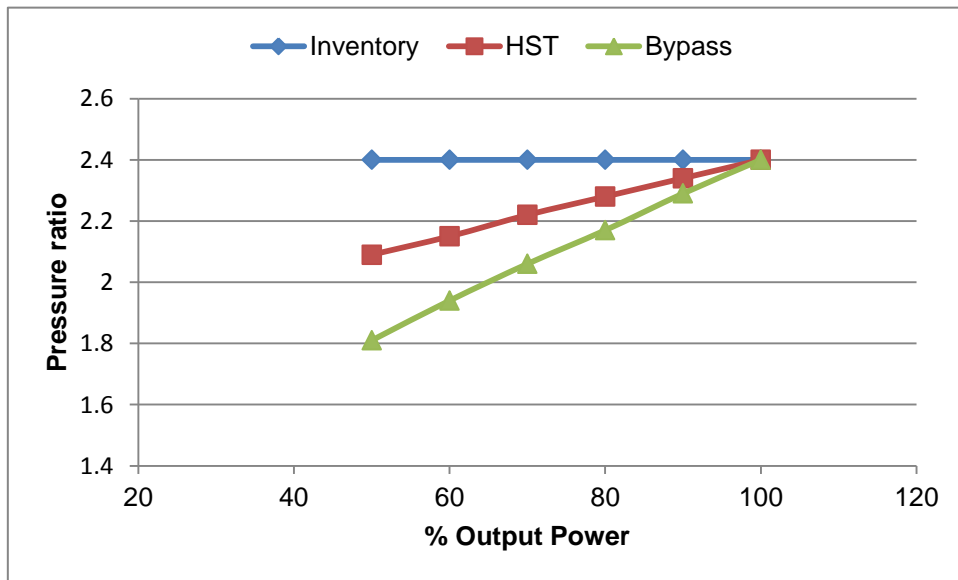


Figure A3 2 Comparison of Control Strategy during Part Load Operations (Pressure ratio)

Appendix B Effect of Working Fluid – Additional Results

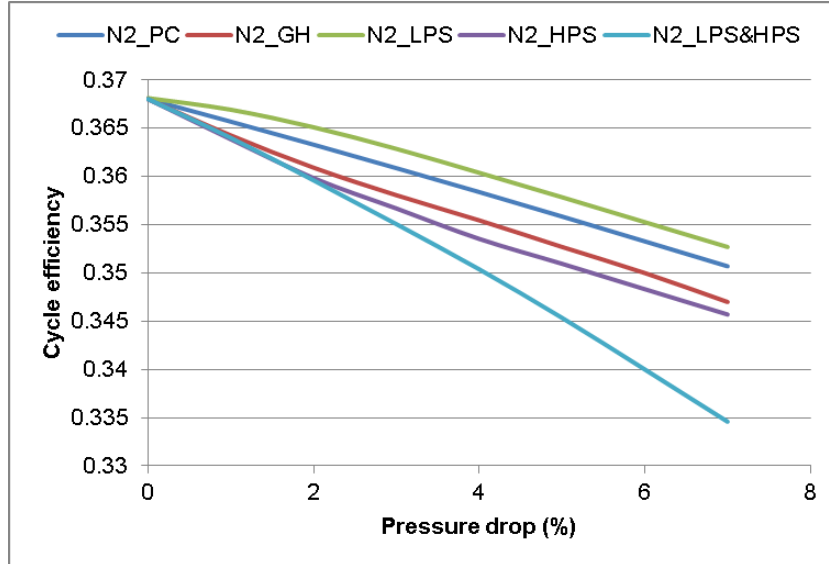


Figure B 1 Effect of Component Pressure drop on nitrogen cycle performance

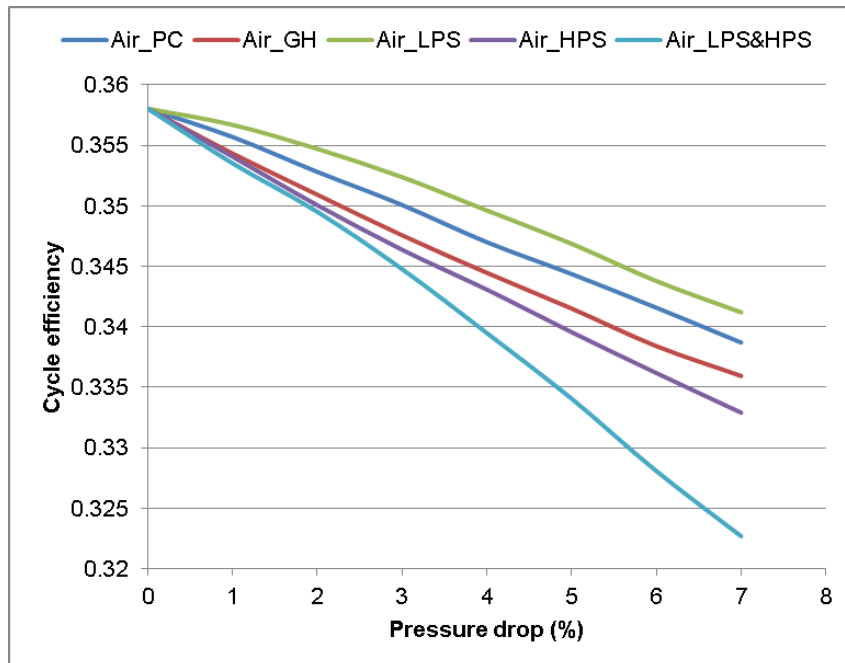


Figure B 2 Effect of Component Pressure drop on air cycle performance

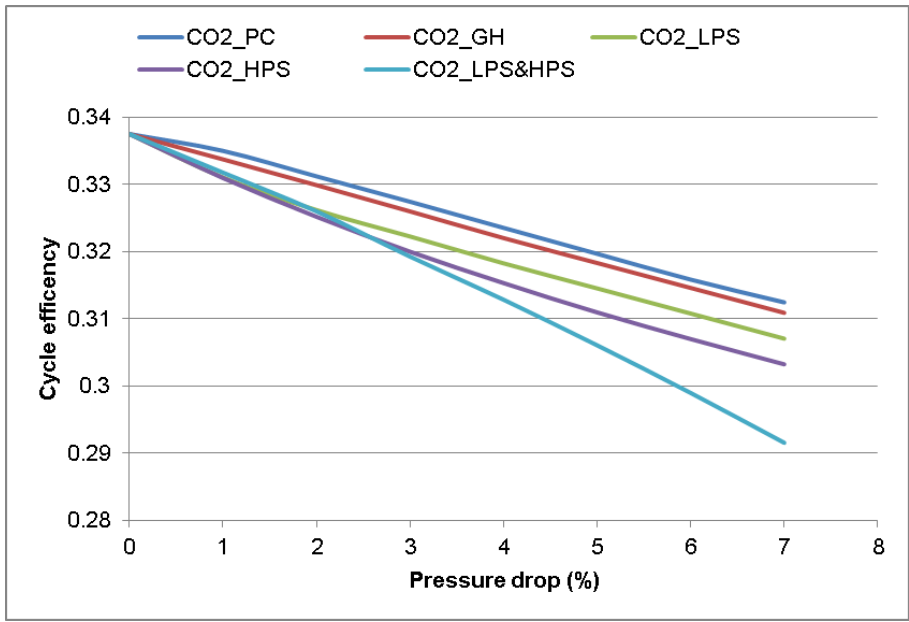


Figure B 3 Effect of Component Pressure drop on carbon dioxide cycle performance

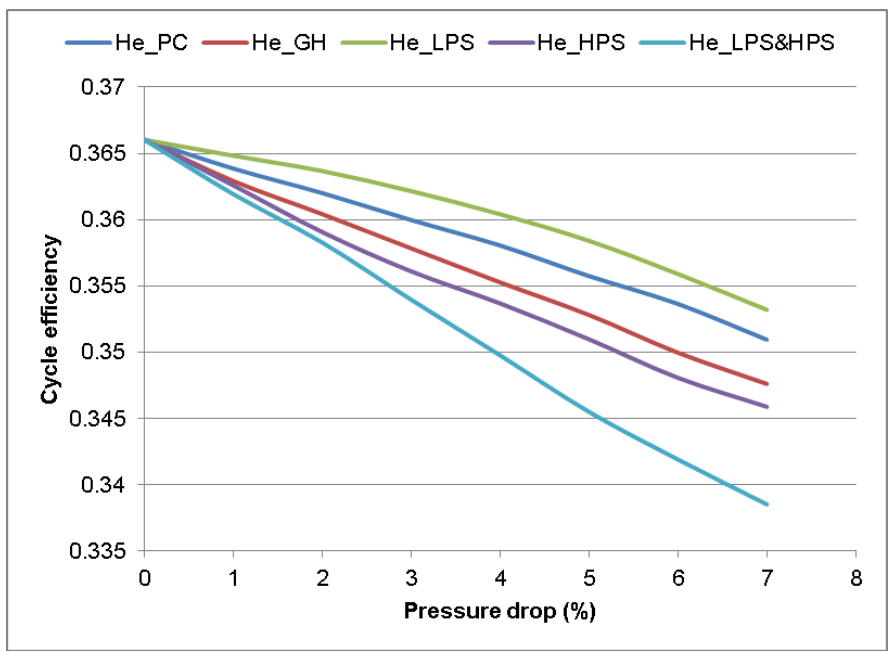


Figure B 4 Effect of Component Pressure drop on helium cycle performance

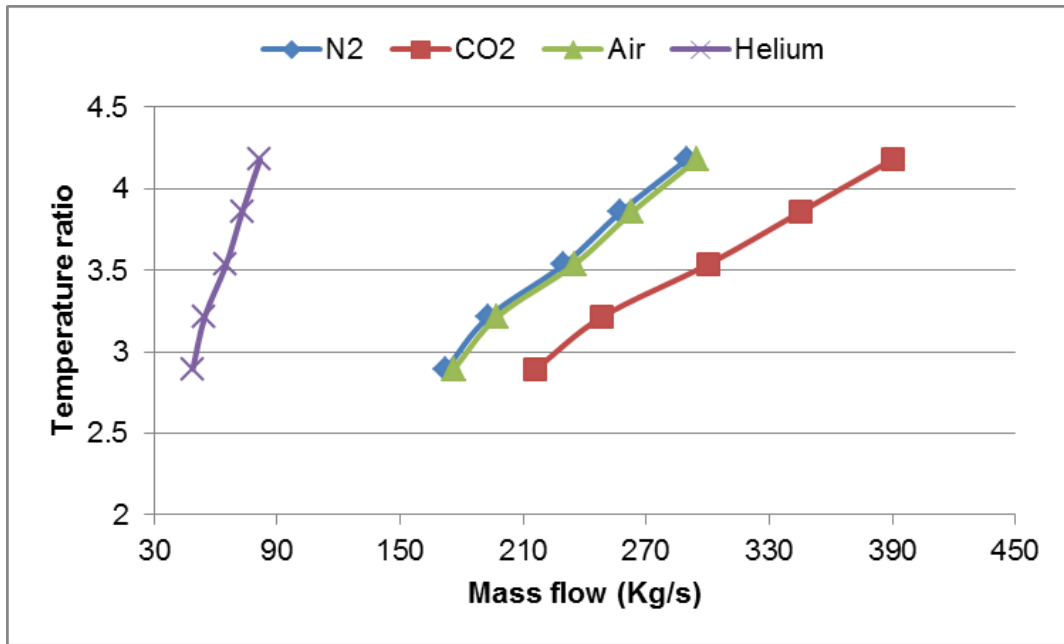


Figure B 5 Case1 – Variation of Mass Flow and Temperature ratio for different Working Fluid

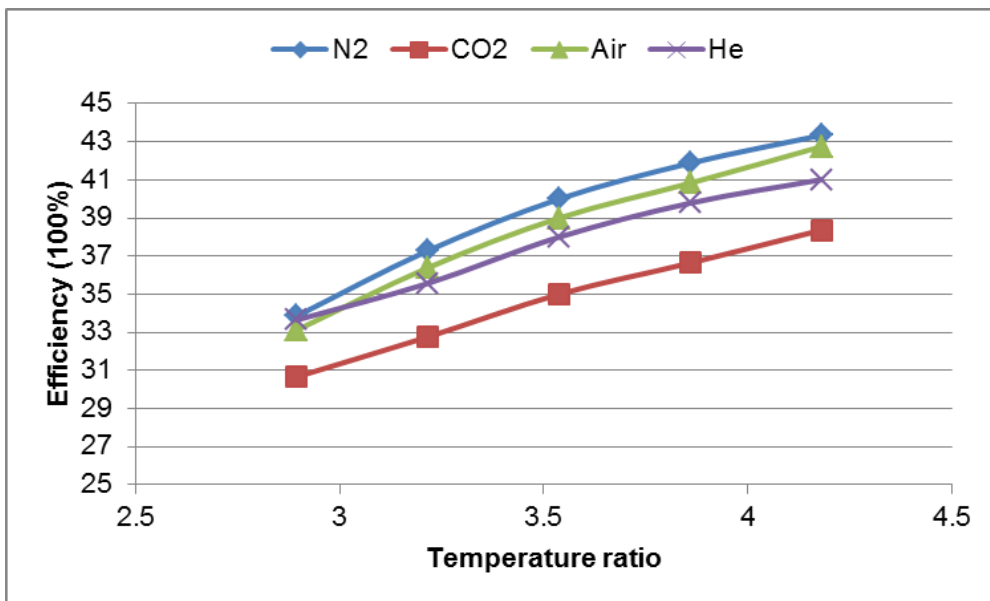


Figure B 6 Case1 - Variation of Cycle Thermal Efficiency at different Temperature ratio

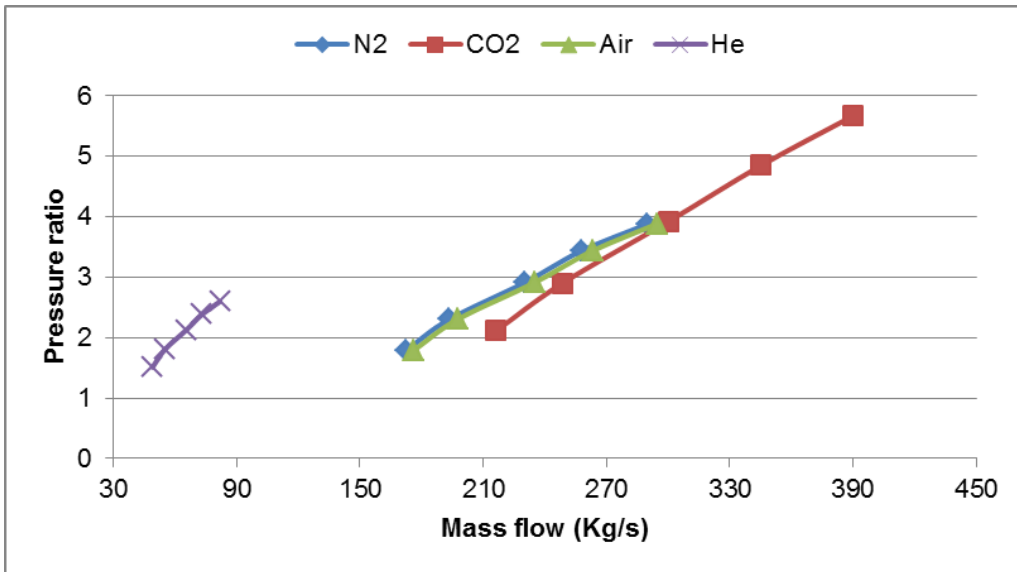


Figure B 7 Case 1 - Variation of Mass Flow and Pressure ratio different Working Fluid

Appendix C Effect of Working Fluid – Additional Results

C.1 U and C Values For Shell and Tube Heat Exchangers

$\dot{Q}/\Delta T$ (W/K)	Cold Side Fluid	Parameter	Hot Side Fluid							
			Low Pressure Gas (< 1 Bar)	Medium Pressure Gas (20 Bar)	Process Water	Low Viscosity Organic Liquid	High Viscosity Fluid	Condensing Steam	Condensing Hydrocarbon	Condensing Hydrocarbon with Inert Gas
1000	Low Pressure Gas (< 1 Bar)	U (W/m ² K)	55	93	102	99	63	107	100	86
		C (E/(W/K))	6.54	6.1	6.03	6.08	6.46	5.9	6.05	6.26
	Med. Pressure Gas (20 Bar)	U (W/m ² K)	93	300	429	375	120	530	388	240
		C (E/(W/K))	6.1	5	4.68	4.7	5.86		4.65	5.4
	Treated Cooling Water	U (W/m ² K)	105	484	938	714	142	1607	764	345
		C (E/(W/K))	6	4.4			5.72			4.9
	Low Viscosity Organic Liquid	U (W/m ² K)	99	375	600	500	130	818	524	286
		C (E/(W/K))	6.08	4.7		4.4	5.8			5.2
High Viscosity Liquid	U (W/m ² K)	68	138	161	153	82	173	155	214	
	C (E/(W/K))	6.41	5.74	5.58	5.71	6.28	5.53	5.6	5.51	
Boiling Water	U (W/m ² K)	105	4.67	875	677	140	1432	722	336	
	C (E/(W/K))	6	4.6			5.73			4.95	
Boiling Organic Liquid	U (W/m ² K)	99	375	600	500	130	818	524	286	
	C (E/(W/K))	6.08	4.7		4.4	5.8			5.2	

5000	Low Pressure Gas (< 1 Bar)	U (W/m ² K)	55	93	102	99	63	107	100	86
		C (E/(W/K))	2.72	1.86	1.88	1.88	2.48	1.88	1.89	2.16
	Med. Pressure Gas (20 Bar)	U (W/m ² K)	93	300	429	375	120	530	388	240
		C (E/(W/K))	1.86	1.27	1.23	1.24	1.76	1.17	1.23	1.34
	Treated Cooling Water	U (W/m ² K)	105	484	938	714	142	1607	764	345
		C (E/(W/K))	1.88	1.21	1.04	1.06	1.6	1.02	1.04	1.25
	Low Viscosity Organic Liquid	U (W/m ² K)	99	375	600	500	130	818	524	286
		C (E/(W/K))	1.88	1.24	1.17	1.19	1.71	1.04	1.18	1.28
High Viscosity Liquid	U (W/m ² K)	68	138	161	153	82	173	155	214	
	C (E/(W/K))	2.4	1.67	1.52	1.56	2.21	1.41	1.57	1.38	
Boiling Water	U (W/m ² K)	105	467	875	677	140	1432	722	336	
	C (E/(W/K))	1.88	1.22	1.04	1.12	1.71	1.03	1.04	1.26	
Boiling Organic Liquid	U (W/m ² K)	99	3.75	600	500	130	818	524	286	
	C (E/(W/K))	1.88	1.24	1.17	1.19	1.71	1.04	1.18	1.28	
30 000	Low Pressure Gas (< 1 Bar)	U (W/m ² K)	55	93	102	99	63	107	100	86
		C (E/(W/K))	1.39	1	0.89	0.91	1.31	0.87	0.91	1.07
	Med. Pressure Gas (20 Bar)	U (W/m ² K)	93	300	429	375	120	530	388	240
		C (E/(W/K))	1	0.46	0.39	0.4	0.83	0.34	0.39	0.53
	Treated Cooling Water	U (W/m ² K)	105	484	938	714	142	1607	764	345
		C (E/(W/K))	0.88	0.38	0.26	0.3	0.76	0.23	0.3	0.43
	Low Viscosity Organic Liquid	U (W/m ² K)	99	375	600	500	130	818	524	286
		C (E/(W/K))	0.91	0.4	0.31	0.37	0.81	0.29	0.35	0.47
High Viscosity Liquid	U (W/m ² K)	68	138	161	153	82	173	155	214	
	C (E/(W/K))	1.3	0.77	0.69	0.72	1.06	0.68	0.71	0.63	
Boiling Water	U (W/m ² K)	105	467	875	677	140	1432	722	336	
	C (E/(W/K))	0.88	0.38	0.28	0.31	0.77	0.23	0.3	0.44	
Boiling Organic Liquid	U (W/m ² K)	99	375	600	500	130	818	524	286	
	C (E/(W/K))	0.91	0.4	0.31	0.37	0.81	0.29	0.35	0.47	

100 000	Low Pressure Gas (< 1 Bar)	U (W/m ² K) C (€/(W/K))	55 1.04	93 0.62	102 0.6	99 0.61	63 0.98	107 0.58	100 0.6	86 0.78
	Med. Pressure Gas (20 Bar)	U (W/m ² K) C (€/(W/K))	93 0.62	300 0.28	429 0.24	375 0.25	120 0.56	530 0.19	388 0.24	240 0.35
	Treated Cooling Water	U (W/m ² K) C (€/(W/K))	105 0.59	484 0.21	938 0.15	714 0.16	142 0.49	1607 0.14	764 0.16	345 0.27
	Low Viscosity Organic Liquid	U (W/m ² K) C (€/(W/K))	99 0.61	375 0.25	600 0.17	500 0.2	130 0.53	818 0.15	524 0.19	286 0.3
	High Viscosity Liquid	U (W/m ² K) C (€/(W/K))	68 0.96	138 0.51	161 0.41	153 0.45	82 0.81	173 0.41	155 0.43	214 0.38
	Boiling Water	U (W/m ² K) C (€/(W/K))	105 0.59	467 0.22	875 0.15	677 0.16	140 0.5	1432 0.14	722 0.16	336 0.28
	Boiling Organic Liquid	U (W/m ² K) C (€/(W/K))	99 0.61	372 0.25	600 0.17	500 0.2	130 0.53	818 0.15	524 0.19	286 0.3
	1 000 000	Low Pressure Gas (< 1 Bar)	U (W/m ² K) C (€/(W/K))	55 1.04	93 0.62	102 0.6	99 0.61	63 0.98	107 0.58	100 0.6
Med. Pressure Gas (20 Bar)		U (W/m ² K) C (€/(W/K))	93 0.62	300 0.28	429 0.24	375 0.25	120 0.56	530 0.19	388 0.24	240 0.35
Treated Cooling Water		U (W/m ² K) C (€/(W/K))	105 0.59	484 0.21	938 0.15	714 0.16	142 0.49	1607 0.14	764 0.16	345 0.27
Low Viscosity Organic Liquid		U (W/m ² K) C (€/(W/K))	99 0.61	375 0.25	600 0.17	500 0.2	130 0.53	818 0.15	524 0.19	286 0.3
High Viscosity Liquid		U (W/m ² K) C (€/(W/K))	68 0.96	138 0.51	161 0.41	153 0.45	82 0.81	173 0.41	155 0.43	214 0.38
Boiling Water		U (W/m ² K) C (€/(W/K))	105 0.59	467 0.22	875 0.15	677 0.16	140 0.5	1432 0.14	722 0.16	336 0.28
Boiling Organic Liquid		U (W/m ² K) C (€/(W/K))	99 0.61	372 0.25	600 0.17	500 0.2	130 0.53	818 0.15	524 0.19	286 0.3
Low Pressure Gas (< 1 Bar)		U (W/m ² K) C (€/(W/K))	55 1.04	93 0.62	102 0.6	99 0.61	63 0.98	107 0.58	100 0.6	86 0.78
Med. Pressure Gas (20 Bar)	U (W/m ² K) C (€/(W/K))	93 0.62	300 0.28	429 0.24	375 0.25	120 0.56	530 0.19	388 0.24	240 0.35	
Treated Cooling Water	U (W/m ² K) C (€/(W/K))	105 0.59	484 0.21	938 0.15	714 0.16	142 0.49	1607 0.14	764 0.16	345 0.27	
Low Viscosity Organic Liquid	U (W/m ² K) C (€/(W/K))	99 0.61	375 0.25	600 0.17	500 0.2	130 0.53	818 0.15	524 0.19	286 0.3	
High Viscosity Liquid	U (W/m ² K) C (€/(W/K))	68 0.96	138 0.51	161 0.41	153 0.45	82 0.81	173 0.41	155 0.43	214 0.38	
Boiling Water	U (W/m ² K) C (€/(W/K))	105 0.59	467 0.22	875 0.15	677 0.16	140 0.5	1432 0.14	722 0.16	336 0.28	
Boiling Organic Liquid	U (W/m ² K) C (€/(W/K))	99 0.61	372 0.25	600 0.17	500 0.2	130 0.53	818 0.15	524 0.19	286 0.3	

Variation	a	b
AES rather than BEM Shell	1.59	-0.155
BEU rather than BEM Shell	0.98	-
450 psig (31.6 bar) rather than 300 psig (22.4 bar) pressure	1.11	-
600 psig (41.8 bar) rather than 300 psig (22.4 bar) pressure	1.25	-
5/8" (15.9 mm) rather than 3/4" (19 mm) tubes	0.90	-
1" (25.5 mm) rather than 3/4" (19 mm) tubes	1.05	-
Stainless steel rather than carbon steel tubes	1.30	0.29
Monel rather than carbon steel tubes	1.16	1.65
Admiralty brass rather than carbon steel tubes	1.42	0.08
Stainless steel rather than carbon steel shell	0.90	0.54
$L/D = 4$	1.50	-
$L/D = 8$	1.30	-
$L/D = 20$	0.87	-

Figure C 1 Values of Constants a and b for respective Variation

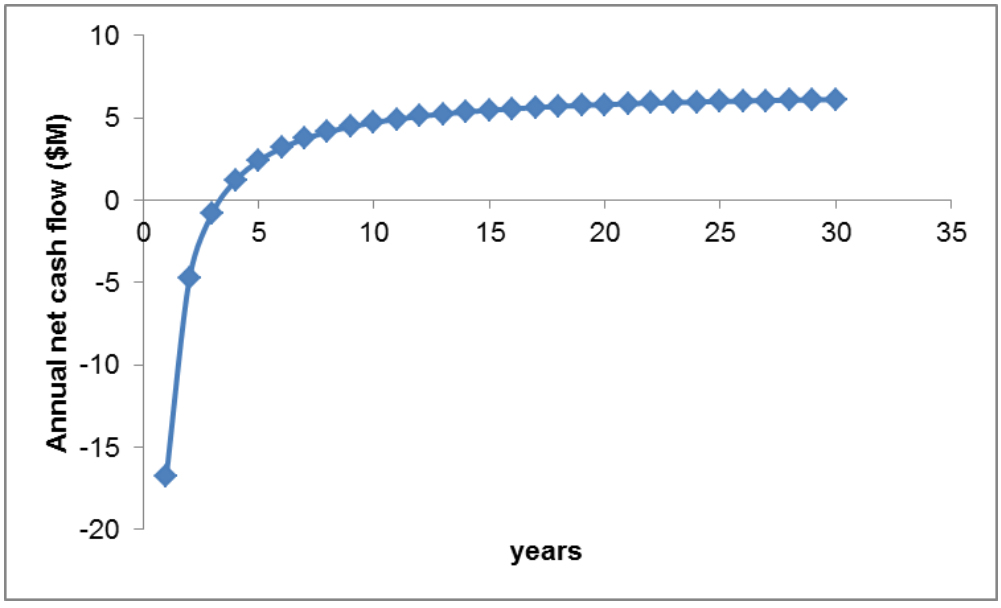


Figure C 2 Cash flow for helium

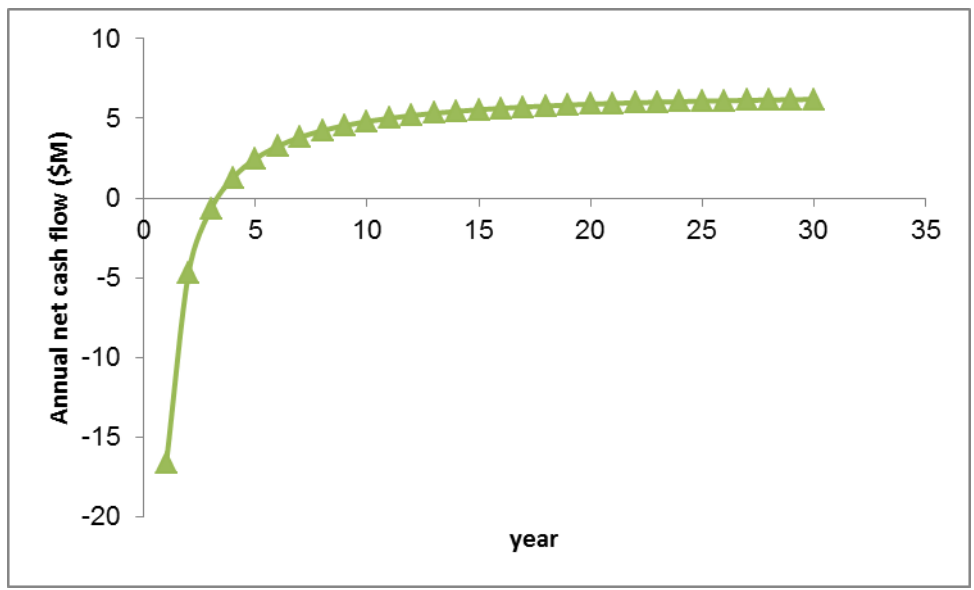


Figure C 3 Cash flow for air